CORSIA SUPPORTING DOCUMENT

CORSIA Eligible Fuels – Life Cycle Assessment Methodology

Version 6 – July 2024

This CORSIA supporting document provides technical information and describes ICAO processes to manage and maintain the ICAO document "CORSIA Default Life Cycle Emissions Values for CORSIA Eligible Fuels", which is referenced in Annex 16 — *Environmental Protection*, Volume IV — *Carbon Offsetting and Reduction Scheme for International Aviation (CORSIA)*, Part II, Paragraph 3.3.2.

Table A shows the origin of the versions to this CORSIA supporting document over time, together with a list of the principal subjects involved.

Table A. Versions of the CORSIA supporting document "CORSIA Eligible Fuels – Life Cycle Assessment Methodology"

Version	*Source(s)*	*Subject(s)*
1	Eleventh Meeting of the Committee on Aviation Environmental Protection	First version of the document.
2	2019 Steering Group Meeting of the Committee on Aviation Environmental Protection	Inclusion of editorial changes and corrections.
3	2020 Steering Group Meeting of the Committee on Aviation Environmental Protection	a) Inclusion of information on ATJ-SPK from ethanol pathways from agricultural residues, forest residues, miscanthus, and switchgrass b) Inclusion of information on HEFA carinata oil pathways c) Inclusion of guidance for submission of lifecycle assessment data d) Inclusion of editorial changes and corrections.
4	2021 Steering Group Meeting of the Committee on Aviation Environmental Protection	a) Inclusion of information on SAF produced from waste gases (ATJ-SPK from ethanol conversion process) b) Inclusion of information on SAF from tallow, soybean oil, and used cooking oil co-processed at petroleum refineries.
5	Twelfth Meeting of the Committee on Aviation Environmental Protection	a) Inclusion of a rationale on the baseline life cycle emissions values for aviation fuel b) Addition of a checklist for the inclusion of new credit pathways. c) Inclusion of information on HEFA jatropha oil pathway d) Addition of information on global ILUC values for several pathways
6	2024 Steering Group Meeting of the Committee on Aviation Environmental Protection	a) Inclusion of information on default core LCA values for beef tallow, poultry fat, lard fat, mixed animal fats, and non-standard coconut b) Inclusion of the process to request the classification of a new feedstock and emission credit to ICAO c) Nomenclature harmonization on the ATJ-SPK conversion processes

CORSIA SUPPORTING DOCUMENT

CORSIA ELIGIBLE FUELS – LIFE CYCLE ASSESSMENT METHODOLOGY

TABLE OF CONTENTS

LIST OF THE PRINCIPAL ACRONYMS

ATJ-SPK	Alcohol to jet synthetic paraffinic kerosene
ASTM	American Society for Testing and Materials
ANL	Argonne National Laboratory
CAEP	Committee on Aviation Environmental Protection
CEF	CORSIA Eligible Fuel
CLCA	Consequential Life Cycle Assessment
CORSIA	Carbon Offsetting and Reduction Scheme for International Aviation
CPO	Crude Palm Oil
CTBE	Brazilian Bioethanol Science and Technology Lab.
DDGS	Distillers Dry Grains and Solubles
FFA	Free Fatty Acids
FOG	Fats, Oils, and Greases
FT	Fischer-Tropsch
GHG	Green House Gas emissions
GWP	Global Warming Potential
HEFA	Hydroprocessed Esters and Fatty Acids
iBuOH	Isobutanol
JRC	Joint Research Center European Commission
LEC	Landfill Emission Credit
LCA	Life Cycle Assessment
LCF	Lower Carbon Aviation Fuel
LCI	Life cycle inventory
MIT	Massachusetts Institute of Technology
MSW	Municipal Solid Waste
NBC	Non-Biogenic Content
PFAD	Palm Fatty Acids Distillate
PSF	Peat Swamp Forest
REC	Recycling Emission Credit
RPO	Refined Palm Oil
SAF	Sustainable Aviation Fuel
SIP	Synthesized Iso-Paraffins
SPK	Synthetic Paraffinic Kerosene
SKA	Synthesized Kerosene with Aromatics
UCO	Used cooking oil
Unicamp	Universidade Estadual de Campinas
WTP	Well to Pump
WTWa	Well to Wake

PART I – ADDING NEW DEFAULT VALUES

CHAPTER 1. **CRITERIA AND PROCESS FOR THE ADDITION OF NEW DEFAULT LIFE CYCLE EMISSION VALUES**

While the vast majority of ground transportation biofuels are currently being produced from a few world regions, in the future, pathways and regions not represented in the results of this technical document will likely also produce SAF.

In order for an additional pathway to be evaluated for inclusion in the ICAO document 'CORSIA Default Life Cycle Emissions Values (core LCA and ILUC) for CORSIA Eligible fuels' the following criteria need to be met:

1. The pathway uses an ASTM certified conversion process or, a conversion process for which the Phase 2 ASTM Research Report has been reviewed and approved by the OEMs

2. The conversion process has been validated at sufficient scale to establish a basis for facility design and operating parameters at commercial scale

3. There are sufficient data on the conversion process of interest to perform LCA modelling.

4. There are sufficient data on the feedstock of interest to perform LCA modelling.

5. There are sufficient data on the region of interest to perform ILUC modelling, where applicable to the pathway.

CAEP designees will determine if the criteria have been met for adding a new pathway, carry out the calculation of default life cycle emission values for the pathway, and communicate the results in this document.

Requests for CAEP to consider a conversion process, feedstock, emission credit, and/or region can be made by ICAO Member States, Observer Organizations, or an approved SCS to the CAEP Secretary in ICAO (caep@icao.int). Further details on the process and data requirements are provided on this Part of this Supporting Document, as follows:

Chapter 2 of this Part provides guidance for submission of lifecycle assessment data, including data required for the calculation of default core LCA values and default ILUC values.

Chapter 3 of this Part defines the process and required data for adding a new emission credit pathway in the CORSIA Framework.

Chapter 4 of this Part defines the process and required data for adding a new feedstock as a waste, residue, or by-product in the CORSIA framework.

When a new region/feedstock/pathway combination is evaluated, ILUC results will be requested from both GTAP-BIO and GLOBIOM models. Each model must be made available to the members of the CAEP Fuels Task Group (FTG), so they can perform their own analysis. However, only the results from model simulations agreed by FTG will be used in calculating new ILUC values. If the ILUC emission results between the two models differ by 8.9 gCO_2e/MJ or less, the average value will be used. When the difference is greater than 8.9 gCO_2e/MJ, the lower of the two values plus 4.45 gCO_2e/MJ will be used. In the event that values cannot be obtained from both models within six months of the request date, the value from one model would be brought forward to CAEP for their potential approval and recommendation to the ICAO Council for inclusion in the default values contained in the ICAO document "CORSIA Default Life Cycle Emissions Values".

CHAPTER 2. GUIDANCE FOR SUBMISSION OF LIFECYCLE ASSESSMENT DATA

2.1 INTRODUCTION

The purpose of this Chapter is to define the minimum requirements of LCA data to be submitted to CAEP-FTG for the definition of default life cycle emission values to be used in CORSIA, in terms of data relevance, adequacy, quality, transparency and accessibility. The scope of this document covers core lifecycle emissions, as well as emissions from induced land use change (ILUC).

The intended audience of this guidance document is any party with an interest in SAF production and use that wishes to submit SAF LCA data to define default life cycle emission values under CORSIA. LCA data adhering to the methodology and data requirements described here may be submitted to the CAEP Secretary in ICAO (caep@icao.int).

2.2 DATA REQUIREMENT FOR THE CALCULATION OF DEFAULT CORE LCA VALUES

Data required for the calculation of default core LCA values for new pathways are listed in Table 1 below.

Table 1: Data to be submitted for the calculation of default core LCA values

#	Parameters	Unit	Note
Category: Feedstock Characteristics			
1	Density	[mass/volume of (dry) feedstock]	At harvest/collection
2	Lower heating value	[energy/mass of (dry) feedstock]	At harvest/collection
3	Higher heating value	[energy/mass of (dry) feedstock]	At harvest/collection
4	Carbon content	[%, mass of (dry) feedstock]	At harvest/collection
5	Sulfur content	[%, mass of (dry) feedstock]	At harvest/collection
6	Moisture content	[%, mass of (dry) feedstock]	At harvest/collection
7	Content of sugar, starch, cellulose, hemicellulose, lignin, vegetable oil, or other energy carrier (as applicable to feedstock of interest)	[%, mass of (dry) feedstock]	At harvest/collection
Category: Material inputs for feedstock generation			
8	Nitrogen	[mass/mass of (dry) feedstock]	
9	Phosphoric acid	[mass/mass of (dry) feedstock]	
10	Potassium oxide	[mass/mass of (dry) feedstock]	
11	Calcium carbonate	[mass/mass of (dry) feedstock]	
12	Insecticide	[mass/mass of (dry) feedstock]	
13	Herbicide	[mass/mass of (dry) feedstock]	
14	Irrigation water	[mass/mass of (dry) feedstock]	
Category: Energy inputs for feedstock generation and collection			
15	Diesel	[energy/mass feedstock]	

16	Liquified petroleum gas	[energy/mass feedstock]	
17	Gasoline	[energy/mass feedstock]	
18	Natural gas	[energy/mass feedstock]	
19	Electricity	[energy/mass feedstock]	
Category: Feedstock transportation			
20	Total transportation distance	[distance]	
21	Transportation mode shares	[%, total transportation distance]	
Category: Material inputs for feedstock to fuel conversion			
22	Feedstock	[mass/total fuel energy yield]	
23	n-Hexane	[mass/total fuel energy yield]	
24	Phosphoric acid	[mass/total fuel energy yield]	
25	Sulfuric acid	[mass/total fuel energy yield]	
26	Ammonia	[mass/total fuel energy yield]	
27	Diamonium	[mass/total fuel energy yield]	
28	Sodium hydroxide	[mass/total fuel energy yield]	
29	Calcium oxide	[mass/total fuel energy yield]	
30	Hydrogen	[mass/total fuel energy yield]	If hydrogen is produced onsite, natural gas demand is requested
31	Enzymes	[mass/total fuel energy yield]	EG. alpha amylase, gluco amylase, cellulase
32	Yeast	[mass/total fuel energy yield]	
Category: Energy inputs for feedstock to fuel conversion			
33	Diesel	[energy/total fuel energy yield]	
34	Liquified petroleum gas	[energy/total fuel energy yield]	
35	Gasoline	[energy/total fuel energy yield]	
36	Natural gas	[energy/total fuel energy yield]	
37	Electricity	[energy/total fuel energy yield]	
38	Hydrogen	[energy/total fuel energy yield]	
Category: Feedstock to fuel conversion process outputs			
39	Fuel product shares	[%, total fuel energy yield]	EG. liquified petroleum gas, naphtha, gasoline, diesel, jet fuels
40	Co- or by-product generation	[quantity/total fuel energy yield]	EG. animal feed, excess electricity
Category: Others			
Note: Not all materials may be relevant to each pathway, and materials that are relevant may be missing. Please add or disregard fields as relevant to the pathway of interest.			

2.3 DATA REQUIREMENT FOR ILUC VALUE CALCULATION OF BIOMASS-BASED FEEDSTOCKS

Table 2 lists the data needed for the ILUC modelling of new pathways and feedstocks with the two models, GTAP-BIO and GLOBIOM. These data fall into two classes: "required" and "recommended". Only seven elements have been classified as required. However, the Table also indicates the default assumptions that will be used for the case where some recommended information is not available.

Table 2: Data to be submitted for the calculation of ILUC values

#	Data	Required / recommended	Rationale
Category: Crop Productivity			
1	Crop yield for the primary product	Required	Required to know the direct land use impact.
2	Crop yield for the secondary products (including transformation losses).	Required	Required to assess the primary crop needs and the displacement effect of coproducts. Information on protein/energy content in the case of protein/energy cakes/distiller grains is recommended, otherwise a default value based on average protein/energy cakes/distiller grains content will be used.
3	Above-ground living biomass at harvest	Required	Required to compute the agricultural biomass sequestration.
4	Below-ground living biomass at harvest	Recommended	Recommended to compute the agricultural biomass sequestration. A default IPCC value will be applied if no information is available. If IPCC does not provide a value, a proxy will be estimated
5	Above-ground living biomass after harvest	Recommended	Recommended to compute the average sequestration time in the field/plantation (e.g. tree biomass remaining for palm plantations, agricultural residue remaining, etc.). If not available, all biomass will be considered harvested.
6	Below-ground living biomass after harvest	Recommended	Recommended to compute average sequestration as it may depend on the crop type (below ground biomass dying in case of annual crops but remaining for some perennials). If not available, all biomass will be considered as removed. Change in soil organic carbon will be computed based on land cover type following IPCC Tier 1 methodology.
7	Typical yields of other neighboring crops where the yield was measured	Required	Required to interpret the yield information provided and extrapolate it to other location. Can be substituted with precise location information on the production site.
8	Fertilizer application assumed for observed yield	Recommended	Recommended, including fertilizer type (organic vs mineral), to interpret the yield information provided (intensification possible or not).
9	Country and/or location	Required	Country required, and more precise location recommended to interpret the yield information provided and extrapolate it to other locations.
10	Production site location	Recommended	

Category: Other Agronomic characteristics			
11	Typical crop calendar	Recommended	Recommended to compute the average biomass in the landscape and represent land competition (e.g. for inter-season cropping). By default, calendar will be based on other annual crops and the feedstock will be assumed in full competition with these.
12	Rotation constraints	Recommended	Recommended to better represent the dynamics of competition with other crops.
13	Typical management tillage practice	Recommended	Recommended to compute the SOC impact. By default, if no specific information available, annual crop management will be assumed to be the same compared to other crops in the country, and perennials will be assumed under no tillage.
14	Typical residue management	Recommended	Recommended to more precisely compute the SOC impact.
15	Typical irrigation practice	Recommended	Recommended to interpret the yield information provided and extrapolate it to other location
16	Crop family and other crops sharing similar characteristics	Recommended	Recommended to interpret the yield information provided and extrapolate it to other location.
17	Any other information of relevance (e.g. land suitability, observed SOC impact, etc.)	Recommended	Recommended to help refine the assessment by modelling teams.
Category: Economic Characteristics			
18	Typical total production cost and farm gate price	Required	Required if not available in international statistics (FAO) to represent correctly the market competition dynamics in the models
19	Input cost shares in total production costs.	Required	Required to better represent the dynamics of input prices in the models.
20	Country Input-Output (IO) table	Recommended	Recommended if missing in the GTAP database. The GTAP-BIO model uses input-output (I/O) tables in its simulation process. If the new feedstock is produced in a country with missing I/O table in the GTAP database, then an I/O table for the country of feedstock is needed. If an I/O table is missing and is not provided, the GTAP team will assign a proxy I/O table.
21	If the products are not part of existing market: Substitutability of the primary and secondary products on any preexisting market	Recommended	Recommended to represent product competition on the current markets. If not available, the product will be assumed in full competition with other product in the same category (e.g. a new vegetable oil will be assumed in competition with other vegetable oil and fats).
22	Any barrier or support to deployment (land conversion or rehabilitation cost, specific dedicated areas, etc.)	Recommended	Recommended for representation of any additional cost or effect on land use change matrix.

2.4 QUALITY

In order to ensure information is coming from a credible source, LCA values submitted to CAEP-FTG must adhere to one of the following criteria in order to be considered for inclusion under CORSIA:

- publication in a peer-reviewed scientific journal;
- publication or dissemination as an academic or archival work (e.g. thesis, textbook, book chapter);
- publication or dissemination by an appropriate agency from a State government (e.g. environmental or transportation agency);
- publication or dissemination by an appropriate intergovernmental agency (e.g. UN body, the International Energy Agency of OECD);
- publication or dissemination by an appropriate non-profit or non-governmental organization (NGO); or
- direct submission to CAEP-FTG of LCA values calculated by an appropriate a) agency from a State government, b) intergovernmental agency, c) non-profit or NGO, or d) private entity.

This list of potential credible data sources is non-exhaustive, and sources beyond those listed here will be considered on a case-by-case basis.

2.5 TRANSPARENCY

Transparency is a key requirement of LCA input values submitted to CAEP-FTG. In order to be considered for inclusion under CORSIA, CAEP-FTG must be able to confirm the accuracy and validity of submitted LCA values, and therefore the calculations must be replicable. To achieve this, all source data must be properly cited, and if it is not otherwise publically accessible, must be provided directly to CAEP-FTG. In addition, the actual model or database used for LCA calculations must be available to CAEP-FTG for verification purposes. This process will be facilitated by the use of existing publically accessible and peer-reviewed LCA calculation tools that are adapted to the evaluation of SAF, where possible. For example, the Greenhouse Gases, Regulated Emissions and Energy Use in Transportation model developed by Argonne National Laboratory in the United States, or BioGrace tool developed by the European Commission (EC 2016).

In order to facilitate the satisfaction of this requirement, ICAO can facilitate setting up non-disclosure agreements (NDAs) between the owners of proprietary fuel production data and technical experts nominated to CAEP-FTG.

2.6 ACCESSIBILITY

Data must be provided in a format conducive to re-calculation and verification, for example a spreadsheet, .csv or .txt file format.

2.7 DATA SUBMISSION PROCESS

Please submit LCA input data that adheres to the methodology and requirements laid out in this document CAEP Secretary in ICAO (caep@icao.int). Questions regarding this document can be directed to the same email address.

CHAPTER 3. **PROCESS FOR ADDING A NEW CREDIT PATHWAY IN THE CORSIA FRAMEWORK**

New credit pathway proponents will complete and provide responses before a new credit pathway is included in the CORSIA Methodologies.

The production of CORSIA Eligible Fuels may generate emission credits that can be subtracted from the actual LCA values to calculate its total L_{CEF}. At the moment, two types of credits are allowed under CORSIA: Avoided Landfill Emissions Credit (LEC) for SAF derived from Municipal Solid Waste (MSW), and Recycling Emissions Credit (REC) for SAF derived from Municipal Solid Waste (MSW).

A new credit pathway may be allowed under CORSIA if approved by the ICAO Council. For that, new credit pathway proponents will complete and substantiate responses to all questions in Table 3 and Table 4. The new credit pathway proponent will submit the tables, with supporting documentation, to the CAEP Secretary in ICAO (caep@icao.int) for review and consideration.

Table 3: Screening Questions for the Development of New Credit Pathways

#	Question	Response		Explanation
1	Are all the emissions reductions associated with the proposed credit occurring outside the scope of the existing CEF methodologies (including ILUC)? (please describe how the emissions reductions are not captured in either Implementation Element "CORSIA Default Life Cycle Emissions Values for CORSIA Eligible Fuels" or Implementation Element "CORSIA Methodology for Calculating Actual Life Cycle Emissions Values).	☐	Yes	
		☐	No	
2	Is jet fuel production a key reason for the overall improvement in GHG emissions? (please describe how the availability of this credit is material for the production of CEF).	☐	Yes	
		☐	No	

If any of the answers to screening questions 1 and 2 are no, the pathway is not eligible. If all the answers are yes, continue to complete Table 4.

Table 4: Proposals for New Credit Pathways

Q#	Question
1	Was the development of the methodology based on similar methodologies? If so, please include a link to or description of the methodology(ies) and which portion of the methodology applies to this proposal. If yes, identify any significant deviations from the similar methodology(ies) (e.g., categories of discrepancy – eligibility, LCA calculation, approach to additionality,

	monitoring) and describe those deviations including explanation for why the deviation is necessary. If no, why not (e.g., no similar methodologies exist).
2	Did the development of the methodology include a stakeholder/peer review process?
3	Provide the approach to quantification monitoring, reporting, and verification for the methodology, including an example calculation addressing full life-cycle accounting, and describe how the full life-cycle accounting was done (e.g., for a change in agricultural practices activity, including any changes in fertilizer), including related emissions outside of the activity boundary.
4	Does the calculation include the potential for an L_{CEF} lower than zero? If yes, describe the situation(s) where this could occur.
5	What are the key elements of the proposed methodology and parameters of the methodology that will need to be audited over time to demonstrate that the GHG reduction occurred?
6	What requirements are included in the proposed methodology to ensure that these emissions reductions are additional (i.e., exceed emissions reductions required by law, regulation, or legally binding mandate, and exceed those that would otherwise occur in a business-as-usual scenario)?
7	What environmental and social risks were considered in the development of the proposed methodology and what safeguards were established to mitigate these risks i.e., water quality and use, soil quality, air quality, conservation, wastes and chemicals, human and labor rights, land use rights, water use rights, local and social development, food security?
8	What requirements are included in the proposed methodology to avoid double counting (including double issuance or double claiming) of credits?
9	Is there a material risk of leakage (i.e., potential increase in emissions elsewhere)? If so, describe how the risk of leakage was addressed in the methodology, including the procedures for deducting leaked emissions from the accounting if relevant. If there is no material risk of leakage, include a brief explanation why.
10	What requirements are in place to ensure emissions reductions are permanent? If the activities include a quantified sequestration component, what requirements are in the proposed methodology to support the economic operator in fulfilling the requirement to demonstrate in a technical report that the emission reductions claimed are permanent (e.g., insurance, buffer pools)?

CHAPTER 4. **GUIDANCE FOR SUBMISSION OF INFORMATION RELATED TO THE CLASSIFICATION OF A FEEDSTOCK AS A WASTE, RESIDUE OR BY-PRODUCT.**

Proponents that intend to request the classification of a feedstock as a waste, residue, or by product should provide supporting information to ICAO, in line with the definitions and guidance provided in Section 4 of the ICAO document “CORSIA methodology for calculating actual life cycle emission values”.

PART II – CALCULATION OF DEFAULT CORE LCA VALUES

CHAPTER 1. **CORE LIFE CYCLE ASSESSMENT METHODOLOGY**

The purpose of this Part is to present the methodology and calculation of the default core life cycle Greenhouse Gas (GHG) emissions of the different Sustainable Aviation Fuel (SAF) pathways that can be used to reduce aircraft operators' offsetting obligations under the Carbon Offsetting and Reduction Scheme for International Aviation (CORSIA).

1.2 BACKGROUND

1.2.1 Eligible fuels under CORSIA

CORSIA eligible fuels (CEF) include Sustainable Aviation Fuels (SAF) and Lower Carbon Aviation Fuels (LCF). At the time of writing, the CAEP has only calculated the default life cycle emissions of SAF pathways, which are documented in this Part.

1.2.2 SAF conversion technologies

In order to be used into commercial flights, an alternative fuel – either eligible under CORSIA or not – has to comply with the ASTM D4054. Among the ASTM certified pathways, a fuel meeting the CORSIA`s sustainability criteria can be eligible as CEF.

As of November 2021, there have been 9 conversion processes approved for aviation alternative fuel production:

1. ASTM D7566 Annex 1 – Fischer-Tropsch hydroprocessed synthesized paraffinic kerosene (FT SPK)

2. ASTM D7566 Annex 2 – Synthesized paraffinic kerosene from hydroprocessed esters and fatty acids (HEFA SPK)

3. ASTM D7566 Annex 3 – Synthesized iso-paraffins from hydroprocessed fermented sugars (SIP)

4. ASTM D7566 Annex 4 – Synthesized kerosene with aromatics derived by alkylation of light aromatics from non-petroleum sources (FT-SKA)

5. ASTM D7566 Annex 5 – Alcohol to jet synthetic paraffinic kerosene (ATJ-SPK)

6. ASTM D7566 Annex 6 – catalytic hydrothermolysis jet (CHJ)

7. ASTM D7566 Annex 7 - synthesized paraffinic kerosene from hydrocarbon-hydroprocessed esters and fatty acids (HC-HEFA SPK)

8. ASTM D-1655 - co-hydroprocessing of esters and fatty acids in a conventional petroleum refinery

9. ASTM D-1655 - co-hydroprocessing of Fischer-Tropsch hydrocarbons in a conventional petroleum refinery.

1.3 LCA GENERAL APPROACH

This Part describes the methodology for, and calculation of, the default core life cycle GHG emissions of SAF.

The core life cycle GHG emissions of the SAF pathways have been calculated using a LCA attributional - or "process-based" approach. Attributional LCA implies accounting mass and energy flows, along the whole value chain. CAEP decided to use attributional analysis for the core LCA GHG emissions

calculations, meaning that no displacement effects related to co-products are accounted for: emissions are allocated across the co-products on the basis of energy content. In contrast, for induced land use change (ILUC) emissions, a consequential approach is taken. Total life cycle GHG emissions (L_{CEF}) values for a given SAF are given by the sum of 'core LCA' emissions calculated with an attributional approach and 'ILUC' emissions calculated with a consequential approach. The focus of this Part is the default 'core LCA' values calculated by CAEP for a number of SAF pathways.

Chapter 1 of this document explains the methodological choices and describes the steps used to calculate default core LCA values.

Chapters 2-6 describe the default core LCA results, broken down by feedstock-to-fuel pathway and grouped per conversion technology.

Chapter 7 provides a summary overview of all pathways for which a default value has been calculated.

1.4 ATTRIBUTIONAL APPROACH FOR CORE LCA CALCULATIONS

1.4.1 System boundary

The system boundary of the CORSIA LCA methodology consists of the full supply chain of SAF production and use. As such, emissions associated with the following stages are accounted for:

- feedstock cultivation;
- feedstock harvesting, collection and recovery;
- feedstock processing and extraction;
- feedstock transportation to processing and fuel production facilities;
- feedstock-to-fuel conversion processes;
- fuel transportation and distribution; and fuel combustion in an aircraft engine.

These lifecycle steps are depicted in Figure 1.

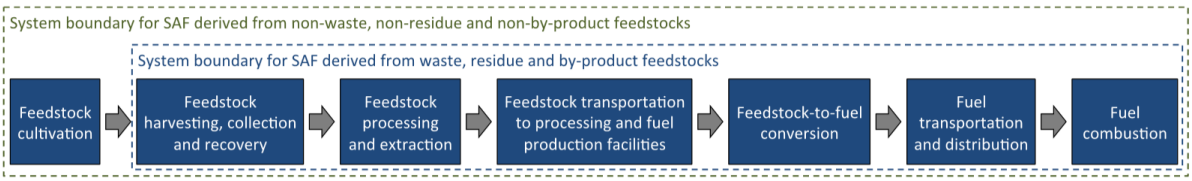

Figure 1: SAF lifecycle steps

The calculated LCA values include emissions generated during on-going operational activities (e.g. operation of a fuel production facility, feedstock cultivation, etc.), as well as emissions embedded in all the streams and utilities used, such as processing chemicals, electricity and natural gas. However, emissions generated during one-time construction or manufacturing activities (e.g. fuel production facility construction, equipment manufacturing) are not included.

According to the type of feedstock (primary products; wastes; residues; or by-products) different approaches are taken for calculating the default core LCA emissions. In particular, waste, residue and by-product feedstocks incur zero GHG emissions during the feedstock production step of the lifecycle;

emissions generated during their collection, recovery and extraction, and processing of wastes, residues and by-products, however, are included.

1.4.2 Emissions species of interest and functional units

CORSIA LCA methodology calculates 100-year global warming potential (GWP) carbon dioxide equivalent (CO_2e) emissions of CO_2, CH_4 and N_2O from well-to-pump activities (WTP), and CO_2 emissions from well-to-wake (WTWa) fuel combustion. 100-year GWP are calculated using the CO_2e values for CH_4 and N_2O from the Intergovernmental Panel on Climate Change (IPCC-AR5) (28 and 265, respectively) (IPCC 2014). Biogenic CO_2 emissions from fuel production or combustion are not included in the calculation per IPCC Fifth Assessment Report 100-year global warming potentials (IPCC 2014).

The functional unit selected for the LCA results is grams of CO_2e per MJ of fuel produced (gCO_2e/MJ_{SAF}) and combusted in an aircraft engine (using the lower heating value for characterizing fuel energy content).

1.4.3 Co-product allocation methodology

In many cases, a SAF production chain will result in the co-production of multiple commodities. These co-products may include other liquid fuels, chemicals, electricity, steam, hydrogen, and/or animal feed. In order to allocate the emissions generated from the entire supply chain amongst all of the valuable outputs of the system, an energy allocation method for co-products is used. Under energy-based allocation, the emissions burdens are allocated to co-products in proportion to their contribution to the total energy content of all the outputs. According to the previously described approach for treating waste, residue and by-product feedstocks, no emissions are allocated to these feedstock categories for their generation.

1.4.4 Data quality

For the purpose of the life cycle assessment methodology developed for CORSIA, the LCA target group screened the available literature on LCA GHG emissions for sustainable aviation fuels. Since there were methodological inconsistencies among different existing studies, tools and datasets, the specific references and inputs to this analysis had to be selected on a case by case, to ensure consistency of the results.

1.4.5 Intended use & aviation fuel baseline

Default core LCA values for SAF - calculated according to the methodology briefly introduced - are compared with baseline LCA GHG values for aviation fuels. This comparison is used in the CORSIA Monitoring, Reporting and Verification (MRV) process to calculate operators' proportional reduction in CO_2 emissions from the use of SAF. These baseline values adopted in Annex 16 Vol IV are 89 gCO_2e/MJ for jet fuel and 95 gCO_2e/MJ for AvGas. The default core LCA values calculated here are intended to be global, and are applicable to any specific world region.

The petroleum aviation fuel baseline includes petroleum fuels from conventional oil and unconventional oil, the latter including enhanced oil recovery (EOR) for crude, offshore deep water recovery, tight/shale oil, and Canadian oil sands.

Modeling teams from the Massachusetts Institute of Technology (MIT), IFP Energies nouvelles (IFPEN) and Argonne National Laboratory (ANL) focused on different parts of the Well to Wake (WTW) GHG emissions for **petroleum-derived jet fuel**. All modelling teams used the CORSIA attributional LCA approach with energy-based allocation to allocate emissions among desired products from petroleum oil, and present average LCA estimates per unit of aviation fuel. The emission estimates were then brought together to yield total WtWa GHG emissions.

WTW GHG emissions for jet fuel production from conventional crude oil in Middle East, North America, Eurasia, Asia & Oceania, Africa, Central & South America, and Europe are estimated and are broken out

into five life cycle stages: crude extraction, crude transportation, crude refining to jet fuels, jet fuel transportation, and jet fuel combustion. In addition, WTW GHG emissions for jet fuel production from unconventional crude sources including offshore deep water crudes, enhanced oil recovery (EOR), shale/tight oil, and Canadian oil sands are evaluated. Three major efforts have been made to fulfil this goal:

MIT calculated crude extraction and transportation emissions using information from work under ASCENT Center of Excellence Project 32. The calculations use, among other items, relationships between each activity of interest, energy expenditure and GHG emissions from several sources, such as EIA, NOAA, EPA, IEA, OPEC, NETL and from the OPGEE and GREET models, to estimate emissions associated with extraction and transportation of various types of crudes around the world.

IFPEN used its Linear Programming (LP) worldwide refinery model (RafGen multi) in order to estimate refining emissions in different world regions. The LP outcomes consist of GHG emissions of the refineries in each world region as well as mass and energy balance data of each unit process within a refinery. For the specific purpose of the baseline estimations, these results are used to develop nine refinery models using GaBi LCA software in order to allocate emissions and energy consumption to jet fuel.

ANL analyzed and published the WTW GHG emissions of jet fuel production from Canadian oil sands and the upstream recovery GHG emissions of shale/tight oil using the ANL GREET life cycle model.[1] ANL also contributed the CO_2 combustion emissions estimate from the GREET model to the analysis effort.

With the above three analysis efforts, the modelling teams determined the GHG emission intensities of all the life-cycle stages associated with jet fuel production from conventional crudes in various regions of the world, and from unconventional crudes (Table 5 and Table 6). These were translated into a global average baseline value by using forecasts about future market shares of conventional crude by world region, and different types of unconventional crude, as presented in Table 7. Based on these data, the baseline for **conventional jet fuel** was set at **89.0 g CO_{2e}/MJ**.

For **Aviation Gasoline** (AvGas), the WTW emissions were based on an estimate of gasoline emissions from an MIT study that informed the CAEP process. This MIT study included 139 GHG emissions points for the well-to-pump (WTP) processes. The refinery stage converted crude oil into gasoline products and considered 113 countries and 687 refineries. 18 different processing units were considered, including distillation, hydro-treating, cracking, coking, and upgrading. Emissions from flaring and fugitive gases were included. The two transportation stages included the movements of crude oil and refined products. Several modes of transport were considered, such as pipeline, tanker, rail, truck, and barge. WTP emissions were calculated for historical years as well as projected to the year 2020. The WTP emissions of AvGas for the year 2020 are estimated at 24.3 gCO_{2e}/MJ.

Aviation gasoline contains tetraethyl lead to prevent engine knock, while automotive gasoline does not. Aviation gasoline on a whole is more similar to premium gasoline than regular/normal gasoline, thus having a higher octane rating to prevent engine knock. Increasing the octane rating of gasoline requires additional refinery processing that result in higher energy expenditure and emissions. These additional refinery

[1] Cai, Hao, et al. "Well-to-wheels greenhouse gas emissions of Canadian oil sands products: Implications for US petroleum fuels." *Environmental science & technology* 49.13 (2015): 8219-8227. Yeh, et al., 2017, "Energy Intensity and Greenhouse Gas Emissions from Tight Oil Production in the Eagle Ford Shale," *Energy and Fuels* 31: 1440-1449. Brandt, et al. 2016, "Energy Intensity and Greenhouse Gas Emissions from Tight Oil Production in the Bakken Formation," *Energy and Fuels*, 30: 9613-9621.

emissions have been estimated based on data from an existing study on higher-octane gasoline[2]. Overall, the change in refinery emissions due to upgrading regular gasoline to premium is estimated at 1.4 g CO_2/MJ.

The standard IPCC value for gasoline combustion emissions is 69.3 gCO_2/MJ[3], which needs to be added to the WTP emissions to complete the quantification of gasoline lifecycle GHG emissions. In total, this approach yields an estimate for lifecycle GHG emissions of **AvGas** in the year 2020 of **95.0 gCO_2e/MJ**.

Table 5: WTW GHG emissions by life-cycle stage for jet fuel production from conventional crudes in various regions of the world

Conventional crudes		Crude Extraction	Crude Transport	Crude Refining	Product Transport	Jet combustion
Middle East	Middle East	6.6	1.8	6.5	1.0	74.0
North America	U.S.	5.8	1.8	1.7	1.0	74.0
	Canada (conventional)	5.8	1.8	1.7	1.0	74.0
	Mexico	5.8	1.8	1.7	1.0	74.0
Eurasia	Russia	10.0	1.8	4.7	1.0	74.0
	Other Europe and Eurasia	10.0	1.8	4.7	1.0	74.0
Asia & Oceania	China	7.1	1.8	5.1	1.0	74.0
	Other Asia	7.1	1.8	3.4	1.0	74.0
Africa	West Africa	10.4	1.8	1.5	1.0	74.0
	North Africa	10.4	1.8	1.5	1.0	74.0
	The rest of Africa	10.4	1.8	1.5	1.0	74.0
Central & South America	Brazil	7.0	1.8	1.7	1.0	74.0
	South America except Brazil	7.0	1.8	1.7	1.0	74.0
Europe	OECD Europe	5.1	1.8	2.3	1.0	74.0

Note: Emissions in red cells are from the MIT analysis; Emissions in yellow cells are from the ANL analysis with GREET; and emissions in green cells are from the IFPEN regional refinery modeling.

Table 6: WTW GHG emissions by life-cycle stage for jet fuel production from unconventional crudes[1]

Unconventional crudes	Crude Extraction	Crude Transport	Crude Refining	Product Transport	Jet combustion
EOR for conventional crude	21.4	1.8	3.3	1.0	74.0
Offshore deep water[2]	7.0	1.8	3.3	1.0	74.0
NGL[3]	17.2				74.0
Tight oil	7.5	1.8	3.3	1.0	74.0
Canadian oil sands	21.3	3.9	3.9	0.5	74.0

Notes:

[1] Emissions in red cells are from the MIT analysis; Emissions in yellow cells are from the ANL analysis with GREET; and emissions in green cells are from the IFPEN regional refinery modeling.

[2] Offshore deep water extraction GHG emission is not available at present. The emission for Brazil extraction is used as a surrogate.

[3] Emissions for all four stages are combined for NGL.

[2] Speth, R. L., et al. "Economic and environmental benefits of higher-octane gasoline." Environmental science & technology 48.12 (2014): 6561-6568.

[3] Intergovernmental Panel on Climate Change (IPCC), "Fifth Assessment Report (AR5)," 2014.

Table 7: Average GHG emissions intensity (gCO_{2e}/MJ) of global jet fuel production, forecast to 2050

		2010-2013	2015	2020	2050
World average	WTP (Well-to-Pump)	14.6	14.5	14.8	15.3
	WTWa (Well-to-Wake)	88.6	88.6	88.8	89.4

1.4.6 Mid-point value definition procedure

The pathway specific analyses described in the next chapters have been performed by various institutions. Each pathway evaluation has been led by a single institution and verified by the others. Results in the calculations have often diverged, as a result of differences in feedstock yields, process inputs, and other parametric assumptions. Therefore, a procedure was required in order to agree upon a single default core LCA value. A threshold equal to 10% of the jet fuel baseline (i.e. 8.9 gCO_2e/MJ_{SAF}) was defined; when the difference between two analyses, for the same pathway, falls within this threshold, the mid-point between the results is taken as the default value. If the difference between two analyses is greater than 8.9 gCO_2e/MJ_{SAF}, harmonization of the parametric assumption was undertaken, or the pathway was split into two in order to better represent physically different systems.

1.4.7 List of the pathways and feedstock analyzed

The different pathways analyzed are reported in Table 8. Pathways are classified by conversion process and type of feedstock. As the feedstock definition in terms of residue, by-product, co-product influences the results, it is worth highlighting how they have been classified in each specific case. A color code is used to describe the feedstock classification: green for residues, wastes and by-products [R,W,B], orange for co-products [C] and blue for main products [M].

Table 8: List of pathways analyzed

Conversion process	Feedstock	Type of feedstock
Fischer-Tropsch (FT)	Agricultural residues	[R]
	Forestry residues	[R]
	Short-rotation woody crops	[M]
	Herbaceous energy crops	[M]
	Municipal solid waste (MSW), 0% non-biogenic carbon (NBC)	[W]
	MSW, NBC (NBC given as a percentage of the non-biogenic carbon content)	[W]
Hydro-processed esters and fatty acids (HEFA)	Tallow	[B]
	Used cooking oil	[W]
	Palm fatty acid distillate	[B]
	Corn oil (from dry mill ethanol plant)	[B]
	Soybean oil	[M]
	Rapeseed oil	[M]
	Camelina oil	[M]
	Palm oil - closed pond	[M]
	Palm oil - open pond	[M]
	Brassica carinata	[M]
	Jatropha	[M]
	Beef tallow, poultry fat, lard fat, mixed animal fats	[W]
	Non-standard coconut	[B]
Synthesized Iso-Paraffins (SIP)	Sugarcane	[M]
	Sugarbeet	[M]
Iso-butanol Alcohol-to-jet (ATJ)	Sugarcane	[M]
	Agricultural residues	[R]
	Forestry residues	[R]
	Corn grain	[M]
	Herbaceous energy crops	[M]
	Molasses	[C]
Ethanol Alcohol-to-jet (ATJ)	Sugarcane	[M]
	Corn grain	[M]
	Agricultural residues	[R]
	Forestry residues	[R]
	Herbaceous energy crops	[M]
	Waste gases	[W]
Hydro-processed esters and fatty acids (HEFA) co-processed at petroleum refineries	Used cooking oil	[W]
	Soybean oil	[M]
	Tallow	[B]

CHAPTER 2. **FISCHER-TROPSCH PATHWAYS**

2.1 PATHWAY DESCRIPTION

The Fischer-Tropsch (FT) pathway is a conversion technology that comprises gasification of biomass, cleaning and conditioning of the produced synthesis gas, and subsequent synthesis to obtain liquid biofuels. A general process flow for FT pathways is shown in Figure 2 below.

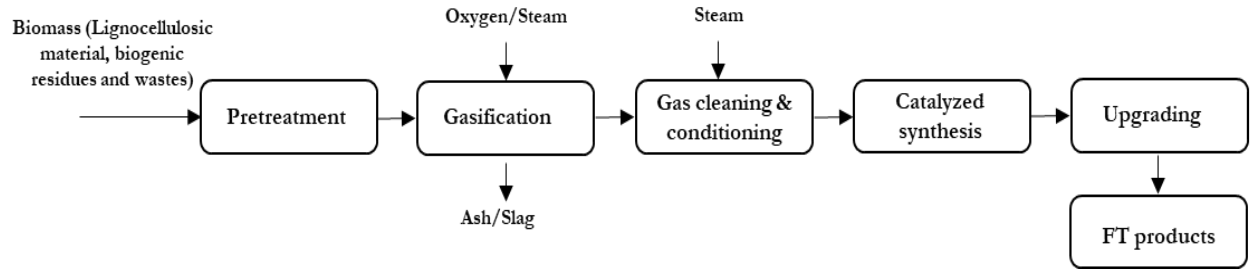

Figure 2: General process flow Fischer-Tropsch pathway

Several lignocellulosic materials, as well as biogenic residues and wastes, can be used for this pathway, due to the theoretical feedstock flexibility that gasification offers. Gasification is a high-temperature (700-1500 ºC) partial oxidation process (using one fifth to one third the oxygen required for full combustion) through which biomass and a gasifying agent (air, oxygen or steam) is converted into synthesis gas, or syngas, principally made of CO, CH_4 and H_2. After gasification, syngas has been cleaned and conditioned to be suitable for catalytic conversion. Along with CO and H_2, syngas contains CH_4, CO_2 and a range of higher hydrocarbons chains (tars) and other pollutants such as H_2S and particulate matter. The main aims of the syngas cleaning stage are: tar removal/cracking; particulate matter removal; and S, N, Cl species removal.

After syngas cleaning, the gas is conditioned to optimize its quality for catalytic synthesis. These steps may include the water-gas shift (WGS) reaction, to adjust the desired H_2/CO ratio, steam reforming to convert larger hydrocarbons, and possibly CO_2 removal if necessary. Finally, the catalytic synthesis of the syngas to the desired product takes place. The process is FT synthesis, in which CO and H_2 gases react in the presence of the catalyst to form liquid hydrocarbons. A further upgrading process is maybe necessary to increase the quality of the fuel, namely isomerization for aviation fuels.

The main drivers of FT process emissions are related to the generation mix for grid electricity, and the energy required for collecting and harvesting the feedstocks. The analysis of each pathway has been under taken considering regional electricity indices, from the World Energy Scenarios (2013). For cultivated energy crop feedstocks, the areal yield of the feedstocks and the fertilizer application rates are important factors as well.

The following sections report the default core LCA calculations for different feedstocks under the FT pathway.

2.2 AGRICULTURAL RESIDUES FT – [R]

Results for FT SAF derived from corn (*Zea mays*) stover and wheat (*Triticum aestivum*) straw are reported here. These are residue feedstocks, and therefore, the system boundary starts at the collection of these materials, without upstream emissions growth. The lifecycle inventory data for these feedstocks are shown

in Table 70 in the appendix. Table 9 shows the total GHG emissions for SAF produced from agricultural residues by FT conversion.

Table 9 report emission factors are calculated both with and without nutrient replacement in the cultivation phase. This difference is needed as typically agricultural residues are left on the field, where they decompose and provide nutrients to the soil. Conversely, if agricultural residues are removed, there may be a soil nutrient deficit, and therefore additional fertilizer has to be applied to maintain agricultural yields. Nutrient replacement is determined on the mass balance of the nutrients removed with the residues. After consideration of these two cases, CAEP determined to proceed with results that do not consider nutrient replacement, because this is consistent with the decision that no upstream generation emissions are included in the life cycle emissions of residue-derived fuels. Therefore, a mid-point value is only calculated for the no nutrient replacement case in Table 9, which is to be used as the default core LCA value for the agricultural residue FT pathway.

Table 9: LCA results for agricultural residues FT pathways [gCO_2e/MJ]

Feedstock	Data provider	Model	Feedstock cultivation and collection	Feedstock transportation	Feedstock-to fuel conversion	Fuel transportation	Total	Midpoint value
Corn Stover (without nutrient replacement)	MIT	GREET	3.3	2.3	0	0.9	**6.5**	**7.7**
	JRC	GREET	2.1	2.3	0	0.9	**5.4**	
	JRC	E3	1.5	4.7	3.3	0.3	**9.7**	
Wheat Straw (without nutrient replacement)	MIT	GREET	3.4	2.3	0	0.9	**6.6**	
	JRC	GREET	6.7	2.3	0	0.9	**10**	
	JRC	E3	1.5	0.5	3.3	0.3	**5.5**	
Corn Stover (with nutrient replacement)	MIT	GREET	11.1	2.3	0	0.9	**14.3**	**n/a**
	JRC	GREET	7.6	2.3	0	0.9	**10.9**	
	JRC	E3	6.1	4.7	3.3	0.3	**14.3**	
Wheat Straw (with nutrient replacement)	MIT	GREET	7.6	2.3	0	0.9	**10.9**	
	JRC	E3	2.1	0.5	3.3	0.3	**6.1**	

MIT calculated the values using the GREET model, while JRC calculated the values with the E3 database tool. ANL provided verification to these values. The E3 database estimates higher gasification and synthesis emissions from the FT process than the GREET model (3.3 g CO_2e/MJ against 0.03 g CO_2e/MJ). The transportation distances between the two models are also different. Emissions from feedstock production in the E3 model are lower for wheat straw because the fertilizer required for nutrient replacement is estimated to be lower (0.0 g N and 0.5 g K_2O instead of 5.0 g N and 0.9 g K_2O).

Despite the differing assumptions, these data are within the 8.9 g CO_2e/MJ threshold, therefore the accepted default core LCA value is 7.7 g CO_2e/MJ.

2.3 FORESTRY RESIDUES FT – [R]

Forest residues are included in this analysis, with the system boundary starting at the collection of these materials. The lifecycle inventory data for this feedstock is shown in Table 71 in the appendix. Table 10 shows the total GHG emissions for SAF produced from forest residues using FT conversion.

Table 10: LCA results for forest residue FT pathways [gCO_2e/MJ]

Feedstock	Data provider	Model	Feedstock cultivation and collection	Feedstock transportation	Feedstock-to- fuel conversion	Fuel transportation	Total	Midpoint value
Forest Residues	MIT	GREET	1.4	3.8	0	0.9	**6.1**	**8.3**
	JRC	GREET	2.4	3.8	0	0.9	**7.1**	
	JRC	E3	3.3	2.9	4	0.3	**10.5**	

MIT calculated the values using the GREET model, while JRC calculated the values with the E3 database. ANL provided verification to these values. AS for the previous case, E3 model estimates higher emissions from the FT process than the GREET (4.0 gCO_2e/MJ rather than 0.03 gCO_2e/MJ). Emissions from feedstock production in the E3 model are higher because of the higher energy demand for feedstock collection (0.26 MJ/kg forest residue rather than Btu rather than 0.14 MJ/kg forest residue).

As the results are within the 8.9 g CO_2e/MJ threshold, the agreed default core LCA value for forest residue FT pathway is 8.3 g CO_2e/MJ.

2.4 SHORT ROTATION WOODY CROPS FT – [M]

The feedstocks in this analysis include poplar (*Populus* spp.), willow (*Salix* spp.), and eucalyptus *(Eucalyptus* spp.). The system boundary considers the growth of these crops, as they are assumed to be grown for the purpose of fuel production. The lifecycle inventory data for these feedstocks are shown in Table 72 in the appendix. Results of the calculation are reported in Table 11.

Table 11: LCA results for short rotation woody crops FT pathways [gCO_2e/MJ]

Feedstock	Data provider	Model	Feedstock cultivation and collection	Feedstock transportation	Feedstock-to- fuel conversion	Fuel transportation	Total	Midpoint value
Poplar	MIT	GREET	6.7	2.3	0	0.9	**9.9**	**12.2**
	JRC	GREET	9.8	2.3	0	0.9	**13**	
	JRC	E3	11.5	0.7	4	0.3	**16.5**	
Willow	MIT	GREET	4.5	2.4	0	0.9	**7.8**	
	JRC	GREET	6.4	2.5	0	0.9	**9.7**	
Eucalyptus	MIT	GREET	6.1	2	0	0.9	**9.1**	
	JRC	E3	5.9	6.3	4.1	0.3	**16.6**	

MIT calculated the values using the GREET model, while JRC calculated the values with the E3 database. ANL provided verification for these values. The E3 Database model has higher gasification and synthesis emissions for the FT conversion process than the GREET (4.0 – 4.1 gCO_2e/MJ against 0.03 gCO_2e/MJ). Transportation distances in the two models are different. Emissions from feedstock production in the E3

model are calculated to be higher for poplar due to the higher fertilizer demand (5.1 g N, 1.4 gP_2O_5, and 3.7 gK_2O instead of 2.0 gN, 0.6 gP_2O_5, and 0.5 gK_2O).

The agreed default core LCA value for short rotation woody crops FT pathway is 12.2gCO_2e/MJ.

2.5 HERBACEOUS LIGNOCELLULOSIC ENERGY CROPS FT – [M]

This analysis includes switchgrass (*Panicum virgatum*) and miscanthus (*Miscanthus sinensis*) feedstocks. These crops are assumed to be grown for the purpose of harvesting biomass for fuel production, therefore the system boundary includes the crop growth step. The relevant lifecycle inventory data for these feedstocks are shown in Table 73 in the appendix. Table 12 shows the total GHG emissions for SAF produced form herbaceous energy crops using FT conversion.

Table 12: LCA results for herbaceous lignocellulosic energy crop FT pathways [gCO_2e/ MJ]

Feedstock	Data provider	Model	Feedstock cultivation and collection	Feedstock transportation	Feedstock-to- fuel conversion	Fuel transportation	Total	Midpoint value
Switchgrass	MIT	GREET	9.8	1.9	0	0.9	**12.7**	
	JRC	GREET	9.9	1.9	0	0.9	**12.7**	
	JRC	E3	6	1.9	3.2	0.3	**11.3**	**10.4**
Miscanthus	MIT	GREET	8.5	1.3	0	0.9	**10.7**	
	JRC	GREET	5.9	1.3	0	0.9	**8**	

MIT calculated the values using the GREET model, while JRC calculated the values with the E3 database. ANL provided verification of these values. The primary difference in the results is related to the higher gasification and synthesis emissions between the two models (3.2 gCO_2e/MJ for E3 against 0.03 gCO_2e/MJ). In addition, the feedstock and fuel transportation distances between the two models differ. Emissions from feedstock production in the E3 model are lower because of the lower fertilizer demand (0.3 gP_2O_5 and 0.0 gK_2O instead of 2.3 gP_2O_5 and 3.2 gK_2O).

The agreed default core LCA value for herbaceous lignocellulosic energy crops FT pathway is 10.4 g CO_2e/MJ.

2.6 FT MUNICIPAL SOLID WASTE – [W]

The FT process can be supplied with Municipal Solid Waste. Unsorted MSW is supposed to be diverted from landfill, therefore no upstream emissions are considered. Moreover, as covered in supplementary materials to the CORSIA implementation elements, credits for avoided emission from landfill (LEC) and additional material recovery (REC) are calculated.

One of the key differences in the lifecycle GHG emissions of MSW derived SAF is that CO_2 emissions from fuel combustion cannot be considered climate neutral, as it is for the biomass-derived SAF. CO_2 from biogenic carbon is supposed to be sequestered in biomass growth; that is not the case of the non-biogenic fractions of MSW feedstock. Therefore, some proportion of the CO_2 from MSW-derived SAF combustion is not entitled to be CO_2 neutral. For example, carbon in the plastic and rubber components of MSW feedstock is derived from fossil fuels, and therefore, CO_2 emissions from this part of the feedstock during fuel production and combustion should be counted against lifecycle GHG emissions. The default core LCA

emissions of SAF produced from MSW are calculated as a function of the non-biogenic content (NBC) of the MSW derived feedstock to account for this.

The lifecycle inventory data for this pathway are reported in Table 74 in the appendix. Table 13 shows the resulting lifecycle GHG emissions for SAF produced from MSW using FT conversion. LEC and REC credits are only included in the calculation of actual LCA emissions for MSW-derived SAF, which is not covered here but is addressed in the ICAO document "CORSIA Methodology for Calculating Actual Life Cycle Emissions Values".

Table 13: LCA results for MSW FT pathways [gCO_2e/MJ]

Feedstock	Data Provider	Model	Non-biogenic carbon (NBC) content	MSW transportation	MSW rejects transportation	Feedstock-to-fuel conversion	Fuel transportation	Fuel combustion	Total	Midpoint value
MSW	MIT	GREET lifecycle inventory (Suresh, 2016)	NBC ≤ 5%	3.9	0.4	2.5	0.9	1.8	**9.5**	**NBC*170.5+5.2**
			5% < NBC ≤ 10%	3.9	0.4	7.3	0.9	5.5	**18**	
			10% < NBC ≤ 15%	3.9	0.4	12.1	0.9	9.2	**26.5**	
			15% < NBC ≤ 20%	3.9	0.4	16.9	0.9	12.9	**35**	
			20% < NBC ≤ 25%	3.9	0.4	21.9	0.9	16.6	**43.6**	
			25% < NBC ≤ 30%	3.9	0.4	26.7	0.9	20.2	**52.1**	
			30% < NBC ≤ 35%	3.9	0.4	31.5	0.9	23.9	**60.6**	
			35% < NBC ≤ 40%	3.9	0.4	36.3	0.9	27.6	**69.1**	
			40% < NBC ≤ 45%	3.9	0.4	41.2	0.9	31.3	**77.7**	
			45% < NBC ≤ 50%	3.9	0.4	46.1	0.9	34.9	**86.2**	

The MSW results in Table 13 are given using non-biogenic carbon (NBC) increments of 5% per step. This generates results that fall within the threshold of 8.9 gCO_2e/MJ (8.5 gCO_2e/MJ among the various steps). LCA values for NBC greater than 50% are not shown because those results exceed 89.0 gCO_2e/MJ, and therefore they cannot be eligible under CORSIA. The differences between each of the NBC categories are apparent in the feedstock-to-fuel conversion and fuel combustion steps of the lifecycle, as anticipated. These results were verified by ANL.

The default core LCA value for MSW-derived is a function of the NBC content in the feedstock, being calculated as NBC*170.5+5.2, where NBC is the % of total C in the feedstock.

CHAPTER 3. **HYDROPROCESSED ESTERS AND FATTY ACIDS PATHWAYS**

3.1 PATHWAY DESCRIPTION

Hydroprocessed esters and fatty acids (HEFA) is a high maturity level and commercially available conversion technology. The HEFA pathway consists of the hydroprocessing of lipid feedstocks to upgrade them to drop-in jet fuels. The whole process consists of various catalytic reactions mechanisms, in the presence of hydrogen (Vásquez et al., 2017); a general process flow for HEFA pathways is shown in Figure 3.

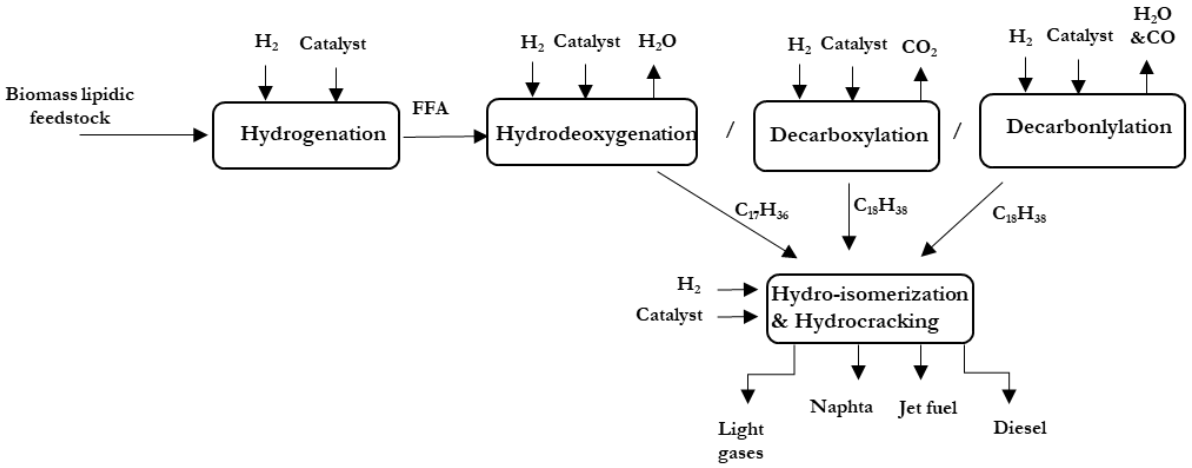

Figure 3: General process flow HEFA pathway

After raw feedstock pre-treatment (i.e. filtration, moisture reduction, etc.), the first process step consists of saturating the double bonds of the lipid chain by catalytic addition of hydrogen - generally known as hydrogenation. Hydrogen addition in a catalytic reactor is also used to remove the carbonyl group after hydrogenation and, simultaneously, to break the glycerol compound, forming propane and chains of free fatty acids (FFA). Then, the carboxylic acid group that remains attached to the FFA has to be removed to form straight paraffin chains; this can be removed through the following three ways:

- hydro-deoxygenation (HDO), in which it reacts with hydrogen to produce a hydrocarbon with the same number of carbon atoms of the fatty acid chain and two moles of water;
- decarboxylation (DCOX), which produces a hydrocarbon with one carbon atom less than the fatty acid chain and a mole of CO_2;
- and decarbonylation (DCO) route, which also produces a hydrocarbon with one carbon atom less, as well as a mole of CO and water.

Alternatively, non-hydrogen processes can be used: these alternative routes to deoxygenation are generally less attractive as they can consume a significant amount of the feedstock.

Other downstream processes are required to improve biofuel properties, namely: isomerization, cracking or cyclization (Alsabawi & Chen, 2012). HEFA-jet is co-produced with diesel for the road sector, and the relative share of the products can be adjusted to meet the market needs; similarly, the amount of the other process outputs (including water, gases such as H_2S, CO, CO_2, CH_4 and C_3H_8) are influenced by the feedstock type and operating conditions, including amongst others the catalyst used, the reaction temperature, and pressure. Industrial optimization has been focusing on developing low cost, robust catalysts for treating complex blends of feedstock.

This section describes the HEFA production pathways from several feedstocks, such as oily crops, oily residues like cooking oil or tallow, as well as co-products from the oil processing industry such as palm fatty acid distillate.

3.2 TALLOW HEFA – [B]

Tallow is produced through rendering of the animal by-products from cattle slaughtering (Seber et al., 2014). If tallow is considered to be a waste or by-product of the beef-production process, then the system boundary for LCA starts at the rendering stage. However, if tallow is considered to be a co-product of the beef production process, then the system boundary for the LCA is extended to include the cattle growth and slaughtering processes. The drivers of emissions identified for the waste HEFA pathways include the mix of sources for electricity generation, hydrogen production, and natural gas production. The lifecycle inventory data for these feedstocks are shown in Table 75 in the appendix. Table 14 shows the total GHG emissions for SAF produced from tallow using HEFA conversion for the two system boundaries considered. CAEP made the decision to consider tallow as a by-product of beef production, therefore a mid-point default core LCA values is only calculated for the case in which the system boundary begins as tallow rendering. The additional data given in Table 14 is for informational purposes only.

Table 14: LCA results for tallow HEFA pathways [gCO_2e/MJ]

Feedstock	Data provider	Model	Feedstock cultivation and collection	Feedstock transportation	Feedstock-to fuel conversion	Fuel transportation	Total	Midpoint value
Tallow (starts at tallow rendering)	MIT	GREET	13.9	0.5	10.5	0.5	**25.3**	**22.5**
	JRC	E3	9.9	0.4	9.3	0.3	**19.8**	
Tallow (starts at cattle growth)	MIT	GREET	310.5	0.4	9.4	0.6	**320.9**	**n/a**
	ANL	GREET	368.3	0.4	9.4	0.6	**378.6**	

MIT calculated the values using a modified GREET model created by Seber et al. (2014), while JRC calculated the values with the E3 database. ANL provided verification to these values. Results for emissions from transportation and HEFA conversion have been quite similar for GREET and E3 database. It is worth noting that that the feedstock production emissions can vary by an order of magnitude, depending on how the system boundary is drawn: a system boundary that considers tallow as a co-product, of beef production, would exclude this pathway from CORSIA definition of SAF. Therefore, tallow is an eligible feedstock only if it is considered as a by-product or a residue from cattle slaughtering.

The agreed default core LCA value for the tallow HEFA pathway is 22.5 gCO_2e/MJ.

3.3 USED COOKING OIL HEFA – [W]

Used cooking oil (UCO) includes vegetable oils recovered from food related activities (Seber et al., 2014). As UCO has been considered as a waste stream, the system boundary starts at the collection and processing

of the UCO. The lifecycle inventory data for this feedstock are shown in Table 76 in the appendix. Table 15 shows the total GHG emissions for SAF produced from UCO using HEFA conversion.

Table 15: LCA results for UCO HEFA pathway [gCO_2e/MJ]

Feedstock	Data Provider	Model	Feedstock cultivation and collection	Feedstock Transportation	Feedstock-to Fuel Conversion	Fuel Transportation	Total	Midpoint value
UCO	MIT	GREET	3.6	0.3	10.5	0.5	**14.8**	**13.9**
	JRC	E3	0	1.7	11	0.3	**13**	

MIT calculated the values using a modified GREET model created by Seber et al. (2014), while JRC calculated the values using the E3 database. ANL provided verification to these values. Emissions from transportation and HEFA conversion are quite similar between the GREET and E3 database. The feedstock production emissions vary, as the GREET model includes collecting and rendering of the UCO, while the E3 model does not. Despite this difference, the net discrepancy in emissions falls within the 8.9 gCO_2e/MJ threshold. The agreed default core LCA value for the UCO HEFA pathway is 13.9 gCO_2e/MJ.

3.4 PALM FATTY ACID DISTILLATE HEFA – [B]

Palm (*Elaeis guineensis*) fatty acid distillate (PFAD) is the collection of volatile fatty acids stripped from the crude palm oil (CPO) during the de-acidification and deodorization processes, to produce refined palm oil (RPO). Typical CPO contains 4-5% (wt.) PFAD. Although PFAD currently has a lower market value than RPO, it is widely used as feedstock for various products, such as laundry soap, animal feed, lubricants, and heating fuel (ICF International, 2015). Table 16 summarizes the process-by-process GHG emissions including feed production, feed transportation, feed-to-fuel conversion, and fuel transportation. The lifecycle inventory data are presented in Table 77 in the appendix.

The results for two cases are presented here. In the first, PFAD is considered a by-product of CPO production, and therefore upstream emissions from palm oil cultivation are not included. In the second, emissions from palm oil cultivation are included. In order to carry out the analysis in a manner consistent with CAEP-agreed upon methodology, the default core LCA value was calculated considering PFAD to be a by-product of CPO production, and upstream emissions were not included.

Table 16: LCA results for PFAD HEFA pathways [gCO_2e/MJ]

Feedstock	Data provider	Model	Feedstock cultivation and collection	Feedstock transportation	Feedstock-to fuel conversion	Fuel transportation	Total	Midpoint value
PFAD (starts at PFAD production)	ANL	GREET	6.6	3.2	14	0.5	**24.3**	**20.7**
	JRC	GREET	4.4	3.1	13.8	0.5	**21.8**	
	JRC	E3	Not provided	Not provided	9.2	0.3	**17.0***	
PFAD (starts at palm production)	ANL	GREET	18	3.2	14	0.5	**35.7**	**n/a**
	JRC	GREET	15.1	3.1	13.8	0.5	**32.6**	

*Note that this total was calculated using emissions for the feedstock production and transportation steps calculated in the GREET model using JRC provided lifecycle inventory data, in order to construct a complete pathway.

ANL calculated the values using the GREET model, while JRC calculated the values by the E3 model. University of Toronto acts as verifier. The results show that the HEFA conversion process is the main contributor of the GHGs, followed by palm farming. The palm oil mill effluent (POME) in this study is assumed to be stored in closed ponds. It is worth noting that the HEFA conversion process in the E3 database has lower GHG emissions than the HEFA process modelled by GREET. Upstream processes for the PFAD HEFA SAF pathway were not evaluated in the E3 database.

The agreed default core LCA value for the PFAD HEFA pathway is 20.7 gCO_2e/MJ.

3.5 CORN OIL HEFA – [B]

Corn oil in the core LCA study is defined as the oil extracted from the distillers dry grains and solubles (DDGS), in a dry mill ethanol plant. Today, corn oil is extracted from dry mill ethanol plants, and it is not edible, but historically, corn oil was a component of DDGS. The US is currently the world largest corn ethanol producer, and it is expected that most US dry mill ethanol plants practice corn oil extraction. However, the mass share of corn oil in the grain is usually less than 5%, and not all of the oil is recoverable, especially from DDGS (ICF International, 2015). Table 17 summarizes the step-by-step GHG emissions including feed production, feed transportation, feed-to-fuel conversion, and fuel transportation used for modeling this pathway. Emissions from the ethanol related processes (fermentation, DDGS separation) are separated from corn oil extraction from DDGS. The lifecycle inventory data is presented in Table 78 in the appendix.

Two different cases were initially considered for this pathway: the first considers corn oil to be a by-product of corn ethanol production, and therefore does not include upstream emissions from corn cultivation, harvesting and transportation (instead the system boundary begins at corn oil production); and the second considers corn oil to be a primary product, and includes emissions from these sources. Ultimately, CAEP agreed to treat corn oil as a by-product, and a mid-point value was calculated on that basis, as shown in Table 17. The data for the other case is displayed here for informational purposes only.

Table 17: LCA results for corn oil HEFA pathways [g CO_2e/MJ]

Feedstock	Data provider	Model	Feedstock cultivation and collection	Feedstock transportation	Feedstock to fuel conversion	Fuel transportation	Total	Midpoint value
Corn Oil (starts at corn oil production)	ANL	GREET	2.5	0.5	14	0.5	**17.5**	**17.2**
	JRC	GREET	2	0.5	13.8	0.5	**16.8**	
Corn Oil (starts at corn farming)	ANL	GREET	30.8	0.5	14	0.5	**45.9**	**n/a**
	JRC	GREET	30.6	0.5	13.8	0.5	**45.4**	
	JRC	E3	44.8		11	1	**56.8**	

ANL calculated the values using the GREET model, while JRC calculated the values using the E3 database tool. University of Toronto acted as verifier. In both models, the upstream emissions are allocated among corn ethanol, DDGS and corn oil using the energy-based allocation method; whereas emissions from the corn oil recovery are assigned only to corn oil. The results show that both corn farming and ethanol fermentation are the main contributors to the WTP GHGs, and that the E3 database has higher emissions for these two processes than GREET. The assumption that the corn oil HEFA pathways should begin at corn oil production, instead of corn grain cultivation, was agreed upon by CAEP. Therefore, the agreed default core LCA value for the corn oil HEFA pathway is 17.2 g CO_2e/MJ.

3.6 OIL CROPS HEFA – [M]

The feedstocks included in this section are the vegetable oils derived from oil crops, namely: soybean (*Glycine max*), rapeseed (*Brassica napus*), and camelina (*Camelina sativa*). The system boundary of the analysis consists of the feedstock production, feedstock transportation, oil extraction, oil transportation, HEFA conversion, as well as HEFA jet fuel transportation and distribution. Four world regions have been considered: the US, the EU, Canada, and Latin America.

The Argonne GREET model and JRC E3 database (E3db) have been used to simulate and verify the core LCA results of the aforementioned oil crops for the HEFA pathways. Key parameters, including energy consumption, the mix of electricity generation sources, nutrients for feedstock production and chemicals for conversion process (nitrogen, phosphate, potash, herbicide and insecticide), oil and meal yields, HEFA jet fuel and co-products yields, etc., of each region were provided by CAEP experts and applied to the simulation. Life cycle inventory (LCI) data associated with crop production, bio-oil extraction, and HEFA conversion is shown in the appendix in Table 79, Table 80, and Table 81, respectively. Note that organic solvent (n-hexane) method is the reference oil extraction method for all three oil crops. E3db has different transportation assumptions relative to GREET; additionally, E3db uses the NEXBTL HEFA conversion technology, whereas GREET uses Honeywell's UOP technology. These differences are reflected in the LCA results presented below.

The LCA results for the soybean HEFA pathway range between 37.7 and 43.0 gCO_2e/MJ, with an agreed final core LCA value of 40.4 gCO_2e/MJ (Table 18). Note that the JRC LCI data for soybean farming (Table 79) represents a weighted average of several sources (Brazil, US, Argentina, and EU) based on their fractions of soybean market in EU. In addition, soy oil extraction using solvents has lower emissions in the EU compared to other regions, because the EU data assumes greater process efficiency (Table 80).

Table 18: LCA results for soybean HEFA [g CO_2e/MJ]

Feedstock	Data source	Model	Cultivation	Feedstock transportation	Oil extraction	Oil transportation	Feedstock to fuel conversion	Fuel transportation	Total	Midpoint value
Soybean	US	GREET	17.9	1.1	7.3	0.7	14	0.5	**41.5**	**40.4**
	EU (BioGrace)	GREET	17.9	1.1	3.7	0.7	13.8	0.5	**37.7**	
	Latin America	GREET	19.5	1	7.7	0.7	13.5	0.5	**43**	
	EU (JRC)	GREET	19.1	1.1	4.1	0.7	14.1	0.5	**39.7**	
	EU (JRC)	E3db	20.6	2.3	3.3	3.3	11.5	0.3	**41.4**	

LCA results for rapeseed HEFA range between 45.0 and 49.7 gCO_2e/MJ, with a default core LCA value of 47.4 g CO_2e/MJ (Table 19). Note that the LCI for Canadian rapeseed farming (Table 79) represents a weighted average of three regions (Manitoba, Saskatchewan, and Alberta), based on their share on the total Canadian production.

Table 19: LCA results for rapeseed HEFA [gCO_2e /MJ]

Feedstock	Data source	Model	Cultivation	Feedstock transportation	Oil extraction	Oil transportation	Feedstock to fuel conversion	Fuel transportation	Total	Midpoint value
rapeseed	US	GREET	28	0.7	4.8	0.5	14	0.5	**48.5**	**47.4**
	EU (BioGrace)	GREET	29.7	0.8	4.5	0.5	13.8	0.5	**49.7**	
	Canada	GREET	24.8	0.7	4.7	0.5	13.9	0.5	**45.0**	
	EU (JRC)	GREET	30.1	0.7	3.5	0.5	14.1	0.5	**49.4**	
	EU (JRC)	E3db	31.4	0.3	3.1	0	11	0.3	**46.1**	

The default core LCA results for the camelina HEFA pathway range between 39.9 and 44.1 g CO_2e /MJ, thus with a final default core LCA value of 42.0 gCO_2e /MJ (Table 20). The nitrogen and phosphorus inputs of camelina farming in Canada are higher than other modelled regions, partially due to the assumption that this crop will be grown on marginal lands (Table 79). Note that camelina oil can also be extracted using a mechanical pressing method in small oil mills (typically with lower oil yields), which may affect LCA results.

Table 20: LCA results for camelina HEFA [gCO₂e /MJ]

Feedstock	Data source	Model	Cultivation	Feedstock transportation	Oil extraction	Oil transportation	Feedstock to fuel conversion	Fuel transportation	Total	Midpoint value
Camelina	US	GREET	23	0.9	2.9	0.5	14	0.5	**41.8**	**42.0**
	Canada	GREET	26.3	0.9	2.7	0.5	13.3	0.5	**44.1**	
	EU (JRC)	GREET	19.4	0.8	4.6	0.5	14.1	0.5	**39.9**	
	EU (JRC)	E3db	25	0	4.8	0.2	11	0.3	**41.3**	

3.7 PALM OIL HEFA – [M]

Two different pathways have been calculated for palm oil HEFA, as two options that can be considered for palm oil production. The main difference takes place at the oil mill in the oil extraction step, where methane represents the main emission released from the palm oil mill effluent (POME) treated in anaerobic ponds, with or without biogas recovery (further referred as methane capture). Today, only a small percentage of global palm oil production capacity in place includes methane capture, typically in the framework of Clean Development Mechanism (CDM) projects; nevertheless, methane capture has been recently identified by the Malaysian Palm Oil Board (MPOB) as one of the key 'entry points' for new palm oil extraction facilities. The total core LCA emissions resulting from the choice of one of these two production options at the oil mill diverge substantially more than the 10% of the aviation fuel baseline (8.9 gCO₂e /MJ), therefore two default core LCA values for palm oil HEFA are calculated and proposed.

The ANL GREET model and the JRC E3db have been used to calculate the default core LCA results. The lifecycle inventory data is presented in Table 77 (palm fruit farming) and Table 82 (palm HEFA processing) in the appendix. The comparison of core LCA results from these data sources is shown in Table 21.

Table 21: LCA results for palm oil HEFA [g CO₂e/MJ]

Conversion technology	Data source	Model	Cultivation	Feedstock transportation	Oil extraction	Oil transportation	Feedstock to fuel conversion (isomerization included)	Fuel transportation	Total	Midpoint value
HEFA with Methane Capture	JRC	E3db	19.8	1.3	4.7	4.6	9.3	0.3	**40**	**37.4**
	ANL	GREET	11.4	0.5	6	2.9	13.5	0.4	**34.7**	
HEFA without Methane Capture	JRC	E3db	19.8	1.3	27.8	4.6	9.3	0.3	**63.1**	**60.0**
	ANL	GREET	11.4	0.5	28.1	2.9	13.5	0.4	**56.9**	

Originally, some significant differences occurred between the two calculation tools, mainly due to divergent estimations of methane emissions from the liquid effluents. Taylor et al. (Taylor et al., 2014) was used as

common reference by ANL and JRC to align these emissions from open ponds; moreover, methane yield is calculated by averaging the values of six references. JRC uses input data published in 2011 by the Malaysian Palm Oil Board (MBOP) (Choo et al., 2011). In this reference, 85% of otherwise emitted methane is captured and destined to productive use: this estimate is on the high end of the possible range of values, which depends on the specific solution adopted and varying from biogas production plants to plastic foils covering the otherwise open pond for effluent treatment.

Following the European Commission stakeholder consultation on draft default values of September 2016, no comments were introduced with respect to input data and values for methane emissions for palm oil mill effluent (Edwards et al., 2017).

The remaining major difference between the two models, for the CAEP exercise, is in the cultivation step. Different assumptions have been used for defining the average percentage of peatland in use prior to January 2008 and December 2007, respectively, for the cultivation of palm, which are aligned to the different values in the respective regulatory frameworks.

Note that oil transportation from the mill to the HEFA conversion facility includes a trans-oceanic transportation of 8795 nautical miles in the case of European data. According to the federation representing the European Vegetable Oil and Protein meal Industry in Europe (FEDIOL), the 70% of palm oil imports is not refined palm oil (the commercial name is Crude Palm Oil, CPO) coming from Malaysia and Indonesia, with the remaining 30% entering Europe as refined palm oil (the commercial name is Refined Bleached and Deodorised, RBD) from the same countries. No palm oil is produced in Europe. Similarly, in GREET, it is assumed that the US imports palm oil mostly from Southeast Asia involving around 10000 nautical miles of palm oil transportation, which leads to comparable, although still significantly different, emissions associated with transportation step.

The agreed default core LCA value for palm oil HEFA with methane capture is 37.4 g CO_2e/MJ, while the value for palm oil HEFA without methane capture is 60.0 g CO_2e/MJ.

3.8 BRASSICA CARINATA HEFA – [M]

This section presents the *Brassica carinata* (hereafter carinata) HEFA pathway. The system boundary of the analysis consists of the carinata oil seeds production (carinata farming), carinata transportation, oil extraction, oil transportation, HEFA conversion, and HEFA jet fuel transportation and distribution. The Argonne GREET model was expanded to simulate and verify the core LCA results. Note that carinata is a primary summer crop in northern US and Canada (the so-called Northern Tier Regions). In the future, carinata as a winter cover crop in Southern Tier Regions such as the Southeast US could be considered, which could impact the core LCA results. Table 22 presents the default core LCA results for the carinata HEFA pathway, which was analyzed by ANL and verified by University of Toronto.

Table 22: LCA result for carinata HEFA pathway [g CO_2e/MJ]

Feedstock	Data source	Model	Cultivation	Feedstock transportation	Oil extraction	Oil transportation	Feedstock to fuel conversion	Fuel transportation	Total
Brassica Carinata	US /Canada	GREET	15.4	0.6	3.9	0.4	13.7	0.4	**34.4**

The ANL core LCA results are based on the HEFA pathways in GREET 2017, where parameters have been updated to use carinata specific inputs. Farming energy and fertilizer application rates collected from the

literature show significant variation as presented in Table 23. For the core LCA value, the cultivation data from Moeller et al. (2017) and Sieverding et al. (2016) have been used, as they are based on practical farming data in the northern US Great Plains. The values are similar to data from other studies, such as D'Avino et al. (2015), collected from Italy. For vegetable oil extraction, the mechanical and organic solvent (n-hexane) method has been considered, based upon existing soybean and rapeseed oil extraction process data. Natural gas, n-hexane, and electricity use for carinata oil extraction are from Rispoli (2014), leading to an estimated total energy use for oil extraction of 2.86 MJ/kg_{oil}. This is in line with previously estimations for rapeseed and camelina (3.06 and 2.00 MJ/kg oil, respectively). The HEFA conversion process for carinata is based on Han et al. (2013), and fuel yield data is from the maximum distillate case of Pearlson et al. (2011), which are the same assumptions of the other HEFA pathways.

Table 23: Farming energy and fertilizer use for brassica carinata

Data source	Region	Farming energy [kJ/ $kg_{dry\ seed}$]	N fertilizer [g/ $kg_{dry\ seed}$]	P fertilizer [g/ $kg_{dry\ seed}$]	K fertilizer [g/ $kg_{dry\ seed}$]
Moeller et al. (2017)/ Sieverding et al. (2016)	US Northern Plains	1729+	26.1‡	3.6‡	0.5‡
Rispoli (2014)	Canada	1163¶	55.8¶	10.8¶	14.5¶
D'Avino et al. (2015)	Italy	1351*	23.6‡	18.2‡	0‡

+ 79 kg of diesel/ha
* 83 L of diesel/ha
‡ conversion from /ha
¶ conversion from /ton oil

As shown in Table 22, the agreed default core LCA value for brassica carinata HEFA is 34.4 gCO_2e/MJ.

3.9 JATROPHA HEFA– [M]

CAEP experts reviewed the recent literature on jatropha in order to identify the most likely pathways for the use of jatropha by-products. The review identified a trend to utilize jatropha fruit as a whole, but there is no common practice on the specific utilization of jatropha by-products yet. This is due to the fact that jatropha is still a semi-wild plant, and its production is mostly at small scale.

Hasselt University researchers reviewed the recent literature on jatropha to obtain information on practices regarding the use of by-products from the oil extraction step. Two papers on optimum sustainable use of jatropha fruit by Alherbawi et al. (2021a, 2021b) proposed multiple alternatives. Using Aspen Plus modelling, and mathematical optimization methods, they evaluated the most efficient pathways for jatropha by-products (Alherbawi et al. 2021a). Considering the net energy use, global warming potential (GWP), water footprint, and net food output, they claim that the seed cake is best utilized as fertilizer. They also claim that fertilizer production can contribute to the food sector with the highest possible food equivalent quantity as compared to detoxification. Seed cake can also be processed for energy production by pyrolysis and anaerobic digestion. Husk and shell could be used for energy through simultaneous saccharification and fermentation (SSF), pyrolysis, anaerobic digestion, or incineration. In their second paper they propose an integrated pathway for jet fuel production utilizing all parts of the jatropha fruit (Alherbawi et al. 2021b). They obtain jet fuel from the oil through hydroprocessing, and they utilize the by-products in order to get jet fuel via Fischer-Tropsch synthesis. Their proposed pathway yields high amounts of jet fuel with a minimum selling price lower than conventional jet fuel, but with high GWP.

Another review on the use of jatropha by-products concludes that through pyrolysis and gasification enough energy as heat or electricity can be produced to cover the energy demand of a biodiesel plant (Piloto-Rodriguez et al. 2020). Concerning pyrolysis, the studies mostly focus on the use of jatropha seed cake as feed. However, they also mention that further research is necessary to increase the yield of bio-oil in case of pyrolysis.

An article by Jingura et al (2018) concentrates on jatropha seed cake and classifies the product streams into three main groups: fertilizer, energy carrier, and industrial chemical products. The energy carrier consists of briquettes, bioethanol, biogas, pyrolytic products, and syngas. They claim that the most promising among these are biogas and briquettes. They also state that the use of the cake as fertilizer is widely practiced. Finally, they summarize by adding work on industrial chemicals such as protein (for animal feed) and biocomposites is underway.

Finally, a review paper by Navarro-Pineda et al. (2016) states the importance of using jatropha plant as a whole, while searching for ways to increase the seed yield and profits from this crop.

Following this literature review, CAEP experts calculated a set of GHG emission values for three scenarios (Figure 4). It is assumed that jatropha meal is used as fertilizer (Scenario 1), as fodder after a detoxification step (Scenario 2) or combusted for electricity production (Scenario 3), while the shells and husks from the process are assumed to be combusted for electricity generation in all scenarios.

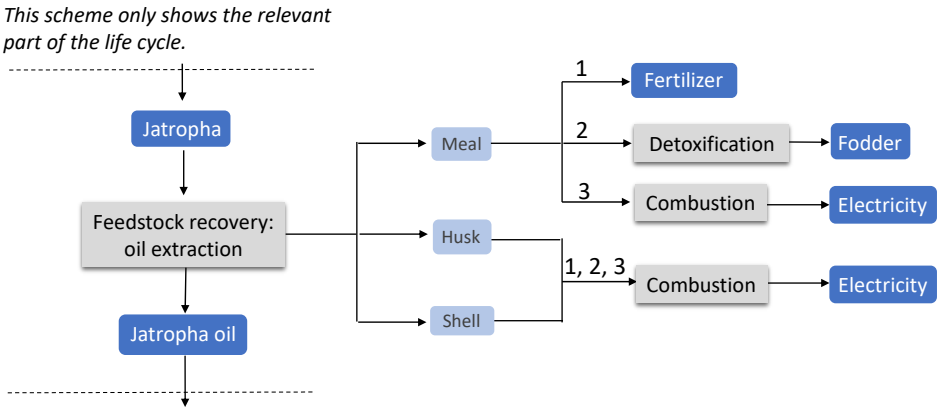

Figure 4: Analyzed pathways for the jatropha by-products

In Scenario 1 jatropha meal is assumed to be used directly as fertilizer, while husk and shell are combusted for electricity generation. Jatropha seed cake and kernel meal have been shown to have comparable nutrient content to other organic fertilizers such as chicken and cow manure (Jingura et al. 2018) with a chemical composition of 4.4-6.5% of nitrogen, 2.1-3% of phosphorus, and 0.9-1.7% of potassium (Achten et al. 2008). Literature examples demonstrate seed cake use as fertilizer for tomatoes, wheat and jatropha (Mambo et al. 2018, Chaturvedi et al. 2012, Ghosh et al. 2012). It has been reported that the toxins in the cake are biodegradable, and they decompose within a few days in soil (Achten et al. 2008).

Scenario 2 considers the use of the meal as fodder, after a detoxification step, while husk and shell are combusted for electricity generation. Jatropha meal is rich in protein (crude protein content: 55% vs soybean meal: 45%), however it contains toxic compounds that limits its use as animal feed. Most of these toxic components (trypsin inhibitor, lectins, tannins, etc.) can be removed by steam treatment (Makkar et al 1997). However, phorbol esters (PE), which are the main source of toxicity in jatropha meal, are not heat labile. Different methods have been proposed for the removal of PEs from jatropha meal (Makkar et al.

2016). Ethanol extraction of the meal was chosen for this analysis, since using polar solvents (ethanol or methanol) is one of the fastest, and most effective methods for PE removal (Gomes et al. 2018). Utilities for the detoxification process are adapted from the techno-economic evaluation of Chico et al., and included within inputs of the oil extraction step since the utilization of the meal as fodder would favor the production of jatropha oil. Detoxified jatropha meal was used as an animal feed ingredient for fish, pigs, and lambs with success (Li et al. 2018, Patil et al. 2015, Wang et al. 2011).

Scenario 3 assumes all the by-products are combusted for electricity production. Assumptions from Stratton et al. (2010) have been used for calculating the electricity generation efficiency in GREET.

The US and India have been considered as world regions for the analysis, and regional electricity mixes were used for each country. The life cycle inventory data are presented from Table 25 through Table 29.

The life cycle inventory data for feedstock cultivation, fuel conversion and transportation steps are identical for all scenarios. However, the inputs/outputs for the oil extraction step differ for each of them (Table 26). In Scenario 2, utilities from the detoxification step are added as inputs, while in Scenario 3 there is no meal output as all by-products are combusted for electricity generation. The electricity inputs are included in brackets, since they are subtracted from the overall electricity generated within the system.

Hasselt University calculated Core LCA values using the GREET model, and ANL verified the calculations. Emissions are distributed among the co-products from the oil extraction step based on their energy contents, in other words allocation factors. These allocation factors differ for each scenario, and applied to each life cycle step prior to the point where these products come out. This is the reason why feedstock cultivation, transportation and oil extraction steps differ from each other for these scenarios, while the emissions after the oil extraction step are identical within each country. The emissions between the US and India differ due to the electricity generation mix used for these countries (Table 28). In India electricity is mostly generated from coal, therefore emissions are higher per MJ of electricity.

Core LCA values for these scenarios are presented in Table 24. The LCA results for the jatropha HEFA pathway range between 42.1 and 50.1 gCO_2e/MJ.

Given that the ILUC values (see Table 105) for scenarios 1 and 3 differ by less than 8.9 gCO2/MJ, the core LCA values for scenario 1 and 3 were combined. The difference between scenarios 1 and 2 is higher than 8.9 gCO2e/MJ, and therefore these core CLA values were not combined. Note that ILUC calculations are only based on the India case. As a result, two core LCA values were computed based on the India data, defined as the mid-point of the range of emissions of scenario 1 and 3 (Jatropha oil HEFA – meal used as fertilizer or electricity input), and the estimated value for scenario 2 (Jatropha oil HEFA – meal used as animal feed after detoxification), respectively. This yields a default core LCA value of 46.9 g CO2e/MJ for scenario 1 and 3, and 46.8 g CO2e/MJ for scenario 2.

Table 24: CLCA values for different scenarios of the jatropha HEFA pathway (in gCO2e/MJ)

Scenario	Region	Feedstock cultivation	Feedstock transportation	Oil extraction	Oil transportation	Jet fuel production	Jet fuel transportation	Total emissions
1	US	24.9	0.71	3.66	0.38	12.1	0.37	42.1
	India	25.9	0.72	3.67	0.38	12.5	0.38	43.6
2	US	27.3	0.78	4.26	0.38	12.1	0.37	45.2
	India	28.4	0.79	4.29	0.38	12.5	0.38	46.8
3	US	29.8	0.85	4.87	0.38	12.1	0.37	48.3

	India	31.0	0.86	4.88	0.38	12.5	0.38	50.1

A scenario where all by-products from the oil extraction step are discarded was initially also considered. However, given that the literature review indicated a desire to utilize the whole fruit the discards-case, this option was not pursued further.

Table 25: Agricultural inputs for jatropha feedstock

	Jatropha, per dry kg
Data source	Stratton et al. 2010
Total N (g)	36.6
P_2O_5 (g)	14.0
K_2O (g)	40.2
Diesel (MJ)	1.50

Table 26: Inputs for the jatropha oil extraction step for all scenarios

	per kg jatropha oil (39.5 MJ)	Stratton et al. 2010, Chico et al. 2013		
Scenario		1	2	3
Inputs	Feedstock (g, dry)	2767	2767	2767
	NG (MJ)	1.80	1.80	1.80
	N-Hexane (MJ)	0.18	0.18	0.18
	Electricity (MJ)	(0.70)	(3.44)	(0.70)
	Ethanol (MJ)	-	0.26	-
Outputs	Meal (MJ)	12.9	10.3	-
	Electricity (MJ)	8.43	5.69	11.3

Table 27: Inputs for HEFA processing of jatropha oil

	per MJ jet fuel	
Data source		GREET (US)
Inputs	Feedstock (g oil)	28.9
	NG (MJ)	0.082
	H_2 (MJ)	0.092
	Electricity (MJ)	0.0046
Outputs	Co-product, propane mix (MJ)	0.074
	Co-product, naphtha (MJ)	0.023

Table 28: Carbon Intensity (C.I.) of regional electricity generation mixes

	US (%)[4]	**India[5] (%)**
C.I (gCO_{2e}/MJ)	125	218

Table 29: Inputs for transportation of feedstock and fuels (Elgowainy et al. 2012)

Jatropha Transportation	
Distance (km)	161; 644
Method	Heavy-duty truck; Train
Share (%)	80; 20
Jatropha Oil Transportation	
Distance (km)	129; 1127
Method	Heavy-duty truck; Train
Share (%)	67; 33
Jet Fuel Transportation	
Distance (km)	837; 1287; 80
Method	Barge; Rail; Heavy-duty truck
Share (%)	8; 29; 63
Jet Fuel Distribution	
Distance (km)	48
Method	Heavy-duty truck

3.10 Beef Tallow. Poultry Fat, Lard fat, and Mixed Animal Fats HEFA [B]

3.10.1 Introduction

This Section describes the data, analysis and results of the modelling of four HEFA pathways from different animal fats. HEFA from beef tallow, HEFA from poultry fat, HEFA from lard fat, and HEFA from mixed animal fats.

While the latter three pathways are new pathways within CORSIA, the former is an update to an existing value previously included in the first edition of the ICAO document "CORSIA default life cycle values for

[4] GREET 2020.

[5] International Energy Agency 2020.

CORSIA eligible fuels". This update is necessary due to the addition of a lifecycle step and higher fidelity modelling of the hydrogen requirements.

Two modelling teams from the European Commission Joint Research Centre (JRC) and University of Hasselt (UH), have been working on the three animal fats feedstock from the slaughterhouses, and the mixed animal fats. Both teams have been working independently with different tools and sources but have been in contact during the entire modelling to discuss the modelling of the pathways. Core LCA emissions from beef tallow-, poultry fat-, and lard fat-based HEFA fuels have been estimated based on literature data and inputs from the industry. Then, the production of these fats (in %) has been assessed using available literature and statistical data. The individual emissions from the three individual HEFA fuels from the animal species have been multiplied by the corresponding production percentages and the results were added up to yield an emissions value for mixed animal fats from slaughterhouse output-HEFA. The core LCA default value is then calculated as the mid-point of the variation between the results of the two modelling teams, for each of the four pathways considered. Given that the feedstocks considered are by-product of the meat producing industry and, therefore, no emissions from induced land-use change are taken into account, the core LCA value is identical to the default value for this pathway.

CAEP FTG experts from the Technical University of Turin (Polito) acted as a verifier between the two modelling teams, aiming at raising the potential issues among the models and highlighting some potential room for reconciliation.

3.10.2 Data and analysis

The system boundaries of the animal fats-based SAF production include the following steps: (1) feedstock transportation from the slaughterhouse to rendering facility, (2) rendering plant, (3) transportation of the rendered products to the fuel production facility, (4) fuel production, and (5) fuel transportation. Compared to the existing analysis for tallow HEFA within CORSIA, step 1 was added against the background that the transportation step from the slaughterhouse to the rendering facility should be part of the fuel lifecycle.

JRC compiled data from the EFPRA (European Fats Processors and Renderers Association) for collection of the slaughterhouses outputs, energy and utilities inputs at the rendering plant, and yield of the rendering among the co-products for the three animal species. Ecoinvent 3.8 database with the system model "allocation, cut-off by classification" is the database used by default. The approach behind relies on that primary production of materials is always allocated to the primary user of a material. When possible, the processes used are European ones representative of the 2021 market. In Europe, three categories of animal by-products exist. Category 1 refers to specified risk materials, transmissible spongiform encephalopathy suspected animals, pet, zoo and experimental animals. Category 2 refers to fallen stock (non ruminants) digestive tract content. For these two categories 1 & 2, hygenisation stage is mandatory based on *Reg. (EC) No 1069/2009* repealing *Reg. (EC) No 1774/2002* (Animal by-products Regulation[12]) and those two slaughterhouse outputs have negative economic values before the hygenisation stage. Then, this hygenisation stage is excluded from the system boundaries for categories 1 & 2 of animal by-products (ABP) in the JRC modelling.

UH compiled US-specific data from USDA (United States Department of Agriculture) for the shares of different animal fats. Rendering energy requirements were estimated as a function of moisture content considering the correlation curve from Lopez (2010) and rendering product ratios for lard from Hicks et al. (2016).[2] The fuel production step and transportation assumptions are from the GREET model, with the exception of the mode of transportation assumption for the transportation to the rendering facility which is taken from the data from the EU rendering industry. Hydrogen requirements for the fuel production step

were augmented based on the fatty acid composition of the different animal fats as from Lopez (2010) and Tolda-Reig et al. (2020).

Table 30 summarizes the general assumptions to estimate the core LCA emissions of animal fats-based SAF production of the two.

Table 30: General assumptions to estimate the core LCA emissions of HEFA fuels from mixed animal fats

Stage	JRC assumptions	UH assumptions
Feedstock transportation to the rendering facility	Market for the transport of goods in Europe, including different lorry classes as well as EURO classes. 64% of trucks > 32 metric tons (average freight load of 16.0 tons) and 36% of trucks of 16-32 metric tons (average freight load of 5.8 tons). Distances are different depending on the animal species: 237, 352, and 319 km respectively for lard, poultry, and beef.	The default transportation distance from the GREET model was used (805 km). Following JRC data, Feedstock was assumed to be transported by truck only (25-ton).
Rendering	Energy requirements depending on the animal species and the ABP categories have been estimated based on EFPRA data.	Energy requirements are estimated as a function of moisture content considering the correlation curve from Lopez 2010[1] and rendering product ratios for lard from Hicks et al. 2016[2].
Rendered product transportation to the fuel production facility	According to default data from CORSIA methodology document, the feedstock is assumed to be transported 150 km by a default average weighted truck in the geography of Europe.	According to default data from the GREET model, 20% of the feedstock was assumed to be transported 644 km by rail and the remaining fraction 161 km by truck (25-ton).
Fuel production	Hydrogen requirements for beef tallow, poultry fat, and lard fat were adjusted considering those for soybean oil based on Capaz et al.[10]. Fatty acid composition of animal fats based on INRA CIRAD AFZ feed tables. Other energy and utilities inputs are equivalent as in the last calculation from CORSIA.[11]	Hydrogen requirements for tallow, poultry fat, and lard were adjusted compared to those for soybean hydrogen consumption based on the molar stoichiometry of the hydroprocessing reactions. Fatty acid composition of animal fats based on Other energy and utilities inputs are equivalent as in the last calculation from CORSIA.[11]
Fuel transportation	According to CORSIA,[11] 250 km are covered by rail.	According to default data from the GREET model, 63%, 8%, and 29% of the fuel were assumed to be transported 80 km by truck, 837 km by barge, and 1288 km by rail, respectively.
Mixed animal fats	According to EFPRA for by-products shares across species, Eurostat 2023 data for European carcass weight slaughtered in slaughterhouses, and Hicks et al[2] for fats share on animals' by-products; beef tallow, poultry fat, and lard fat respectively account for 14%, 13%, and 73%.	According to data from the USDA,[3] tallow, poultry fat, and lard compromise 56%, 23%, and 21% of animal fat production in the USA, respectively.

The feedstocks involved in this pathway include slaughterhouse outputs from beef, poultry, and pigs' slaughtering. These feedstocks are assumed to have zero GHG emissions associated with them as they are considered a by-product derived from the slaughterhouses.

The rendering stage refers to the heat treatment of fat, bone, offal, and related material derived from carcasses of livestock. In this process, the slaughterhouse outputs are crushed and subsequently heated inside a cooking chamber by means of indirect steam, obtaining rendered lipids, Meat and Bone Meal (MBM), and water. Table 31 summarizes the inputs and outputs of the rendering process.

JRC assumes that the hygenisation part is excluded out of the system boundaries for the categories 1[6] & 2[7] for animal by-products based on the European context.[12] Indeed, hygenisation stage is mandatory in Europe for categories 1 & 2 products and thus the economic value of those slaughterhouse outputs is negative before the hygenisation. It is assumed that categories 1 & 2 have a 27.4% share among the European slaughterhouse outputs based on EFPRA 2021 data. The required process as stated in the European Parliament and Council[12] is to elevate the temperature at 133°C during 20 minutes at 3 bars pressure. The initial temperature is supposed equal to 5°C to allow the storage of organic matters. As the waste thermal capacity is not known, the water thermal capacity has been taken into account as the worst-case scenario. Water has one of the highest thermal capacity. It results into 2.73 MJ to elevate the temperature from 5°C to 133°C at 3 bars pressure and to evaporate the water. The efficiency has been assumed equal to 95%. Heat and electricity consumptions are based on EFPRA data as well as transportation distances from the slaughterhouses to the rendering plant. Each animal species has its own inputs.

UH assumes that energy requirements for the rendering depend on moisture content. Lopez et al. 2010[1] provides a correlation curve of rendered products vs energy use corresponding to the amount of water removal from animal by-products of cattle and chicken. Accordingly, rendering of chicken by-products consumed more energy than cattle by-products due to higher water content (60% for chicken vs 49% for cattle by-products). Meat and bone meal ratio, with respect to fats, produced from rendering was similar for the two feedstocks. Using the correlation curve from Lopez et al. 2010[1] and rendering product ratios for lard from Hicks et al. 2016[2], rendering inputs for lard were estimated. In order to assess the amount of animal fat production in the world, WSU made use of data from USD[9] to come up with conversion coefficients for the amount of animal fat production per animal in the U.S. These conversion coefficients are then applied to OECD-FAO worldwide meat production data to find the fat production worldwide (Table 35 and Table 36). The production share was calculated for each type of animal fat.

Table 31: Inputs and outputs of the rendering of animal by-products. Data expressed per kg of rendered product, aka unrefined fat

Parameter	Unit	Beef		Poultry		Lard	
		JRC[8]	UH[1,4]	JRC[4]	UH[1]	JRC[4]	UH[1,2]
Inputs							
Slaughterhouse waste	kg	6.20	3.6	8.46	4.8	7.05	3.4
Light Fuel oil for steam generation	MJ	0	2.22	0	3.45	0	2.39
Diesel	MJ	0	0.02	0	0.02	0	0.02
Heat, from natural gas	MJ	13.88	3.47	10.42	5.36	7.62	3.75
Electricity low voltage	MJ	1.62	1.04	1.73	1.1	1.26	0.85
Animal fat	MJ	0	1.82	0	2.81	0	1.97

[6] Category 1 refers to specified risk materials, transmissible spongiform encephalopathy suspected animals, pet, zoo and experimental animals

[7] Category 2 refers to fallen stock (non ruminants) digestive tract content

[8] Data sources are based on European Parliament and Council,[12] and EFPRA data

Outputs							
Rendered product (as unrefined fat)	kg	1.00	1.00	1.00	1.00	1.00	1.00
MBM	kg	1.54	0.82	1.70	0.91	1.75	0.49
Water	kg		1.75		2.88		1.93
Other							
Total energy input	MJ	15.50	8.56	12.1	12.7	8.88	8.98
Moisture content	—		49%		60%		57%
Lower heating value of animal fat	MJ/kg	38.8[9]	40.1	38.8[9]	39.5	38.8[9]	40.1
Lower heating value of MBM	MJ/kg	17.7[9]	17.0	17.7[9]	17.0	17.7[9]	17.0
Allocation to fat (energy criteria)	—	58.4%	74%	55.9%	72%	55.4%	83%
Production share (over total animal fat production)	—		56%		23%		21%

The fuel production stage refers to the transformation of rendered product into SAF, which requires the upgrading of the feedstock, and its subsequent hydrotreatment and isomerization. Table 32 summarizes the inputs and outputs of the transformation of animal fats into HEFA fuels.

Table 32: Inputs and outputs of the transformation of unrefined animal fats into HEFA fuels. Data expressed per kg of jet fuel

Parameter	Unit	Beef		Poultry		Lard	
		JRC[10]	UH[1,4]	JRC[6]	UH[1]	JRC[6]	UH[1,2]
Inputs							
Unrefined animal fat	kg	1.23	1.27	1.23	1.27	1.23	1.27
Phosphoric acid	g	0.75	0	0.75	0	0.75	0
Sodium hydroxide	g	1.20	0	1.20	0	1.20	0
Natural gas	MJ	2.6	3.60	2.60	3.60	2.60	3.60
Electricity low voltage	MJ	0.28	0.20	0.28	0.20	0.28	0.20
Hydrogen	MJ	4.80	2.74	5.99	3.29	5.31	3.09
Outputs							
Jet fuel	kg	1.00	1.00	1.00	1.00	1.00	1.00
Co-product	MJ	0.48	0.10	0.48	0.10	0.48	0.10
Propane fuel mix	kg	0	0.074	0	0.074	0	0.074
Naphta	kg	0	0.023	0	0.023	0	0.023
Other							
Total energy input	MJ	7.68	6.54	8.87	7.09	8.19	6.89

[9] Dry, compiled from Phyllis database

[10] Data sources are based on Li, Mupondwa and Tabil,[15], IFEU study, INRAE CIRAD AFZ feed tables, and PlasticsEurope eco-profiles.[16]

Next to the hydrotreatment, JRC assumes that 50% of the hydrotreated fuel is isomerised. This is a common stage for the three animal fats categories. Isomerisation process is based on Hedden and Jess, 1994[13] (Hedden and Jess, 1994) summarized in Table 33. UH included the standard GREET assumptions for the fuel production step, and isomerization-related inputs are included therefore in Table 32.

Table 33: Inputs for the isomerisation process, per kg of jet fuel. For UH, isomerization inputs are included in Table 32

Parameter	Unit	JRC[11]
Inputs		
Hydrotreated fuel	kg	1.00
Heat from steam	MJ	2.60
Sodium hydroxide	g	1.20
Electricity low voltage	MJ	0.26
Hydrogen	mg	6.00
Outputs		
Jet fuel	kg	1.00
Other		
Total energy input	MJ	2.86

JRC assumes that after the rendering plant, the unrefined fat is transported with an averaged European truck over 150 km to the hydrotreatment plant. The hydrotreatment is based on NexBTL process (IFEU by order of Neste Oil, 2006) with a European configuration and low efficiency, running with rapeseed oil feedstock. Based on (Li et al., 2018), hydrogen consumption has been adjusted to the three unrefined oil as the higher the unsaturated fatty acids are, the higher the H2 consumption is. The composition of the studied feedstock is based on INRAE-CIRAD-AFZ feed tables. Hydrogen from SMR process comes from Industry 2.0 database representing the data calculated by PlasticsEurope[16] and available as an eco-profile. Hydrotreated fuel bears 98.9% of the environmental impacts of the process, based on an energetic allocation. The final fuel is assumed to be transported by train over 250 km.

UH assumes that hydrogen consumption of tallow during upgrading to HEFA fuel might differ from poultry fat and lard since they have different fatty acid compositions. As seen in Table 37 at the end of Appendix A, tallow contains more saturated fatty acids than poultry fat and lard which would result in less hydrogen consumption during the hydrogenation phase of upgrading to HEFA fuels. Table 37 also shows the fatty acid content for soybean which is highly unsaturated compared to tallow. Inputs for the upgrading of tallow to HEFA fuel in CORSIA is from Seber et al. 2014. Here, data from Pearlson 2011[6] on soybean HEFA was used, and hydrogen consumption for tallow has not been adjusted. 27 kg of hydrogen gas was used per MT of soybean oil and the same was assumed for tallow. In an attempt to update the hydrogen consumption for tallow, and provide inputs for poultry fat and lard, the molar stoichiometry of the hydroprocessing reactions were utilized.[7] For this, reaction molar stoichiometry in the reactor (from a combination of reactions from unsaturated triglycerides to saturated ones, propane loss, and decarboxylation) was calculated for soybean oil, tallow, poultry fat, and lard. Then, using the hydrogen input for soybean oil from CORSIA Supporting information (Table 81 in the Supporting Information), the amount of hydrogen was adjusted for tallow,

[11] Data sources are based on Hedden and Jess.[13]

poultry fat, and lard. Natural gas and electricity as utility inputs were kept the same as in Table 81 from CORSIA.

3.10.3 Results

Table 34 summarizes the estimated GHG emissions from animal fat-based SAF production from the two modelling teams by lifecycle step.

The variation between the JRC and UH emission estimates range from 1.70g CO_{2e}/MJ SAF (in case of poultry fat HEFA) to 4.32 g (for lard fat HEFA), which is less than the 8.9g variation that defines the boundary of a pathway within CORSIA. Therefore, Table 34 also contains the proposed default values for the three separate HEFA fuels, and for the mixed animal fat-based SAF production computed as the weighted average of GHG emission from each specific pathway. The default values are defined by the mid-point value of the variation in the calculated lifecycle emissions from the modelling teams.

As a result of the analysis, the following default values were obtained:

Beef tallow HEFA: 29.7 gCO_{2e}/MJ

Poultry fat HEFA: 33.7 gCO2e/MJ

Lard fat HEFA: 27.8 gCO2e/MJ

Mixed animal fats HEFA: 28.6 gCO2e/MJ

Table 34: Estimated GHG emissions from animal fat-based SAF production. Data in g CO2e/MJSAF

Stage	Beef Tallow-HEFA		Poultry Fat-HEFA		Lard fat-HEFA		Mixed animal fats HEFA	
	JRC	UH	JRC	UH	JRC	UH	JRC	UH
Production share	14%	56%	13%	23%	73%	21%	—	—
Transport to the rendering facility	4.03	5.80	6.07	7.50	3.40	6.13	3.85	6.26
Rendering	15.81	10.60	12.97	14.80	9.50	12.20	10.83	11.90
Transport to the SAF facility	0.45	0.35	0.45	0.35	0.45	0.35	0.45	0.35
SAF production	11.34	10.50	13.21	11.50	12.15	10.90	12.18	10.81
SAF distribution	0.16	0.40	0.16	0.40	0.16	0.40	0.16	0.40
Total	***31.78***	***27.65***	***32.85***	***34.55***	***25.66***	***29.98***	***27.46***	***29.73***
Final default value	***29.7***		***33.7***		***27.8***		***28.6***	

When explaining the differences in results, the following observations can be made:

- Concerning the transport to the rendering facility, JRC assumes the use of a representative market share of trucks in Europe encompassing several types of trucks (size): UH assumes the use of heavy trucks only. Moreover, transportation distances differ in the two world regions considered.

- JRC assumes higher energy requirements during the rendering stage, possibly due to a stronger animal by-products regulation in Europe with regard to the process and use. Related to the different

scope and categorization of animal by-products, the feedstock as slaughterhouse outputs appear to be rather a waste and thus with a lower fat content as already valorized for other purposes. This leads to higher GHG emissions than those of UH (Table 31).

- For the fuel production stage, one difference in assumptions is the hydrogen requirement that have been assumed for the different rendered fats.

Table 35: Production coefficients for animal fats calculated using data from reference 8, UH analysis

Production Coefficients for Animal Fats,		
Apply to FAO Meat production values		
	Production Coefficient (fat/meat) Animal	
Tallow		
Edible	0.037	All Cattle
Inedible	0.141	All Cattle
Technical	0.048	All Cattle
Lard & Grease		
Lard	0.010	Pork
Choice White Grease	0.045	Pork
Poultry Fat		
Total	0.041	Poultry
Sheep Tallow		
Total	0.129	Sheep

Table 36: Worldwide production of animal fats estimated[8,9]

Parameter	Average 2019-21
Beef (inedible)	13,299,099
Beef (edible)	2,593,429
Swine (inedible)	4,986,178
Swine (edible)	1,160,856
Sheep (edible and inedible)	2,020,305
Poultry	5,467,994
TOTAL	29,527,861
TOTAL, million MT (no sheep)	27.5
TOTAL inedible*, million MT (no sheep)	23.8

Table 37: Fatty acid compositions of animal fats assumed in the UH analysis, soybean oil for comparison purposes

Fatty acid (FA)	Tallow[1]	Poultry fat[1]	Lard[5]	Soybean oil[6]
C14:0	3.1	1.1	1.6	0.12

C16:0	25.2	22.9	25.1	11.4
C16:1	3.7	7.8	2.8	0.14
C18:0	18.5	5.4	12.6	5.3
C18:1	44.5	41.5	36.5	35.4
C18:2	3.0	18.2	16.5	39.7
C18:3	0.7	0.9	1.1	5.4
C20:4			0.3	
C22:5			0.2	
Others	1.3	2.2	3.3	2.54
∑Saturated	46.8	29.4	39.3	16.8
∑Unsaturated	51.9	68.4	57.4	80.6
Unsaturated/Saturated	1.11	2.33	1.46	4.79

3.10.4 References

1. [1] Lopez et al. 2010, Ind. Eng. Chem Res., 49, 2419-2432.
2. [2] Hicks, T.et al. 2016 Meat Industry Protein By-Products: Sources and Characteristics in "Protein By-products: Transformation from Environmental Burden into Value-Added Products.
3. [3] a) Poultry Slaughter 2021 Summary (February 2022) USDA, National Agricultural Statistics Service;
4. b) Livestock Slaughter 2021 Summary (April 2022) USDA, National Agricultural Statistics Service;
5. c) Fats and Oils: Oilseed Crushings, Production, Consumption and Stocks 2021 Summary (March 2022) USDA, National Agricultural Statistics Service.
6. [4] Chen. R. et al. 2017 Updates on the Energy Consumption of the Beef Tallow Rendering Process in GREET (October 9, 2017).
7. [5] Toldra-Reig et al. 2020, Appl. Sci., 10, 3644.
8. [6] Pearlson, M. 2011, M.S.Thesis: A Techno-Economic and Environmental Assessment of Hydroprocessed Renewable Distillate Fuels.
9. [7] Li, X. et al. Bioresource Technology 249 (2018) 196–205.
10. [8] a) Poultry Slaughter 2021 Summary (February 2022) USDA, National Agricultural Statistics Service;
11. b) Livestock Slaughter 2021 Summary (April 2022) USDA, National Agricultural Statistics Service;
12. c) Fats and Oils: Oilseed Crushings, Production, Consumption and Stocks 2021 Summary (March 2022) USDA, National Agricultural Statistics Service.
13. [9] OECD-FAO Agricultural Outlook 2022-2031 - © OECD 2022
14. [10] Capaz, R.S. et al. (2021) 'The carbon footprint of alternative jet fuels produced in Brazil: exploring different approaches', Resources, Conservation and Recycling, 166(October 2020), p. 105260. doi:10.1016/j.resconrec.2020.105260.
15. [11] CORSIA ICAO (2022) CORSIA Supporting Document - CORSIA Eligible Fuels-Life Cycle Assessment Methodology - Version 5.
16. [12] European Parliament and Council (2009) Regulation (EC) No 1069/2009, Official Journal of the European Union.
17. [13] Hedden, K. and Jess, A. (1994) IKARUS Project.
18. [15] Li, X., Mupondwa, E. and Tabil, L. (2018) 'Technoeconomic analysis of biojet fuel production from camelina at commercial scale: Case of Canadian Prairies', Bioresource Technology, 249(September 2017), pp. 196–205. doi:10.1016/j.biortech.2017.09.183.
19. [16] PlasticsEurope (2005) Eco-profiles of the European Plastics Industry. Reformer Hydrogen.

3.11 NON-STANDARD COCONUT HEFA [B]

3.11.1 Introduction

Two CAEP modelling teams from the National Institute of Advanced Industrial Science and Technology (AIST) and Hasselt University (UH), have worked on the calculation of a default core LCA value for the non-standard coconuts HEFA. Both teams have worked independently but have been in contact during the entire modelling to discuss the modelling of the pathway. Core LCA emissions from non-standard coconuts HEFA fuels have been estimated based on literature data and industry inputs from a crude coconut oil producer.The core LCA default value is then calculated as the mid-point of the variation between the results of the two modelling teams Both modelling teams have also performed sensitivity analysis in order to populate the "pathway specifications" column of the default values table for non-standard coconut HEFA. As a result, a correction value that is equivalent to the calculated sensitivity of the pathway to the use of coal for hydrogen production is applied.

CAEP experts from Politecnico di Torino (Polito) acted as the verifier of the calculations of the two modelling teams.

3.11.2 Data and analysis

The system boundaries of the non-standard coconut SAF production follows the steps defined in the ICAO document "CORSIA Methodology for Calculating Actual Life Cycle Emissions Values": (1) production at source (e.g., feedstock cultivation); (2) conditioning at source (e.g., feedstock harvesting, collection, and recovery); (3) feedstock processing and extraction; (4) feedstock transportation to processing and fuel production facilities; (5) feedstock-to-fuel conversion processes; (6) fuel transportation and distribution to the blend point; (7) fuel transportation from the blending point to the aircraft uplift location; and (8) fuel combustion in an aircraft engine. Given that non-standard coconuts are classified as by-products in the positive list of the ICAO document "CORSIA Methodology for Calculating Actual Life Cycle Emissions Values" (Fourth Edition, March 2024), they are assumed to incur zero emissions during the feedstock production, i.e., life cycle stage 1.

AIST assumed that processes up to Crude Coconut Oil (CCO) production take place in Indonesia, while SAF production and distribution processes take place in Japan as shown in Figure 5. Unless otherwise specified, carbon intensities and GHG emissions are referred from GREET Version 45VH2 (2023). In the feedstock pre-treatment and coconut oil extraction, two processes (copra production and CCO production) are relevant. For copra production process, coconuts are dried by sun and/or smoked by coconut husks derived from the feedstock itself, therefore, no energy input for drying is considered. Only a small amount of electricity input (for lighting purpose) and sulfur input (for preventing decay) are considered. CCO production process is to have mechanical extraction process followed by chemical oil extraction process. Input of steam (to be produced from coal boiler), water, solvent (n-hexane), and grid electricity are considered. Output of the mechanical process, copra expeller, is to be an input of chemical process. From the chemical process, copra expeller pellet is output. Copra expeller pellet (meal) is utilized as animal feed and then regarded as a co-product. Emissions are allocated to such a co-product on energy basis.

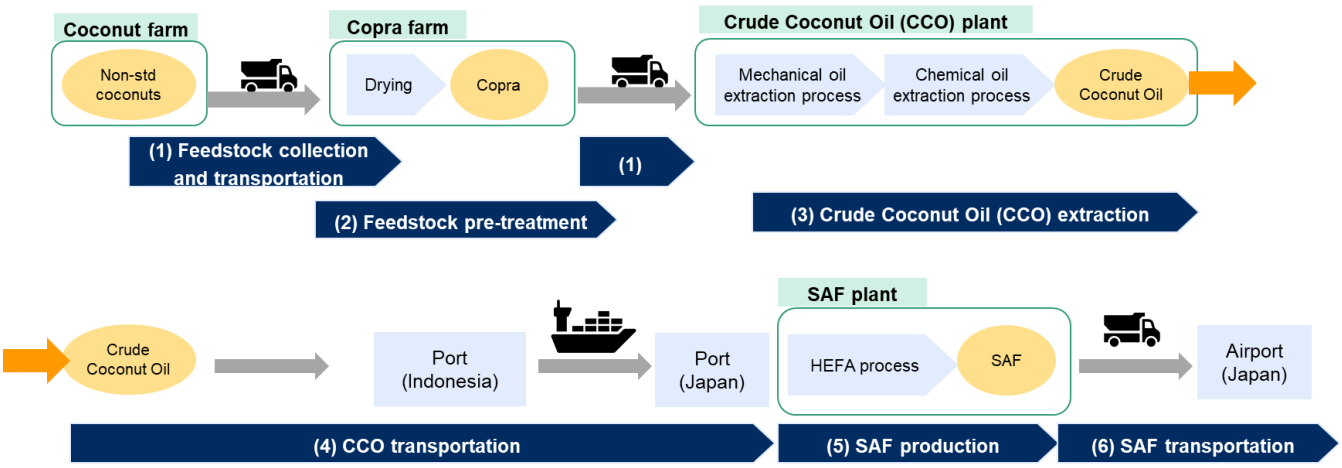

Figure 5: System boundaries, AIST assumption

The UH modelling assumed that the feedstock collection and transportation and the coconut oil extraction take place in The Philippines. Particularly, the coconut collection is assumed to take place in the Davao region as this area has the largest share of coconut farms in the country. [1] The coconuts are then assumed to be transported to the feedstock pre-treatment and coconut oil extraction facility. The extracted crude coconut oil is then transported from The Philippines (Port of Davao) to Europe (Port of Rotterdam) where the HEFA fuel is assumed to be produced. The fuel production step and transportation assumptions are from the GREET 2023 model (Excel version). Hydrogen requirements for the fuel production step were augmented based on the fatty acid composition of the crude coconut oil. [2] Carbon intensities and GHG emissions are referred from GREET 2023.

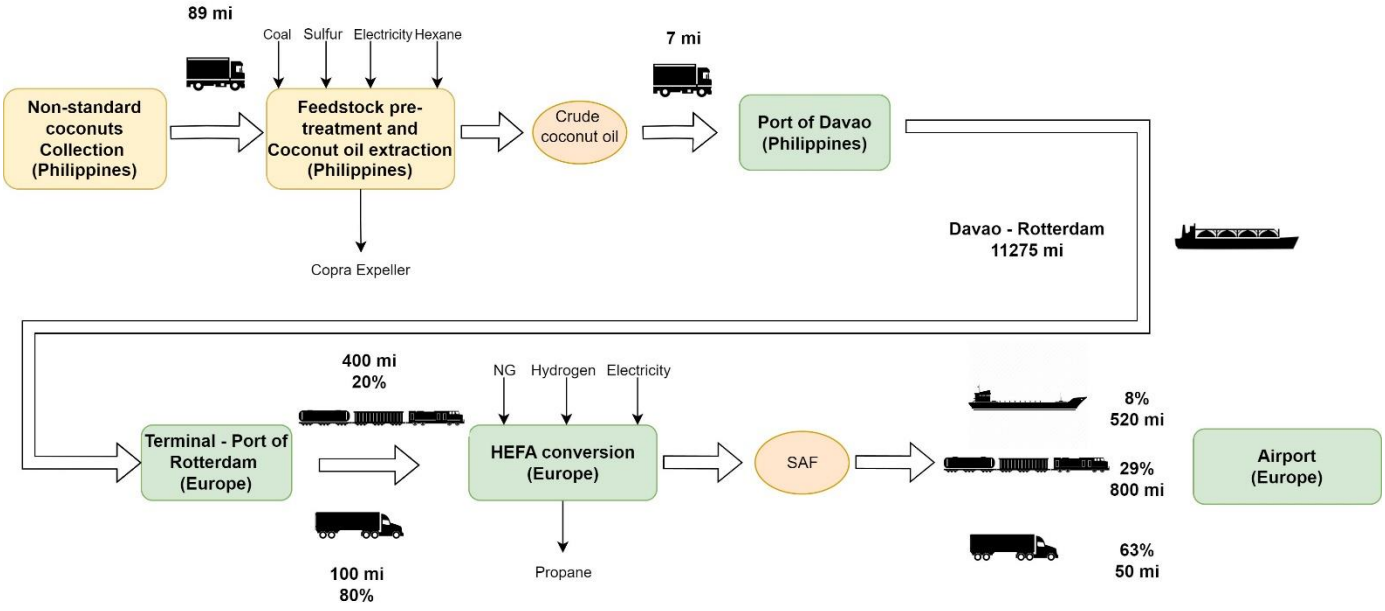

Figure 6: System boundaries, UH assumption

Table 38 summarizes the general assumptions used by the two modelling teams to estimate the core LCA emissions of non-standard coconuts SAF production.

Table 38: General assumptions to estimate the core LCA emissions of HEFA fuels from non-standard coconut

Stage	AIST assumptions	UH assumptions
Feedstock collection and transportation	Coconuts are harvested manually, therefore no energy input is considered. Coconuts are transported from coconut farm to copra farm for 88 miles by medium heavy truck. Copra is transported from copra farm to CCO plant for 7 miles by medium heavy truck. Back-hauls are regarded to be empty and taken into account.	Coconut collection is assumed to take place in the Davao region, in The Philippines which has the national largest share of coconut farms.[1] The feedstock is assumed to be transported for 143 km by medium-truck to the feedstock pre-treatment and crude coconut oil facility. Back-hauls are regarded to be empty and taken into account.
Feedstock pre-treatment	For copra production process, coconuts are dried by sun and/or smoked by coconut husks derived from the feedstock itself, therefore, no energy input for drying is considered. Only a small amount of electricity input (for lighting purpose) and sulfur input (for preventing decay) are considered.	Input of electricity (for lighting purpose) and sulfur (for preventing decay) is assumed in feedstock processing. [3] The electricity mix of The Philippines is considered as electricity grid.[4]
Crude coconut oil extraction	For CCO production process, mechanical extraction process followed by chemical oil extraction process is conducted. Input of steam (heated by coal), solvent (n-hexane), and grid electricity is considered. As an output in addition to CCO, copra expeller pellet (meal) is produced as a co-product (animal feed).	Input of steam (to be produced from coal boiler), water, solvent (hexane), and grid electricity is assumed. Output of copra expeller from mechanical process and copra expeller pellet from chemical process are assumed. They are utilized as feed, therefore regarded as co-product. Emissions are allocated to such co-product on energy basis. Data source: [5] The electricity mix of The Philippines is considered as electricity grid.[4]
Crude coconut oil transportation to the fuel production facility	CCO is transported from CCO plant to port in Indonesia for 99 miles by heavy truck, from Indonesia to Japan for 3,573 miles by oceanic tanker, and from port in Japan to SAF plant for 10 miles by heavy truck. Back-hauls are regarded to be empty and taken into account.	The extracted coconut oil is assumed to transported first by truck (11 km) to the Port of Davao from where it is transported to the Port of Rotterdam, in Europe. Transportation by ocean tanker (18145 km).
Fuel production	Hydrogen required are calculated based on the molar stoichiometry of the hydro-processing reactions. Fatty acid composition of coconut oil is from Ministry of Education, Culture, Sports, Science and technology, Japan (2020). Other energy and utilities inputs are referred to the default data from GREET 2019 as it keeps the consistency to other HEFA pathways. The upstream emission factors of natural gas and hydrogen are calculated to reflect the scenario in Japan where LNG is imported from Australia.	Hydrogen requirements for coconut oil were adjusted compared to those for soybean hydrogen consumption based on the molar stoichiometry of the hydroprocessing reactions. Fatty acid composition of coconut oil based on. [2] Other energy and utilities inputs are equivalent as in the last calculation from CORSIA.

Fuel transportation and distribution	31 miles of heavy truck transport from SAF plant to blending point, then to airport is assumed. Back-haul is regarded to be empty and taken into account.	According to default data from the GREET model, 63%, 8% and 29% of the fuel were assumed to be transported 80 km by truck, 837 km by barge, and 1288 km by rail, respectively. Back-haul is regarded to be empty and taken into account.

Table 39 and Table 40 summarize inputs and outputs of the feedstock pre-treatment and crude coconut oil extraction processes. Both modeling teams rely here on the same data source [3,5], so the parameters are identical.

Table 39: Inputs and outputs of the feedstock pre-treatment [3]

		Non-standard coconut	
Parameter		**AIST**	**UH**
Inputs	***Unit***		
Electricity	MJ/ton copra	23	23
Sulfur	ton/ton copra	0.001	0.001

Table 40: Inputs and outputs of the coconut oil extraction [5]

		Non-standard coconut	
Parameter		**AIST**	**UH**
Inputs	***Unit***		
Coal	Btu/lb CCO	1600	1600
Electricity	Btu/lb CCO	464.6	464.6
n-Hexane	Btu/lb CCO	43.5	43.5
Outputs			
Crude coconut oil (CCO)	lb CCO/ ton dry copra	1459.6	1459.6
Coconut oil LHV	MJ/kg	37.8	37.8
Copra expeller LHV	MJ/kg	15.7	15.7
Allocation factor (energy)	%	85.5	85.5

The fuel production stage refers to the transformation of rendered product into SAF, which requires the upgrading of the feedstock, and its subsequent hydrotreatment and isomerization. Table 44 summarizes the inputs and outputs of the transformation of coconut oil into HEFA fuel.

AIST assumed that hydrogen consumption of CCO during upgrading to HEFA fuel differ from other vegetable oils such as soy oil and palm oil. As seen in Table 41, CCO contains less unsaturated fatty acids than soybean oil, and fatty acid compositions of coconut oil distribute among smaller numbers of C and closer to those of jet fuel compared to soybean oil, requiring less hydrogen input. Hydrogen input is calculated based on the molar stoichiometry of each process of hydrogeneration, propane cleave, hydrodeoxygenation, decarboxylation and hydrocracking. For hydrocracking process, composition of paraffins just before hydrocracking process is calculated and it is assumed that straight-chain paraffins of C16 or longer are cracked by one hydrogen molecule. Natural gas and electricity inputs, as well as yield and outputs of co-products, are assumed to be equivalent to ones used to calculate default values of other HEFA pathways as it keeps the consistency. The upstream emission factors of natural gas and hydrogen in Japan are calculated to reflect the scenario in Japan where LNG is imported from Australia as shown in Table 42. AIST assumed that natural gas is extracted and liquified in Australia, and LNG is transported

from Australia to Japan via ocean tanker, vaporized and distributed. Likewise, to calculate emissions from production of hydrogen, AIST assumed that hydrogen is produced from imported LNG, instead of domestic natural gas and counted emissions associated with supply of imported LNG. Table 44 summarizes inputs and outputs of the transformation of coconut oil into HEFA fuel.

Table 41: Fatty acid compositions of coconut oil assumed in the AIST analysis, and soybean oil for comparison purpose

Parameter	**Coconut oil [wt%] [6]**	**Soybean oil [wt%] [7]**
C6:0	0.60	
C8:0	8.28	
C10:0	6.09	
C12:0	46.71	
C14:0	17.27	0.12
C16:0	9.28	11.4
C16:1		0.14
C18:0	2.89	5.3
C18:1	7.09	35.4
C18:2	1.70	39.7
C18:3		5.4
C20:0	0.10	
Others		2.54
Total saturated	91.2	16.8
Total unsaturated	8.8	80.6
Unsaturated/saturated	0.10	4.79

Table 42: Upstream emission factors of Natural Gas and Hydrogen in Japan

GHG	**Upstream EF of Natural Gas [g/mm BTU-HEFA]**			**Upstream EF of Hydrogen [g/mm BTU-HEFA]**	
	Ref.) US (domestic)	**Ref.) US (imported LNG)**	**Japan (imported LNG)**	**Ref.) US (domestic)**	**Japan (imported LNG)**
VOC	11.1	10.36	9.47	13.8	12.27
CO	35.0	28.40	23.86	36.1	25.37
CH4	210.8	276.79	263.35	239.3	289.80
N2O	1.5	0.39	0.075	1.74	0.45
CO2	6624	13154	12708	75344	81193

UH assumes that hydrogen consumption of coconut oil during upgrading to HEFA fuel might differ from soybean oil due to different fatty acid compositions. As seen in Table 43, coconut oil contains more saturated fatty acids than soybean oil which would result in less hydrogen consumption during the hydrogenation phase of upgrading to HEFA fuels. To calculate the hydrogen consumption for coconut oil, the molar stoichiometry of the hydroprocessing reactions were employed.[8] For this, reaction molar stoichiometry in the reactor (from a combination of reactions from unsaturated triglycerides to saturated ones, propane loss, and decarboxylation) was calculated for coconut oil. Then, using the hydrogen input for soybean oil, provided in Table 81, the amount of hydrogen was adjusted for coconut oil. Natural gas and

electricity as utility inputs were kept the same as in Table 81 from this document.

Table 43: Fatty acid compositions of coconut oil and soybean oil assumed in the UH analysis

Parameter	**Coconut oil [wt%] [2]**	**Soybean oil [wt%] [7]**
C6:0	0.39	
C8:0	5.04	
C10:0	4.07	
C12:0	38.11	
C14:0	19.43	0.12
C16:0	13.17	11.4
C16:1		0.14
C18:0	2.50	5.3
C18:1	12.52	35.4
C18:2	4.76	39.7
C18:3	0.04	5.4
Others	4.76	2.54
Total saturated	82.68	16.8
Total unsaturated	17.28	80.6
Unsaturated/saturated	0.21	4.79

Table 44: Inputs and outputs of the transformation of coconut oil into HEFA fuel

		Non-standard coconuts	
Parameter		**AIST**	**UH**
Inputs	***Unit***		
Coconut oil	lb/ lb fuel	1.27	1.27
Natural Gas	Btu/lb-CCO	1548	1548
Electricity	Btu/lb-CCO	88	88
Hydrogen	Btu/lb-CCO	973	925
Outputs			
Jet fuel	lb	1.00	1.00
Propane	lb/ lb fuel	0.099	0.099
Total Energy Input	Btu/ lb fuel	2609	2561

3.11.3 Results

Table 45 summarizes the estimated GHG emissions from non-standard coconut based HEFA production from the two modelling teams by lifecycle step.

The calculated values by AIST and UH are 27.24 g-CO_2e/MJ and 26.55 g-CO_2e /MJ, respectively. Therefore, the variation is less than the 8.9 g variation that defines the boundary of a pathway within CORSIA. Table 45 also contains the proposed default value for the HEFA fuel. The default value is defined by the mid-point value of the variation in the calculated lifecycle emissions from the modelling teams.

The following default value was obtained:

Non-standard coconut HEFA: 26.90 g-CO2e/MJ

Table 45: Estimated GHG emissions from non-standard coconuts SAF production. Data in g-CO2e/MJ$_{SAF}$

Stage	Non-standard coconuts	
	AIST	UH
Feedstock pre-treatment	0.19	0.11
Feedstock transportation to oil extraction facility	1.13	1.29
Coconut oil extraction	14.42	13.45
Transport to the SAF facility	1.05	2.25
SAF production	10.36	9.07
SAF transportation	0.09	0.38
Total	***27.24***	***26.55***
default value	***26.90***	

Although the result difference between the two modelling teams is relatively limited, the following observations can be made:

Differences in the feedstock pre-treatment and coconut oil extraction values may be related to the assumed production sites (Indonesia and The Philippines). Concerning the transport to the SAF facility, the value computed by UH modelling team is higher due to the larger distance covered by the ocean tanker to transport the extracted crude coconut oil from the Philippines to Europe.

The SAF production values' differences are influenced by the assumed location for the production facility, considered to be in Japan (AIST) and Europe (UH). Consequently, the results are affected by the relative electricity mix assumed. Furthermore, the amount of hydrogen consumption differs due to varying the fatty acid composition employed by the two respective modelling teams. AIST also calculated the production emission factor of natural gas and hydrogen since imported LNG from Australia is mainly used in Japan. As for the SAF transportation differences, UH considers GREET default data whereas AIST adjusts the transportation to the specific Japan location.

3.11.4 Sensitivity analysis

This section presents the method and results of a sensitivity analysis for a set of 6 different parameters applied to the non-standard coconut conversion pathway analyzed.

The following parameters were considered in the sensitivity analysis:

- Transportation: UH assumes an alternative arrival port in Europe. The Port of Genova is considered as alternative to the Port of Rotterdam. AIST assumes that, although the bulk density of coconut is larger than copra, the coconut meat portions can be utilized to produce crude coconut oil. Hence, coconut is less efficient to transport compared to copra. For container volume rise, 14.4 kg of coconuts (=5.76 kg of coconut meat) is equal to 9 kg of copra. Thus, an alternative scenario with adjusted energy intensity is computed in the sensitivity analysis.

Moreover, an alternative port of arrival in Japan is assumed (Port of Kushiro). Finally, an alternative SAF transportation scenario is developed in the sensitivity analysis.

- Heat requirements: The non-standard coconuts HEFA pathway requires external heat sources during the coconut oil extraction process and during the HEFA conversion process. Those requirements are assumed to be satisfied by natural gas and are varied from -20% to 20%.

- Coal requirements: The non-standard coconut HEFA pathway requires coal during the coconut oil extraction process. Those requirements are assumed to be satisfied by natural gas and are varied from -20%, to 20%.

- Electricity requirements: electricity requirements throughout the lifecycle are varied by -20%, and 20%.

- Heat source: As mentioned above, the default value is modelled by assuming that external heat requirements are satisfied by natural gas. In the sensitivity analysis, the effect of using coal is quantified.

- Hydrogen source: Hydrogen is an important input in the SAF production. In the default value it is assumed that hydrogen is produced from natural gas by means of steam methane reforming. A sensitivity analysis was performed to quantify the emission effect of hydrogen from a zero carbon source, and hydrogen from pet coke.

The following results were obtained in the sensitivity analysis conducted by AIST:

Feedstock transportation: Baseline: Energy intensity of coconut transport is equal to copra = 1.13 g-CO_2e/MJ, origin-to-destination = 1914 Btu/ton-mile, Back-haul = 1789 Btu/ton-mile
Alternative: energy intensity of coconut transport is different from copra due to loading density = 1.71 (+0.58) g-CO_2e/MJ, origin-to-destination = 2991 Btu/ton-mile, back-haul = 2796 Btu/ton-mile.

CCO transportation: Baseline: Port of Dumai to Port of Chiba (Eastern Japan) = 1.05 g-CO_2e/MJ; Alternative: Port of Jakarta to Port of Kushiro (Northern Japan) = 1.17 g CO2eq/MJ (+0.12)

SAF transportation: Baseline: 31 miles of truck transport = 0.09 g-CO_2e/MJ
Alternative: 19 miles of barge and 29 miles of pipeline = 0.06 (-0.03) g-CO_2e/MJ

Coal used as source of heat instead of natural gas in HEFA conversion step = 29.22 (+1.98) g-CO2e/MJ

Table 46: Sensitivity analysis results for power, coal and natural gas requirements obtained by AIST

Variation in g-CO_2e/MJ	-20%	-10%	Baseline	+10%	+20%
Power requirements	-1.35	-0.68	27.24	+0.67	+1.34

Coal/NG requirements	-2.82	-1.41	27.24	+1.40	+2.81

Table 47: Sensitivity analysis results source of hydrogen production obtained by AIST

g-CO_2e/MJ	Natural Gas (baseline)	Pet Coke	Nuclear (thermo-chemical water cracking)	Nuclear (HTGR)
GHG emission	27.24	32.38 (+5.14)	23.93 (-3.31)	23.61 (-3.63)

The following results were obtained in the sensitivity analysis conducted by UH:

CCO transportation: Baseline: Port of Davao to Port of Rotterdam = 26.55 g-CO_2e/MJ; Alternative Port of Davao to Port of Genova = 26.19 (-0.38) g-CO_2e/MJ

Coal used as source of heat instead of natural gas in HEFA conversion step = 28.92 (+2.37) g-CO2e/MJ

Table 48: Sensitivity analysis results for power, coal and natural gas requirements obtained by UH

Variation in g-CO_2e/MJ	-20%	-10%	Baseline	+10%	+20%
Power requirements	-1.12	-0.59	26.55	+0.60	+1.12
Coal/NG requirements	-2.69	-1.34	27.24	+1.34	+2.69

Table 49: Sensitivity analysis results source of hydrogen production obtained by UH

g-CO_2e/MJ	Natural Gas (baseline)	Pet Coke	Nuclear (thermo-chemical water cracking)	Nuclear (HTGR)
GHG emission	26.55	31.75 (+5.20)	23.72 (-2.83)	23.42 (-3.13)

As a result, emission changes for more than 4 g-CO_2e/MJ for the following parameter for both modelling teams.

- Source of hydrogen (baseline: natural gas (UH) or imported LNG (AIST), alternative: pet coke)

This indicates that the pathway specification needs to be included as a condition to apply this default value. The proposed pathway specification is “The default value is valid if the hydrogen used is not

produced from coal. If hydrogen is produced from coal, a correction value of 5.17 g-CO_2e/MJ shall be added to the core LCA value." The correction value is computed as below:

$$Correction\ value = Midpoint\_sensitivityLCA\ -\ defaultLCAvalue_{proposed}$$

$$= \frac{31.75 + 32.38}{2}\ -\ 26.90 = 5.17\ \frac{gCO_2eq.}{MJ}$$

3.11.5 References

1. Authority PS. Selected statistics on agriculture and fisheries. Diliman, Quezon City: Philippine Statistics Authority, 2022.
2. Liu RJ, Guo X, Cheng M, et al. Effects of chemical refinement on the quality of coconut oil. *J Food Sci Tech Mys* 2019; **56**(6): 3109-16.
3. Puspaningrum T, Indrasti NS, Indrawanto C, Yani M. Life cycle assessment of coconut plantation, copra, and charcoal production. *Glob J Environ Sci M* 2023; **9**(4): 653-72.
4. Ember. The Philippines electricity generation by source. 2023. https://ember-climate.org/countries-and-regions/countries/philippines-the/.
5. Yani M, Toruan DPML, Puspaningrum T, Sarfat MS, Indrawanto C. Life cycle assessment of coconut oil product. *IOP Conference Series: Earth and Environmental Science* 2022; **1063**(1): 012017.
6. Ministry of Education C, Sports, Science and technology, Japan Standard Tables of Food Composition in Japan. 2020. https://www.mext.go.jp/a_menu/syokuhinseibun/mext_01110.html.
7. Pearlson M. A Techno-Economic and Environmental Assessment of Hydroprocessed Renewable Distillate Fuels: Massachusetts Institute of Technology; 2011.
8. Li X, Mupondwa E, Tabil L. Technoeconomic analysis of biojet fuel production from camelina at commercial scale: Case of Canadian Prairies. *Bioresource Technol* 2018; **249**: 196-205.

CHAPTER 4. SYNTHESIZED ISO-PARAFFINS PATHWAYS

4.1 PATHWAY DESCRIPTION

Synthesized iso-paraffins (SIP) pathway is a biochemical conversion technology in which SAF is produced biologically, through sugar fermentation. Microorganisms to synthetize a hydrocarbon molecule called farnesene, that can be upgraded to farnesane. Farnesane can be blended with petroleum-derived fuel. The general process for this pathway is shown in Figure 7.

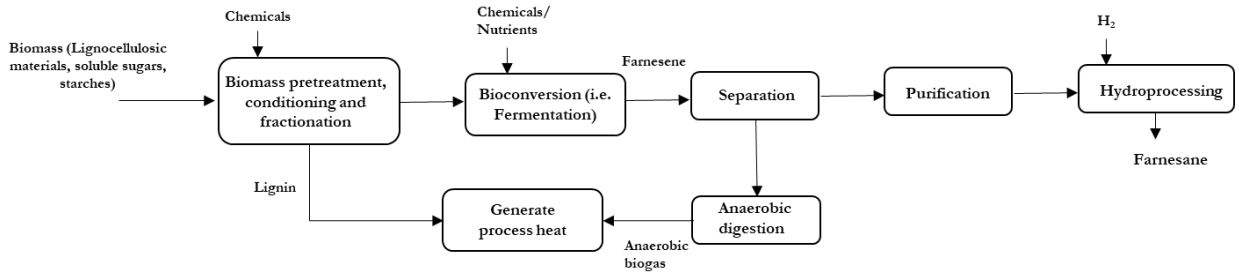

Figure 7: General process flow synthesized iso-paraffins pathway (source: Wang et al., 2016)

This pathway can be fed with sugarcane (*Saccharum officinarum*), or other sugar plants such as sugar beets (*Beta vulgaris* subsp. *vulgaris*), sweet sorghum (*Sorghum bicolor*), halophytes and cellulosic sugars. In the first step, biomass is pretreated by enzymatic hydrolysis, and the solubilized C5 and C6 sugars are separated and concentrated; the pretreated material undergoes the biological conversion to produce an intermediate hydrocarbon; and finally, it is oligomerized and hydrotreated to SAF fuel (Davis et al. 2013). This direct sugar-to-hydrocarbon (DSHC) fermentation pathway has been developed by Amyris (Amyris Inc. 2014c). In this process, sugars are fermented into a farnesene, and then hydrogenated to produce farnesane, which has to be further hydrocracked and isomerized to obtain jet fuel. Lignin, as well as other streams unsuitable for farnesene production, are separated and energetically valorized to support process utility demands. As per the ASTM 7566 standard, the resulting SAF can be blended with fossil fuel up to 10%.

4.2 SIP SUGARCANE – [M]

The GREET model modified by MIT, and JRC E3db, were used to calculate the core LCA results for sugarcane SIP; LCI data for these pathways were provided by technical experts from MIT, JRC and Universidade Estadual de Campinas (Unicamp). The initial comparison of core LCA results from these three data sources is shown in Table 50. All the models consider fermentation of sucrose to farnesene performed in Brazil, followed by hydro-treating to upgrade farnesene to farnesane.

Table 50: Initial comparison of core LCA results for sugarcane SIP

Conversion technology	Data source	Model	Cultivation	Feedstock transportation	Fermentation and upgrading	Farnesene transportation	Fuel transportation	Total emissions
SIP	MIT	GREET	17.6	2.8	11.4	-	0.3	**32.1**
	JRC	E3db	20.9	1.9	10.4	-	0.3	**33.5**
	Unicamp	CA-GREET	11.3	-*	14.8	0.2	0.3	**26.6**

*Crop transportation emissions are included in the cultivation emissions for the Unicamp data

The MIT core LCA results are based on an adaptation of the mass and energy balances presented by Staples et al. (2014). Sugarcane cultivation and transportation data are from the GREET 2016 default for Brazilian sugarcane; the sugarcane composition, sucrose yield, and utility requirements for sugarcane milling have been estimated from Dias et al. (2009); co-generation of heat and electricity from bagasse is modelled on the basis of Murphy et al. (2004). The assumed farnesene yield from sucrose is from a fuel producer, as documented in Karatzos et al. (2014). Utility requirements for fermentation and farnesene separation are based off of Vasudevan et al. (2012), Najafpour (2007) and Couper et al. (2012); farnesane yields from farnesene are assumed to be 95% of the stoichiometric value, which has been also used to determine H_2 requirements for hydro-treating. Utility requirements for hydro-treating are based on Pearlson et al. (2013). SIP jet fuel transportation assumptions are the default modes and distances assumed for Brazilian sugarcane ethanol in GREET 2016.

For calculating the core LCA values for this pathway, JRC took sugarcane cultivation and transportation assumptions are from E3db default for Brazilian sugarcane. The sugarcane composition is from Kaltschmitt et al. (2001); the assumptions regarding sucrose yield, utility requirements for sugarcane milling, and co-generation of heat and electricity from bagasse are from Macedo et al. (2008). Farnesene yield is based on values reported by a fuel producer and re-assessed by the US National Advanced Biofuels Consortium (NABC), as documented in Karatzos et al. (2014). Farnesane from farnesene yield and the associated H_2 demand for hydrotreating are based on the stoichiometry value. SIP jet fuel transportation assumptions are based on the default modes and distances from E3db.

The Unicamp core LCA results are based on an analysis documented by Moreira et al. (2014), with the results regenerated assuming energy based emissions allocation in order to be consistent with the CAEP core LCA methodology.

The comparison of these three data sources reveals a number of discrepancies, affecting the core LCA results. Apart from the notable difference in the feedstock cultivation emissions, due to difference in yields and input assumptions, another relevant one is due to the farnesene yields: MIT assumes 17% (wt.) yield of farnesene from sucrose, JRC assumes 13%, and the Unicamp analysis assumes higher farnesene yields and sugarcane quality (the exact values used in the Unicamp analysis cannot be revealed due to their proprietary nature). These differences impact on the yield of 1 kg of farnesene, in terms of 42.6 kg of sugarcane required for MIT analysis, 65.3 kg of sugarcane for JRC, and 27.2 kg of sugarcane required in the Unicamp analysis.

The MIT and JRC assumptions are based on farnesene yields that have already been demonstrated at relevant scale, whereas the Unicamp study reflects improvements in farnesene yield and sugarcane quality, targeted by fuel producers. Therefore, in order to better reflect the current state of sugarcane SIP technology, in a manner that is consistent with the approach taken by CAEP in its agreed core LCA methodology and analyses, it has been agreed to use the MIT and JRC core LCA results, as shown in Table 51.

Table 51: LCA results for sugarcane SIP pathway

Conversion technology	Data source	Model	Cultivation	Feedstock transportation	Fermentation and upgrading	Fuel transportation	Total emissions	Midpoint value
SIP	MIT	GREET	17.6	2.8	11.4	0.3	**32.1**	**32.8**
	JRC	E3db	20.9	1.9	10.4	0.3	**33.5**	

The core LCA results in Table 51 range from 32.1 to 33.5 gCO_2e/MJ, with an agreed default core LCA value of 32.8 gCO_2e/MJ.

A comparison of the agricultural inputs for sugarcane cultivation in the MIT and JRC analyses, as well as the data from the Brazilian Bioethanol Science and Technology Lab (CTBE) used for the sugarcane SIP pathway, is given in Table 83 in the appendix. The differences in P_2O_5, K_2O, $CaCO_3$ or lime, and pesticide application have a relatively small impact on lifecycle emissions: less than 1 gCO_2e per kg sugarcane. On the other hand, differences in the assumed rate of N application and diesel used for cultivation and harvesting between the MIT and CTBE analyses result in differences of approximately 4 and 2 gCO_2e per kg sugarcane, respectively (4 gCO_2e is equivalent to approximately 16% of total CO_2e emissions from sugarcane cultivation in the MIT analysis).

4.3 SIP SUGARBEET – [M]

The sugarbeet SIP pathway has been modelled for being consistent with the sugarcane SIP. Both processes are based on the fermentation of sugars to hydrocarbon intermediates and subsequent hydrotreating to drop-in jet fuel. Similar to the other pathways, the input dataset covers the following steps: feedstock cultivation, feedstock transportation, sugar to drop-in jet production, and final fuel transportation. The lifecycle inventory data for this feedstock is shown in Table 84 in the appendix. In the JRC analysis, the cultivation inputs are based on data from the Cofédération Générale de la Betterave (CGB, a sugar producers group), CIBE 2013 (International Confederation of European Beet Growers) and the Food and Agricultural Organization (FAO) of the United Nations, with a yield of 76.9 t/ha and a water content of 74%. The sugar content is assumed to be 0.171 $kg/kg_{moist.sugarbeet}$ (Kaltschmitt et al., 1997), and the energy inputs for the SIP process have been assumed to be partially offset by energy recovered from biogas generation from sugarbeet pulp (Eder & Schulz 2006, Karatzos et al. 2014, Wang et al., 2016). The resulting yield is 0.57 $MJ_{farnesene}/MJ_{sugarbeet}$. In the model 0.96 kg of farnesene are to be hydrogenated to produce a 1 kg of SAF.

In the MIT analysis, the inputs for sugarbeet cultivation and transportation to the biorefinery are based on Edwards (Edwards et al., 2017). Sugar content is assumed to be 0.167 $kg/kg_{moist.sugarbeet}$ (Buchspies et al., 2016). Methane yield from anaerobic digestion of sugarbeet pulp is estimated from Zieminski et al. (2017), and co-generation of heat and power from the biogas is estimated considering the efficiencies reported by Pöschl et al. (2010). The resulting yield of farnesene is 0.45 MJ $MJ_{farnesene}/MJ_{sugarbeet}$. The heat and electricity requirements for fermentation are taken from Najafpour (2007) and Couper et al. (2012), and the utility requirements for farnesene separation are estimated from Vasudevan et al. (2012). In the MIT analysis 1.01 kg of farnesene is assumed to be needed to produce 1 kg of SAF, assuming 95% stoichiometric yield.

The results for the JRC and MIT analyses of the sugarbeet SIP pathway are shown below in Table 52. A number of factors contribute to the discrepancy between the data: the two analysis rely on differing data sources for sugarbeet cultivation, as described above; moreover, MIT assumes a lower sugar yield from sugarbeet, resulting in a 21% lower energetic yield of farnesene per unit feedstock. The process slightly differs, in term of assumptions about biogas yield from sugarbeet pulp and CHP cogeneration efficiencies. Despite the differences in the input and assumptions, the data are within the threshold of 8.9 gCO_2e/MJ,

therefore the agreed default core LCA value for the sugarbeet SIP pathway has been calculated as midpoint: 32.4 gCO_2e/MJ.

Table 52: LCA results sugarbeet SIP pathways

Conversion technology	Data source	Model	Cultivation	Feedstock transportation	SIP production	Fuel transportation	Total emissions	Midpoint value
SIP from sugarbeet	JRC	E3db	11	0.9	16.6	0.3	**28.8**	**32.4**
	MIT	GREET	23.4	1.4	10.8	0.4	**36.0**	

CHAPTER 5. ALCOHOL-TO-JET PATHWAYS

5.1 PATHWAY DESCRIPTION

The alcohol-to-jet (ATJ) pathway is a biochemical conversion process for producing jet fuel blendstock from alcohols. ATJ provides a means for producing SAF from a wide variety of resources, therefore offering opportunities for alcohol producers to enter the aviation market (Geleynse et al., 2018). SAF produced through ATJ pathway is referred to ATJ-SPK (synthetic paraffinic kerosene) and it has been approved by ASTM D7566. Currently, ATJ-SPK produced from an ethanol or butanol intermediates are allowed up to a 50% maximum blend.

Several feedstocks can be used for this pathway, but while fermentation of sugars from edible plants is the most common practice to produce alcohol derivatives, fermentation from non-edible plants require other advance techniques involving pre-treatment, specific microbes and additional process units.

A general process description for the ATJ pathway is shown in Figure 8.

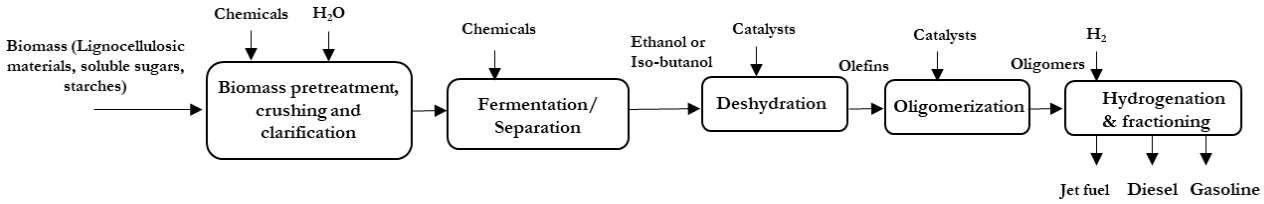

Figure 8: General process flow alcohol-to-jet pathway

After biomass pre-treatment and conditioning, alcohols can be produced through fermentation processes. A typical three-step ATJ process that converts alcohols to jet fuel has been demonstrated (Byogy Renewables 2011). The process includes alcohol dehydration, oligomerization, and hydrogenation.

5.2 SUGARCANE ISO-BUTANOL ATJ – [M]

This section covers the sugarcane ATJ pathway. MIT and CTBE used modified versions of the GREET model, and JRC used the E3db, to calculate the core LCA results shown in Table 53. Input data have been provided by technical experts from MIT, JRC, and CTBE. All of these analyses consider isobutanol (iBuOH) as the intermediate alcohol, which is then dehydrated and oligomerized to jet fuel.

Table 53: Initial comparison of core LCA results for sugarcane iso-butanol ATJ [gCO_2e/MJ]

Conversion technology	Data source	Model	Cultivation	Feedstock transportation	Fermentation and upgrading	iBuOH transportation	Fuel transportation	Total emissions
ATJ	MIT	GREET	12.4	1.9	6.0	-	3.6	**23.9**
	JRC	E3db	17.7	1.6	7.7	1.8	3.1	**31.9**
	CTBE	GREET	13.1	1.7	6.7	-	0.5	**22.0**

The MIT core LCA results are based on mass and energy balances presented in Staples et al. (2014) for the iBuOH pathway. The sugarcane cultivation and transportation assumptions are the GREET 2016 default assumptions for Brazilian sugarcane; the sugarcane composition, sucrose yield, and utility requirements for sugarcane milling are estimated from Dias et al. (2009); co-generation of heat and electricity from bagasse is modelled on the basis of Murphy & McKeogh (2004). iBuOH yield from sucrose is based on 85% of the stoichiometric maximum, as suggested by Dugar & Stephanopoulos (2011). Utility requirements of iBuOH fermentation and distillation have been obtained from Najafpour (2007), Couper et al. (2012) and Mei (2006). Jet fuel yields from iBuOH and the associated utility requirements are based on data provided by a fuel producer; and the ATJ fuel transportation assumptions are the default modes and distances assumed for Brazilian sugarcane ethanol in GREET 2016.

For the JRC core LCA results, sugarcane cultivation and transportation assumptions are from E3db for Brazilian sugarcane; the sugarcane composition is from Kaltschmitt & Hartmann (2001) and Macedo (2008). Sucrose yield, utility requirements for sugarcane milling, and co-generation of heat and electricity from bagasse are from Klein-Marcuschamer & Turner (2013); the yield of iBuOH from sucrose, and the associated utility requirements are based on data from Tao (2014) and Dunn (2014). Jet yield from iBuOH and the associated utility requirements are based on data provided by a fuel producer; and the jet fuel transportation assumptions are based on the default modes and distances from E3db.

The CTBE LCI data is from an analysis that is fully documented in Klein (in preparation), with the results regenerated in GREET 2016, with energy emissions allocated accordingly to CAEP core LCA methodology.

Differences between MIT, JRC and CTBE results are shown in Table 53. JRC analysis assumes that iBuOH production and upgrading occur at separate facilities, therefore there are emissions associated with iBuOH transportation, whereas the MIT and CTBE analyses assume that these operations are co-located. MIT and JRC assume inter-continental transportation for the finished jet fuel product, reflecting the geographic origin of the feedstock and assuming regions for fuel uplift, whereas the CTBE analysis assumes regional use of the fuel (all three analysis assume Brazil as the origin of the sugarcane feedstock).

Harmonization of the assumptions have been proposed, in order to make a consistent comparison of core LCA results. iBuOH transportation step has been removed from the JRC results, and the jet fuel transportation emissions are assumed to be equivalent to those calculated for the sugarcane SIP pathway. Second, the average of the jet fuel transportation emissions from the MIT and JRC results has been applied to the CTBE. The core LCA results from the three datasets, following the harmonization process, are presented in Table 54. Comparisons of the inputs used are available in Table 85 in the appendix.

Table 54: LCA results for sugarcane iso-butanol ATJ [gCO_2e/MJ]

Conversion technology	Data Source	Model	Cultivation	Feedstock transportation	Fermentation and upgrading	Fuel transportation	Total emissions	Midpoint value
ATJ	MIT	GREET	12.4	1.9	6	0.3	**20.7**	**24.0**
	JRC	E3db	17.7	1.6	7.7	0.3	**27.3**	
	CTBE	GREET	13.1	1.7	6.7	0.3	**21.8**	

The results in Table 54 range from 20.7 to 27.3 gCO_2e/MJ, with an agreed midpoint default core LCA value of 24.0 gCO_2e/MJ.

5.3 AGRICULTURAL RESIDUES ISO-BUTANOL ATJ – [R]

Corn stover is considered a suitable agricultural residue for the ATJ pathway. The source for the MIT provided data is Staples et al. (2014) and the source for the JRC provided data is the E3 database (Ludwig-Bolkow Systemtechnik GMBH, 2006); detailed LCI data from both sources are given in Table 86 in the appendix. Table 55 shows the GHG emissions results for SAF produced from agricultural residues. Agricultural residues have been considered as waste feedstocks; therefore, the system boundary starts at the collection of these waste materials, without upstream emissions for the cultivation phase.

It is worth noting that the values in Table 55 are shown both with and without emissions associated with nutrient replacement. As for other pathways, when agricultural residues are left on the field, they decompose providing nutrients to the soil. Conversely, if agricultural residues are removed, there may be a soil nutrient deficit, and therefore additional fertilizer may have to be applied to maintain yields. The lifecycle GHG emissions of these pathways vary among the studies, depending on whether or not the emissions associated with nutrient replacement are included in the lifecycle analysis. However, to stay consistent with the CAEP methodology to not include upstream emissions for residue-derived SAF, the default value for this pathway was calculated without nutrient replacement. The data including nutrient replacement is provided below in Table 55 for information only.

Table 55: LCA results for agricultural residues iso-butanol ATJ pathway [gCO_2e/MJ]

Feedstock	Data Provider	Model	Feedstock collection	Feedstock Transportation	Feedstock to Fuel Conversion	Fuel Transportation	Total emissions	Midpoint value
Corn Stover (without nutrient replacement)	MIT	GREET	3.3	1.2	27	0.5	**31.9**	**29.3**
	JRC	E3	2.4	7.9	15.3	0.3	**25.9**	
	JRC	GREET	3	3.5	23.7	0.5	**30**	
Corn Stover (with nutrient replacement)	MIT	GREET	13.8	1.2	26.2	0.5	**41.7**	**n/a**
	JRC	E3	10.1	7.9	15.3	0.3	**33.6**	
	JRC	GREET	11.9	2.5	23.7	0.5	**37.6**	

There are some differences in the results based on the MIT and JRC datasets. Feedstock transportation emissions from the JRC data (7.9 gCO_2e/MJ) are higher than those from the MIT data (1.2 gCO_2e/MJ), driven primarily by an assumption of greater transportation distances in the E3 database. In addition, differences in feedstock-to-fuel conversion are present, due to assumed net heat demand for fermentation of lignocellulosic feedstock to isobutanol (0.04 $MJ_{nat.gas}/MJ_{SAF}$ in MIT data versus 0.01 $MJ_{nat.\ gas}/MJ_{SAF}$ in JRC data), and the source and quantity of cellulase enzymes for bioconversion of lignocellulosic feedstock to isobutanol (0.85 $g_{cellulase}/MJ_{SAF}$ versus 1.62 $g_{cellulase}/MJ_{SAF}$).

In order to further investigate the differences between the MIT and JRC results, the JRC source data for the feedstock collection and feedstock-to-fuel conversion steps was input into GREET, and the results are shown in the third line of each feedstock category in Table 55, where the data provider is JRC and the model is GREET. These results are between the lower bound results from the E3 database, and the upper bound results from GREET using data from Staples et al. (2014).

Finally, it was agreed to consider the assumption without nutrient replacement. Therefore, the agreed default core LCA value for the agricultural residues ATJ pathway is 29.3 [gCO_2e/MJ].

5.4 FORESTRY RESIDUES ISO-BUTANOL ATJ – [R]

The system boundary for forest residue ATJ starts at the collection of this residual material and therefore does not include any cultivation emissions. The source for the MIT provided data is Staples, et al. (2014) and the source for the JRC provided data is the E3 database (mainly based on LudwigBolkow S. GMBH, 2006). The lifecycle inventory data associated with both of these results are shown in Table 87. Table 56 shows the lifecycle GHG emissions results for SAF produced from forest residues using ATJ conversion.

Table 56: LCA results for the forest residue iso-butanol ATJ pathway [gCO_2e/MJ]

Feedstock	Data Provider	Model	Feedstock collection	Feedstock transportation	Feedstock-to- fuel conversion	Fuel transportation	Total emissions	Midpoint value
Forest Residues	MIT	GREET	1.6	2.1	20.5	0.5	**24.7**	**23.8**
	JRC	E3	3.9	3.6	15	0.3	**22.8**	

The main source of differences in the E3 database results compared to the MIT/GREET results is due to the energy inputs for forestry residue collection and transportation, differences in feedstock-to-fuel conversion emissions for the net heat demand for fermentation to iso-butanol (0.04 $MJ_{nat.gas}/MJ_{SAF}$ in MIT data versus 0.01 $MJ_{nat.gas}/MJ_{SAF}$ in JRC data), and the source and quantity of enzymes for bioconversion of the feedstock to isobutanol (0.85 $g_{cellulase}/MJ_{SAF}$ versus 1.62 $g_{cellulase}/MJ_{SAF}$).

The agreed default core LCA value for the forestry residues ATJ pathway is 23.8 gCO_2e/MJ.

5.5 CORN GRAIN ISO-BUTANOL ATJ – [M]

Two independent analyses were compared for this pathway, in order to determine an appropriate default core LCA value: one carried out by MIT, and the other by JRC. The LCA results from the MIT and JRC analyses are shown in Table 57. The differences in the LCA data are related to the inventories used: E3db assumes corn grain yield of 7.1 t/ha, conversely to a yield of 10.4 t/ha in the underlying GREET 2017 data; DDGS yield of 0.31 $kg/kg_{corn\ grain}$ in E3db versus 0.28 $kg/kg_{corn\ grain}$ in GREET 2017. The lifecycle inventory data for this pathway is shown in Table 78 (corn farming) and Table 88 (ethanol ATJ pathway) in the appendix.

Table 57: LCA results corn grain iso-butanol ATJ pathway [gCO_2e/MJ]

Conversion technology	Data source	Model	Cultivation	Feedstock transportation	Fermentation and upgrading	Jet fuel transportation	Total emissions	Midpoint value
Corn grain iBuOH ATJ	MIT	GREET	15.9	0.9	38.8	0.4	**56.0**	**55.8**
	JRC	E3db	22.5	0.6	32.1	0.3	**55.5**	

In the MIT analysis the life cycle inventory data for corn grain cultivation, harvesting, and transportation to a biorefinery are taken from GREET 2017, with a moisture content of 15.5%. The corn grain milling process is based on data from Kwiatkowski et al. (2006) and Mei (2006). Fermentation yields of iBuOH

from corn starch are estimated as 85% of theoretical maximum based on Dugar & Stephanopolous (2011), and the heat and electricity requirements for fermentation are taken from Najafpour (2007) and Couper (2012). Similar to the corn grain ethanol ATJ pathway, the co-products to which an emissions burden is allocated are distiller dry grains and solubles (DDGS) and corn oil. The quantity of these co-products generated during iBuOH fermentation, as well as the quantity of inputs of alpha and gluco-amylase, yeast, ammonia, sodium hydroxide, sulfuric acid and calcium oxide for iBuOH fermentation were estimated based on the corn ethanol dry mill process in GREET 2017. Iso-butanol is assumed to be dehydrated, oligomerized and hydrotreated to jet fuel in a manner similarly to the Gevo process. Process data provided to MIT from Gevo was used to estimate jet yields from iBuOH, and the requirements of heat, electricity, and hydrogen for upgrading. Note that the Gevo processing data are proprietary, and provided to MIT under a non-disclosure agreement. Subsequent analysis of the data provided under the NDA has been published in the peer-reviewed literature (Staples et al. 2014), and forms the basis for the LCA data presented here. Finally, the SAF product is assumed to be transported by heavy-duty diesel truck, barge and rail to the final fueling point, according to the default GREET 2017 assumptions for renewable jet fuel transportation (Staples et al., 2014).

In the JRC analysis the life cycle inventory data for corn grain cultivation, harvesting and transportation to the conversion plant are taken from the E3db and are aligned with input data used for default value calculation in the EU Renewable Energy Directive – Recast (Edwards et al., 2017) for corn (14% moisture content) characterized by an average agricultural yield value of 7.13 tons/ha/yr. The fermentation process of iBuOH is calculated based on assumptions in Ramey & Yang 2004 with updated data from Ramey (2008) and Tao et al. (2014). Similar to MIT, JRC modelled the upgrading process from iso-butanol to jet fuel following steps compatible with the Gevo process (Johnston, 2017) with some differences with respect to the required hydrogen input compared to input data used by MIT.

The agreed default core LCA value for the corn grain iBuOH ATJ pathway is 55.8 gCO_2e/MJ.

5.6 HERBACEOUS ENERGY CROPS ISO-BUTANOL ATJ – [M]

Three analyses were performed for this pathway, in order to determine default core LCA value. MIT modelled the switchgrass and miscanthus iBuOH ATJ pathways, and JRC modelled the switchgrass iBuOH ATJ pathway only, as representative for herbaceous energy crops. The lifecycle inventory data for this pathway is shown in Table 73 (input for herbaceous energy crops farming) and Table 88 (input for ethanol ATJ processes) in the appendix The LCA results from the MIT and JRC analyses are compared in Table 58.

Table 58: LCA results herbaceous energy crops iso-butanol ATJ pathway [gCO_2e/MJ]

Conversion technology	Data source	Model	Cultivation	Feedstock transportation	Fermentation and upgrading	Jet fuel transportation	Total emissions	Midpoint value
Miscanthus iBuOH ATJ	MIT	GREET	12.5	1.4	27.7	0.4	**42.1**	**43.4**
Switchgrass iBuOH ATJ	MIT	GREET	14.9	2.1	27	0.4	**44.5**	
	JRC	E3db	9.9	3.1	31.4	0.3	**44.7**	

Fermentation and upgrading emissions for the herbaceous lignocellulosic pathways are substantially lower than those for the corn grain iBuOH ATJ pathway, as calculated by MIT. This is due to the assumption of use of the lignin for CHP energy recovery. The CHP is assumed to offset electricity and heat demands for

fermentation and upgrading, therefore contributing to lower emissions. In the MIT analysis, the LCI data for switchgrass and miscanthus cultivation, harvesting, and transportation to a biorefinery are from GREET 2017, on a dry matter basis. The yields and process inputs of the dilute acid pretreatment, needed to extract monomer sugars were estimated from Kumar & Murthy (2011). Fermentation yields of iBuOH from C5 and C6 sugars are estimated as 85% and 60% of theoretical maximum, respectively, based on Dugar & Stephanopolous (2011), and the heat and electricity requirements for fermentation are taken from Najafpour (2007) and Couper (2012). Lignin cogeneration of heat and power via biomass is assumed to partially offset utility demands for the fuel production process, according to electricity and process heat generation efficiencies from Murphy & McKeogh (2004). Inputs of cellulase, yeast, sulfuric acid and ammonia for iBuOH fermentation are estimated based on the switchgrass and miscanthus ethanol processes in GREET 2017. Iso-butanol is assumed to be dehydrated, oligomerized and hydrotreated to jet fuel in a manner similar to the Gevo process. Process data from Gevo, provided to MIT under an NDA as described above, was used to estimate jet yields from iBuOH, and the requirements of heat, electricity, and hydrogen for upgrading (Staples et al. 2014). Finally, the jet fuel product is assumed to be transported by heavy-duty diesel truck, barge and rail to the final fueling point, according to the default GREET 2017 assumptions on renewable jet fuel transportation.

In the JRC analysis, the life cycle inventory data for switchgrass cultivation, harvesting and transportation to the conversion plant are based on Groode & Heywood (2008), considering the conversion of switchgrass to lignocellulosic ethanol. As a result, differences from the analysis performed by MIT are mostly due to the cultivation conditions and practices, namely with respect to the use of pesticides. The conversion process input data are substantially the same as those used for the corn grain iBuOH ATJ pathway. Similar to corn grain iBuOH ATJ pathway, the upgrading of iBuOH-to-jet (Gevo process (Johnston, 2017)) with some differences with respect to the required hydrogen input compared to input data used by MIT.

The agreed default core LCA value for the herbaceous lignocellulosic iBuOH ATJ pathway is 43.4 gCO_2e/MJ.

5.7 MOLASSES ISO-BUTANOL ATJ – [C]

This pathway is based on the sugarcane iBuOH ATJ pathway. The fuel production is from sugar-derived iso-butanol, which is subsequently converted to drop-in fuel via dehydration, oligomerization, and hydrotreating. Two different approaches are considered for the calculation of this pathway: the first one assumes the same value of sugarcane iBuOH pathway, while the second assumes that sugar is separated for sale as a food product and fermentation of the molasses for biofuel production. In both the cases molasses has been considered as a co-product of the main production.

5.7.1 Fermentation of all sugars -JRC

This approach was proposed by JRC in order to guarantee consistency with the analysis carried out for the sugarcane iBuOH ATJ pathway. For the purpose of this analysis, it is assumed that a company producing biofuel from sugarcane is most likely to ferment all available sugars, including what can be – if ideally separated from the process stream – called molasses. This pathway is designed around a plant optimized to produce biofuels from sugarcane, rather than sugar for use as food. This is consistent with the modelling of sugarcane iBuOH ATJ pathway. This approach leads to the conclusion that the amount of sugar that could be attributed to molasses is processed simultaneously with the other sugar content in the juice extracted from the sugarcane, and thus with the same emissions associated. Assuming the same factor for conversion efficiency, regardless of impurities (and a possible somewhat lower efficiency following the fermentation of molasses compared to the fermentation of sugarcane) the carbon intensity of the two feedstocks (sugarcane and molasses) can be assumed to be equal (Figure 9). Hence, the model for the sugarcane iBuOH ATJ pathway can be used to attribute emissions to molasses iBuOH ATJ pathway.

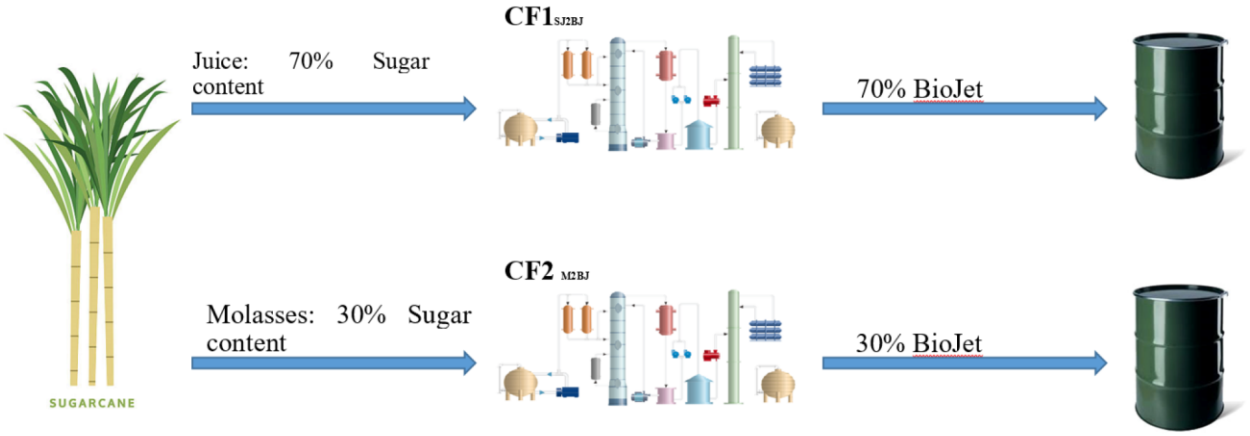

Figure 9: Conceptual description of the JRC approach: proportionality between sugar attributed to molasses and juice

5.7.2 Sugar separation for sale as food product - MIT

MIT worked in parallel to model the molasses iBuOH ATJ pathway, under the assumption that the sugar was produced for sale as a food product, and only the molasses was fermented for iBuOH production. The other major product of sugar milling, sugarcane bagasse, was considered as a fuel used for co-generation similar to all other sugarcane pathways modelled by MIT. The molasses iBuOH ATJ process considered in this approach is shown below in Figure 10. Alcohols can be converted to pure hydrocarbons in the jet fuel range through a process of dehydration, oligomerization, hydrogenation, and fractionation. ATJ-SPK was qualified in April 2016 under the ASTM7566 standard as aviation alternative fuel for blending up to 30% (recently increase to 50%) with fossil-based jet fuel.

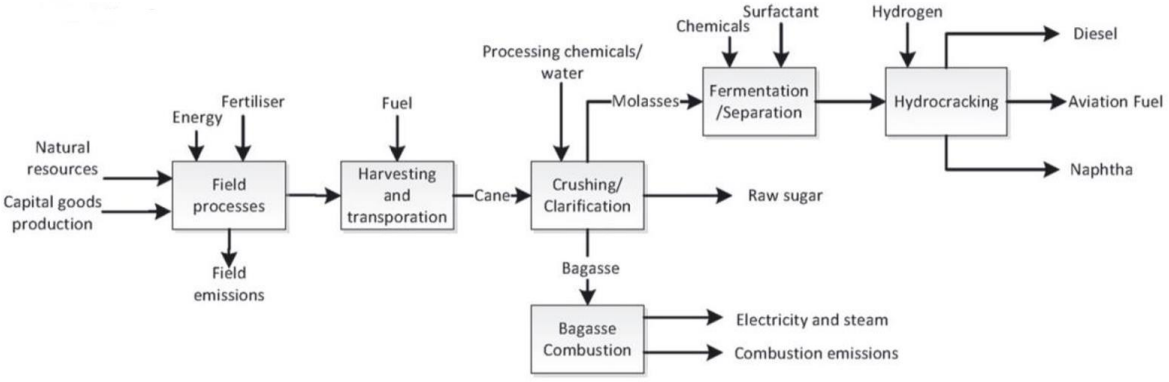

Figure 10: Process flows for SAF production from sugarcane molasses (source: Cox et al. 2014)

The molasses iBuOH ATJ pathway as illustrated in Figure 10 has been modelled using GREET. It was modelled under the assumption that the sugar milling, molasses fermentation, and jet fuel production are carried out at the same facility. Bagasse is used for cogeneration of heat and electricity which satisfies all the energy requirements for the aforementioned processes, with some extra energy also being produced and utilized outside the system boundary.

Data for a number of different sources was used to carry out the LCA for this pathway. The data for the sugarcane farming and transportation stages are from pre-defined processes on GREET: "Sugarcane

Farming" and "Brazil Sugarcane". For the sugarcane milling stage, data on sugar, molasses, and bagasse yield, and process energy and heat requirements were drawn from Tsiropoulos (2014) and Lobo (2007). Lower heating value of bagasse was obtained from Tsiropoulos (2014), lower heating value of molasses from J.H. Park et al. (2016), and lower heating value of sugar from GREET. These heating values along with bagasse heat and electricity yield were employed in determining the emissions allocation (on the basis of energy) between sugar, molasses, and the excess energy from bagasse.

The allocation factor for molasses was calculated to be 20.9% of all emissions from sugarcane farming and transportation and sugar milling. Data for the molasses fermentation stage was obtained from Tsiropoulos et al. (2014) and Khatiwada et al. (2016). Fermentation yields of iBuOH from C5 and C6 sugars are estimated as 85% and 60% of theoretical maximum, respectively (Dugar & Stephanopolous, 2011), and process data provided to MIT from Gevo was used to estimate jet yields from iBuOH, and the requirements of heat, electricity, and hydrogen for upgrading. Finally, the finished jet fuel product is assumed to be transported by heavy-duty diesel truck, barge and rail to the final fueling point, according to the default GREET 2017 assumptions on renewable jet fuel transportation. A similar exercise was carried out by ARB in 2015 (ARB 2015), which achieved similar outputs with an allocation factor of about 29.8% for molasses.

Despite the modeling differences between MIT and JRC analyses, the independent analyses of the molasses iBuOH AJT pathway gave similar results, as shown in Table 59.

Table 59: LCA results for the molasses iBuOH ATJ pathway [gCO_2e/MJ]

Conversion technology	Data source	Model	Cultivation	Feedstock transportation	Fermentation and upgrading	Jet fuel transportation	Total emissions	Midpoint value
Molasses iBuOH ATJ	JRC	E3db	17.7	1.6	7.7	0.3	**27.3**	**27.0**
	MIT	GREET	17.8	2.1	6.4	0.3	**26.6**	

Results are within the threshold, therefore the agreed default core LCA value for the molasses iBuOH ATJ pathway is 27.0 gCO_2e/MJ.

5.8 SUGARCANE ETHANOL ATJ – [M]

The fuel production pathway considered in this section is sugarcane derived-ethanol, that is subsequently converted to drop-in fuel via dehydration, oligomerization and hydrotreating. The system boundary includes sugarcane cultivation and harvesting, transportation of the feedstock to a drop-in fuel production facility, fermentation to ethanol and upgrading to a drop-in fuel slate and finished jet fuel transportation and distribution. Three independent LCA sources for the sugarcane ethanol-to-jet fuel pathway are compared in Table 60: an updated version of the pathway described in Staples et al. (2014) and modelled in GREET.net (v.1.3.0.13239); the pathway modelled by JRC in the E3db; and a modified version of the pathway described in Bonomi et al. (2016), Chagas et al. (2016) and Klein et al. (2018). The lifecycle inventory data for this pathway is shown in Table 89 in the appendix.

Table 60: LCA results for sugarcane ethanol ATJ pathway [gCO_2e/MJ]

Data source	Model	Cultivation and harvesting	Feedstock transportation	Fermentation and EtOH upgrading	Jet fuel transportation	Total emissions	Midpoint value
MIT	GREET	13.7	1.6	4.6	0.4	**20.4**	
JRC	E3db	17.5	1.6	7.7	0.4	**27.2**	**24.1**
CTBE	ReCiPe	19.9	2.1	5.3	0.4*	**27.7**	

*Note that these emissions were not initially included in the CTBE data. Therefore, the value for jet fuel transportation emissions from the other data points were adopted to maintain consistency.

The MIT analysis draws on a number of sources to calculate the LCA value for sugarcane ethanol ATJ. For sugarcane cultivation and harvest, and transportation to the fuel production facility, the emissions and inputs are assumed to correspond to the default values in GREET.net for the "Sugarcane Production for Brazil Ethanol Plant" process. In addition, the jet fuel transportation step is assumed to correspond to the default "Renewable Jet Fuel Transportation" process in GREET.net. For sugarcane milling, Dias et al. (2009) was used to estimate the efficiency of sugar extraction, and process heat and electricity requirements, and Murphy & McKeogh (2004) was used to estimate electricity and heat co-generation from the co-produced bagasse. 85% of the theoretical maximum ethanol yield from glucose was assumed (Dugar & Stephanopolous, 2011). Pumping, agitation and aeration electricity requirements for saccharification and fermentation are taken from Najafpour (2007) and Couper et al. (2012). Ethanol distillation, dehydration, oligomerization and hydrotreating yields, and the electricity, process heat and hydrogen requirements, are based on Mei (2006) and proprietary data from Byogy.

The JRC data on sugarcane ethanol ATJ is based on the default sugarcane ethanol pathway aligned with the EU RED2 input values (Edwards et al., 2017) and related references, with the yield and utility requirements of the ethanol production and upgrading to jet based on the publicly available version of GREET (GREET-2016), computed with the E3db used by JRC.

The CTBE data is based on three recent studies: Bonomi et al. (2016), Chagas et al. (2016) and Klein et al. (2018). In contrast to Klein et al. (2018), it is not assumed that green diesel is used to substitute fossil diesel in agricultural operations, and in straw recovery from the field and transportation to the biorefinery. Ethanol dehydration, oligomerization and upgrading is based on Arvidsson & Lundin (2011), Heveling et al. (1998) and Gruber et al. (2012).

The largest differences in the sugarcane ethanol ATJ data are in the cultivation and harvesting steps, and fermentation and ethanol upgrading steps. For the agricultural step, the assumed areal yield of sugarcane (86.7, 62.6 and 76.0 metric ton/ha in the MIT, JRC and CTBE analyses, respectively) is one key difference in the LCA inventories. In addition, the CTBE analysis draws on a larger set of inputs for inventory (e.g. accounting for gypsum application to the soil, and emissions from transportation of straw, vinasse, and inputs), which contributes to higher calculated agricultural emissions. For the fermentation and ethanol upgrading step, a significant contributor to the difference in emissions is the assumed yield of drop-in fuel from ethanol (0.54 kg/kg of ethanol in the MIT and JRC analyses, compared to 0.45 kg/kg in the CTBE analysis). Despite these differences, the overall LCA results from the three data sources are within 10% of the aviation fuel baseline (8.9 gCO_2e/MJ) threshold.

The agreed default core LCA value for sugarcane ethanol ATJ is 24.1 gCO_2e/MJ.

5.9 CORN GRAIN ETHANOL ATJ – [M]

The fuel production pathway considered in this section is corn grain derived-ethanol, that is subsequently converted to drop-in fuel via dehydration, oligomerization and hydrotreating. The system boundary includes corn grain cultivation and harvesting, transportation of the feedstock to a drop-in fuel production facility, fermentation to ethanol and upgrading to a drop-in fuel slate, and finished jet fuel transportation and distribution. Two independent LCA sources for the corn grain ethanol-to-jet fuel pathway are compared in Table 61: an updated version of the pathway described in Staples et al. (2014) and modelled in GREET.net (v.1.3.0.13239); and the same pathway as modelled by JRC in the E3db. The lifecycle inventory data for this pathway is shown in Table 90 in the appendix.

Table 61: LCA results for corn grain ethanol ATJ pathway [gCO_2e/MJ]

Data source	Model	Cultivation and harvesting	Feedstock transportation	Fermentation and EtOH upgrading	Jet fuel transportation	Total emissions	Midpoint value
MIT	GREET	21.3	1.2	42.7	0.4	**65.6**	**65.7**
JRC	E3db	31.2	2.1	32	0.4	**65.7**	

The MIT analysis draws on a number of sources to calculate the LCA value for corn ethanol ATJ. For corn grain cultivation and harvest, and transportation to the fuel production facility, the emissions and inputs are assumed to correspond to the default US values in GREET.net for the "Corn Production for Biofuel Refinery" process. In addition, the jet fuel transportation step is assumed to correspond to the default "Renewable Jet Fuel Transportation" process in GREET.net. For corn grain milling, Mei (2006) was used to estimate the efficiency of starch extraction, and process heat and electricity requirements, and saccharification and fermentation efficiencies of 98% and 85%, respectively, of the theoretical maximums were assumed (Dugar & Stephanopolous 2011). Pumping, agitation and aeration electricity requirements for saccharification and fermentation are taken from Najafpour (2007) and Couper et al. (2012). Ethanol distillation, dehydration, oligomerization and hydrotreating yields, and the electricity, process heat and hydrogen requirements, are based on (Mei, 2006) and proprietary data from Byogy.

The JRC data is based on the corn grain ethanol ATJ pathway as modelled in the E3. The JRC data on corn grain ethanol ATJ is based on the default corn grain ethanol pathway aligned with EU RED2 input values (Edwards et al., 2017) and related references with the yield and utility requirements of the ethanol production and upgrading to jet based on the publicly available version of GREET (GREET-2016), computed with the E3db used by JRC.

The largest differences in the corn grain ethanol ATJ data from MIT and JRC are in the cultivation and harvesting, and fermentation and ethanol upgrading steps. On the agricultural step, the difference in the assumed areal yield of corn grain (10.4 metric ton/ha in the MIT analysis, compared to 7.1 metric tonnes/ha in the JRC analysis) drives the discrepancy in emissions. For the fermentation and ethanol upgrading step, a significant contributor to the difference in emissions is the quantity of natural gas for process heat required for distillation, dehydration, oligomerization and hydrotreating (8.4 MJ/kg of ethanol input in the MIT analysis, compared to 2.1 MJ/kg in the JRC analysis). Despite these differences, the overall LCA results from the two data sources are within 10% of aviation fuel baseline threshold (8.9 gCO_2e/MJ).

Therefore, the agreed default core LCA value for corn grain ethanol ATJ is 65.7 gCO_2e/MJ.

AGRICULTURAL RESIDUES ETHANOL ATJ – [R]

The fuel production pathway considered in this section is agricultural residues derived-ethanol, that is subsequently converted to drop-in fuel via dehydration, oligomerization, and hydrotreating. The system boundary includes feedstock collection, transportation of the feedstock to a drop-in fuel production facility, fermentation to ethanol and upgrading to a drop-in fuel slate, and finished jet fuel transportation and distribution. Two different ATJ conversion plant layouts, standalone and integrated designs, are considered. In the standalone configuration, it is assumed that an ATJ facility takes ethanol from the market or a separate ethanol production facility, while the integrated configuration assumes co-locating the ATJ process with ethanol production. The integrated plant layout enables heat integration, so reduction to CLCA emissions per MJ of fuel. Two LCA values of agricultural residues ethanol ATJ pathways are presented in Table 62.

Table 62: LCA results for agricultural residues ethanol ATJ pathway [gCO_2e/MJ]

Conversion Design	Data source	Model	Feedstock collection	Feedstock transportation	Jet fuel production	Jet fuel transportation	Total emissions
Standalone	Consensus model	GREET	3.5	3.1	32.7	0.4	**39.7**
Integrated	Consensus model	GREET	3.6	3.2	17.4	0.4	**24.6**

For ethanol production from agricultural residues, the corn stover ethanol production pathway in GREET was used. Table 91 presents the inputs and outputs of the ethanol production pathway. Note that the integrated case utilizes the electricity from the ethanol production for the ATJ process, which was adjusted. For the ATJ process, FTG's CLCA modeling group has reviewed and collected the life-cycle inventory of the ethanol-to-jet process from various research papers as well as the industry data (Mei, 2006; Braz et al., 2018; Crawford et al., 2016, Byogy, and LanzaTech). For the integrated case, adjusted natural gas and electricity inputs for the ATJ-SPK from ethanol conversion process were considered to model system integration between ethanol production and jet conversion processes. The system integration enables reduced intensity of the ethanol purification process, and heat and electricity generated from ethanol production are sufficient to eliminate the external natural gas and electricity requirements for the ATJ-SPK from ethanol process (Han et al., 2017). Table 91 presents the life-cycle inventories of the ATJ process.

FTG's CLCA modeling group agreed to have ANL calculate the CLCA values using the new consensus datasets for the pathways using the GREET model. The calculations have been verified by Hasselt University and approved by the modelling team.

Therefore, the agreed default core LCA values for standalone and integrated agricultural residues ethanol ATJ are 39.7 and 24.6 gCO_2e/MJ, respectively.

FOREST RESIDUES ETHANOL ATJ – [R]

The fuel production pathway considered in this section is forest residues derived-ethanol, that is subsequently converted to drop-in fuel via dehydration, oligomerization, and hydrotreating. The system boundary includes feedstock collection, transportation of the feedstock to a drop-in fuel production facility, fermentation to ethanol and upgrading to a drop-in fuel slate, and finished jet fuel transportation and distribution. Two different ATJ conversion plant layouts, standalone and integrated designs, are considered. In the standalone configuration, it is assumed that an ATJ facility takes ethanol from the market or a separate ethanol production facility, while the integrated configuration assumes co-locating the ATJ process with

ethanol production. The integrated plant layout enables heat integration, so reduction to CLCA emissions per MJ of fuel. Two LCA values of forest residues ethanol ATJ pathways are presented in Table 63.

Table 63: LCA results for forest residues ethanol ATJ pathway [gCO_2e/MJ]

Conversion Design	Data source	Model	Feedstock collection	Feedstock transportation	Jet fuel production	Jet fuel transportation	Total emissions
Standalone	Consensus model	GREET	1.8	2.4	35.5	0.4	**40.0**
Integrated	Consensus model	GREET	1.8	2.4	20.3	0.4	**24.9**

For ethanol production from forest residues, GREET was used. Table 91 presents the inputs and outputs of the ethanol production pathway. Note that the integrated case utilizes the electricity from the ethanol production for the ATJ process, which was adjusted. For the ATJ process, FTG's CLCA modeling group has reviewed and collected the life-cycle inventory of the ethanol-to-jet process from various research papers as well as the industry data (Mei, 2006; Braz et al., 2018; Crawford et al., 2016, Byogy, and LanzaTech). For the integrated case, adjusted natural gas and electricity inputs for the ATJ-SPK from ethanol conversion process were considered to model system integration between ethanol production and jet conversion processes. The system integration enables reduced intensity of the ethanol purification process, and heat and electricity generated from ethanol production are sufficient to eliminate the external natural gas and electricity requirements for the ATJ-SPK from ethanol process (Han et al., 2017). Table 91 presents the life-cycle inventories of the ATJ process.

FTG's CLCA modeling group agreed to have ANL calculate the CLCA values using the new consensus datasets for the pathways using the GREET model. The calculations have been verified by Hasselt University and approved by the modelling team.

Therefore, the agreed default core LCA values for standalone and integrated forest residues ethanol ATJ are 40.0 and 24.9 gCO_2e/MJ, respectively.

HERBACEOUS ENERGY CROPS ETHANOL ATJ – [M]

The fuel production pathways considered in this section are herbaceous lignocellulosic energy crops (miscanthus and switchgrass) derived-ethanol, that is subsequently converted to drop-in fuel via dehydration, oligomerization, and hydrotreating. The system boundary includes cultivation, feedstock collection, transportation of the feedstock to a drop-in fuel production facility, fermentation to ethanol and upgrading to a drop-in fuel slate, and finished jet fuel transportation and distribution. Two different ATJ conversion plant layouts, standalone and integrated designs, are considered. In the standalone configuration, it is assumed that an ATJ facility takes ethanol from the market or a separate ethanol production facility, while the integrated configuration assumes co-locating the ATJ process with ethanol production. The integrated plant layout enables heat integration, so reduction to CLCA emissions per MJ of fuel. Two sets of the LCA values of miscanthus and switchgrass ethanol ATJ pathways are presented in Table 64.

Table 64: LCA results for miscanthus and switchgrass ethanol ATJ pathway [gCO_2e/MJ]

Feedstock	Conversion Design	Data source	Model	Cultivation and feedstock collection	Feedstock transportation	Jet fuel production	Jet fuel transportation	Total emissions
Miscanthus	Standalone	Consensus model	GREET	8.8	1.4	32.7	0.4	**43.3**
	Integrated	Consensus model	GREET	9.0	1.4	17.4	0.4	**28.3**
Switchgrass	Standalone	Consensus model	GREET	9.6	1.2	32.7	0.4	**43.9**
	Integrated	Consensus model	GREET	9.8	1.2	17.4	0.4	**28.9**

For ethanol production from miscanthus and switchgrass, GREET was used. Table 91 presents the inputs and outputs of the ethanol production pathway. Note that the integrated case utilizes the electricity from the ethanol production for the ATJ process, which was adjusted. For the ATJ process, FTG's CLCA modeling group has reviewed and collected the life-cycle inventory of the ethanol-to-jet process from various research papers as well as the industry data (Mei, 2006; Braz et al., 2018; Crawford et al., 2016, Byogy, and LanzaTech). For the integrated case, adjusted natural gas and electricity inputs for the ATJ-SPK from ethanol conversion process were considered to model system integration between ethanol production and jet conversion processes. The system integration enables reduced intensity of the ethanol purification process, and heat and electricity generated from ethanol production are sufficient to eliminate the external natural gas and electricity requirements for the ATJ-SPK from ethanol process (Han et al., 2017). Table 91 presents the life-cycle inventories of the ATJ process.

FTG's CLCA modeling group agreed to have ANL calculate the CLCA values using the new consensus datasets for the pathways using the GREET model. The calculations have been verified by Hasselt University and approved by the modelling team.

Therefore, the agreed default core LCA values for standalone and integrated miscanthus ethanol ATJ are 43.3 and 28.3 gCO_2e/MJ, respectively. The agreed default core LCA values for standalone and integrated switchgrass ethanol ATJ are 43.9 and 28.9 gCO_2e/MJ, respectively.

WASTE GAS ETHANOL TO JET, VIA MICROBIOLOGIC CONVERSION ROUTE [W]

The "waste gas ethanol to jet, via microbiologic conversion route" refers to Sustainable Aviation Fuels produced from a waste gas stream which is made of materials with inelastic supply and no economic value[12]. The term waste, used in the definition, refers to processing gasses or exhaust gases which are produced as an unavoidable and unintentional consequence of the production process in industrial installations, and for these default values, processed via a microbiological conversion step.

The default values have been calculated within clear system boundaries, based on the assumption that the waste gases were previously flared, without any energy being recovered from them. Therefore it is fundamental to apply these values and/or the proposed methodological approach, according to the proper case and within appropriate system boundaries. CAEP agreed upon using an updated life- cycle inventory

[12] *CORSIA DEFINITION OF WASTE: Wastes are materials with inelastic supply and no economic value. A waste is any substance or object which the holder discards or intends or is required to discard*

of updated ethanol-to-jet process for cellulosic ethanol pathways for standalone and integrated systems, the so called "consensus model".

CAEP used a "carbon-neutral" approach to produce these default values, since emissions from waste gas flaring offset the waste gas-derived emissions from fuel production and use. Under this assumption, the previous fate of the carbon atoms in the waste gas does not differ with the net realization of CO_2 emissions from airplane use, nor is the production process from which these were derived influenced by diverting these gases for aviation fuel production as there was no energy recovery from the gases.

Table 65 shows the total GHG emissions for SAF produced from waste gas, via a microbiologic conversion route, under these system boundaries. The standalone default values are applicable to an E2J facility that uses ethanol that was produced at a separate ethanol production facility. The integrated default values are applicable to a co-located facility where heat is integrated between the two systems (ethanol production and hydrocarbon production) so that no additional energy is required to meet the heat demand for the E2J process.

Table 65: core LCA results for waste gas pathways, via microbiologic conversion route

	Data Source	**Model**	**Waste gases to Ethanol**	**Ethanol to jet**	**Fuel transportation**	**core LCA default value [gCO_2e/MJ]**
Standalone	Consensus database	Consensus Model	21.5	19.8	1.0	42.4
Integrated	Consensus database	Consensus Model	21.5	7.5	0.4	29.4

As the gases are diverted from a previous point of emission, but without being now considered as a net emission elsewhere (e.g., the airplane), it is fundamental to guarantee (e.g., have an assessment) that the emissions from the process generating these gases keeps reporting the associated GHG emission in the national registry as a part of the GHG inventory and/or equivalent reporting obligation. This information should be made available to, and verifiable by, the SCS and be part of the information that is passed through the chain of custody from the producer to the relevant CORSIA database.

The calculations used a carbon-neutral approach since emissions from waste gas flaring offset the waste gas-derived emissions from fuel production and use. Figure 11 presents the system boundary of the waste gas ethanol-to-jet pathway. Note that a portion of the microorganism inputs for ethanol production is available as a co-product, which can be used as an animal feed.

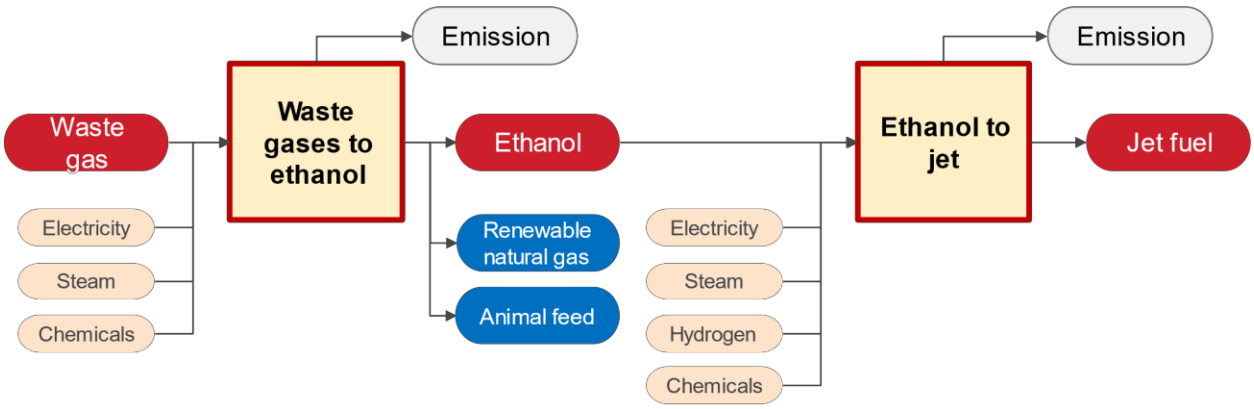

Figure 11: The system boundary of the waste gas ethanol-to-jet pathways

Table 66 provides the mass/energy information used for ethanol production from waste gas.

Table 66: Major parameters for the waste gases to ethanol and ethanol to jet processes

Waste gases to Ethanol	Inputs	Waste gas[+]	1.86 mmBtu (409 kg)
		Electricity	148,000 Btu
		Natural gas	62,600 Btu
	Outputs	Ethanol	1.02 mmBtu
		Renewable natural gas	0.028 mmBtu
		Biomass for animal feed	0.127 mmBtu
Ethanol to jet	Inputs	Ethanol	1.02mmBtu
		Electricity	28,100 Btu
		Natural gas	58,900 Btu
		Hydrogen	31,900 Btu
	Outputs	Jet and diesel	1.0 mmBtu

[+] Carbon content: 27% | moisture content: 4%

For the ethanol-to-jet process, the LCA calculations considered two datasets representing life cycle inventories of standalone and integrated configurations, which are provided in Table 67.

Table 67: Life-cycle inventories of the ATJ-SPK from ethanol process

Inputs		**Standalone**	**Integrated**
Feedstock (ethanol)	MJ	1.06	1.06
Hydrogen	MJ	0.06	0.06
Natural gas	MJ	0.18	**0**
Electricity	MJ	0.02	**0**
Total Energy Input	MJ	1.32	1.12
Outputs			
Jet fuel and energy products	MJ	1	1
Jet energy share in total energy output (%)		75%	75%
Energy efficiency (%)		76%	90%

It is worth remarking that the calculations and results apply only to the case where gases were previously flared without any energy recovery. In any other case, the assumptions and the approach taken would not hold and cannot be used to derive actual values.

CHAPTER 6. **HYDROPROCESSED ESTERS AND FATTY ACIDS CO-PROCESSED AT PETROLEUM REFINERIES**

6.1 LCA APPROACHES TO CO-PROCESSED HEFA

Two complementary approaches were used to calculate the core LCA values of SAFs produced from used cooking oil, soybean oil, and tallow co processed in petroleum refineries, as follows:

- Bottom-up approach: Co-processing was simulated using a linear programming (LP) model for petroleum refineries. The LP model considers 5 vol% of bio-feedstock inputs to two insertion points (hydrotreater [HDT] and hydrocracker [HYK]). The LP model estimates the input and output streams of each process in modeled petroleum refineries with and without co-feeding of bio-feedstocks.
- Top-down approach: A top-down approach was carried out to compute core LCA values for co-processing using results from available studies. The top-down approach is used for validating results from the bottom-up approach.

Generally, the same system boundary used for standalone SAF was used to calculate core LCA values for co-processed SAF (see Figure 12). The feedstock production stage covers all inputs to produce three types of bio-feedstocks (soybean oil, used cooking oil [UCO], and tallow). However, UCO and tallow are considered as waste and therefore do not take into account emission burdens of feedstock production except for collection, recovery, extraction, and processing. Transportation and distribution used the same assumptions which were used for "standalone" SAF. For jet fuel combustion, CO2 emissions from the combustion of co-processed SAFs are considered carbon-neutral, like standalone SAFs.

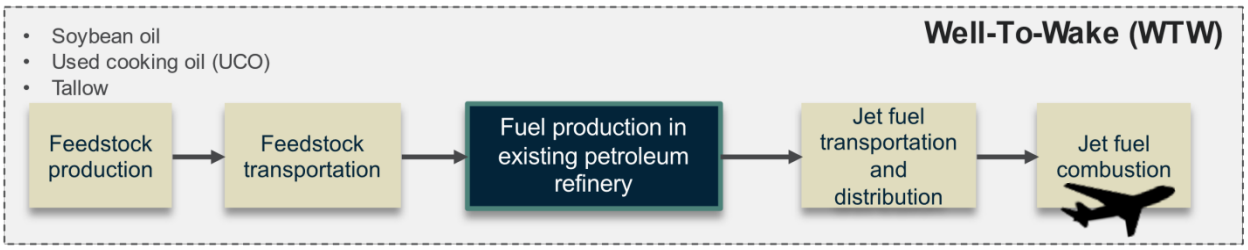

Figure 12: The system boundary of co-processed SAFs in a petroleum refinery

Regarding the allocation method, Figure 13 describes the marginal approach used for calculating the refinery carbon intensity of co-processed SAFs. The marginal approach allocates all changes in inputs and outputs in a scenario with co-processing of biogenic feedstocks vs. a scenario without co- processing of biogenic feedstocks. It requires normalizing the crude oil inputs and evaluating the changes in energy use, refinery emissions, and fuel production. Note that biogenic carbon emissions from the refinery are considered carbon neutral.

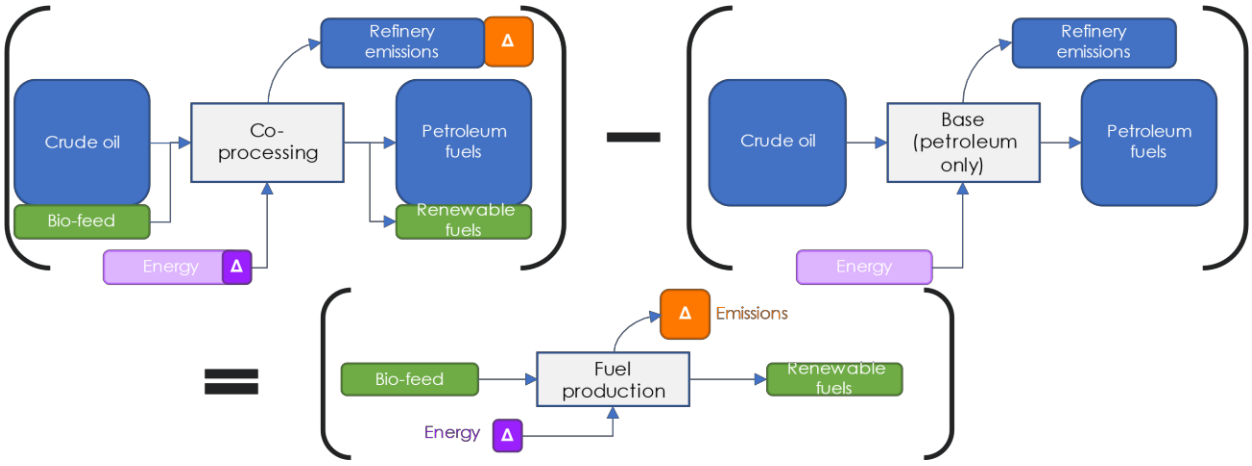

Figure 13: Schematic of the marginal analysis used for calculating the refinery carbon intensity of co-processed SAFs. After normalizing the crude oil inputs, the baseline (petroleum only) case is subtracted from the co-processing case. All the changes in energy use and emissions are then allocated to renewable fuel production

Bio-feedstocks are inserted into either a hydrotreater or hydrocracker, which would generate renewable fuels including jet and diesel. Since renewable fuels are only produced from the co- processing units, we use energy allocation among products for this process. When the so-called process- level energy allocation is used, the refinery carbon intensities remain the same for all 'renewable fuel' products (i.e., renewable jet and diesel) from the process.

6.2 REFINERY EMISSIONS: BOTTOM-UP APPROACH

From the LP results, the refinery carbon intensities (CIs) of co-processing cases are calculated using the marginal approach as shown in Figure 14. The refinery CIs of co-processing are compared with those of standalone hydroprocessed esters and fatty acids (HEFA) pathways in CORSIA.

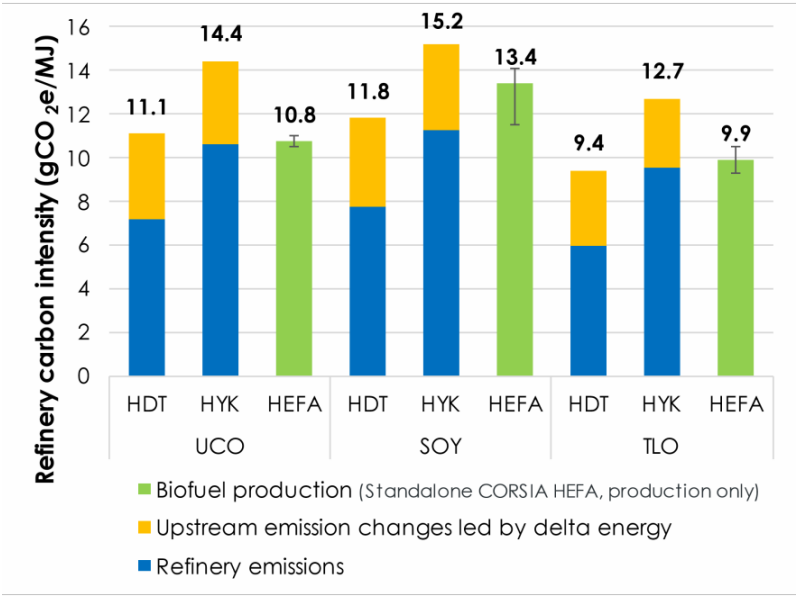

Figure 14: Refinery carbon intensity (gCO2e/MJ) using the marginal approach. UCO: used cooking oil, SOY: soy oil, TLO: tallow, HDT: biofeed inserted to hydrotreater, HYK: biofeed inserted to hydrocracker. Biofuel production (green bars) represents the averaged fuel production emission values of standalone CORSIA neat HEFA pathways. The error bars represent the ranges in the CORSIA supporting document

The results show that hydrocracker cases output slightly higher emissions compared to hydrotreater cases mainly due to higher hydrogen requirements per unit of renewable fuel production. However, overall, the refinery CIs are quite comparable (<3.5 g/MJ difference) when using the same bio- feedstock.

6.3 REFINERY EMISSIONS: TOP-DOWN APPROACH

The top-down approach utilizes publicly available data from established co-processing refineries, literature, and CORSIA neat HEFA values to compare to the bottom-up LCA values presented in Section 6.2. Figure 15 summarizes the results for the refinery step.

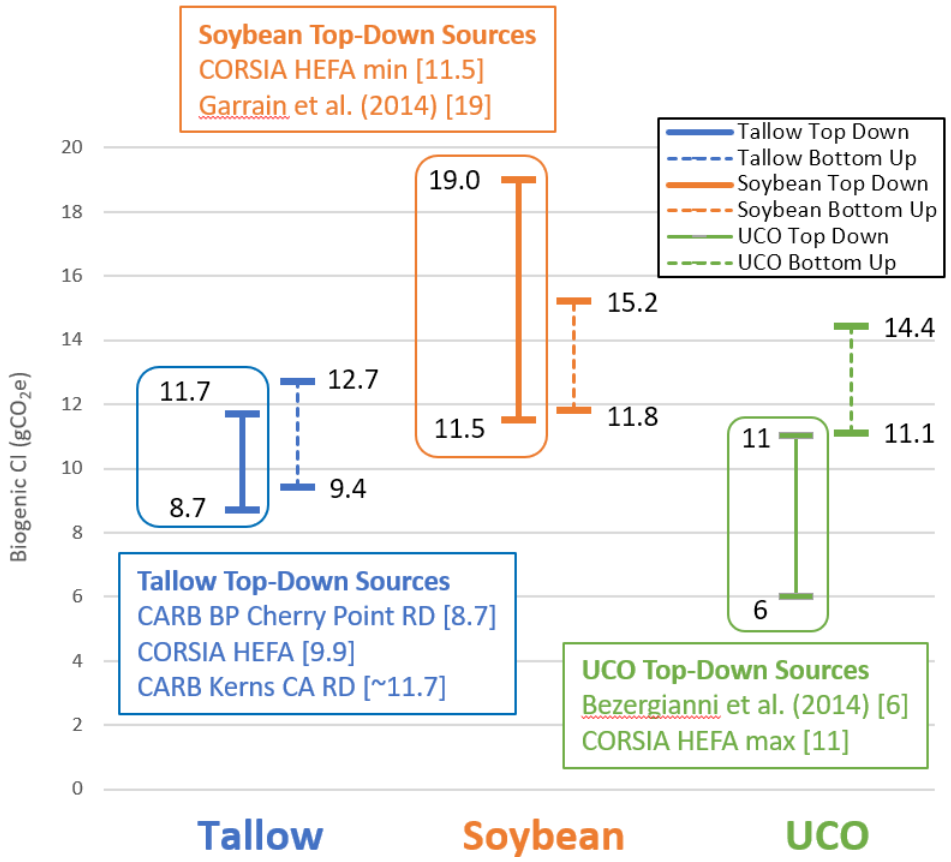

Figure 15: Comparison of biogenic bottom-up LCA values to top-down estimated LCA, refinery production emissions only

For tallow, a set of reference values was compiled from the literature. These include: (1) BP's application for a certified pathway within the California Air Resources Board (CARB) Low Carbon Fuel Standard (LCFS) for renewable Diesel (RD) produced by co-processing with tallow at the Cherry Point facility in Washington state (CARB, 2019); (2) the midpoint value for feedstock-to-fuel conversion step in CORSIA HEFA (ICAO, 2019); and (3) Kerns' application for the same pathway as BP (CARB,2020). The refinery-level CLCA emissions are shown in Figure 15. We note that the Kerns value is estimated, because the LCA breakout is redacted in the publicly available report. Thus, the average fraction of tallow rendering carbon intensity divided by the total carbon intensity, excluding finished fuel transportation (well to tank), is calculated from the BP Cherry Point and CORSIA HEFA sources. This fraction (.584) is used to estimate the tallow rendering emissions for Kerns (17.3gCO2e/MJ) which is then subtracted from the reported well-to-tank RD production emissions (29.567gCO2e/MJ), along with the reported tallow transport emissions

(0.634gCO2e/MJ). This results in the 11.7gCO2e/MJ maximum value for top-down tallow CI shown in Figure 15. Although the Kerns report also lists a margin of safety CI addition and a propoane allocation factor, these are again redacted and not explicitly accounted for in this estimate. As seen in Figure 15, the top-down and bottom-up CI values are generally well-aligned.

For soybean, two sources are used: the minimum value for production from CORSIA neat HEFA; and data from Garrain et al. (2014). The CI value for production emissions was calculated using a fraction of production emissions intensity of the total intensity from CORSIA HEFA, multiplied to the biogenic CI calculated from Garrain et al. (2014). As shown in Figure 15, the bottom-up values are completely within the top-down range of CI values.

For used cooking oil, the first source is from Bezergianni et al. (2014). The CI value for production emissions was calculated in the same manner as for soybean (see Section 3.2.3). The value likely deviates from the bottom-up LCA values due to the differences in input fossil feedstock used (Heavy Atmospheric Gas Oil vs. middle distillates). This study also did not report details of energy content broken out for each fuel product, so some simplifying assumptions were made to estimate the CI. These factors may be contributing to the misalignment between the top-down and bottom-up values. However, the co- processing bottom-up value closely matches (11.1gCO2e/MJ) the CORSIA HEFA max value (11gCO2e/MJ).

6.4 CLCA VALUES OF CO-PROCESSED USED COOKING OIL, SOYBEAN OIL, AND TALLOW

The CLCA values, including both co-processing and the rest of the supply chain, of co-processed fuels show consistent trends and comparable results with those of standalone neat HEFA production pathways in CORSIA, as shown in Figure 16.

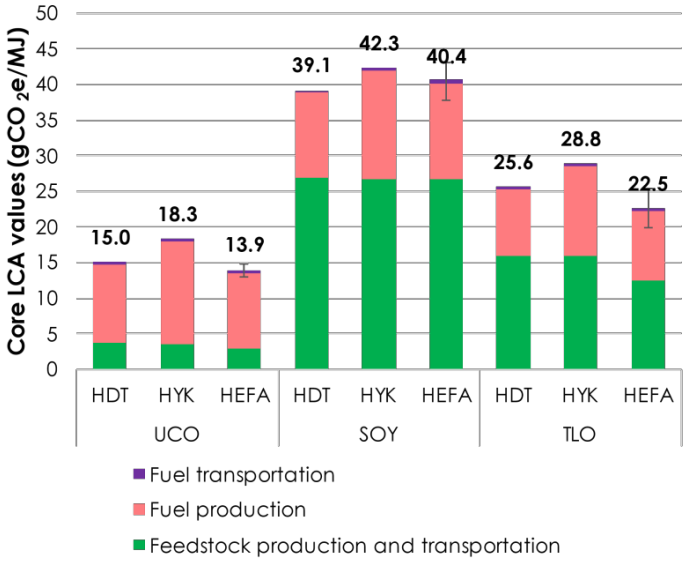

Figure 16: CLCA values of co-processed SAFs using the marginal approach (bottom-up). UCO: used cooking oil, SOY: soy oil, TLO: tallow, HDT: biofeed inserted to hydrotreater, HYK: biofeed inserted to hydrocracker. Biofuel represents the averaged fuel production emission values of standalone CORSIA neat HEFA pathways. The error bars represent the ranges in the CORSIA supporting document. The fuel production stage (pink bars) represents the refinery CI in Figure 14

Since the CLCA values of co-processed fuels are within the agreed definition of a default LCA value (<8.9 gCO2e/MJ) for each feedstock, the midpoint value was adopted as a default LCA value for each feedstock, as shown in Table 68.

Table 68: CLCA values of co-processed SAFs in terms of gCO2e/MJ. HDT: biofeedstock inserted to hydrotreater, HYK: biofeedstock inserted to hydrocracker.

Feedstock	**Insertion point**	**Feedstock production / transportation**	**Fuel production**	**Fuel transportation**	Total	**default core LCA value** (gCO_2e/MJ)
used cooking oil (UCO)	HDT	3.6	11.1	0.3	15.0	16.7
	HYK	3.6	14.4	0.3	18.3	
Soybean oil	HDT	27.0	11.8	0.3	39.1	40.7
	HYK	26.8	15.2	0.3	42.3	
tallow	HDT	15.9	9.4	0.3	25.6	27.2
	HYK	15.8	12.7	0.3	28.8	

CHAPTER 7. **SUMMARY OF DEFAULT CORE LCA VALUES**

Table 69 summarizes the list of SAF pathways for which default core LCA values have been agreed for use under CORSIA.

Table 69: Summary of default core LCA values to date

Conversion process	**Feedstock**	**Default core LCA value [gCO_2e/MJ]**
Fischer-Tropsch (FT)	Agricultural residues	7.7
	Forestry residues	8.3
	MSW, 0% NBC	5.2
	MSW, NBC as % of total C	NBC*170.5+5.2
	Short-rotation woody crops	12.2
	Herbaceous energy crops	10.4
Hydro-processed esters and fatty acids (HEFA)	Tallow	22.5
	Used cooking oil	13.9
	Palm fatty acid distillate	20.7
	Corn oil	17.2
	Soybean oil	40.4
	Rapeseed oil	47.4
	Camelina	42
	Palm oil - closed pond	37.4
	Palm oil - open pond	60
	Brassica carinata	34.4
	Jatropha	46.8
Synthesized Iso-Paraffins (SIP)	Sugarcane	32.8
	Sugarbeet	32.4
Iso-butanol Alcohol-to-jet (ATJ)	Sugarcane	24.0
	Agricultural residues	29.3
	Forestry residues	23.8
	Corn grain	55.8
	Herbaceous energy crops	43.4
	Molasses	27.0
Ethanol Alcohol-to-jet (ATJ)	Sugarcane	24.1
	Corn grain	65.7
	Agricultural residues - standalone	39.7
	Agricultural residues - integrated	24.6
	Forest residues - standalone	40.0
	Forest residues - integrated	24.9
	Miscanthus - standalone	43.3
	Miscanthus - integrated	28.3
	Switchgrass - standalone	43.9
	Switchgrass - integrated	28.9

	Waste gases (Ethanol produced via microbiologic conversion route, Standalone conversion design)	42.4
	Waste gases (Ethanol produced via microbiologic conversion route, Integrated conversion design)	29.4
Hydro-processed esters and fatty acids (HEFA) co-processed at petroleum refineries	Tallow	27.2
	Used cooking oil	16.7
	Soybean oil	40.7

REFERENCES

Achten, W. M. J. et al. (2008). Jatropha biodiesel production and use. Biomass and Bioenegy, 32, 1063-1084.

Alherbawi et al. (2021a). Optimum sustainable utilization of the whole fruit of Jatropha curcas: An energy, water and food nexus approach. Renewable and Sustainable Energy Reviews, 137, 110605.

Alherbawi et al. (2021b). A novel integrated pathway for Jet Biofuel production from whole energy crops: A Jatropha curcas case study. Energy Conversion and Management, 229, 113662

Argonne National Laboratory. The greenhouse gases, regulated emissions, and energy use in transportation (GREET) computer model GREET1_2020. Argonne, IL; 2020.

Argonne National Laboratory. (2015). Retrieved 09 30, 2016, from Greenhousegases, Regulated Emissions, and Energy use in Transportation (GREET) Model: http://greet.es.anl.gov/

Arvidsson, M., & Lundin, B. (2011). Process integration study of a biorefinery producing ethylene from lignocellulosic feedstock for a chemical cluster. MS Thesis, Chalmers University of Technology, 2011: http://publications.lib.chalmers.se/records/fulltext/140886.pdf

Bonomi, A., Cavalett, O., Cunha, M. P. D., & Lima, M. A. (2016). Virtual Biorefinery. Cham: Springer International Publishing.

Buchspies, B., M. Kaltschmitt (2016), Life cycle assessment of bioethanol from wheat and sugar beet discussing environmental impacts of multiple concepts of co-product processing in the context of European Renewable Energy Directive, Biofuels, 7(2), p. 141-153

Byogy Renewables (2011). Alcohol To Jet (ATJ) Emerging Through ASTM. ICAO Aviation And Sustainable Alternative Fuels Workshop, Montreal Canada.

CARB, 2017. Co-processing of biogenic feedstocks in petroleum refineries. Draft Staff Discussion Paper. Retrieved from https://ww3.arb.ca.gov/fuels/lcfs/lcfs_meetings/020717_staffdiscussionpaper.pdf

Cashman, S. A., Moran, K. M., & Gaglione, A. G. (2015). Greenhouse gas and energy life cycle assessment of pine chemicals derived from crude tall oil and their substitutes. Journal of Industrial Ecology, 20(5), 1108-1121.

Chagas, M.F., R.O. Bordonal, O. Cavalett, J.L.N. Carvalho, A. Bonomi Jr., and N. La Scala. "Environmental and economic impacts of different sugarcane production systems in the ethanol biorefinery." Biofuels, Bioproducts and Biorefining, 10(1), 2016: 89-106.

Chaturvedi, S. et al. (2012). Bio-diesel waste as tailored organic fertilizer for improving yields and nutritive values of Lycopercicum esculatum (tomato) crop. Journal of Soil Science and Plant Nutrition, 12 (4), 801-810.

Chico, F. et al. (2013). Techno-economic evaluation for producing suitable animal feed protein from jatropha curcas press cake, M.S. Thesis, Wageningen University and Research.

Choo, Y. M., Muhamad, H., Hashim, Z., Subramaniam, V., Puah, C. W., & Tan, Y. A. (2011). Determination of GHG contributions by subsystems in the oil palm supply chain using the LCA approach. *The International Journal of Life Cycle Assessment, 16*, 669-681.

Couper, J. R., Penney, W. R., & Fair, J. R. (2012). Chemical Process Equipment-Selection and Design, Chapter 10 (Revised 3rd Edition). Butterworth-Heinemann.

Cox, K., Renouf, M., Dargan, A., Turner, C., & Klein‐Marcuschamer, D. (2014). Environmental life cycle assessment (LCA) of aviation biofuel from microalgae, Pongamia pinnata, and sugarcane molasses. Biofuels, Bioproducts and Biorefining, 8(4), 579-593.

D'Avino, L., Dainelli, R., Lazzeri, L., & Spugnoli, P. (2015). The role of co-products in biorefinery sustainability: energy allocation versus substitution method in rapeseed and carinata biodiesel chains. Journal of Cleaner Production, 94, 108-115.

Davis, R., Tao, L., Tan, E. C. D., Biddy, M. J., Beckham, G. T., Scarlata, C., ... & Knorr, D. (2013). Process design and economics for the conversion of lignocellulosic biomass to hydrocarbons: dilute-acid and enzymatic deconstruction of biomass to sugars and biological conversion of sugars to hydrocarbons (No. NREL/TP-5100-60223). National Renewable Energy Lab.(NREL), Golden, CO (United States).

Dias, M. O., Ensinas, A. V., Nebra, S. A., Maciel Filho, R., Rossell, C. E., & Maciel, M. R. W. (2009). Production of bioethanol and other bio-based materials from sugarcane bagasse: integration to conventional bioethanol production process. Chemical Engineering Research and Design, 87(9), 1206-1216.

Dugar, D. & Stephanopoulos, G. (2011). Relative potential of biosynthetic pathways for biofuels and bio-based products. *Nature Biotechnology*, 29(12), 1074-1078.

Dunn, J. B., Adom, F., Sather, N., Han, J., Snyder, S., He, C., ... & You, F. (2015). Life-cycle Analysis of Bioproducts and their Conventional Counterparts in GREET (No. ANL/ESD-14/9 Rev.). Argonne National Lab.(ANL), Argonne, IL (United States).

Edwards, R., M. Padella, J. Giuntoli, R. Koeble, A. O'Connell, C. Bulgheroni, and L. Marelli. Definition of input data to assess GHG default emissions from biofuels in EU legislation, Version 1c – July 2017, (2017). DOI: 10.2790/658143

Elgowainy, A. et al. (2012) Life Cycle Analysis of Alternative Aviation Fuels in GREET. Argonne National Laboratory, Argonne, IL, USA.

Fiorentino, G., Ripa, M., Mellino, S., Fahd, S., & Ulgiati, S. (2014). Life cycle assessment of Brassica carinata biomass conversion to bioenergy and platform chemicals. Journal of cleaner production, 66, 174-187.

Geleynse, S., Brandt, K., Wolcott, M., Garcia-Perez, M., & Zhang, X. (2018). The Alcohol-to-Jet Conversion Pathway for Drop‐In Biofuels: Techno‐Economic Evaluation. ChemSusChem.

Ghosh et al. (2012). Value addition of jatropha cake and its utilisation as manure in jatropha and other crops. In: Carels, N., Sujatha, M., Bahadar, B. (eds.) Jatropha, Challenges for a New Energy Crop: Volume 1: Farming, Economics and Biofuel, pp. 355–368. Springer Science + Business Media, New York.

Gomes, et al. (2018) Current strategies for the detoxification of jatropha curcas seed cake: A review. J. Agric. Food. Chem.66, 2510-2522.

Groode, T. A., & Heywood, J. B. (2008). Biomass to ethanol: potential production and environmental impacts (Vol. 69, No. 06).

Gruber, P. R., Peters, M. W., Griffith, J. M., Al Obaidi, Y., Manzer, L. E., Taylor, J. D., & Henton, D. E. (2012). U.S. Patent No. 8,193,402. Washington, DC: U.S. Patent and Trademark Office.

Han, J., Elgowainy, A., Palou-Rivera, I., Dunn, J. B., & Wang, M. Q. (2011). Well-to-wheels analysis of fast pyrolysis pathways with the GREET model (No. ANL/ESD/11-8). Argonne National Lab.(ANL), Argonne, IL (United States).

Heveling, J., Nicolaides, C. P., & Scurrell, M. S. (1998). Catalysts and conditions for the highly efficient, selective and stable heterogeneous oligomerisation of ethylene. Applied Catalysis A: General, 173(1), 1-9.

Intergovernmental Panel on Climate Change (IPCC), Climate Change 2014 Synthesis Report, 2014. https://www.ipcc.ch/pdf/assessment-report/ar5/syr/SYR_AR5_FINAL_full.pdf [accessed August 30, 2016]

International Energy Agency (IEA) (2020). India 2020 Energy Policy Review.

Jingura, R. M. et al. (2018). Technical Options for Valorisation of Jatropha Press-Cake: A Review, Waste Biomass Valorization 9, 701-703.

Johnston, G. (Gevo): Alcohol to jet - isobutanol; ICAO Seminar on alternative fuels 2017, ICAO Headquarters, Montréal, 8-9 February 2017

Kaltschmitt, M., & Reinhardt, G. A. (1997). Nachwachsende Energieträger. In Grundlagen, Verfahren, ökologische Bilanzierung. Vieweg, Braunschweig/Wiesbaden.

Kaltschmitt, M., Hartmann, H (2001). Energie aus Biomasse: Grundlagen, Techniken und Verfahren.

Karatzos, S., McMillan, J. D., & Saddler, J. N. (2014). The potential and challenges of drop-in biofuels. *Report for IEA Bioenergy Task, 39*.

Khatiwada, D., Venkata, B. K., Silveira, S., & Johnson, F. X. (2016). Energy and GHG balances of ethanol production from cane molasses in Indonesia. Applied energy, 164, 756-768.

Klein, B. C., Chagas, M. F., Junqueira, T. L., Rezende, M. C. A. F., de Fátima Cardoso, T., Cavalett, O., & Bonomi, A. (2018). Techno-economic and environmental assessment of renewable jet fuel production in integrated Brazilian sugarcane biorefineries. Applied Energy, 209, 290-305.

Klein, B.C. et al. (*in preparation*). Techno-economic and environmental assessment of renewable jet fuel production in integrated Brazilian sugarcane biorefineries.

Klein-Marcuschamer, D., Turner, C., Allen, M., Gray, P., Dietzgen, R. G., Gresshoff, P. M., ... & Speight, R. (2013). Technoeconomic analysis of renewable aviation fuel from microalgae, Pongamia pinnata, and sugarcane. Biofuels, Bioproducts and Biorefining, 7(4), 416-428.

Kumar, D., & Murthy, G. S. (2011). Impact of pretreatment and downstream processing technologies on economics and energy in cellulosic ethanol production. Biotechnology for biofuels, 4(1), 27.

Kwiatkowski, J. R., McAloon, A. J., Taylor, F., & Johnston, D. B. (2006). Modeling the process and costs of fuel ethanol production by the corn dry-grind process. Industrial crops and products, 23(3), 288-296.

Li Y. et al (2018) Substitution of soybean meal with detoxified Jatropha curcas kernel meal: effects on performance, nutrient utilization, and meat edibility of growing pigs. Asian Australas. J. Anim. Sci. 31(6):888.

Lobo, P. C., Jaguaribe, E. F., Rodrigues, J., & Da Rocha, F. A. A. (2007). Economics of alternative sugar cane milling options. Applied Thermal Engineering, 27(8-9), 1405-1413.

Ludwig-Bolkow Systemtechnik GMBH. (2006). *E3 Database*. Retrieved May 15, 2017, from http://www.e3database.com/

Macedo, I. C., Seabra, J. E., & Silva, J. E. (2008). Greenhouse gases emissions in the production and use of ethanol from sugarcane in Brazil: the 2005/2006 averages and a prediction for 2020. Biomass and bioenergy, 32(7), 582-595.

Makkar, H.P.S. et al. (1997) Studies on Nutritive Potential and Toxic Constituents of Different Provenances of Jatropha curcas. J. Agric. Food Chem. 45, 3152-3157.

Makkar, H. P. (2016). State-of-the-art on detoxification of Jatropha curcas products aimed for use as animal and fish feed: A review. Anim. Feed Sci. Technol. 2016, 222, 87−99

Mei, F. (2006). Mass and energy balance for a corn-to-ethanol plant (MS thesis, Washington University). http://crelonweb.eec.wustl.edu/theses/Masters/Fan%20Mei%20-Master%20thesis.pdf

Moeller, D., Sieverding, H. L., & Stone, J. J. (2017). Comparative Farm-Gate Life Cycle Assessment of Oilseed Feedstocks in the Northern Great Plains. BioPhysical Economics and Resource Quality, 2(4), 13.

Moreira, M., Gurgel, A. C., & Seabra, J. E. (2014). Life cycle greenhouse gas emissions of sugar cane renewable jet fuel. Environmental science & technology, 48(24), 14756-14763.

Murphy, J.D. & McKeogh, E. (2004). Technical, economic and environmental analysis of energy production from municipal solid waste. *Renewable Energy*, 29, 1043-1057.

Najafpour, G.D. (2007). Biochemical engineering and biotechnology, Elsevier B.V., chapters 3 and 6.

Navarro-Pineda, F. S. et al. (2016). Advances on the processing of Jatropha curcas towards a whole-crop biorefinery. Renewable and Sustainable Energy Reviews, 54:247-269.

Park, J. H., Lee, C. H., Joo, J. B., Bae, D. H., Shun, D., Moon, J. H., ... & Park, J. (2016). Fuel characteristics of molasses-impregnated low-rank coal produced in a top-spray fluidized-bed reactor. Drying technology, 34(9), 1095-1106.

Patil, S.S. et al. (2015). Effect of feeding detoxified Jatropha curcas meal on carcass characteristics and meat quality in lambs. Indian J. Anim. Sci. 85(3), pp. 307–310.

Pearlson, M. N. (2011). A techno-economic and environmental assessment of hydroprocessed renewable distillate fuels (Doctoral dissertation, Massachusetts Institute of Technology).

Pearlson, M., Wollersheim, C., & Hileman, J. (2013). A techno-economic review of hydroprocessed renewable esters and fatty acids for jet fuel production. Biofuels, Bioproducts and Biorefining, 7(1), 89-96.

Piloto-Rodríguez et al. (2020). An approach to the use of *Jatropha curcas* by-products as energy source in agroindustry Energy Sources, Part A: Recovery, Utilization, and Environmental Effects.

Pöschl, M., Ward, S., & Owende, P. (2010). Evaluation of energy efficiency of various biogas production and utilization pathways. Applied Energy, 87(11), 3305-3321.

Ramey, D. E., & Yang, S. T. (2005). Production of butyric acid and butanol from biomass (No. DOE-ER86106). Environmental Energy Inc., Blacklick, OH (United States).

Ramey, D., E., ButylFuel, LLC, Blacklick (2008). Butanol: The Other Alternative Fuel. http://nabc.cals.cornell.edu/Publications/Reports/nabc_19/19_4_6_Ramey.pdf

Renouf, M. A., Pagan, R. J., & Wegener, M. K. (2011). Life cycle assessment of Australian sugarcane products with a focus on cane processing. The International Journal of Life Cycle Assessment, 16(2), 125-137

Rispoli, K. (2014). Life cycle and supply assessment of aviation biofuels in the Canadian context (MS Thesis, University of Toronto). https://tspace.library.utoronto.ca/handle/1807/82670

Seber, G., Malina, R., Pearlson, M. N., Olcay, H., Hileman, J. I., & Barrett, S. R. (2014). Environmental and economic assessment of producing hydroprocessed jet and diesel fuel from waste oils and tallow. *Biomass and Bioenergy*, *67*, 108-118.

Sieverding, H. L., Zhao, X., Wei, L., & Stone, J. J. (2016). Life-cycle assessment of oilseeds for biojet production using localized cold-press extraction. Journal of environmental quality, 45(3), 967-976.

Spliethoff, H., Kaltschmitt, M., & Mory, A. (2001). Energie aus Biomasse: Grundlagen, Techniken und Verfahren.

Staples, M. D., Malina, R., Olcay, H., Pearlson, M. N., Hileman, J. I., Boies, A., & Barrett, S. R. (2014). Lifecycle greenhouse gas footprint and minimum selling price of renewable diesel and jet fuel from fermentation and advanced fermentation production technologies. Energy & Environmental Science, 7(5), 1545-1554.

Stratton, R.W. et al. (2010) Life Cycle Greenhouse Gas Emissions from Alternative Jet Fuels. MIT and Partnership for Air Transportation and Emissions Reduction, Cambridge, MA, USA.

Suresh, P. (2016). Environmental and economic assessment of transportation fuels from municipal solid waste. Massachusetts Institute of Technology. Cambridge: MIT.

Tao, L., Tan, E. C., McCormick, R., Zhang, M., Aden, A., He, X., & Zigler, B. T. (2014). Techno-economic analysis and life cycle assessment of cellulosic isobutanol and comparison with cellulosic ethanol and n-butanol. Biofuels, Bioproducts and Biorefining, 8(1), 30-48.

Taylor, P. G., Bilinski, T. M., Fancher, H. R., Cleveland, C. C., Nemergut, D. R., Weintraub, S. R., ... & Townsend, A. R. (2014). Palm oil wastewater methane emissions and bioenergy potential. Nature Climate Change, 4(3), 151.

Total, Amyris to market renewable jet fuel from commercial flights, Biomass Magazine.

Tsiropoulos, I., Faaij, A. P., Seabra, J. E., Lundquist, L., Schenker, U., Briois, J. F., & Patel, M. K. (2014). Life cycle assessment of sugarcane ethanol production in India in comparison to Brazil. The International Journal of Life Cycle Assessment, 19(5), 1049-1067.

Vasudevan, V., Stratton, R. W., Pearlson, M. N., Jersey, G. R., Beyene, A. G., Weissman, J. C., ... & Hileman, J. I. (2012). Environmental performance of algal biofuel technology options. Environmental science & technology, 46(4), 2451-2459

Wang H. et al. (2011). Effects of replacing soybean meal by detoxified Jatropha curcas kernel meal in the diet of growing pigs on their growth, serum biochemical parameters and visceral organs. Anim. Feed Sci. Technol. 170, pp. 141–146.

Wang, M., Han, J., Dunn, J. B., Cai, H., & Elgowainy, A. (2012). Well-to-wheels energy use and greenhouse gas emissions of ethanol from corn, sugarcane and cellulosic biomass for US use. Environmental research letters, 7(4), 045905.

Wang, W. C., Tao, L., Markham, J., Zhang, Y., Tan, E., Batan, L.; Warner, E.; Biddy, M: (2016). Review of biojet fuel conversion technologies. Golden: NREL (National Renewable Energy Laboratory).

Ziemiński, K., & Kowalska-Wentel, M. (2017). Effect of different sugar beet pulp pretreatments on biogas production efficiency. Applied biochemistry and biotechnology, 181(3), 1211-1227.

APPENDIX

Table 70: Lifecycle inventory for agricultural residues FT

Feedstock	Corn Stover (w nutrient replacement)			Wheat Straw (w nutrient replacement)		Corn Stover		Wheat Straw	
Data Provider	ANL /MIT (US)	ANL /MIT (EU)	JRC	ANL /MIT (US)	JRC	MIT	JRC	MIT	JRC
Feedstock Production									
N [$g/kg_{dry\ feedstock}$]	8.8	5.6	9.6	5.5	0	0	0	0	0
P_2O_5 [$g/kg_{dry\ feedstock}$]	2.4	3.1	2.1	1.4	1.9	0	0	0	0
K_2O [$g/kg_{dry\ feedstock}$]	15.0	13.4	15.8	1.0	0.5	0	0	0	0
Energy [$Btu/kg_{dry\ feedstock}$]	246.5	144.4	244	255.0	144	246.5	244	255.0	155
Yield (kg/ha)	5,500	5,000	N/A	-	3,256	5,500	N/A	-	3,256
Feedstock Transportation									
Distance	153.2	153.2 *	500	153.2 *	50	153.2	500	153.2 *	50
Method	Heavy-duty truck	Heavy-duty truck	Truck	Heavy-duty truck	Truck	Heavy-duty truck	Truck	Heavy-duty truck	Truck
FT Conversion									
Efficiency (%)	50	50	41	50	41	50	41	50	41
Jet Fuel Transportation									
Distance (km)	1,288;837; 644	1,288*;837*;644*	250	1,288; 837;644	250	1,288;837; 644	250	1,288; 837;644	250
Method	Rail;Barge; Pipeline	Rail*;Barge*; Pipeline*	Train	Rail;Barge;Pipeline	Train	Rail;Barge; Pipeline	Train	Rail;Barge; Pipeline	Train
Share (%)	7; 33; 60	7*; 33*;60*	100	7; 33; 60	100	7; 33; 60	100	7; 33; 60	100
Reference	(Argonne National Laboratory, 2015) (Spatari et al, 2005)	(Neeft & et al, 2012) (Gabrielle et al., 2014a)	(Sawyer & Mallarino, 2007) (Kaltschmitt & Hartmann, 2001)	(US Department of Energy, 2016)	(Kaltschmitt & Hartmann, 2001) (Giuntoli et al., 2013) (Sikkema et al., 2010) (Sultana, Kumar, & Harfield, 2010)	(Argonne National Laboratory, 2015) (Spatari et al, 2005)	(Sawyer & Mallarino, 2007) (Kaltschmitt & Hartmann, 2001)	(Giuntoli et al., 2013) (Sikkema et al., 2010) (Sultana, Kumar, & Harfield, 2010)	(Kaltschmitt & Hartmann, 2001) (Giuntoli et al., 2013)

* Where regionally specific data was unavailable, US values were used instead (as a default / reference point).

Table 71: Lifecycle inventory for forestry residues FT

Feedstock	Forest Residues		
Data Provider	ANL / MIT (US)	ANL / MIT (EU)	JRC
Feedstock Production			
N [g/kg$_{\text{dry feedstock}}$]	0	0	0
P_2O_5 [g/kg$_{\text{dry feedstock}}$]	0	0	0
K_2O [g/kg$_{\text{dry feedstock}}$]	0	0	0
Energy [Btu/kg$_{\text{dry feedstock}}$]	146.4	146.4*	244.2
Yield (kg/ha)	500 *	500	500 *
Feedstock Transportation			
Distance (km)	144.8	144.8 *	50
Method	Heavy-duty truck	Heavy-duty truck	Truck
FT Conversion			
Efficiency (%)	50	50	47
Jet Fuel Transportation			
Distance (km)	1,288; 837; 644	1,288*; 837*; 644*	250
Method	Rail; Barge; Pipeline	Rail*; Barge*; Pipeline*	Train
Share (%)	7; 33; 60	7*; 33*; 60*	100
Reference	(Argonne National Laboratory, 2015) (Han et al., 2011)	(Brandao et al, 2011)	(Lindholm et al., 2010) (Hamelinck et al., 2005)

* Where regionally specific data was unavailable, US values were used instead (as a default / reference point).

Table 72: Lifecycle inventory for short rotation woody crops FT

Feedstock	Poplar			Willow		Eucalyptus	
Data Provider	ANL / MIT (US)	ANL / MIT (US)	JRC	ANL / MIT (US)	ANL / MIT (US)	ANL / MIT (US)	JRC
Feedstock Production							
N [g/kg$_{dry\ feedstock}$]	2.2	5.2	5.1	1.7	3.2	3.1	17.7
P_2O_5 [g/kg$_{dry\ feedstock}$]	0.7	0.9	1.4	0.7	0.6	2.4	6.8
K_2O[g/kg$_{dry\ feedstock}$]	0.6	3.3	3.7	1.1	1.4	0.6	14.2
Energy [Btu/kg$_{dry\ feedstock}$]	296.1	296.1 *	228.3	204.4	204.4*	251.8	262
Yield (kg/ha)	8,500 *	8,500	10,000	8,500 *	8,500	9,000	12,900
Feedstock Transportation							
Distance (km)	80.5	80.5 *	50	80.5	80.5 *	80.5 *	500
Method	Heavy-duty truck	Heavy-duty	Truck	Heavy-duty truck	Heavy-duty truck	Heavy-duty truck	Truck
FT Conversion							
Efficiency (%)	50	50	47	50	50	50	38
Jet Fuel Transportation							
Distance (km)	1,288; 837;644	1,288*; 837*; 644*	250	1,288; 837;644	1,288*; 837*; 644*	1,288; 837; 644*	250
Method	Rail; Barge ;Pipeline	Rail*; Barge*; Pipeline*	Train	Rail; Barge; Pipeline*	Rail*; Barge*; Pipeline*	Rail; Barge; Pipeline	Train
Share (%)	7; 33; 60	7*; 33*; 60*	100	7; 33; 60	7*; 33*; 60*	7; 33; 60	100
Reference	(Argonne National Laboratory, 2015)	(Gabrielle et al., 2014a) (Gabrielle et al., 2014b)	(UNEP, 2013)	(Argonne National Laboratory, 2015)	(Gabrielle et al., 2014a) (Gabrielle et al., 2014b) (Brandao et al., 2011)	(US Department of Energy, 2016)	(Paustian, 2006) (Bernd et al., 2012)

Table 73: Lifecycle inventory for herbaceous energy crops FT

Feedstock	Switchgrass			Miscanthus	
Data Provider	ANL / MIT (US)	ANL / MIT (EU)	JRC	ANL / MIT (US)	ANL / MIT (EU)
Feedstock Production					
N [g/kg$_{dry\ feedstock}$]	5.4	5.8	5.1	5.1	3.0
P_2O_5 [g/kg$_{dry\ feedstock}$]	2.5	0.9	0.3	1.1	0.6
K_2O [g/kg$_{dry\ feedstock}$]	3.5	4.1	0	3.2	5.2
Energy [Btu/kg$_{dry\ feedstock}$]	74.4	74.4 *	8	56.9	56.9*
Yield (kg/ha)	13,000	12,000	12,285	18,800	20,700
Feedstock Transportation					
Distance (km)	105.6	105.6 *	160.9	82.6	82.6 *
Method	Heavy-duty truck	Heavy-duty truck	Truck	Heavy-duty truck	Heavy-duty truck
FT Conversion					
Efficiency (%)	50	50	41	50	50
Jet Fuel Transportation					
Distance (km)	1,288; 837; 644	1,288*; 837*; 644*	250	1,288; 837; 644	1,288*; 837*; 644*
Method	Rail; Barge; Pipeline	Rail*; Barge*;	Train	Rail; Barge; Pipeline	Rail*; Barge*; Pipeline*
Share (%)	7; 33; 60	7*; 33*; 60*	100	7; 33; 60	7*; 33*; 60*
Reference	(Argonne National Laboratory, 2015) (Wang et al., 2012)	(Laboratory, 2015) (Wang et al., 2012) (Smeets et al., 2009) (Gabrielle et al., 2014a) (Gabrielle et al., 2014b)	(Groode & Heywood, 2008)	(Argonne National Laboratory, 2015) (Wang et al., 2012)	(Smeets et al., 2009) (Gabrielle et al., 2014a) (Gabrielle et al., 2014b)

* Where regionally specific data was unavailable, US values were used instead (as a default / reference point).

Table 74: Lifecycle inventory for municipal solid waste FT. Note that the assumed proportion of non-biogenic carbon (NBC) content was varied to estimate life cycle emissions as a function of NBC

Parameters		Value	Unit
MSW characteristics [Suresh 2016]	Energy content	20.9	MJ/kg_{MSW} (pre-processed and dried MSW)
	Carbon content	0.51	kg/kg_{MSW} (pre-processed and dried MSW)
	Sulfur content	2.5	g/kg_{MSW} (pre-processed and dried MSW)
	Ash/inorganic content	0.11	kg/kg_{MSW} (pre-processed and dried MSW)
MSW transportation to biorefinery	GHG intensity of trucking to biorefinery	0.88	$kgCO_2e$/tonne-km
	Distance to biorefinery	32.2	km
Feedstock-to-fuel conversion	Olivine	1.4	$kg/tonne_{MSW}$
	Conversion efficiency	54	%

Table 75: Lifecycle inventory for tallow HEFA

Data Provider		MIT	JRC
Cattle lifecycle (per cattle raised)	Enteric emissions	1430 kg_{CO2e}/cow	-
	Manure emissions	54 kg_{CO2e}/cow	-
Cattle slaughter (per mass of slaughtered cattle)	Yield	3.89 kg_{cow}/kg_{tallow}	3.45 kg_{cow}/kg_{tallow}
	Natural gas demand	1.3 MJ_{NG}/ kg_{cow}	-
	Electricity demand	0.23 MJ_{NG}/ kg_{cow}	-
Rendering (per mass of oil rendered from tallow)	Natural gas	8.39 MJ_{NG}/ kg_{tallow}	5.3MJ NG /kg tallow
	Electricity	0.63 MJ electricity / kg tallow	3.0 MJ electricity / kg tallow
HEFA conversion (per kg of oil)	Natural gas	4.88 MJ NG / kg oil in	0.011 MJ / MJ HVO
	Electricity	0.22 MJ electricity / kg oil in	0.0015 MJ / MJ HVO
References		(Seber et al., 2014) (Lopez, Mullins, & Bruce, 2010)	Confidential

Table 76: Lifecycle inventory for UCO HEFA

Data provider		MIT	JRC
Rendering (per mass of UCO)	Natural gas	1.45 MJ NG / kg UCO	5.30 MJ_{NG}/kg_{UCO}
	Electricity	0.15 MJ electricity / MJ UCO	3.0 $MJ_{electricity}/kg_{UCO}$
	Oil yield	0.73 $kg_{rendered\ oil}/kg_{UCO}$	-*
HEFA conversion (per kg oil)	Natural gas	4.88 MJ NG / kg oil in	0.01098 MJ / MJ HVO
	Electricity	0.22 MJ electricity / kg oil in	0.0015 MJ/ MJ HVO
References		(Seber et al., 2014) (Lopez, Mullins, & Bruce, 2010)	Confidential

* Energy requirements for this step (i.e. de-watering and filtering) are already included in the natural gas and electricity input values. The reason for this is that there is no specific rendering yield, for this can strongly vary depending on the feedstock quality.

Table 77: Lifecycle inventory for PFAD HEFA

Product, Farming	**Palm (per kg dry FFB)**	
Data provider	ANL	JRC
Total N (g)	10.5	7.54
P_2O_5 (g)	0	2.63
K_2O (g)	0	14.54
$CaCO_3$ (g)	0	0
Herbicide (G)	0	1.12
Insecticide (g)	0	0
Diesel (kJ)	241.55	128.58
Gasoline (kJ)	0	0
NG (kJ)	0	0
LPG (kJ)	0	0
Electricity (kJ)	0	0
Total fossil energy (kJ)	241.55	128.58
References	(Stratton et al., 2010) (Argonne National Laboratory, 2015)	(Neeft et al., 2012)
Product, oil extraction	**PFAD (per kg oil)**	
Feedstock (kg dry FFB)	68.8	
Total fossil energy (kJ)	1061.54	
References	(Choo et al., 2011)	

Table 78: Lifecycle inventory for corn oil HEFA

Product, Farming	**Corn (per kg dry corn grain)**	
Data provider	ANL	JRC
Total N (g) *	17.74	20.34
P_2O_5 (g) *	6.45	6.29
K_2O (g) *	6.78	7.3
$CaCO_3$ (g) *	59.76	7.3
Herbicide (g) *	0.27	0
Insecticide (g) *	0	0.24
Diesel (kJ) *	166.57	0
Gasoline (kJ)	49.75	0
NG (kJ) *	45.83	0
LPG (kJ) *	60.67	0
Electricity (kJ) *	15.54	0
Total fossil energy (kJ) *	338.37	262.4
References	(Argonne National Laboratory, 2015)	(International Fertilizer Association, 2010)
Product, oil extraction	**Corn Oil (per kg oil)**	
Feedstock (kg dry)	103.38	
Total fossil energy (kJ)	618.8	
References	(Argonne National Laboratory, 2015)	

* Note that ultimately corn oil was treated as a by-product, and therefore fertilizer and energy use for corn grain cultivation was not considered in the life cycle emissions. This data is here for information purposes only.

Table 79: Agricultural inputs for soybean, rapeseed and camelina feedstocks

	Soybean, per bushel (52.2 lbs, dry)				**Rapeseed, per dry kg**				**Camelina, per dry kg**			
Region	**Europe**	**US**	**Latin America**	**JRC**	**Europe**	**US**	**JRC**	**Canada**	**Europe**	**US**	**Canada**	**JRC**
Total N (g)	51.8	48.1	60.2	45.8	48.7	54.7	48.5	52.1	37.5	43	51.3	37.5
P_2O_5 (g)	221	186.7	670.7	397.9	12	15.3	10.9	15.3	7.3	17.4	25.6	7.3
K_2O (g)	150.3	299.1	713.7	382.7	17.6	2.9	14.7	2.6	0	11.6	0	0
$CaCO_3$ (g)	1535	0	3775	4134	12	0	106.9	0	0	0	0	0
Herbicide (g)	37.1	17.9	50.3	30.7	0.3	0.3	1.7	0.3	0	0	1	0
Insecticide (g)	0.7	0.4	15.7	0.6	0.1	0	0.5	0.1	0	0	0	0
Diesel (Btu)	14099	12985	7878	16627	994.4	505.3	966.8	491.2	1306	1118	1068	1306
Gasoline (Btu)	0	2902	0	0	0	0	0	0	0	0	0	0
NG (Btu)	660.7	933.1	0	0	0	1.1	0	0.8	0	0	0	0
LPG (Btu)	335.5	725.7	0	0	0	0	0	0	0	0	0	0
Electricity (Btu)	149.7	886.6	821.6	0	0	12.7	0	11.7	0	0	0	0

Data source:

1. GREET (2016)
2. GHGenius, 4.01a. (2012)
3. BioGrace I v.4d and BioGrace II v.3 (2012)
4. Raucci, G.S. et al. (2015). Greenhouse gas assessment of Brazilian soybean production: a case study of Mato Grosso State, Journal of Cleaner Production, 96: 418-425
5. Canola Council of Canada. (2017). Canadian Canola Statistics. http://www.canolacouncil.org/markets-stats/statistics.
6. Statistics Canada. (2017). Table 001-0010, 001-0017, 001-0068, 004-0210 - CANSIM (database). http://www5.statcan.gc.ca/cansim. Accessed 2017-09-15
7. Canadian Grain Commission (2014). Quality of western Canadian canola 2014. https://www.grainscanada.gc.ca/canola/harvest-recolte/2014/hqc14-qrc14-6-en.htm. Accessed 2017-09-15
8. Agriculture Research and Extension Council of Alberta. (2011). Energy Conservation and Energy Efficiency. Edmonton. http://www.areca.ab.ca/projects/manuals.html
9. Colorado State University (1998). Estimating Farm Fuel Requirements. Fort Collins. http://www.ext.colostate.edu/pubs/farmmgt/05006.pdf.
10. Manitoba Agricultural Services Corporation (2017). Manitoba Management Plus Program (MMPP) Fertilizer Data Browser. www.masc.mb.ca/masc.nsf/mmpp_browser_fertilizer.html
11. Smart Earth Seeds (2017). MIDAS Camelina. http://smartearthseeds.com/index.php/camelina/camelina-midas
12. Dangol, N. et al. (2015) Life cycle anlalysis and production potential of camelina biodiesel in the Pacific Northwest; American Society of Agricultural and Biological Engineers, Vol. 58(2): 465-475, ISSN 2151-0032; DOI 10.13031/trans.58.10771
13. Foulke, T. et al. (2013) Is biodiesel from camelina right for you. University of Wyoming-Extension. www.sare.org/content/download/71599/1019535/file/B1249.pdf
14. Paustian, K., et al (2006) IPCC Guidelines for National Greenhouse Gas Inventories; IPCC National Greenhouse Inventories Programme; published by the Institute for Global Environmental Strategies (IGES), Hayama, Japan on behalf of the Intergovernmental Panel on Climate Change (IPCC), 2006; http://www.ipcc-nggip.iges.or.jp/public/2006gl/pdf/4_Volume4; http://www.ipcc-nggip.iges.or.jp/public/2006gl/vol5.html
15. Perego, C. (2015) From biomass to advanced biofuel: the green diesel case; Sinchem Winter School, February 16-17, 2015, Bologna; http://www.sinchem.eu/wp-content/uploads/2015/01/15-Perego-ENI.pdf
16. Petre, S. M. et al. (2013) Life cycle assessment: by-products in biofuels production battle; rapeseed vs camelina sativa L.; AgroLife Scientific Journal - Volume 2, Number 1
17. Toncea, I. et al. (2013) The seed's and oil composition of camelia - first Romanian cultivar of camelina (Camelina sativa, L. Crantz); Romanian Biotechnological Letters, Vol. 18, No. 5
18. International Fertilizer Association: fertilizer use by crop http://www.fertilizer.org/ifa/Home-Page/STATISTICS
19. Kraenzlein, T. (2011) Energy Use in Agriculture. Chapter 7.5 in CAPRI model documentation: Editors: W. Britz, P. Witzke. Available at: http://www.capri-model.org/docs/capri_documentation_2011.pdf.
20. EMEP/EEA Air pollutant emission inventory guidebook - 2013
21. FAOSTAT data accessed in October 2016
22. Ecoinvent report no. 17 - Chapter 9: Soybean, The life cycle inventory data, Version July 2009
23. A. Pradhan, D.S. Shrestha, A. McAloon, W. Yee, M. Haas, J.A.Duffield, 2011, "Energy Life-cycle assessment of soybean biodiesel revisited", Transactions of the ASABE, Vol. 54(3): 1031-1039
24. Ecoinvent report no. 17 - Chapter 9: Soybean, The life cycle Inventory Data, Version July 2009
25. CENBIO (Centro Nacional de Referência em Biomassa), 2009, "Complete Project report"
26. Muzio, J. et al. (2009) Argentina's Technical Comments on biodiesel from soy bean 02/04/09 INTA document IIR-BC-INF-14-08 by Instituto Nacional de Technologia Agropecuaria (INTA).

27. Hilbert, J.A. et al. (2010) Comparative analysis of energy consumption and GHG emissions from the production of biodiesel from soybean under conventional and no-till farming systems. Communication to JRC and DG-TREN. INTA document IIR-BC-INF-06-09 by Instituto Nacional de Technologia Agropecuaria (INTA)
28. CAPRI model documentation http://www.capri-model.org/docs/capri_documentation_2011.pdf

Table 80: Inputs for oil extraction from soybean, rapeseed and camelina feedstocks

	Soybean, per lb. oil				Rapeseed, per lb. oil				Camelina, per lb. oil			
Region	Europe	US	Latin America	JRC	Europe	US	JRC	Canada	Europe	US	Canada	JRC
Feedstock (g, dry)	2099	2107	2066	2099	1050	977.2	998.9	945.9	1050	1129	1129	1050
Electricity (Btu)	258.2	312.8	312.8	258.2	205.8	176.3	165.4	170.6	205.8	36.1	36.1	205.8
NG (Btu)	1447	1757	2068	1447	989.7	1044	624.7	981.6	989.7	503.4	503.4	989.7
#2 Fuel Oil (Btu)	0	13.5	16	0	0	0	0	0	0	275.7	275.7	0
#6 Fuel Oil (Btu)	0	27	32	0	0	0	0	0	0	0	0	0
Coal (Btu)	0	865	1018	0	0	0	0	0	0	0	0	0
Biomass (Btu)	0	27	32	0	0	0	0	0	0	0	0	0
Landfill gas (Btu)	0	13.5	16	0	0	0	0	0	0	0	0	0
N-Hexane (Btu)	58.2	56.8	56.8	58.2	68.8	96.1	63.6	93	68.8	43.8	43.8	68.8
Meal (g, dry)	1646	1645	1645	1646	569.3	504.7	531.7	488.5	569.3	656.2	656.2	569.3

Data source:
1. GREET (2016)
2. GHGenius, 4.01a. (2012)
3. BioGrace I v.4d and BioGrace II v.3 (2012)
4. Schneider, L. & Finkbeiner, M. (2013) Life Cycle Assessment of EU Oilseed Crushing and Vegetable Oil Refining. Sustainable Engineering. Report commissioned by FEDIOL. http://www.fediol.eu/data/Full%20FEDIOL%20LCA%20report_05062013_CR%20statement.pdf

Table 81: Inputs for HEFA processing of vegetable oils from soybean, rapeseed and camelina feedstocks

	Soybean, per lb jet fuel				Rapeseed, per lb jet fuel				Camelina, per lb jet fuel			
Region	Europe	US	Latin America	JRC	Europe	US	JRC	Canada	Europe	US	Canada	JRC
Feedstock (g oil)	556.0	577.1	577.1	556.0	556	577.1	556.0	577.1	556	577.1	577.1	556.0
H_2 (Btu)	317.4	1736	1736	317.4	317.4	1736	317.4	1736	317.4	1736	1736	317.4
NG (Btu)	3820	1548	1548	3820	3669	1548	3669	1548	3669	1548	1548	3669
Electricity (Btu)	33.9	87.7	87.7	33.9	146	87.7	146.0	87.7	146	87.7	87.7	146.0
Co-product, propane mix (Btu)	0.0	1370	1370	0.0	0	1370	0	1370	0	1370	1370	0
Co-product, naphtha (Btu)	189.6	437.0	437.0	189.6	189.6	437.0	189.6	437.0	189.6	437.0	437.0	189.6

Data source:
1. GREET (2016)
2. BioGrace I v.4d and BioGrace II v.3 (2012)
3. Lindfors, R.: Neste Oil's Roles in Itaka Project: Production of NEXBTL Renewable Aviation Fuel; Madrid, 22 October 2014; http://www.core-jetfuel.eu/Shared%20Documents/Roger_Lindfors_Neste_Oil%E2%80%99s_roles_Itaka_project.pdf
4. Reinhardt, G. et al. (2006) An Assessment of Energy and Greenhouse Gases of NExBTL; Institute for Energy and Environmental Research Heidelberg GmbH (IFEU). By order of the Neste Oil Corporatioin, Porvoo, Finland; Final Report;
Heidelberg, June 2006

Table 82: Lifecycle inventory for palm oil HEFA pathway (without agricultural inputs)

Feedstock	**Palm Oil**		
Data provider		JRC	ANL
Feedstock transportation			
Input	Diesel (MJ/tkm)	2.2378	2.7959
Plant oil extraction			
Input	FFB (MJ/MJ_{oil})	1.8079	1.1172
	Grid electricity (MJ/MJ_{oil})	0.000066	0.0042
	Diesel (MJ/MJ_{oil})	0.00375	0.0243
Output	CH_4 emissions (g/MJ_{oil})	0.831(open pond) 0.125(close pond)	0.736 (open pond) 0.110(close pond)
	N_2O emission (g/MJ_{oil})	0.00084	-
	Heat (MJ/MJ_{oil})	0.0177	0.0181
	Crude vegetable oil (MJ)	1	1
Oil transport			
Input	Diesel (MJ/tkm)	0.8111	1.0175
	Heavy fuel oil (MJ/tkm)	2.2717	1.9571
Feedstock to fuel conversion			
Input	NG (MJ/MJ_{BTL})	0.08576	0.081627
	Vegetable oil (MJ/MJ_{BTL})	1.02385	1.183235
	H_3PO_4 (kg/MJ_{BTL})	1.68778E-05	-
	NaOH (kg/MJ_{BTL})	2.70028E-05	-
	N_2 (kg/MJ_{BTL})	4.91944E-06	-
	Electricity (MJ/MJBTL)	0.00686	0.004624
	GH_2 (MJ/MJBTL)	0.017	0.091586
Output	BTL-like fuel (MJ)	1	1
	Steam (MJ/MJ_{BTL})	0.004712	0.1148

Table 83: Lifecycle inventory for sugarcane SIP pathway

Feedstock		**Sugarcane**	
Data provider		JRC	MIT
Cultivation and harvesting			
Inputs	Diesel [MJ/$kg_{sugarcane}$]	0.01	0.038
	Pesticides [g/$kg_{sugarcane}$]	0.037	0.048
	N-fertilizer [g/$kg_{sugarcane}$]	0.91	0.93
	$CaCO_3$-fertilizer [g/$kg_{sugarcane}$]	1.02	5.2
	K_2O-fertilizer [g/$kg_{sugarcane}$]	1.02	1.51
	P_2O_5-fertilizer [g/$kg_{sugarcane}$]	0.32	0.32
Outputs	Sugar cane [kg]	1	1
Sugar cane to farnesene			
Inputs	Sugar cane [MJ/$MJ_{farnesene}$]	4.23	3.52
	CaO [g/$MJ_{farnesene}$]	0.73	0.95
	Lubricants [g/$MJ_{farnesene}$]	0.010	-
Outputs	Farnesene [MJ]	1	1
	Electricity [MJ/$MJ_{farnesene}$]	0.026	0.330
	CH_4 [g/$MJ_{farnesene}$]	0.0041	-
	N_2O [g/$MJ_{farnesene}$]	0.0020	-
Farnesene to jet fuel			
Inputs	Farnesene [MJ/$MJ_{jet\ fuel}$]	0.91	1.03
	H_2 [g/$MJ_{SAF\ fuel}$]	0.86	0.91
Outputs	Jet fuel [MJ/$MJ_{SAF\ fuel}$]	1	1

Table 84: Lifecycle inventory for sugarbeet SIP pathway

Feedstock		**Sugarbeet**	
Data provider		JRC	MIT
Cultivation and harvesting			
Input	Pesticides [g/$kg_{dry\ sugarbeet}$]	0.89	0.80
	Diesel oil [MJ/$kg_{dry\ sugarbeet}$]	0.17	0.17
	N-ferilizer [g/$kg_{dry\ sugarbeet}$]	5.70	5.72
	K_2O-fertilizer [g/$kg_{dry\ sugarbeet}$]	4.26	4.24
	P_2O_5-fertilizer [g/$kg_{dry\ sugarbeet}$]	2.43	2.44
	Sugar beet seeding material [g/$kg_{dry\ sugarbeet}$]	0.18	-
	CaO-fertilizer [g/$kg_{dry\ sugarbeet}$]	9.91	17.6
Sugar beet to farnesene			
Input	Sugar beet [MJ_{dry}/$MJ_{farnesene}$]	1.77	1.98
	Electricity [MJ/$MJ_{farnesene}$]	0.024	-
	Steam [MJ/$MJ_{farnesene}$]	0.065	-
	Sulfuric acid [g/$MJ_{farnesene}$]	-	0.15
	Sodium carbonate [g/$MJ_{farnesene}$]	-	0.044
	Hydrochloric acid [g/$MJ_{farnesene}$]	-	0.021
	Formaldehyde [g/$MJ_{farnesene}$]	-	0.13
	Pet coke [MJ/$MJ_{farnesene}$]	-	0.045
Output	Farnesene [MJ/$MJ_{farnesene}$]	1.00	1.00
	Electricity [MJ/$MJ_{farnesene}$]	-	0.03
Farnesene to jet fuel			
Inputs	Farnesene [MJ/$MJ_{SAF\ fuel}$]	0.91	1.03
	H_2 [g/$MJ_{SAF\ fuel}$]	0.86	0.91
Output	Jet fuel [MJ/$MJ_{SAF\ fuel}$]	1.00	1.00

Table 85: Lifecycle inventory for sugarcane iso-butanol ATJ pathway

Data provider		MIT	JRC	CTBE
Sugarcane cultivation				
Inputs	N[g /$kg_{sugarcane}$]	0.93	0.91	1.3
	P_2O_5 [g /$kg_{sugarcane}$]	0.32	0.32	0.11
	K_2O [g /$kg_{sugarcane}$]	1.51	1.02	1.28
	$CaCO_3$ [g /$kg_{sugarcane}$]	5.2	1.02	5.26
	Pesticides [g /$kg_{sugarcane}$]	0.048	0.037	0.018
	Diesel [MJ//$kg_{sugarcane}$]	0.0384	0.0101	0.0014
ATJ Conversion parameters				
Inputs	kg $_{sugarcane}$/kg $_{total\ fuel}$	28	21.1	28.2
	kg $_{CaCO3}$/kg $_{total\ fuel}$	0.0271	0.0186	0.0172
	kg_{H2}/kg $_{total\ fuel}$	0.0148	0.0072	0.0148*
	kg_{NG}/$kg_{total\ fuel}$	0.02	-	
Outputs	$kWh_{co\text{-}prod.\ elec.}$/$kg_{total\ fuel}$	2.49	0.28	4.44
	kg $_{co\text{-}prod.\ Naphtha}$/kg $_{total\ fuel}$	-	0.18	0.15

Table 86: Lifecycle inventory for agricultural residues iso-butanol ATJ pathway

Data provider			MIT	JRC
Corn stover collection and field treatment	Inputs	Diesel fuel [MJ/kgcorn stover]	0.30	0.17
		HDPE [g/kgcorn stover]	0.37	-
		Nitrogen [g/kgcorn stover]	8.77	9.61
		Phosphoric acid [g/kgcorn stover]	2.51	2.08
		Potassium Oxide [g/kgcorn stover]	15.04	15.77
Feedstock transportation	Inputs	Diesel fuel [MJ/kg corn stover]	0.11	7.5
Fermentation to iso-butanol	Inputs	Feedstock [kg/MJ_{SAF}]	0.15	0.16
		Natural gas for process heat [MJ/MJ_{SAF}]	0.03	0.01
		Cellulase [g/MJ_{SAF}]	1.4	0.84
		Yeast [g/MJ_{SAF}]	0.30	0
		Sulfuric acid [g/MJ_{SAF}]	4.1	3.69
		Ammonia [g/MJ_{SAF}]	2.7	2.23
		Sodium hydroxide [g/MJ_{SAF}]	-	4.06
		Calcium oxide [g/MJ_{SAF}]	-	1.64
		Corn steep liquor [g/MJ_{SAF}]	2.4	2.33
		Diammonium phosphate [g/MJ_{SAF}]	0.30	0.25
	Outputs	Co-produced electricity [kJ/MJ_{SAF}]	41.0	73.33
		iBuOH [g/MJ_{SAF}]	30.5	30.7
iBuOH upgrading to drop-in fuels	Inputs	iBuOH [g/MJ_{SAF}]	30.5	30.7
		Natural gas for process heat [MJ/MJ_{SAF}]	0.06	0.07
		Hydrogen [g/MJ_{SAF}]	0.19	0.2
	Outputs	Heavy oil [MJ/MJ_{SAF}]	0.03	-
		Naphtha [MJ/MJ_{SAF}]	-	0.22
		Diesel [MJ/MJ_{SAF}]	0.08	-
		Jet fuels [MJ/MJ_{SAF}]	1.0	1

Note: All corn stover is in units of dry biomass

Table 87: Lifecycle inventory for forest residues iso-butanol ATJ pathway

Data provider			MIT	JRC
Forest residue collection	Inputs	Diesel fuel [$MJ/_{kg forest residue}$]	0.15	0.23
Feedstock transportation	Inputs	Diesel fuel [$MJ/_{kg forest residue}$]	0.14	0.83
Fermentation to iso-butanol	Inputs	Feedstock [kg/MJ_{SAF}]	0.15	0.16
		Natural gas for process heat [MJ/MJ_{SAF}]	0.032	0.01
		Cellulase [g/MJ_{SAF}]	1.4	0.84
		Yeast [g/MJ_{SAF}]	0.30	0
		Sulfuric acid [g/MJ_{SAF}]	4.1	3.69
		Ammonia [g/MJ_{SAF}]	2.7	2.23
		Sodium hydroxide [g/MJ_{SAF}]	-	4.06
		Calcium oxide [g/MJ_{SAF}]	-	1.64
		Corn steep liquor [g/MJ_{SAF}]	2.4	2.33
		Diammonium phosphate [g/MJ_{SAF}]	0.30	0.25
	Outputs	Co-produced electricity [kJ/MJ_{SAF}]	90.0	73.33
		iBuOH [g/MJ_{SAF}]	30.5	30.7
iBuOH upgrading to drop-in fuels	Inputs	iBuOH [g/MJ_{SAF}]	30.5	30.7
		Natural gas for process heat [MJ/MJ_{SAF}]	0.02	0.07
		Hydrogen [g/MJ_{SAF}]	0.19	0.2
	Outputs	Heavy oil [MJ/MJ_{SAF}]	0.03	-
		Naphtha [MJ/MJ_{SAF}]	-	0.22
		Diesel [MJ/MJ_{SAF}]	0.08	-
		Jet fuels [MJ/MJ_{SAF}]	1	1

Note: All forest residue is in units of 30% moisture content

Table 88: Lifecycle inventory for corn grain iso-butanol ATJ pathway (without agricultural inputs)

Data provider			MIT	JRC
Corn grain drying	Inputs	Natural gas for process heat [MJ/MJ_{corn}]	-	0.0089
		Electricity [MJ/MJ_{corn}]	-	0.0015
Fermentation to isobutanol	Inputs	Corn grain [MJ/MJ_{iBuOH}]	2.16	2.38
		Natural gas for process heat [MJ/MJ_{iBuOH}]	0.13	0.23
		Electricity [MJ/MJ_{iBuOH}]	0.055	0.060
		Gluco amylase [g/MJ_{iBuOH}]	0.083	-
		Yeast [g/ MJ_{iBuOH}]	0.042	-
		Sulfuric acid [g/ MJ_{iBuOH}]	0.071	-
		Ammonia [g/ MJ_{iBuOH}]	0.28	-
		Sodium hydroxide [g/ MJ_{iBuOH}]	0.34	-
		Calcium oxide [g/ MJ_{iBuOH}]	0.16	-
		Alpha amylase [g/ MJ_{iBuOH}]	0.039	-
	Outputs	DDGS [MJ/MJ_{iBuOH}]	0.76	0.89
		iBuOH [MJ/MJ_{iBuOH}]	1	1
		Corn oil [MJ/MJ_{iBuOH}]	0.049	-
iBuOH upgrading to drop-in fuels	Inputs	iBuOH [MJ/MJ_{SAF}]	1.00	1.02
		Electricity [MJ/MJ_{SAF}]	0.021	0.021
		Natural gas for process heat [MJ/MJ_{SAF}]	0.26	0.23
		Hydrogen [MJ/MJ_{SAF}]	0.041	0.030
	Outputs	Jet fuels [MJ/MJ_{SAF}]	1	1

Table 89: Lifecycle inventory sugarcane ethanol ATJ pathway

Data provider			MIT	JRC	CTBE
Sugarcane cultivation	Inputs	N [$g/kg_{sugarcane}$]	0.93	0.91	1.3
		P_2O_5 [$g/kg_{sugarcane}$]	0.32	0.32	0.11
		K_2O [$g/kg_{sugarcane}$]	1.51	1.02	1.28
		$CaCO_3$ [$g/kg_{sugarcane}$]	5.20	1.02	5.26
		Pesticides [$g/kg_{sugarcane}$]	0.048	0.037	0.018
		Diesel [$MJ/kg_{sugarcane}$]	0.038	0.010	0.0014
Fermentation to Ethanol	Inputs	H_2SO_4 [g/MJ_{EtOH}]	-	0.43	-
		Cyclohexane [g/MJ_{EtOH}]	-	0.028	-
		CaO [g/MJ_{EtOH}]	0.62	0.51	0.37
		Lubricants [g/MJ_{EtOH}]	-	7.3E-06	-
		Sugarcane [kg/MJ_{EtOH}]	0.62	0.64	*0.60*
	Outputs	Electricity [MJ/MJ_{EtOH}]	0.20	0.018	*0.28*
		Ethanol [MJ]	1	1	1
Alcohol upgrading to drop-in fuels	Inputs	EtOH [MJ/MJ_{SAF}]	1.78	1.02	2.10
		Electricity [MJ/MJ_{SAF}]	-	0.021	-
		Natural gas for process heat [MJ/MJ_{SAF}]	-	0.23	-
		Hydrogen [MJ/MJ_{SAF}]	0.072	0.03	0.11
	Outputs	Jet [MJ/MJ_{SAF}]	1	1	1
		Diesel [MJ/MJ_{SAF}]	0.25	-	0.083
		Naphtha [MJ/MJ_{SAF}]	0.36	-	0.46
		Heavy oil [MJ/MJ_{SAF}]	0.078	-	-

Table 90: Lifecycle inventory corn grain ethanol ATJ pathway

Data provider			MIT	JRC
Corn grain cultivation	Inputs	Nitrogen [$g/kg_{corn\ grain}$]	15.08	20.34
		P_2O_5 [$g/kg_{corn\ grain}$]	5.48	6.29
		K_2O [$g/kg_{corn\ grain}$]	5.76	7.3
		$CaCO_3$ [$g/kg_{corn\ grain}$]	50.80	7.3
		Pesticides [$g/kg_{corn\ grain}$]	0.00023	0.00024
		Diesel [$MJ/kg_{corn\ grain}$]	0.29	0.2624
	Outputs	Corn grain [kg]	1	1
Fermentation to Ethanol	Inputs	Alpha amylase [g/MJ_{EtOH}]	0.038	0.032
		Gluco amylase [g/MJ_{EtOH}]	0.084	0.068
		Yeast [g/MJ_{EtOH}]	0.041	0.035
		Sulfuric acid [g/MJ_{EtOH}]	0.067	0.059
		Ammonia [g/MJ_{EtOH}]	0.27	0.225
		Sodium hydroxide [g/MJ_{EtOH}]	0.34	0.282
		Calcium oxide [g/MJ_{EtOH}]	0.16	0.134
		Natural gas for process heat [MJ/MJ_{EtOH}]	0.13	0.335
		Electricity [MJ/MJ_{EtOH}]	0.054	0.023
		Corn grain [kg/MJ_{EtOH}]	0.13	0.100
	Outputs	Ethanol [MJ]	1.00	1.000
		DDGS [MJ/MJ_{EtOH}]	0.75	0.649
		Corn oil [MJ/MJ_{EtOH}]	0.048	0.087
Alcohol upgrading to drop-in fuels	Inputs	EtOH [MJ/MJ_{SAF}]	1.78	1.120
		Electricity [MJ/MJ_{SAF}]	0.041	0.025
		Natural gas for process heat [MJ/MJ_{SAF}]	0.52	-
		Hydrogen [MJ/MJ_{SAF}]	0.072	0.060
	Outputs	Jet [MJ/MJ_{SAF}]	1	1.000
		Diesel [MJ/MJ_{SAF}]	0.25	-
		Naphtha [MJ/MJ_{SAF}]	0.36	-
		Heavy oil [MJ/MJ_{SAF}]	0.078	-

Table 91: Lifecycle inventory cellulosic ethanol ATJ pathway (agreed set of input between JRC and ANL)

Ethanol production		Agricultural residues		Forest residues		Miscanthus		Switchgrass	
Inputs	**Units**	Standalone	Integrated	Standalone	Integrated	Standalone	Integrated	Standalone	Integrated
Biomass feedstock	dry kg	0.13	0.13	0.13	0.13	0.13	0.13	0.13	0.13
Natural gas	MJ	-	-	.042	.042	-	-	-	-
Diesel	MJ	0.0024	0.0024	.0044	.0044	0.0024	0.0024	0.0024	0.0024
Cellulase	g	1.33	1.33	1.33	1.33	1.33	1.33	1.33	1.33
Yeast	g	0.33	0.33	0.33	0.33	0.33	0.33	0.33	0.33
Sulfuric acid	g	4.30	4.30	4.30	4.30	4.30	4.30	4.30	4.30
Ammonia	g	0.52	0.52	0.52	0.52	0.52	0.52	0.52	0.52
NaOH	g	1.46	1.46	1.46	1.46	1.46	1.46	1.46	1.46
CaO	g	0.95	0.95	0.95	0.95	0.95	0.95	0.95	0.95
Corn steep liquor	g	1.63	1.63	1.63	1.63	1.63	1.63	1.63	1.63
DAP	g	0.17	0.17	0.17	0.17	0.17	0.17	0.17	0.17
Urea	g	0.26	0.26	0.26	0.26	0.26	0.26	0.26	0.26
Outputs									
Ethanol	MJ	1	1	1	1	1	1	1	1
Electricity before use for ATJ conversion	MJ	0.11	0.088	0.11	0.088	0.11	0.088	0.11	0.088

Ethanol-to-jet		Agricultural residues		Forest residues		Miscanthus		Switchgrass	
Inputs	**Units**	Standalone	Integrated	Standalone	Integrated	Standalone	Integrated	Standalone	Integrated
Ethanol	MJ	1.06	1.06	1.06	1.06	1.06	1.06	1.06	1.06
Hydrogen	MJ	0.06	0.06	0.06	0.06	0.06	0.06	0.06	0.06
Natural gas	MJ	0.18	0	0.18	0	0.18	0	0.18	0
Electricity	MJ	0.02	0	0.02	0	0.02	0	0.02	0
Total Energy Input	**MJ**	**1.32**	**1.12**	**1.32**	**1.12**	**1.32**	**1.12**	**1.32**	**1.12**
Outputs									
Jet fuel and other energy products	MJ	1	1	1	1	1	1	1	1
Jet energy share in total energy output (%)		75%	75%	75%	75%	75%	75%	75%	75%
Energy efficiency (%)		**76%**	**92%**	**76%**	**92%**	**76%**	**92%**	**76%**	**92%**

References for Appendix

International Fertilizer Association. (2010). Retrieved from Fertilizer use by crop 2006/7: http://www.fertilizer.org/ifa/Home-Page/STATISTICS

Neeft, J., & et al. (2012). Retrieved from Biofuel Greenhouse gas emissions: Align Calculations in Europe (BioGrace), Version BioGrace I v.4d and BioGrace II v.3: http://www.biograce.net

Gabrielle, B., Gagnaire, N., Massad, R. S., Dufossé, K., & Bessou, C. (2014a). Environmental assessment of biofuel pathways in Ile de France based on ecosystem modeling. *Bioresource technology*, *152*, 511-518.

Gabrielle, B., Bamière, L., Caldes, N., De Cara, S., Decocq, G., Ferchaud, F., ... & Richard, G. (2014b). Paving the way for sustainable bioenergy in Europe: technological options and research avenues for large-scale biomass feedstock supply. *Renewable and Sustainable Energy Reviews*, *33*, 11-25.

Sawyer, J., & Mallarino, A. (2007, August). *Iowa State University.* Retrieved from Nutrient removal when harvesting corn stover: http://www.ipm.iastate.edu/ipm/icm/2007/8-6/nutrients.html

Giuntoli, J., Boulmanti, A. K., Corrado, S., Motegh, M., Agostini, A., & Baxter, D. (2013). Environmental impacts of future bioenergy pathways: the case of electricity from wheat straw bales and pellets. *GCB Bioenergy*, *5*, 497-513.

Sikkema, R., Junginger, M., Pichler, W., Hayes, S., & Faaij, A. P. (2010). The international logistics of wood pellets for heating and power production in Europe: Costs, energy-input and greenhouse gas balances of pellet consumption in Italy, Sweden and the Netherlands. *Biofuels, Bioproducts and Biorefining*, *4*(2), 132-153.

Sultana, A., Kumar, A., & Harfield, D. (2010). Development of agri-pellet production cost and optimum size. *Bioresource Technology*, *101*, 5609-5621.

Brandao, M., i Canals, L. M., & Clift, R. (2011). Soil organic carbon changes in the cultivation of energy crops: Implications for GHG balances and soil quality for use in LCA. *Biomass and Bioenergy*, *35*(6), 2323-2336.

Lindholm, E. L., Berg, S., & Hansson, P. A. (2010). Energy efficiency and the environmental impact of harvesting stumps and logging residues. *Eur. J. Forest Res.*, *129*, 1223-1235.

Hamelinck, C. N., Suurs, R. A., & Faaij, A. (2005). International bioenergy transport costs and energy balance. *Biomass and Bioenergy*, *29*, 114-134.

Paustian, K. (2006). *Institute for Global Environmental Strategies.* Retrieved from IPCC Guidelines for National GHG Inventories: http://www.ipcc-nggip.iges.or.jp/public/2006gl/pdf/4_Volume4

Bernd, F., Reinhardt, G., Malavelle, J., Faaij, A., & Fritsche, U. (2012, February). Retrieved from Global Assessments and Guidelines for Sustainable Liquid Biofuels - a GEF Targeted Research Project.

Smeets, E. M., Lewandowski, I. M., & Faaij, A. P. (2009). The economical and environmental performance of miscanthus and switchgrass production and supply chains in a European setting. *Renewable and sustainable energy reviews*, *13*(6-7), 1230-1245.

Lopez, D., Mullins, J., & Bruce, D. (2010). Energy life cycle assessment for the production of biodiesel from rendered lipids in the US. *Ind Eng Chem Res*, *49*(2), 419-432.

Stratton, R. W., & et al. (2010). *Life Cycle Greenhouse Gas Emissions from Alternative Jet Fuels.* MIT and Partnership for Air Transportation Noise and Emissions Reduction, Cambridge, MA, USA.

PART III – CALCULATION OF INDUCED LAND USE CHANGE VALUES

CHAPTER 1. **INTRODUCTION**

ICAO and its Member States have agreed to implement a Global Market-based Measure (GMBM) scheme in the form of the Carbon Offsetting and Reduction Scheme for International Aviation (CORSIA) to curb aviation emissions (ICAO, 2016). The use of sustainable aviation fuels (SAF) may play a critical role for mitigating emissions in the GMBM scheme, particularly given that other energy sources, such as natural gas and electricity, are not viable in aviation because of the requirements on the performance or specifications for jet fuels (Petter and Tyner, 2014; Radich, 2015). Thus, it is important to know to what extent SAF can help reduce carbon emissions from international aviation.

The Committee on Aviation Environmental Protection (CAEP) of ICAO assessed the wide range of issues related to emission reductions from the use of sustainable aviation fuels. CAEP employed life-cycle analysis (LCA) for evaluating greenhouse gas (GHG) emissions associated with all stages in the production and use of a fuel and for comparing emission profiles between SAF and petroleum-based fuels. Promoting crop-based SAF may encourage cropland expansion and cause GHG emissions from land use change. As a result of land competition between croplands and natural lands, interactions among markets, and trade among regions, land use change and related emissions may become a global phenomenon that goes beyond the regions expanding biofuels production. This is called biofuels induced land use change (ILUC) emissions. The CAEP agreed to include the ILUC emissions in the emissions estimates of the LCA of SAF. CAEP decided that the sum of the core life-cycle emissions and the ILUC emissions is defined as the total life-cycle emissions for a SAF pathway, which is compared with the baseline life cycle emissions values for aviation fuels to determine whether and to what extent the SAF can mitigate emissions. In CORSIA, these baseline values are equal to 89 gCO_2e/MJ for jet fuel and 95 gCO_2e/MJ for AvGas.

Biofuels ILUCs and their associated emissions have been widely examined in the literature (Ahlgren and Di Lucia, 2014; Broch et al., 2013; Khanna and Crago, 2012; Warner et al., 2014; Wicke et al., 2012). These review papers indicate that there are important disparities among models in the baseline assumptions, shock size, simulation approach, and the data used in calculating emissions. Previous studies have estimated ILUC and associated emissions induced by first-generation biofuels or second-generation biofuels for road transportation (Dunn et al., 2013; Havlík et al., 2011; Hertel et al., 2010; Keeney and Hertel, 2009; Kicklighter et al., 2012; Laborde and Valin, 2012; Mosnier et al., 2013; Searchinger et al., 2008; Taheripour et al., 2017a; Taheripour and Tyner, 2013; Taheripour et al., 2011; Taheripour et al., 2017b; Tyner et al., 2010; Valin et al., 2015). SAF ILUC emissions have not been estimated in the literature. Nevertheless, studies for road biofuels indicated that estimating ILUC emissions is subject to notable uncertainty, and uncertainties in economic models can be amplified through the uncertainties in the carbon accounting models (Plevin et al., 2015; Taheripour and Tyner, 2013).

For estimating SAF ILUC emissions, noting the considerable uncertainty for estimating biofuels ILUC emissions, two well-established economic equilibrium models, GTAP-BIO and GLOBIOM, were employed in parallel in CAEP. GTAP-BIO and GLOBIOM are two economic models that have been extensively employed in estimating biofuels induced land use change and related emissions. They belong to two different branches of economic models. GTAP-BIO is a computable general equilibrium model developed at the Center for Global Trade Analysis Project (GTAP) at Purdue University. GLOBIOM is a partial equilibrium mathematical programming (constrained optimization) model developed at the International Institute for Applied Systems Analysis (IIASA). GLOBIOM has its roots in FASOM developed by Bruce McCarl at Texas A&M. However, FASOM is US focused, while GLOBIOM is global with more detailed representation for the EU. GTAP-BIO has been used mainly for evaluating biofuels policies in the U.S., and GLOBIOM has focused mainly on EU policies, although both models have experience with analysis in other regions.

The measurement of ILUC emissions usually consists of two steps. The global land use change is first estimated through an economic equilibrium model, and then GHG emissions associated with the estimated

land use changes can be measured by applying an emission accounting model. An emission accounting model accounts for at least three major sources of emissions released to the atmosphere due to ILUC, including (1) emissions due to changes in vegetative living biomass (natural vegetation and average agricultural landscape) carbon stock, (2) emissions due to changes in soil carbon stock, and (3) emissions debt equivalent to forgone carbon sequestration (Plevin et al., 2014a; Searchinger et al., 2008; Taheripour and Tyner, 2013). GTAP-BIO runs with its coupled emission factor model, AEZ-EF created for the California Air Resource Board (CARB), while GLOBIOM has emission factors embedded within the model.

GTAP-BIO (AEZ-EF) and GLOBIOM have different structures, and use data sets, parameters and emission factors from different sources. For these reasons, the results of the two models can differ. In the context of the CAEP work, 22 pathways, including 6 starch & sugar pathways, 6 vegetable oil pathways, and 10 cellulosic pathways, were simulated in the two models, respectively. The two modeling teams worked closely to compare the land use change and emissions results and to explore the main drivers of the differences. Based on the comparison analysis, the two teams reconciled some data and assumptions employed in the two models to reflect new literature data and aligned assumptions. Substantial progress has been made for all pathways in reducing the gap between the two model assessments through these harmonization efforts. The ILUC emissions for the starch & sugar pathways have reached close agreement, in terms of the total ILUC emission intensity between GTAP-BIO and GLOBIOM. However, the ILUC emission differences for several vegetable oil pathways remain large, mainly due to the difference in the livestock rebound effect, demand responses, and other factors. Even though the ILUC emission difference for several cellulosic pathways is also relatively large, these pathways generally have negative or small emission intensities.

This report aims to document the methodology and the technical information used for estimating ILUC emissions for SAF pathways. The rest of this technical report is structured as follows:

- Section 2 describes the SAF pathways for evaluation and the development of shock sizes for the pathways.
- Section 3 introduces the two models, GTAP-BIO and GLOBIOM, employed and provides a detailed descriptive comparison between GTAP-BIO (including AEZ-EF) and GLOBIOM from the perspective of data, modeling framework, and emission factors.
- In section 4, the data updates and model modifications made in both models for the purpose of estimating SAF ILUC emissions are summarized and discussed.
- The ILUC emission results from GTAP-BIO and GLOBIOM are provided and compared in Section 5.
- Section 6 discuss the sensitivity of key data and parameters in modelling ILUC emissions.
- Section 7 documents the agreed method for calculating default ILUC emission intensity value based on GTAP-BIO and GLOBIOM results,
- and Section 8 discusses the process for developing additional ILUC values.

CHAPTER 2. **SUSTAINABLE AVIATION FUEL PATHWAYS AND SHOCK SIZES**

2.1 **SAF PATHWAYS**

A complete SAF pathway is defined by the fuel conversion technology, the feedstock, and the region where SAF will be produced and consumed. For this task, CAEP focus on the American Society for Testing and Materials (ASTM) approved technologies including Hydrotreated Esters of Fatty Acids (HEFA), Fischer-Tropsch (FT)[13], Synthesized Iso-Paraffins (SIP), Alcohol (isobutanol)-To-Jet (ATJ-SPK from isobutanol), and Alcohol (ethanol)-To-Jet (ATJ-SPK from ethanol)[14] (ASTM, 2018) using land-based feedstocks. This analysis currently focuses on SAF produced in four regions including the US, EU, Brazil, and Malaysia/Indonesia since they are leading producers of conventional road biofuels and major consumers of petroleum jet fuel. Furthermore, CAEP only studied pathways using feedstocks that could lead to induced land use change. That is, SAF produced from feedstocks such as agricultural and forestry residues, waste tallow, used cooking oil (UCO), municipal solid waste (MSW), and microalgae are not included as they have low risk in generating induced LUC emissions.

In total, there are twenty-two pathways, as presented in Table 92 All these pathways were simulated in both GTAP-BIO and GLOBIOM.

Table 92: SAF pathways for ILUC emission value estimation

Description		Technology and feedstock																
		ATJ-SPK from isobutanol				ATJ-SPK from ethanol				SIP		HEFA				FTJ		
		Corn	Sugarcane	Miscanthus	Switchgrass	Corn	Sugarcane	Miscanthus	Switchgrass	Sugarcane	Sugar beet	Soy oil	Rapeseed oil	Palm oil	Carinata oil	Poplar	Miscanthus	Switchgrass
Region	USA	**1**		**3**	**5**	**6**		**8**	**10**			**13**			**17**	**19**	**20**	**22**
	Brazil		**2**				**7**			**11**		**14**			**18**			
	EU			**4**				**9**			**12**		**15**				**21**	
	Malaysia & Indonesia													**16**				

[13] FTJ represents both FT-SPK and FT-SKA and the two are not distinguished.

[14] In April 2018, ASTM International revised the Standard Specification for Aviation Turbine Fuel Containing Synthesized Hydrocarbons (ASTM D7566 Annex A5) to add ethanol as an approved feedstock in addition to isobutanol for producing ATJ synthetic paraffinic kerosene. The approved blend level (percentage of SAF allowed when blended with petroleum-based jet fuel) for ATJ was also increased from 30% to 50% in the revision. The approved blend level is 10% for SIP and 50% for ATJ and HEFA.

2.2 **SHOCK SIZE DEVELOPMENT**

The size of the SAF expansions (termed "shocks" by the modellers) is the difference in SAF production for the target year between the scenario with aviation fuel deployment and a counterfactual where biofuels remain fixed at the base year production levels, for a pathway in a particular region. GTAP-BIO has a base year of 2011 and GLOBIOM uses 2010 as its reference. 2035 is used as the target year to be consistent with the Global Market-based Measure (GMBM) scheme. Since there was negligible SAF production in the base year of the models, the estimated production projected in 2035 would be the SAF shock.

To estimate ILUC emissions of an SAF pathway, the projected SAF production (shock size) of the pathway is needed in the simulation as the driver of global land use changes. The shock sizes of the SAF expansions are developed based the International Energy Agency (IEA) 450 Scenario[15] projections from the World Energy Outlook (WEO) (IEA, 2015a). The "IEA 450" Scenario provided the projection of global SAF production in 2025 and 2040 (IEA, 2015a). The 2035 SAF production, 2596 Petajoules (PJ) or 21.2 Billion Gallons Gasoline Equivalent (BGGE), was interpolated linearly based on those projections. The global projection is further allocated to the regional level based on information in WEO and Southeast Asia Energy Outlook (SAEO) (IEA, 2015b) and pathway level with the consideration of feedstock availability, economic feasibility, and road biofuels coproduct shares. Pathway-level SAF shocks were first developed, and other biofuel and bioenergy coproducts are calculated based on the fuel output shares implied by a technology.

The regional shares for the USA (29%), Brazil (19%), and EU (17%) are calculated from the total biofuel consumption levels in 2040 projected in the New Policies Scenario in WEO (IEA, 2015a). The level of S.E. Asia biofuels projection in 2040 is from the New Policies Scenario in Southeast Asia Energy Outlook (IEA, 2015b), which is 9 million of tonnes of oil equivalent (Mtoe). The Malaysia & Indonesia share (3%) was estimated by assuming it is 60% of total S.E. Asia, which is approximately the historical jet fuel consumption ratio between Malaysia & Indonesia and S.E. Asia (EIA, 2015). The regional shares are used to split the projected world total SAF in 2035 into regional levels. The four regions account for 67% of the total SAF production.

In each region, the pathway shares are estimated with the consideration of the economic feasibility of technology, the feedstock availability in a region, and the share of road biofuels coproduct. Table 93 presents fuel output energy shares between SAF and road biofuel coproducts for the four pathways. It was decided that the coproduced road biofuels are shocked in conjunction with their corresponding SAF, and emissions are allocated on an energy basis. These shares are in line with the shares applied in core LCA analyses except for HEFA. For the HEFA pathways, it was assumed that 10% of renewable diesel could be used as SAF, so that the SAF share increased from 15% in the max renewable diesel scenario to 25%.

[15] The 450 Scenario is the most aggressive scenario projected by IEA. It depicts a pathway to limit the rise of the long-term average global temperature to two degrees Celsius (2 °C) compared with pre-industrial levels.

Table 93: Fuel output energy shares by pathway

Pathway	Output energy shares	
	SAF	Road
HEFA	25%	75%
Grain ATJ	100%	0%
Sugarcane ATJ	88%	12%
Grain ATJ-SPK from ethanol	76%	24%
Sugarcane ATJ-SPK from ethanol	62%	38%
FT	25%	75%
SIP	100%	0%
Perennial crops ATJ	100%	0%
Perennial crops ATJ-SPK from ethanol	74.5%	25.5%

The HEFA pathway has relatively lower life-cycle cost of production compared with other pathways since the technology is relatively more mature (Diederichs et al., 2016). However, the vegetable oil feedstocks availability and the high share of road biofuels coproduct are two important constraints for the expansion of HEFA SAF. For this reason, CAEP also assumed a particular constraint that, for non-cellulosic pathways, the volume of feedstock used for SAF production could not exceed the current production level. In 2015, soybean (*Glycine max*) oil production in the USA was around 10 million tons (Mt) or about 2.8 billion gallons (BG) (USDA, 2016e). About 2.2 Mt soybean oil was used for biodiesel production, accounting for 45% of the total biodiesel feedstock (other biodiesel feedstocks include 7% rapeseed oil, 10% corn (*Zea* mays) oil, 38% fats, grease, and others; the total biodiesel production was 1.27 BG in 2015) (EIA, 2016). CAEP assumed that the soy oil HEFA pathway would account for 2.2% of the total SAF production in 2035, which requires feedstock of around 6 Mil. Mt soy oil after considering coproducts. Similar pathway shares for the HEFA pathways are assigned in other regions. The total soybean oil production in Brazil in 2014 was around 7.76 Mt, which was about 2.17 BG. Total rapeseed (*Brassica napus*) oil production in EU was about 10 Mt in 2015, of which 6.1 Mt was used in biodiesel or renewable diesel production (USDA, 2016a). In 2015, Malaysia & Indonesia produced 0.46 BG biodiesel from palm (*Elaeis guineensis*) oil, of which 0.14 BG were exported. The palm oil produced in Malaysia & Indonesia was over 14.8 BG (USDA, 2016c, d).

Given the higher existing supply of corn and sugar crops and smaller coproduct shares for ATJ and SIP, CAEP assigned relatively higher pathway shares in the global SAF portfolio for these pathways. CAEP assigned a pathway share of 4% to the USA corn ATJ-SPK from ethanol/isobutanol and the two sets of sugarcane (*Saccharum officinarum*) pathways in Brazil, and 3% to the EU sugar beet (*Beta vulgaris* ssp. *vulgaris*) SIP pathway. In 2014, the US corn production was around 350 Mt, and Sugarcane production in Brazil was around 600 Mt. Sugar beet production in 2014 in EU was over 100 Mt (USDA, 2016b). The feedstock requirement for these pathways is small compared with the existing production.

The 2011 US DOE's billion-ton study update (Perlack et al., 2011) estimated 0.4 billion dry tons of potential energy crop could be produced for biomass source for biofuels in 2030. The feedstock projection is more than enough for producing 6.8 BGGE (including coproducts) cellulosic FT/ ATJ-SPK from ethanol/isobutanol biofuels, assuming 8% of the total SAF production in 2035 would be from cellulosic FT/ATJ-SPK from isobutanol/ethanol in the USA. It also indicated the large potential of non-LUC feedstock (over 3.6 billion dry tons agricultural and forest residue and waste). Similarly, large potential has been estimated in the case of the EU (EEA, 2007, 2013). Also, the shock size for cellulosic biofuels used

in Valin et al. (2015) was 123 PJ or 1 BGGE for 2020 diesel production from miscanthus (*Miscanthus sinensis*). Given that the coproducts from cellulosic biofuels can replace the diesel used for road, it is reasonable to have a shock size for cellulosic FT/ATJ-SPK from isobutanol/ethanol of 1.7 BGGE in 2035. Furthermore, the "other SAF" includes low ILUC risk pathways or other LUC-inducing SAF pathways not yet included. The "other SAF" accounts for about 50% of the world total SAF production. The estimated SAF production in 2035 after applying the assumed pathway shares is presented in Table 94.

Table 94: SAF projection in 2035, by region and technology

Region	SAF pathway	Pathway Share	SAF production	
			PJ	BGGE
USA	Soy oil HEFA	2.2%	57	0.47
	Corn ATJ-SPK from isobutanol/ethanol	4.0%	104	0.85
	Miscanthus FT/ATJ-SPK from isobutanol/ethanol	2.7%	69	0.57
	Switchgrass FT/ATJ-SPK from isobutanol/ethanol	2.7%	69	0.57
	Poplar FT	2.7%	69	0.57
	Other SAF including: Carinata oil HEFA*	14.4% (0.25%)	373 (6.5)	3.05 (0.053)
Brazil	Soy oil HEFA	1.7%	44	0.36
	Sugarcane SIP	4.0%	104	0.85
	Sugarcane ATJ-SPK from isobutanol/ethanol	4.0%	104	0.85
	Other SAF including: Carinata oil HEFA*	9.3% (0.25%)	243 (6.5)	1.98 (0.053)
EU	Rapeseed oil HEFA	2.5%	65	0.53
	Miscanthus FT/ATJ-SPK from isobutanol/ethanol	2.0%	52	0.42
	Sugar beet SIP	3.0%	78	0.64
	Other SAF	9.2%	238	1.94
Malaysia & Indonesia	Palm HEFA	2.0%	52	0.42
	Other SAF	0.5%	13	0.11
Other regions		33.2%	862	7.04
Total		100.0%	2596	21.2

* Carinata grown as a secondary crop that avoids other crops displacement

For including new pathways not already considered in Table 94, the shock size for new pathways must be decided such that the original shock size development framework is not affected. For new pathways using new feedstock, the shock can be added to the list by disaggregating them from "other pathways" in the original development. However, for the new pathways using an already listed feedstock (e.g., corn or miscanthus), feedstock availability has been considered in developing the shock of existing pathways using these feedstocks so that they cannot be disaggregated from "other pathways". Also, to not affect shock sizes of already listed pathways, CAEP assigns, for new pathways, the same SAF shock size as the existing pathways using the same feedstock. This latter addition is considered without changing the total shock size, which means the new pathway is considered as an alternative route to the pathway from which it replicates the shock size. For example, US corn ATJ-SPK from ethanol was a pathway added after the original shock

development was completed, so it was assigned a 104 PJ SAF shock, like the US corn ATJ-SPK from isobutanol pathway (only for the simulation purpose), while the two pathways together are assumed to produce 104 PJ SAF to be consistent with the SAF production projections. The setup facilitates the comparison of the results and accounts for potential nonlinearity caused by shock size. In this respect, it is still consistent with the original shock size development, and it paves the way for developing shocks for new pathways in the future. Also, the fuel coproduct shocks are calculated based on the fuel coproduct shares presented in Table 93. The finalized shock sizes for pathways tested for CAEP/11 are presented in Table 95.

Table 95: Shock sizes for SAF pathways

Region	SAF pathway	Jet	Fuel coproduct	Total	Jet	Fuel coproduct	Total
		PJ	PJ	PJ	BGGE	BGGE	BGGE
USA	Soy oil HEFA	57.1	171.3	228.4	0.47	1.40	1.86
	Carinata oil HEFA*	6.5	19.5	26.0	0.05	0.16	0.21
	Corn ATJ-SPK from isobutanol	103.8	0.0	103.8	0.85	0.00	0.85
	Corn ATJ-SPK from ethanol	103.8	32.2	136	0.85	0.26	1.11
	Miscanthus FT	69.2	207.7	276.9	0.57	1.70	2.26
	Miscanthus ATJ-SPK from isobutanol	69.2	0.0	69.2	0.57	0.00	0.57
	Miscanthus ATJ-SPK from ethanol	69.2	23.7	92.9	0.57	0.19	0.76
	Switchgrass FT	69.2	207.7	276.9	0.57	1.70	2.26
	Switchgrass ATJ-SPK from isobutanol	69.2	0.0	69.2	0.57	0.00	0.57
	Switchgrass ATJ-SPK from ethanol	69.2	23.7	92.9	0.57	0.19	0.76
	Poplar FT	69.2	207.7	276.9	0.57	1.70	2.26
Brazil	Soy oil HEFA	44.1	132.4	176.5	0.36	1.08	1.44
	Carinata oil HEFA*	6.5	19.5	26.0	0.05	0.16	0.21
	Sugarcane SIP	103.8	0.0	103.8	0.85	0.00	0.85
	Sugarcane ATJ-SPK from isobutanol	103.8	14.1	117.9	0.85	0.12	0.96
	Sugarcane ATJ-SPK from ethanol	103.8	64.6	168.5	0.85	0.53	1.38
EU	Rapeseed oil HEFA	64.9	194.7	259.6	0.53	1.59	2.12
	Miscanthus FT	51.9	155.8	207.7	0.42	1.27	1.70
	Miscanthus ATJ-SPK from isobutanol	51.9	0.0	51.9	0.42	0.00	0.42
	Miscanthus ATJ-SPK from ethanol	51.9	17.8	69.7	0.42	0.15	0.57
	Sugar beet SIP	77.9	0.0	77.9	0.64	0.00	0.64
Malaysia & Indonesia	Palm jet HEFA	51.9	155.8	207.7	0.42	1.27	1.70

* Carinata grown as a secondary crop that avoids other crops displacement

2.3 **ILUC EMISSION INTENSITY**

To be consistent with the core LCA analysis and the literature convention, the ILUC emission intensity is calculated for each pathway. The simulations conducted for each pathway are independent. Land use change results are translated to total ILUC emissions by summing emissions (E) over emission category (i), land transition (j), AEZ (k), and region (r), and the ILUC emission intensity is calculated by weighting the total emissions over the 25 year amortization period (AP) and the total energy output (EO) (Equation 1). As a result, the ILUC emission intensity has a unit of grams CO_2-equivalent per megajoule (g CO_2e/MJ).

$$ILUC\ emission\ intensity = \frac{\sum_{i,j,k,r} E_{i,j,k,r}}{AP \times EO} \quad (1)$$

An amortization period of 25 years is used, as agreed by CAEP. This value is a compromise between the European use of 20 years and the US value of 30 years[16]. Note that the equation implies that the total emissions are weighted over all energy outputs from an SAF pathway on the energy basis. That is, energy content in non-fuel energy coproducts (e.g., electricity or biogas) will also be included in the denominator in ILUC emission intensity calculation. Note that only three pathways including Brazil sugarcane ATJ-SPK from isobutanol, Brazil sugarcane SIP, and EU sugar beet SIP pathways have non-fuel energy coproducts (electricity or biogas).

[16] The amortization period is usually a decision made by policy-makers. The choice of amortization approach and period may play an important role in affecting ILUC emission intensity (see O'hare et al., 2009 for different amortization approaches). Most US work used 30-year amortization period while most EU work used 20-year amortization period.

CHAPTER 3. **GTAP-BIO AND GLOBIOM**

3.1 **DATA AND MODELING FRAMEWORK**

GTAP-BIO is a multi-sector multi-region Computable General Equilibrium (CGE) model, based primarily on the standard GTAP database which is the database used by the existing well-known CGE models worldwide. This data set includes the Social Accounting Matrices (SAM) of 140 countries/regions covering 57 economic sectors. Biofuel sectors are added to the SAM tables. In addition, this data base includes data on land cover items (including cropland, forest, and pasture land), crop production, and harvested area all by Agro-Ecological-Zone (AEZ). It also provides data on the production and consumption of energy, emissions, and trade obtained from trusted data sources (Aguiar et al., 2016). Biofuels produced across the world plus their by-products were introduced into the latest version of this standard database which represents the world economy in 2011. This database is geographically aggregated into 19 regions for biofuel analysis. The GTAP-BIO model represents production functions for goods and services; derived demand equations for intermediate and primary inputs (including land by AEZ, labor, capital, and resources); equations to represent households and government demands for goods and services; and equations to model bilateral trade for each pair of countries. Market clearing conditions maintain all markets in equilibrium. These equations endogenously determine supply and demand quantities for all goods and services. This model uses a nesting structure to determine demands for animal feed items by livestock sectors. This nesting structure allows substitution among substitutable feed items in response to changes in relative prices. The parameters of this model which govern land allocation were tuned according to recent observations of land use changes across the world. The latest version of this model, documented in Taheripour et al. (2017b), takes into account multiple cropping and conversion of unused cropland to crop production.

GLOBIOM is a partial equilibrium constrained optimization model of agriculture, forestry and bioenergy sectors. The model was developed using a bottom-up setting based on grid cell information, providing the biophysical and technical cost information through specific activity models: the vegetation model EPIC for crops, the Gridded Livestock of the World database and the digestibility model RUMINANT for livestock, and the G4M model for forestry. These models estimate productivity and environmental indicators for different management based on input data on soil and climate, feeding practices and net primary productivity. In GLOBIOM, as in GTAP-BIO, production, demand and international trade evolve with the endogenous adjustment of prices. However, GTAP-BIO traces trade of all goods and services across the world, while GLOBIOM only focuses on trade of primary and secondary agricultural and forestry products. Prices are fixed for the non-land based sectors (energy, industry, services). Market equilibrium is determined through mathematical optimization which allocates land and other resources to maximize the sum of consumer and producer surplus (Valin et al., 2015).

Land cover in GTAP-BIO includes cropland (including cropland pasture and unused cropland), pasture, and (accessible managed) forest. Cropland pasture is marginal cropland that is used by the livestock industry and can move to crop production. GLOBIOM includes cropland, grassland, forest, and other natural land. Pasture and forest in GTAP are close to grassland and forest in GLOBIOM, but the data come from different sources. Other natural land (including abandoned land) in GLOBIOM is defined as land not classified as cropland, grassland or forest in the initial land cover data (2000). Abandoned land in GLOBIOM is accounted for separately. Differences in land categories and their emission stocks can be important drivers leading to different ILUC emissions.

GTAP-BIO has the base year of 2011. With this database, the model determines ILUCs associated with each biofuel pathway using a comparative static approach. This approach isolates the impacts of expansion in production of each biofuel pathway (or a shock in production) from all other factors that may affect the global economy. Thus, this approach isolates the impacts for each biofuel production for a given target and determines how that expansion affects the allocation of land across its alternative uses. The new allocation

of land is compared with the allocation of land in the base data to determine ILUCs. GLOBIOM is dynamic-recursive and follows a forward-looking approach. The model is calibrated on the base year 2000. The first step is to establish a baseline from 2000 to 2020. This baseline considers the major changes in the global economy affecting land use, such as population increase, GDP development, diet shifts, and yield increases. In the current baseline, biofuel incorporation levels are kept constant after 2010. This baseline is compared to a scenario where aviation and road transportation fuel are deployed in addition to the macroeconomic development and other policy changes. The biofuel shock is implemented as a progressive increase between 2010 and 2020 in order to remain close to the base year on which GTAP-BIO is operating. In essence, the biofuel impacts are the delta between the baseline and the simulation with the biofuel shock. Assessing impact on longer time period would indeed make the assessment deeply baseline-dependent, whereas the time horizon 2020 is very close to current land use context.

There are important differences in data, model structure, and even scenario implementation methods. However, both models estimate ILUC emissions following the same accounting convention. First, land use impacts were calculated for expansion in each biofuel. Then ILUCs were converted to ILUC emissions. In other words, if the two models resulted in similar land use change outcomes and similar emission factors were used, then the ILUC emission results would be comparable. Table 96 summarizes some important modeling differences between GTAP-BIO and GLOBIOM.

Table 96: Descriptive comparison between GTAP-BIO and GLOBIOM

	GTAP-BIO (Taheripour et al., 2017b)	GLOBIOM (Valin et al., 2015)
Model framework	A large-scale global CGE model which uses social accounting matrices by region in combination with trade and biophysical data to obtain ILUC	A grid-based global partial equilibrium model, bottom-up, starting from land and technology to markets and consumers, with embedded biophysical process models
Sector coverage	All economic sectors are represented including disaggregated sectors for crops, livestock, forestry, energy (including biofuels) industries, and services	Focus on land-based sectors: agriculture (including livestock), forestry, and bioenergy
Regional coverage	Global (aggregated into 19 regions in the version used for biofuel simulations, but these are aggregated from 140 global regions)	Global (28 EU Member states + 29 regions)
Resolution on production side	Data on land use, crop production, and harvested area are aggregated from a grid cell level to 18 agro-ecological zones (AEZs). SAM tables are at the national level.	Detailed grid-cell level (>10,000 units worldwide)
Time Horizon	Comparative static using 2011 base year.	Dynamic model with ten-year time steps
Land data source	2011 GTAP land database, see Peña-Lévano et al. (2015) for details.	Global Land Cover 2000 dataset with more detailed cover maps for EU (CORINE Land Cover 2000)

	GTAP-BIO (Taheripour et al., 2017b)	GLOBIOM (Valin et al., 2015)
Market data source	2011 GTAP database (Aguiar et al., 2016; Peña-Lévano et al., 2015) developed based on official data collected by the World Bank, FAOSTAT, USITC, and several other data sources.	FAOSTAT and EUROSTAT
Modeling trade	Covers global trade in all goods and services. GTAP uses Armington assumptions to model trade relationships (imperfect substitution between domestic and imported goods and also between imports from different regions)	Bilateral trade for agricultural and wood products, with non-linear transportation costs. Products are traded in physical units as homogenous goods.
Primary factors of production	More detailed on economic resources (labor, capital, land, and natural resources), implied by social accounting matrices	No limit on labor, capital, and energy sources. More detail on non-energy natural resources (land and water).
Land use change mechanisms	Substitution of land use at the regional and AEZ level. Nested CET approach is used for land transformation on the supply side of the market for land; adjustments were made for new cropland productivity.	Grid-based. Constrained mathematical optimization model. Land conversion possibilities allocated to grid-cells taking into account suitability, protected areas.
Representation of production technology	Production technologies are implied in the regional input-output tables from an extended GTAP database (with new sectors introduced for feedstocks and biofuel industries). Constant Elasticity of substitution (CES) production function is used in all sectors.	Detailed biophysical model estimates for agriculture and forestry with several management systems Literature reviews for biofuel processing.
Crop production and yield response	Aggregated 13 crop categories represent all crops in the FAO database including silages, forages, fodders, and planted grass. Crops for biofuels production are disaggregated independently. The crop yields in base data match with the FAO database. CES production function is used for all crops. Thus, changes in the prices of primary factors of production may encourage substitution among these inputs so that crop yield may respond endogenously, according to the embedded regional yield to price elasticities.	18 crops are modeled for the world with nine additional crops for EU representing 84% of global harvested area. Fodder and planted grasses covered through the grassland land cover. An exogenous yield growth trend is implemented in both baseline and biofuels simulation scenarios. Endogenous yield responses are modeled as farmer decisions on (1) shifts between rainfed management types and change in rotation practices; (2) investments in irrigated systems; and (3) change in allocation across spatial units with different suitability.

	GTAP-BIO (Taheripour et al., 2017b)	GLOBIOM (Valin et al., 2015)
Demand side representation	Demand for each sector (good/service) has two components: 1) Final demand including household consumption, government consumption, and net trade and 2) Intermediate demand which represents consumptions of good and services by firms. One representative utility maximizing agent per region determines the final demand for goods and services based on changes in income and relative prices.	Crop and grass consumptions are explicitly modelled for different livestock management systems. Processing industry for oilseeds, woody products, and bioenergy. Food and wood products are consumed directly by one representative agent per region, reacting to the price of products. No cross-price elasticities considered for final consumer except in the case of vegetable oil products.
Multiple cropping and unused land responses	Multi-cropping and unused land responses are modelled together through a calibrated parameter based on historical crop harvest frequency (CHF) trend by region and AEZ.	Multi-cropping at crop level in the base data, with an exogenous trend by crop but no further price induced intensification. The unused agricultural land is currently limited to abandoned land after 2000.

3.2 **EMISSION ACCOUNTING**

ILUC emissions can be categorized into natural vegetation carbon (carbon stored in forest, pasture, etc.), natural vegetation reversion (foregone sequestration), agricultural biomass carbon, soil organic carbon (SOC), and peatland oxidation. Even though in each category, there could be differences in assumptions, data sources, and accounting boundaries between GTAP-BIO and GLOBIOM, ILUC emission results are decomposed into these categories to facilitate results communication and comparison.

Natural vegetation carbon includes carbon stored in above- and below-ground living biomass for forest, pasture, cropland pasture. For forest conversion, both the AEZ-EF and GLOBIOM models also consider dead wood, litter, understory, and harvested wood products (HWP). The carbon sequestration in HWP was added in GLOBIOM calculation for CAEP. AEZ-EF used data from various sources for forestry biomass carbon including Gibbs et al. (2014), IPCC (2006), Saatchi et al. (2011), Woodall et al. (2008), Earles et al. (2012), etc. IPCC (2006) data were used for pasture biomass carbon. Cropland pasture was assumed to have the carbon stock equal to half of the pasture value for the corresponding land transition. GLOBIOM uses data from Forest Resource Assessment (FAO, 2010) for forestry and Ruesch and Gibbs (2008) for other natural vegetation and grassland.

In AEZ-EF, foregone sequestration was accounted only for converting forest since it assumed that forest, if not converted, can still sequester carbon at a certain rate. The natural vegetation reversion in GLOBIOM is similar to the foregone sequestration in AEZ-EF, while it was accounted only for converting abandoned land. For AEZ-EF, forest regrowth data from Lewis et al. (2009) and Myneni et al. (2001) are used. GLOBIOM assumed that abandoned land, if not brought back to production, would revert to forest or other natural land. It follows the EPA (EPA, 2010) method in determining the share of reforestation on abandoned land (to be the same with the share of forest or other natural vegetation already observed on fertile land in the same region). Constant carbon stock is used for other natural vegetation reversion. The assumption GLOBIOM was recently updated to only allow natural vegetation reversion to other natural land.

A recent update in GTAP-BIO allows increasing the use of unused cropland as a land source for crops (biofuels feedstock) production (Taheripour et al., 2017a; Taheripour et al., 2017b). The unused cropland

may have carbon stock in the natural vegetation grown on the land, and it may have higher carbon sequestration in soil compared with the cropland under cultivation. Thus, there could be land use change emissions from bringing unused cropland back to production. Unused land change was disaggregated from the cropland intensification responses, and it was assumed that the emission factors for converting unused cropland are the same with those for converting cropland pasture. The emissions from converting unused land may be compared to the emissions from converting other natural land or abandoned land in GLOBIOM.

Agricultural biomass carbon accounts for carbon changes in agricultural biomass including aboveground and belowground (root and rhizome) biomass. Crop yield, root-to-shoot ratio, harvest index, and effective carbon fraction are key factors in determining the agricultural biomass carbon. The formula used for calculating agricultural biomass carbon is similar for both models. The average carbon stock on cropland is calculated as an average over the cultivation cycle of crops and plantations. This source of sequestration corresponds to the change of land cover and is not to be confused with the accounting of the biomass harvested, which follows here the carbon neutrality assumption (the sequestered carbon is not accounted as sent back to the atmosphere through the biofuel combustion). In AEZ-EF, biomass carbon for annual crops is calculated based on updated crop yield from GTAP-BIO while GLOBIOM uses crop yields in the EPIC model. For palm tree biomass carbon, 34.9 t C/ha was used originally in AEZ-EF but was updated to 48 t C/ha to match GLOBIOM according to the latest literature.

Soil organic carbon (SOC) accounts for organic carbon changes in soil. Natural land (forest, pasture, grass land) usually have significantly higher SOC compared with cropland. SOC sequestration in land growing perennial crops is much higher than in land growing annual crops. Peatland mineral carbon oxidation is not included here. Both models used data from the Harmonized World Soil Database for SOC. GLOBIOM used the IPCC Tier 1 approach while AEZ-EF made some modifications based on the IPCC Tier 1 approach, and different parameters might be applied (e.g., factors for perennial/tree crops, etc.). AEZ-EF also accounts for N_2O (about 10% of the SOC). For both models, the period of SOC accounting does not vary with the amortization period.

Peatland mineral carbon oxidation is separated from soil organic carbon given the importance. It accounts for soil emissions from peatland drainage in Indonesia and Malaysia. Originally, AEZ-EF uses data from Page et al. (2011) (95 t CO_2 /ha/year) while GLOBIOM data is from the mean level (61 t CO_2 /ha/year) of a literature survey. Both models aligned the peat oxidation factor to 38.1 t CO_2 /ha/year based on the new literature data.

3.3 **MODEL INFORMATION SOURCES**

The source of model information for GTAP-BIO and GLOBIOM are presented in Table 97.

Table 97: The sources of model information for GTAP-BIO and GLOBIOM

Information	Source/link
GTAP website	https://www.gtap.agecon.purdue.edu/
GTAP 9 Data Base	https://www.gtap.agecon.purdue.edu/databases/v9/default.asp https://www.gtap.agecon.purdue.edu/resources/res_display.asp?RecordID=5172
GTAP 9 Land Use and Land Cover	https://www.gtap.agecon.purdue.edu/models/landuse.asp https://www.gtap.agecon.purdue.edu/resources/res_display.asp?RecordID=4844
GTAP FAQ	https://www.gtap.agecon.purdue.edu/resources/faqs/index.aspx
GLOBIOM website	https://globiom.org/
GLOBIOM documentation	https://pure.iiasa.ac.at/id/eprint/18996/1/GLOBIOM_Documentation.pdf

CHAPTER 4. DATA UPDATES AND MODEL MODIFICATIONS

4.1 MODEL AND DATA RECONCILIATION

Both GTAP-BIO and GLOBIOM are well-established models in the literature and had been used for estimating induced land use change emissions of road biofuels. For the CAEP work, the starting point of GTAP-BIO was the version of the model documented in Taheripour et al. (2017b), and the version of GLOBIOM used was the one used in Valin et al. (2015). Road biofuels technologies had been introduced into the two models for previous studies, but SAF technologies were not. For estimating SAF ILUC emissions, SAF pathways and their feedstocks (if not previously introduced) need to be introduced into GTAP-BIO and GLOBIOM database and model. For consistency, the average technology conversion yield (Table 98) used for core life-cycle emissions estimation is employed for both models.

Table 98: Technology conversion yield

Technology	Feedstock	SAF	Other fuel	Overall fuel	Electricity	Biogas	DDGS
		MJ/t	MJ/t	MJ/t	MJ/t	MJ/t	t/t
ATJ-SPK from isobutanol	Corn	7233		7233			0.31
	Sugarcane	1541	209	1750	312		
	Miscanthus	5752		5752			
	Switchgrass	5441		5441			
ATJ-SPK from ethanol	Corn	4970	1541	6511			0.29
	Sugarcane	809	504	1313	394		
	Miscanthus	5330	1824	7154			
	Switchgrass	5330	1824	7154			
SIP	Sugarcane	853		853	187		
	Sugar beet	1227		2289		1092	
HEFA	Soy oil	9445	28334	37778			
	Rapeseed oil	9522	28565	38087			
	Palm oil	9445	28334	37778			
	Carinata oil	9472	28416	37888			
FT	Miscanthus	2029	6088	8117			
	Switchgrass	2100	6300	8400			
	Poplar	2246	6737	8982			

Note: DDGS yield is in fresh tons.

The GTAP-BIO and the GLOBIOM team worked closely to compare model results and investigate key drivers to the difference between model results. The most important drivers included livestock rebound response for vegetable oil pathways, palm-related issues (e.g., palm yield, peat oxidation factor, etc.), emissions from converting abandoned land and unused land, cropland intensification responses through multi-cropping and use of unused land, trade modelling framework, land use change patterns in Brazil, and biomass carbon and soil organic carbon for cellulosic crops. Based on the comparison and investigation,

some of the data and assumptions in the two models were updated and reconciled. Table 99 summarizes the changes in the two models during the reconciliation process. The modifications and updates are discussed in more detail in Sections 4.2 and 4.3 for GTAP-BIO and GLOBIOM, respectively.

Table 99: Changes made in the models in reconciliation

Item	Interpretation and changes made
Palm kernel oil	GLOBIOM added palm kernel oil based on FAO data into database and modeling framework.
Palm oil extraction efficiency	GLOBIOM increased palm oil extraction efficiency to reflect the latest data.
Palm biomass carbon	The palm tree biomass carbon sequestration rate in AEZ-EF was increased from 34.9 t C/ha to 48 t C/ha to reflect the new data in the literature.
Immature palm area and palm yield responses	In GTAP-BIO, cropland extensification parameters in Malaysia and Indonesia are adjusted to consider 10-12% immature palm expansion in the region. The palm yield response in Malaysia and Indonesia in GTAP-BIO was lowered by decreasing the palm yield to price elasticity to reflect the new data. In GLOBIOM, the immature palm area in Indonesia is adjusted down to 20% from 30% based on new data from Statistics Indonesia.
Peat oxidation emission factor	The peat oxidation emission factor in AEZ-EF was decreased from 95 tons CO_2/ha/year (Page et al., 2011) to 38.1 t CO_2e/ha/year. GLOBIOM decreased the peat oxidation emission factor from 61 t CO_2/ha/year to the same value (38.1 t CO_2e/ha/year)
Palm expansion on peatland	GLOBIOM decreased the share of palm expansion on peatland from 32% to 20% for Indonesia while 34% is still used for Malaysia. GTAP-BIO uses an endogenous value with a max of 33% for Malaysia and Indonesia.
Land use change pattern in Brazil	The elasticity and the land conversion costs governing the expansion of cropland into forest in Brazil are adjusted in GLOBIOM based on the data and results from GLOBIOM-Brazil.
Emissions from converting unused cropland	In GTAP-BIO, emission factors for converting unused cropland are set to be equal to those of converting cropland pasture in a region
Harvested wood products	In GLOBIOM, harvested wood products (HWP) from forest are considered following an approach similar to the one in AEZ-EF.
Cellulosic crop yields	The ILUC group (both GTAP-BIO and GLOBIOM) adjusted the average cellulosic yields to the yields used by core LCA group. That is, the average dry matter yields after accounting for post-harvest loss targeted were 15.0 t/ha for USA miscanthus, 11.4 t/ha for USA switchgrass, 8.5 t/ha for USA poplar, and 16.6 t/ha for EU miscanthus.
Cellulosic crop biomass carbon	GTAP-BIO (AEZ-EF) and GLOBIOM aligned cellulosic crop biomass carbon based on the recent literature estimation.
Multi-cropping responses	GLOBIOM included multi-cropping trends at crop level so as harvested areas can be distinguished from cultivated area.
Soil organic carbon for cellulosic crops	GLOBIOM updated soil organic carbon for cellulosic crops.

4.2 **MODIFICATIONS AND UPDATES MADE IN GTAP-BIO AND AEZ-EF**

4.2.1 Introduce SAF pathways into GTAP-BIO

For the purpose of this study, CAEP makes necessary modifications in the database and the model of GTAP-BIO. The major modifications include (1) introducing miscanthus (*Miscanthus sinensis*), switchgrass (*Panicum virgatum*), and poplar (*Populus* spp.) in the database and model, (2) incorporating SAF pathways in the database and model, (3) splitting coproducts for SAF in the database and modelling coproducts (both SAF and fuel coproducts enter the blender sector and then supply transportation industries; the co-produced electricity enters the existing electricity industry), (4) modify the constant elasticity of transformation nesting structure to introduce cropland supply for cellulosic crops by nesting miscanthus, switchgrass, and poplar with cropland pasture, (5) tuning parameters governing land transformation, cropland pasture productivity response, and cropland intensification responses.

Following Taheripour et al. (2011) and Taheripour and Tyner (2013), the constant elasticity of transformation (CET) land supply nest for cellulosic cropland and cropland pasture is separated from other cropland to introduce transformation parameters for more flexible governing land transformation to cellulosic corps. The parameters reflect that cellulosic crops will more likely be grown on cropland pasture. The production and cost data for feedstocks and pathways are drawn from literature. Cellulosic feedstocks are introduced as intermediate inputs in biofuels production. Biofuels, either aviation or road biofuels coproducts, produced from SAF pathways are nested with other biofuels. Leontief (fixed coefficient) production is used for SAF production in the top (intermediate inputs) nest so that the technology conversion yields remain unchanged in the simulation. A blender industry processes biofuels and blends them with petroleum fuels to supply either road or aviation transportation. Other coproducts including DDGS, electricity, and gas are treated the same as the existing products in the model by nesting them with their respective existing products using a high elasticity of substitution.

To introduce production technologies for cellulosic crops and SAF into GTAP-BIO database, CAEP developed cost shares of production based on the best available literature information (Buchspies and Kaltschmitt, 2016; Diederichs et al., 2016; Edwards et al., 2016; Elgowainy et al., 2012; Klein, Marcuschamer et al., 2013; Pearlson et al., 2013; Staples et al., 2014; Stratton, 2010; Taheripour and Tyner, 2013). The costs of production were obtained from the literature, mostly techno-economic analysis, and adjusted to 2011$ to match the GTAP 2011 database. The Chemical Engineering Plant Cost Index (CEPCI) was used for adjusting capital costs, and the Industrial Chemicals Producer Price Index (PPI) was used for adjusting chemical prices (CEPCI, 2016; U.S. Bureau of Labor Statistics, 2018). Since in the base year of 2011, the production of cellulosic crops and SAF were negligible, a tiny amount of dummy production was introduced to facilitate the simulation process. Cellulosic crops were disaggregated from the other coarse grains (Oth_CrGr) sector, and the SAF sectors were disaggregated from the energy intensive industries (En_int_ind). In particular, the production of 10,000 tons of cellulosic crops was assumed in the USA and EU, and these crops were dedicated for biofuels production. The AEZ-level crop yields for the US (shown in Table 100) were provided by the Argonne National Laboratory (ANL) while the miscanthus yields in EU were estimated based on the US miscanthus yield and their relationship with corn and wheat. It was assumed that the post-harvest loss is 20% for miscanthus and 12% for switchgrass. The cost structure has to be carefully aligned to the land rent, crop prices, and assumed production level in the database while targeting crop yield and technology conversion yields to maintain the production traceability. Regarding miscanthus, the cost share is different between the US and EU mainly because of the higher average miscanthus land rental rate in EU. The land (AEZs) cost shares for producing cellulosic crops are closely linked to the yield (both AEZ-level and country-average) and the assumed production distribution. In the US, the AEZ with higher cellulosic crop yield was assigned with higher production, and the production was uniformly distributed in EU (1000 tons in each AEZ) to maintain a reasonable country-average crop yield (e.g., 16.6 tons/ha for EU miscanthus). For each cellulosic crop, the AEZ cost shares match the production share across AEZs so that the rental rate (per ha) would be proportional to the crop yield across AEZs.

Furthermore, cellulosic crops are modelled as dedicated energy crops, and the overall average cellulosic crop yields in GTAP-BIO were targeted to the CLCA crop yields with technical shifters to maintain consistency. The average dry matter yields after accounting for post-harvest loss targeted were 15.0 t/ha for USA miscanthus, 11.4 t/ha for USA switchgrass, 8.5 t/ha for USA poplar, and 16.6 t/ha for EU miscanthus.

Table 100: Post-loss dry matter yield for cellulosic crops (t / ha)

Sector	USA			EU
	Miscanthus	Switchgrass	Poplar	Miscanthus
AEZ4	-	-	-	9.2
AEZ7	7.6	5.8	4.5	0.0
AEZ8	10.5	5.5	5.8	12.0
AEZ9	13.1	6.9	7.9	14.5
AEZ10	17.1	9.2	10.8	19.8
AEZ11	16.9	13.6	11.8	24.2
AEZ12	13.8	14.6	10.7	25.0
AEZ13	7.5	2.9	3.5	16.8
AEZ14	10.0	3.2	4.4	25.0
AEZ15	-	-	-	15.8
AEZ16	-	-	-	21.5

Figure 17 explains several important economic responses that occur when an increase in demand for an agricultural commodity for producing biofuels is introduced into the system. There are three margins: demand margin, intensive margin, and extensive margin. The estimation of LUC induced from biofuels measures the land conversion from forest or pasture at the extensive margin, crop switching, and changes in multi-cropping, unused land, and cropland pasture. The demand margin reflects the market-mediated responses in the global economy due to changes in consumption and trade. As a response to higher crop prices encouraged by biofuels production, households and firms will reduce their crop consumption and may increase consumption of its substitute. As domestic prices increase relative to world prices, net exports will decrease. The effects are transferred to other countries through international trade, and other countries may respond with changes in consumption or production. The intensive margin includes intensification in crop production as a response to an increase in the commodity price through (1) substituting land with other inputs in production (2) multiple cropping practices or use of existing cropland, and (3) technical improvements. Finally, the expansion in extensive margin implies land transformation from forest, pasture, or other cropland to producing biofuel feedstocks. When land is converted from forest or pasture to cropland, the productivity of the land will likely be different from the existing cropland. Also, land transformations directly affect the supply and demand of other land-using industries (i.e., other crops, livestock, forestry) due to the scarcity of the land endowment. This links to the responses for those industries. As a result of the domestic and international responses, land conversion from forest, pasture, cropland pasture and unused land to cropland in each region will be accounted as LUC induced by biofuel production.

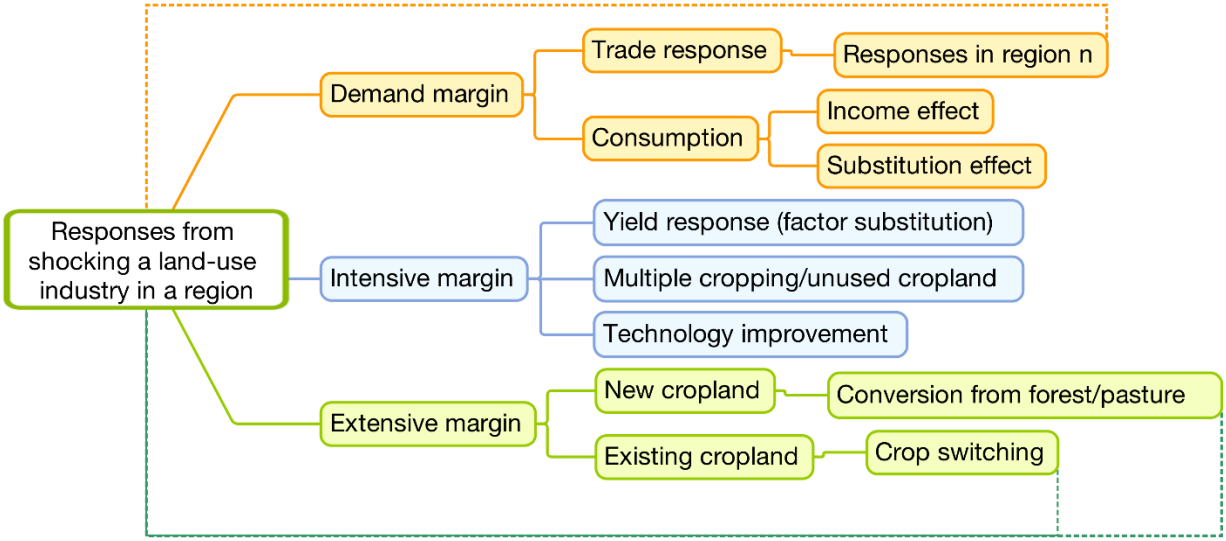

Figure 17: Market-mediated responses from a biofuels policy in GTAP-BIO

4.2.2 Introducing cellulosic crops into AEZ-EF

AEZ-EF was modified and updated for this analysis to include cellulosic crops and to reflect the latest literature data[17]. Plevin (2017) documented the major changes and data sources. For cellulosic feedstocks (switchgrass, miscanthus, and poplar), agricultural biomass carbon (ABC) and soil organic carbon (SOC) are two categories that were updated. Both ABC and SOC are critical for cellulosic crops. As perennial crops with high crop yield, both biomass carbon and SOC for cellulosic crops are significantly higher than the typical row crops. The soil organic carbon emission factors were provided by Argonne National Laboratory's Carbon Calculator for Land Use Change from Biofuels (CCLUB) model (Qin et al., 2016; Dunn et al., 2016). The data indicate that SOC would increase if converting cropland, cropland pasture, or even pasture in many AEZs to producing cellulosic crops. Also, land growing miscanthus tends to have higher SOC compared with growing switchgrass or poplar. For example, in AEZ 10 in the USA, SOC would increase by 1.26 t C/ha/year if converting annual cropland for growing miscanthus. The figure would be 0.5 and 0.18 t C/ha/year for growing switchgrass and poplar, respectively.

The formula used for calculating ABC (IPCC Tier1 approach) is presented in Equation 2 (see Plevin et al. (2014b) for more details). The parameters used for cellulosic crop biomass carbon calculation are presented in Table 101. The crop yields simulated in GTAP-BIO are used in the formula to take into account yield changes in the simulation. A timing parameter of 0.5 is used for annual crops, representing the assumption that that carbon sequestrated in annual crops stays for a half year. Harvest index depicts the share of above-ground biomass that is harvested. CAEP employs the literature estimations of cellulosic crop biomass carbon to calibrate the timing parameter for cellulosic crops[18].

[17] The modifications for adding cellulosic crops were completed in collaboration with Dr. Richard Plevin, one of the original creators of the CARB AEZ-EF model. The changes were made in the Python version of AEZ-EF. Some important emission factors and assumptions were then updated to reflect the new literature data and the progress of model reconciliation between GTAP-BIO and GLOBIOM.

[18] For example, Dohleman et al. (2012) estimated the miscanthus below-ground biomass carbon to be 12.7 t /ha considering rhizome biomass, root biomass and deep root biomass. The poplar biomass carbon was estimated to be 12.2 t C/ha assuming an 8-year rotation (roots lasts for 5-7 coppicing cycles) (estimated by IIASA). The timing parameters were estimated based on these literature values.

$$\textbf{Crop biomass carbon} = \frac{\textit{Timing parameter} \cdot \textit{crop carbon fraction} \cdot \textit{dry crop yield} \cdot (1+R{:}S)}{(1-\textit{loss fraction}) \cdot (HI)} \quad \textbf{(2)}$$

Table 101: Parameters used for calculating agricultural biomass carbon for cellulosic crops

Parameter	Post-harvest loss fraction	Harvest index (HI)	Root-to-shoot ratio (R:S)	Crop C fraction	Source
Miscanthus	0.12	0.9	0.41	0.45	Zhuang et al. (2013)
Switchgrass	0.2	0.9	0.72	0.45	Garten et al. (2010); Zhuang et al. (2013)
Poplar	0	0.9	0.40	0.45	Garten et al. (2011); Winans et al. (2015)

4.2.3 Palm related responses and emission factors

Malaysia and Indonesia are the world largest palm oil producers, together accounting for 85% of world palm oil production in 2014 (FAOSTAT, 2017). Oil palm expansion in Malaysia and Indonesia has been at the expense of forest clearance and peatland drainage, both of which considerably contribute to carbon emissions. The peatland ecosystem is one of the most efficient carbon sinks as it accumulates decayed vegetation or organic matter over thousands of years (Hugron et al., 2013). Drainage of peatlands, peat swap forest particularly, for industrial oil palm plantation in Malaysia and Indonesia has led to the important loss of soil carbon. Due to substitutions among vegetable oils and international trade, producing biofuels from any vegetable oil in any region would encourage palm oil expansion in Malaysia and Indonesia. In other words, ILUC emissions results, particularly for vegetable oil pathways, are very sensitive to the palm related parameters. Thus, several important palm related emission factors are examined in this section.

The life cycle for a typical palm plantation is planting (or replanting) followed by about three years of no yield, followed by a rapid increase in yield for about seven years. Then plateauing for about ten years followed by a sharp decline afterward (Shean, 2012). Because of the development period of palm plantation, the immature area of palm may also expand due to biofuel shocks. GTAP-BIO used the FAO data to represent the average yield of the existing trees (harvested areas) in each region so that immature area was not included. This was modified by adjusting cropland extensification parameters in Malaysia and Indonesia to consider 10-12% immature palm related to replanting of plantations in the region. That is, 10-12% of the palm planation area used for SAF production is immature palm area. It reflects immature palm area share in a steady state.

As a response to higher land prices caused by the expansion in biofuels, palm fruit production would intensify by using relatively less land but relatively more other inputs. This price induced yield response is included in GTAP-BIO endogenously. It is also a way to reflect the historical yield increase in the model. The yield response in the model directly affects the yield in the updated database. In GTAP-BIO, the yield elasticity used for palm in Malaysia and Indonesia was assumed to be the same as the yield elasticity used for corn in the USA. However, the yield growth of US corn has been significantly stronger than it for palm in the past decades. Thus, the palm yield response in GTAP-BIO was tuned and adjusted. Following a set of sensitivity tests, a lower yield to price elasticity (0.05) was assigned to palm produced in Malaysia & Indonesia to take into account the recently observed stagnation in palm yield growth in this region.

AEZ-EF was using 34.9 t C/ha for palm tree biomass carbon based on the estimation from Harris (2011) and EPA (2012). The estimation did not account for below-ground biomass carbon. A recent study from Khasanah et al. (2015) reported estimation of 37.7 - 42.1 t C/ha for palm aboveground carbon stock. Apply the root-to-shoot ratio of palm trees to the aboveground biomass carbon value gives a total palm biomass carbon of about 48 t C/ha. Thus, the palm biomass carbon was updated to 48 t C/ha.

The peat oxidation emission factor was 95 tons CO_2/ha/year (Page, Rieley, and Banks, 2011) in AEZ-EF. It was at the high-end in the literature, and it is a uniform value used for any peatland. In a recent study, Miettinen et al. (2017) pointed out that peat oxidation factors should be differentiated by peatland type. The study suggested using 55 t CO_2/ha/year for pristine peat swamp forest (PSF), 45.3 t CO_2/ha/year for degraded peat swamp forest, 35.6 t CO_2/ha/year for tall shrub/secondary forest, and 19.8 t CO_2/ha/year for ferns/low shrub/clearance. For the purpose of this study, CAEP overlaid the peatland map used in Miettinen et al. (2016) with the Indonesia palm concession map from the Global Forest Watch (GFW, 2017) to estimate the available peatland for palm expansion in the region. The results (Table 102) show that for Sumatra and Borneo, Indonesia, there are about 2.4 Mil. ha of palm concession on peatland with tiny pristine PSF and 0.42 Mil. ha of degraded PSF. Over 1 Mil. ha has been used under industrial palm plantations. The estimation is in line with the recent literature study by Austin et al. (2017). The weighted average peat oxidation value based on Table 102 is 38.1 t CO_2/ha/year. Thus, CAEP decreased the peat oxidation value from 95 t CO_2/ha/year to 38.1 t CO_2/ha/year[19].

Table 102: Available peatland for palm expansion and associated peat oxidation factors

Land category	Peat area (Mil. ha)	Emission factor (CO_2/ha/year)
Pristine peat swamp forest (PSF)	0.04	55
Clearance (open area)	0.06	19.8
Ferns/low shrub	0.11	19.8
Tall shrub/secondary forest	0.26	35.6
Degraded PSF	0.42	45.3
Small-holder area (existing palm)	0.45	0
Industrial plantations (existing palm)	1.08	0
Total/average	2.42	38.1

4.2.4 Including emissions from converting unused cropland

GTAP-BIO recently introduced cropland intensification response to allow multi-cropping and the use of the existing unused cropland. The conversion of unused cropland to crop production may lead to LUC emissions. In other words, if assuming no land use change emissions from bringing back unused cropland to production, the ILUC emissions will be underestimated. This was not previously considered by GTAP-BIO (AEZ-EF) since the two cropland intensification responses, multi-cropping and the use of unused cropland, were modeled jointly so that the two cannot be distinguished when extrapolating land transition matrices based on land use change results. For the purpose of this study, CAEP estimates the shares between multi-cropping and unused cropland in land use change results for each AEZ and region using cropping intensity maps provided by Ray and Foley (2013) and Siebert et al. (2010). The shares are further refined based on Taheripour et al. (2017a) to be consistent with GTAP-BIO. Given limited literature estimations, CAEP assumed that the emission factors for converting unused cropland are the same as those for converting cropland pasture.

[19] Malaysia does not have a publicly available palm concession map, so only peat oxidation factor estimated for Indonesia was used to represent both Malaysia and Indonesia.

4.3 **MODIFICATIONS AND UPDATES IN GLOBIOM**

4.3.1 Revision of palm plantation expansion emissions

Dynamics of expansion of palm plantation in Southeast Asia and its impact on carbon stock in forest and peatland is crucial for the outcome of the scenario of palm oil HEFA but also for other pathways based on vegetable oil, due to substitution effects. Assumptions used for GLOBIOM preliminary results were based on previous reviews of the literature performed in 2013 and 2014 and fully documented in Valin et al. 2015. Two important parameters are used in GLOBIOM to estimate GHG emissions related to palm oil expansion: i) the share of palm plantation expansion occurring into land covers on peat; ii) the emission factor applied to plantations cultivated on peatland. At the time of the 2013-2014 review, the limited number of references available to look at these important questions had been highlighted and some first uncertainty range estimated based on the published literature. New literature has now been produced over the past couple of years that could be used to update and improve these important parameters, as explained below.

New evidence on the trend of expansion into peatland has been provided by recent studies for the period following 2010-2015 in Indonesia. In particular, Austin et al. (2017) have analyzed the expansion trend of plantations into peatland using more precise remote sensing imagery than previously performed. This remote sensing study identified and validated the position of plantations up to the years 2016 and 2017. A more official peatland map was used by Austin and colleagues' analysis, produced by the Ministry of Agriculture of Indonesia (2011), compared to Gurnaso et al. (2013) who used an earlier peatland map from Wetlands International (Wahyunto & Suryadiputra, 2008). Although these two maps were not directly compared in that study, the results obtained in Austin et al. show a notable difference in the patterns calculated, in particular for the period 2005-2010 where estimates from Gurnaso were revised down for Sumatra. It is interesting to note that although the trend of expansion into peatland has been observed to decline in Sumatra for the period 2010-2015, the upward trend for expansion in Kalimantan is confirmed by Austin et al. This is an important finding because according to the same study, the share of all plantations expanding into Kalimantan has been increasing, to reach 61% in 2010-2015. If the same trend as observed in 2010-2015 were to be observed in 2015-2020, the share of expansion into peatland would be for Indonesia 20%. The previous assumption in GLOBIOM for expansion of palm plantation into peatland was set at 32% for the Indonesian average based on the results of Gurnaso et al. (2013). In view of the more up-to-date evidence from the peer-reviewed literature, this parameter was changed in the model from 32% to 20%.

Another important change in the emission calculation related to peat relates to the emission factor applied to palm plantation. GLOBIOM had been using an estimate of 60.8 tCO_2-eq/ha/year for palm plantations, based on a literature review documented in Valin et al. 2015. Although these estimates still seem to reflect a certain compromise within the large range of values provided by the literature (including the IPCC emission factor of 55t CO_2-eq/ha/year for plantations), none of the models reviewed had considered so far peatland emissions associated with other disturbed land use types. However, Austin et al. (2017) calculated for Indonesia in what land cover type the peatland drained for palm cultivation had been expanding. The results showed that one-third of expansion (31%) had taken place in forest over the period 2010-2015 (mostly secondary), while 32% had been on swamp and swamp scrubland and 15% into scrubland, savannah or bare land. The remaining 22% went into agricultural land. The GTAP-BIO team conducted the same calculation for both Indonesia and Malaysia and obtained similar findings, as explained in Section 4.2.3. For this reason, the GLOBIOM peatland emission factor for Indonesia and Malaysia was revised down from 60.8 tCO_2/ha/year to the same value of 38.1 tCO_2/ha/year of converted peat for palm cultivation as in the GTAP-BIO model.

Furthermore, based on time series based on FAOSTAT and the Indonesian Ministry of Agriculture, the estimate found for the share of total area under cultivation was around 70% for Indonesia, due to the high rate of expansion leading to large areas of new unproductive plantations. Newly retrieved time series

spanning until 2017 led to an upward revision of this share to 80%. This is equivalent to an increase of yield for palm plantation in Indonesia of 14%.

4.3.2 Foregone sequestration accounting

Abandoned land is accounted for in the GLOBIOM framework when the demand for agricultural products decreases (e.g., beef demand in the EU) or when agricultural yield improvement is faster than food demand change. Using abandoned land to grow bioenergy feedstock is part of the chain of impacts in the model when implementing a bioenergy demand shock. This implies a carbon cost if this land is being left without management for a long time in the counterfactual scenario (baseline). With an amortization period of 25 years for C stock change in the CAEP ILUC context, SOC regeneration is being accounted in GLOBIOM, and living biomass reversion is also considered in this land. Therefore, the GLOBIOM results have shown that the use of abandoned land could have a high carbon opportunity cost.

An important part of the discussion on the C debt incurred from using abandoned land concerns the living biomass C accumulation rate on this land when left idle. The approach taken in GLOBIOM has been to assume a mix of other natural vegetation and natural forest reversion in the absence of land management. The share of other natural vegetation versus forest regrowth is determined by the initial shares of each land cover type in each simulation grid-cell. Assuming full forest regrowth over 25 years, or only natural vegetation regrowth typically leads to higher or lower carbon stocks, respectively, compared to the approach assumed here. Due to the high carbon cost of forest, the sequestered carbon stock after 25 years can be very different depending on whether reversion goes to one of the land use types, or to the others, and therefore what mix of land covers the reversion is composed of.

Accounting for the C opportunity costs of using abandoned land is fundamental to properly assess the full extent of emission impact for a region where cropland is decreasing, like Europe. However, it also introduces some asymmetry in the treatment of opportunity cost when comparing with other locations where cropland would be increasing. Indeed, expanding into abandoned land is attributed an opportunity cost with some forest regrowth, whereas expanding into other natural vegetation does not receive any extra opportunity cost other than the vegetation covering it, because C accumulation is assumed to have reached an equilibrium, and no further forest regrows. This asymmetry, therefore, leads to higher opportunity cost for regions with more abandoned land, compared to some others with less or no abandoned land. In forward-looking modelling, this is an even greater problem as abandoned land projections are model and baseline assumption dependent. In our previous sets of results, the same feedstocks expanding in similar biomes in different regions would then be attributed different opportunity costs depending on the land abandonment context, which does not appear consistent. For this reason, to create a more even treatment of feedstock impact across different geographies, the choice was made to account in GLOBIOM only for the reversion to other natural vegetation as part of the foregone sequestration. This prevents, in this case, having different accounting of carbon opportunity costs due to differences in the mix of vegetation regrowth in the regions considered. This, however, also means that the opportunity cost accounted for is at a rather low bound of possible estimates.

4.3.3 Crop specific soil organic carbon impacts

Some new assumptions for the modeling of soil organic carbon (SOC) were also implemented in GLOBIOM to better take into account the differentiated impacts of some particular types of crops. The initial version of GLOBIOM used for biofuel policy analysis was relying on an IPCC Tier 1 approach for the global accounting of SOC, and all annual crops were so far assumed having the same management coefficient depending on their level of input. Perennials plantations were assumed on their side having the same SOC stock as grassland. The examination of more recent literature allowed some more precise characterization of the impact of some bioenergy crops on SOC. In particular, a study led by the Argonne National Laboratory (Qin et al., 2016) analyzed the specific SOC impact for the different land cover of the cultivation of corn, switchgrass, miscanthus, and poplar. They found through soil process modeling that

corn cultivation on cropland was increasing SOC compared to other crops due to the effect of residues. They confirmed, however, that this effect was not strong enough to fully mitigate the impact of expanding corn on grassland or other natural vegetation. The SOC impact of corn would nonetheless be lower than the impact from other crops. The authors also performed the same analysis for lignocellulosic feedstocks and obtained the much higher level of carbon sequestration in the soil. Miscanthus appeared to sequester large quantities of carbon on all type of land, whereas switchgrass would have a neutral impact on grassland but a much higher impact than corn in the case of cropland. Last, poplar would increase SOC stock on cropland but have a negative impact on grassland.

The findings from Qin et al. (2016) were implemented in the GLOBIOM modeling. The study also provided cellulosic crop SOC data used in AEZ-EF. For this purpose, the management coefficient F_i used in the IPCC method to calculate the SOC content of the soil was updated in the model. Due to the uncertainty of the management, low input annual crops outside of the EU were previously assigned a coefficient F_i=1 (default input) and the intensive systems had an improved high input coefficient of F_i=1.04 or 1.11 depending on the climate zone (see IPCC, 2006, Chapter 5 for all the default coefficients). The improved management coefficient supposedly reflects a situation where residues are returned to the soil, which is the case of corn. However, because a number of other crops do not return this amount of residues, or these residues are harvested and used, as often in the EU, the convention was changed for the SOC accounting for these crops and kept only the F_i improved coefficient for the case of corn. This change gives an advantage to corn in the case where it expands into cropland (other crops having now a F_i=1) but maintains the same reduced impact as previously assumed for expansion into grassland, in line with the increased input coefficient definition. For perennials, a SOC-specific coefficient was also introduced to reflect the improved effects of plantations on cropland, and in the case of miscanthus for grassland.

4.3.4 Biomass carbon stock in cellulosic crops

The initial GLOBIOM version used for biofuel policies only considered cellulosic feedstock in the EU. Different perennial feedstocks were introduced in the US, introduced on areas suitable in the model for short rotation coppices (Havlik et al., 2011) and with biophysical parameters aligned with the parameterisation chosen in GTAP-BIO (see Section 4.2.2). The above and below ground living biomass category in GLOBIOM displays in particular a similar range of magnitude for the different miscanthus pathways, in the EU and the US. The sequestration assumptions are presented in Table 103 and vary depending on the perennial plantation type.

Table 103: Perennial plantation carbon sequestration observed in living biomass

	Average yield (t dm/ha/yr) (1)	Above-ground living biomass (tC/ha) (2)	Below-ground living biomass (tC/ha) (3)	Total average biomass on harvest cycle (tC/ha) (4) = (2) +(3)	Sequestration to yield ratio (5) = (4) / (1) / CF*
EU Miscanthus	15.7	5.6	13.3	18.9	2.56
US Miscanthus	14.1	5.0	11.9	16.9	2.56
US Switchgrass	11.3	3.6	5.4	9.0	1.69
US Poplar	7.8	5.2	6.0	11.2	2.88

*with a carbon fraction (CF) of 0.5 for poplar and 0.47 for grassy crops.

4.3.5 Land use change in Brazil

The GLOBIOM version used for CAEP is calibrated using the same parameterization for Brazil as in the global model version (Havlík et al., 2011; Havlík et al., 2014) and provides a good pattern of expansion of deforestation in the region (Valin et al., 2013). In order to improve the behaviour of the model in response to Brazil shocks, the model results were compared with similar tests performed with a more detailed version of GLOBIOM dedicated to Brazil specific scenarios, called GLOBIOM-Brazil (Câmara et al., 2015; Soterroni et al., 2018). GLOBIOM-Brazil is based on a more detailed resolution of the land use change (half-degree grid for Brazil, versus 2-degree grid for the standard representation), and explicitly model policy constraints in Brazil related to the Forest Code and the soybean moratorium, as well as dynamic modelling of multi-cropping. This version is however still under development for many other features and does not incorporate many features necessary for CAEP scenario, such as land abandonment, vegetable oil markets, or aviation fuel supply chains. Therefore, GLOBIOM-Brazil has been used here mainly for the sake of comparison and calibration improvement on the sugar cane shocks.

Preliminary testing with GLOBIOM-Brazil on a shock of sugar cane suggests lower expansion into forest compared to previous results. In GLOBIOM-Brazil, only 12% of cropland expansion occurs into forest. This number should, however, be interpreted with caution as it was performed for a different shock size and longer time-frame as the one considered here. However, considering GLOBIOM-Brazil takes better into account local policies in Brazil, it was decided to recalibrate the land use expansion function in GLOBIOM to better mimic this expansion pattern. Only conversion cost of cropland into forest was adjusted, conversion cost of grassland into forest was kept unchanged.

4.3.6 Harvested wood products

Accounting of harvested wood products (HWP) was not originally considered in GLOBIOM. Sequestration in HWP can be important in countries with a forestry sector oriented towards manufactured products as carbon get sequestered in these products for long time periods after a forest is harvested. HWP accounting was added to the GLOBIOM GHG emission accounting used for CAEP.

To introduce HWP in GLOBIOM, the estimation of HWP coefficients from Earles et al. (2012) was implemented. These authors provide estimates of carbon stock kept in products or released into the atmosphere for each country and at different time periods: 0 years, 15 years, 30 years, etc. To use these coefficients in the context of the CAEP calculation, a 25-year coefficient was derived based on linear interpolation from the 15-year and 30-year estimates. HWP coefficients were applied to land use emissions from deforestation only, in line with the focus of the Earles et al. (2012) study. Therefore, no HWP were considered for clearing of other natural vegetation.

4.3.7 Crop cultivated areas

Crop area in GLOBIOM was initially calibrated using solely FAOSTAT data, which only provides harvested areas per crop. The multi-cropping intensity increase was represented as an increase in average yield trend for all the annual crops in each region, following data from Ray and Foley (2013). As a consequence, cultivated areas for some crops like rice were still overestimated in Asia, and for the case of Brazil, corn and soybean had the same multi-cropping intensity shift.

For the CAEP, all the data from GLOBIOM have been revised to take into account the multi-cropping intensity of each crop in the different regions, adjusting the cultivated area projections accordingly. For this purpose, a combination of the dataset from the IFPRI SPAM model (You and Wood, 2006) and from MIRCA2000 (Siebert et al., 2010) were used to recalibrate all the crops multi-cropping intensities for the base year. Trends for multi-cropping intensity increase from Ray and Foley (2013) were kept, except for India and China where some regional studies were used, as explained in the GLOBIOM documentation. In the case of Brazil, the multi-cropping trend was recalibrated to fit the data provided by Brazilian experts.

CHAPTER 5. **RESULTS**

5.1 **ILUC EMISSION INTENSITY**

The ILUC emission intensity results from GTAP-BIO and GLOBIOM for the 22 SAF pathways are presented in Table 104. The starch and sugar pathways had small absolute differences (gap less than 6 g CO_2e/MJ) in ILUC emissions between the two models. All cellulosic pathways provide negative or very small ILUC emission values from both models due to the high soil carbon sequestration and biomass carbon from producing cellulosic crops, even though the difference can be large between the two models for these cellulosic pathways (e.g., a difference of around 50 g CO_2e MJ^{-1} for US miscanthus ATJ-SPK from isobutanol). The gaps for HEFA pathways other than EU rapeseed oil HEFA remained large, mainly driven by the difference in the livestock rebound effect and vegetable oil demand responses. Out of the 22 pathways simulated in both models, nine pathways have an absolute difference (gap) that is less than 10 g CO_2e/MJ while eight pathways have a gap over 20 g CO_2e/MJ.

Table 104: ILUC emission intensity for SAF pathways, in g CO2e/MJ

Region	Feedstock	Conversion Process	Pathway Specifications	GTAP-BIO	GLOBIOM	GAP
USA	Corn grain	Alcohol (isobutanol) to jet		22.5	21.7	0.8
USA	Corn grain	Alcohol (ethanol) to jet		24.9	25.3	0.4
Brazil	Sugarcane and Molasses	Alcohol (isobutanol) to jet		7.4	7.2	0.2
Brazil	Sugarcane	Alcohol (ethanol) to jet		9.0	8.3	0.7
Brazil	Sugarcane	Synthesized iso-paraffins (SIP)		14.2	8.4	5.8
EU	Sugar beet	Synthesized iso-paraffins (SIP)		20.3	20.0	0.3
USA	Soy oil	Hydroprocessed esters and fatty acids (HEFA)		20.0	50.4	30.4
USA	Carinata oil	Hydroprocessed esters and fatty acids (HEFA)	Feedstock is grown as a secondary crop that avoids other crops displacement	-12.9	-25.9	13.0
Brazil	Soy oil	Hydroprocessed esters and fatty acids (HEFA)		22.5	117.9	95.4
Brazil	Carinata oil	Hydroprocessed esters and fatty acids (HEFA)	Feedstock is grown as a secondary crop that avoids other crops displacement	-15	-24.9	9.9
EU	Rapeseed oil	Hydroprocessed esters and fatty acids (HEFA)		20.7	27.5	6.8
Malaysia & Indonesia	Palm oil	Hydroprocessed esters and fatty acids (HEFA)		34.6	60.2	25.6
USA	Miscanthus	Fischer-Tropsch (FT)		-37.3	-10.6	26.7
USA	Miscanthus	Alcohol (isobutanol) to jet		-58.5	-8.7	49.8

USA	Miscanthus	ATJ-SPK from ethanol		-47.1	-8.2	38.9
USA	Switchgrass	Fischer-Tropsch (FT)		-8.2	2.5	10.7
USA	Switchgrass	Alcohol (isobutanol) to jet		-18.9	10.2	29.1
USA	Switchgrass	Alcohol (ethanol) to jet		-15.2	8.4	23.6
USA	Poplar	Fischer-Tropsch (FT)		-9.6	-0.6	9.0
EU	Miscanthus	Fischer-Tropsch (FT)		-9.3	-26.5	17.2
EU	Miscanthus	Alcohol (isobutanol) to jet		-16.6	-35.5	18.9
EU	Miscanthus	Alcohol (Ethanol) to jet		-12.7	-27.8	15.1
India	Jatropha	Hydroprocessed esters and fatty acids (HEFA)	Meal used as fertilizer or electricity input	-27.3	-22.2	5.1
India	Jatropha	Hydroprocessed esters and fatty acids (HEFA)	Meal used as animal feed after detoxification	-41.9	-52.6	10.7
Global	Soy oil	Hydroprocessed esters and fatty acids (HEFA)		21.3	88.1	66.8
Global	Corn grain	Alcohol (isobutanol) to jet		37.7	25.2	12.5
Global	Corn grain	Alcohol (ethanol) to jet		40.7	30.4	10.3
Global	Rapeseed oil	Hydroprocessed esters and fatty acids (HEFA)		24.1	27.8	3.7
Global	Sugarcane and Molasses	Alcohol (isobutanol) to jet (ATJ)		11.4	6.8	4.6
Global	Sugarcane	Alcohol (ethanol) to jet		16.8	4.0	12.8
Global	Sugarcane	Synthesized iso-paraffins (SIP)		26.8	6.6	20.2
Global	Sugar beet	Synthesized iso-paraffins (SIP)		13.0	9.5	3.5
Global	Miscanthus	Fischer-Tropsch (FT)		-16.7	-8.5	8.2
Global	Miscanthus	Alcohol (isobutanol) to jet		-28.0	-13.8	14.2
Global	Miscanthus	Alcohol (ethanol) to jet		-23.4	-11.0	12.4
Global	Switchgrass	Fischer-Tropsch (FT)		5.3	5.2	0.1
Global	Switchgrass	Alcohol (isobutanol) to jet		3.1	7.7	4.6
Global	Switchgrass	Alcohol (ethanol) to jet		3.7	5.9	2.2
Global	Poplar	Fischer-Tropsch (FT)		11.4	5.8	5.6
Global	Carinata oil	Hydroprocessed esters and fatty acids (HEFA)	Feedstock is grown as a secondary crop that avoids other crops displacement	-9.8	-15.5	5.7
Global	Camelina oil	Hydroprocessed esters and fatty acids (HEFA)	Feedstock is grown as a secondary crop that avoids other crops displacement	-11.4	-15.4	4.0

In the following sections, the detailed results for each pathway are discussed. The global feedstock area increase is decomposed into all other land area sources including forest, pasture, crop switching, multi-cropping (GTAP-BIO and GLOBIOM) & unused cropland (GTAP-BIO), cropland pasture (GTAP-BIO), other natural land (GLOBIOM), and abandoned land (GLOBIOM). Even though the same technology conversion yield and shock size are used for a pathway in both models, the area increase in the biofuels feedstock can still be very different. For pathways that have comparable feedstock area change predicted by GTAP-BIO and GLOBIOM, the composition of the area sources and the associated emission factors may determine the total emissions. The total emissions of each pathway are also decomposed into major emission sources (see section 3.2 for details) including carbons in natural vegetation, foregone sequestration, agricultural biomass, soil organic carbon (SOC) and peatland oxidation.

5.2 REGIONAL ILUC VALUES

5.2.1 USA CORN ATJ-SPK FROM ISOBUTANOL

The 25-year ILUC emission intensity for the USA corn ATJ-SPK from isobutanol pathway is 22.5 g CO_2e/MJ from GTAP-BIO and 21.7 g CO_2e/MJ from GLOBIOM. Even though the total emission intensity from the two models are close, there could be important differences in regional results, market-mediated responses, and the decomposition of land use change and emissions. Figure 18 compares the global land use change decomposition and emission decomposition between the two models for the USA corn ATJ-SPK from isobutanol pathway. The (net) total bar level in the land use change decomposition indicates the feedstock harvested area increase, which is a reflection of crop yield, technology conversion yield, meal coproduct substitution, and other market-mediated responses.

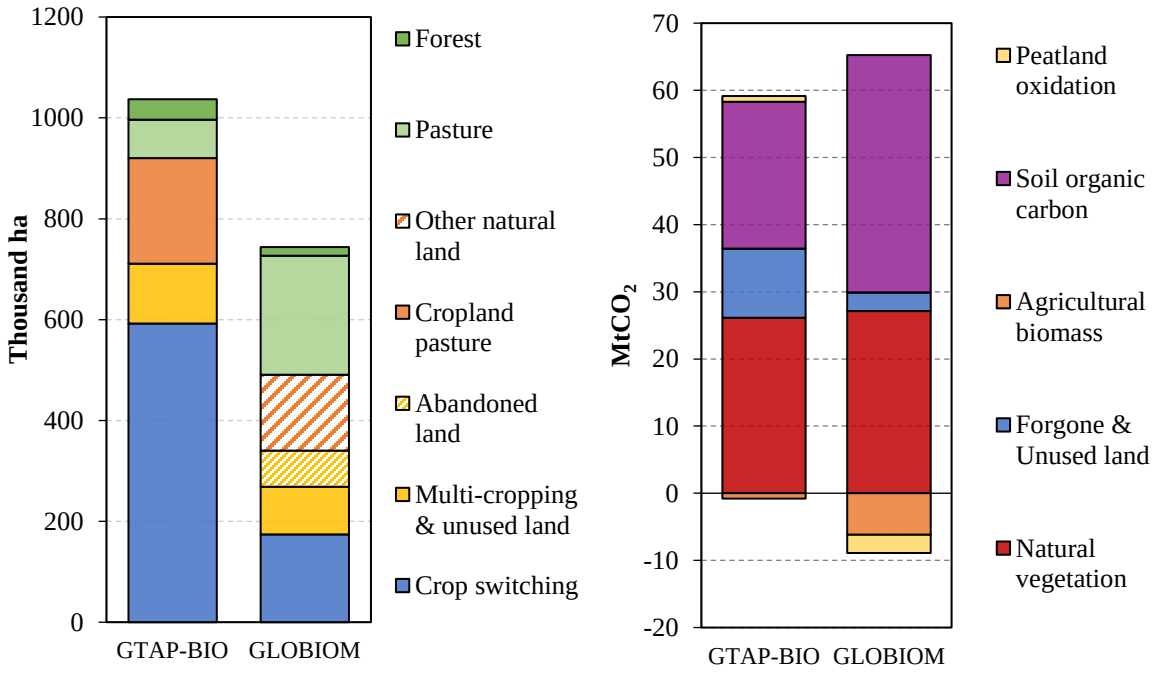

Figure 18: Land use change decomposition (left) and emission decomposition (right) for the USA corn alcohol (isobutanol) to jet pathway

For producing 104 PJ ATJ-SPK from isobutanol fuels, 14.4 million tons (Mt) of corn are directly needed, while 4.4 Mt DDGS would be coproduced for substituting corn or other feed crops in livestock sectors.

GTAP-BIO projected the global corn production would increase by 9.4 Mt, and 91% of the increase would be grown in the USA. GLOBIOM estimated 8.9 Mt global corn increase with 96% of which being produced in the USA. The corn demand responses and the DDGS displacement pattern are the two drivers to the difference in the total corn production.

In GTAP-BIO, the shock of the USA corn ATJ-SPK from isobutanol led to 1.04 Mha increase in the global coarse grains harvested area. The decomposition indicates that there is strong decrease in other crop areas or crop switching (0.59 Mha). Cropland pasture accounts for 0.21 Mha and multi-cropping and unused cropland provides 0.12 Mha with the rest provided by forest and pasture. In GLOBIOM, the global corn harvested area increased by 0.74 Mha due to the ATJ-SPK from isobutanol shock, of which 0.17 Mha was from crop switching, 0.09 Mha was from multi-cropping, 0.22 Mha was from other natural land or abandoned land, and 0.25 Mha was from pasture (0.24 Mha) and forest. GLOBIOM has higher corn yield in the baseline (9.01 vs. 8.95 t/ha) and stronger yield response for corn compared with GTAP-BIO, which partly explains the much smaller corn area increase in GLOBIOM.

Crop switching plays the most important role in supplying corn area in GTAP-BIO. This was because the coproduced DDGS also displaced other feed crops so that land originally growing those crops were converted to growing corn. In GLOBIOM, DDGS displaced relatively less other feed crops but more corn, which explains the smaller crop switching and smaller total crop production increase. GLOBIOM baseline was recently updated, which also increased the contribution of abandoned land in the USA. The change led to closer results for the USA corn ATJ-SPK from isobutanol pathway between GTAP-BIO and GLOBIOM as low-emission land such as cropland pasture and unused land played an important role in supplying cropland in GTAP-BIO.

Both GTAP-BIO and GLOBIOM estimated little land conversion from forest and pasture in the USA. GTAP-BIO indicated Sub-Saharan Africa, Brazil, and other South America countries are major regions of deforestation and pasture conversion. Pasture conversion in Brazil (0.15 Mha) is a major land source in GLOBIOM.

The total emissions from natural vegetation are comparable between the two models (26-27 $MtCO_2$). GLOBIOM results showed larger emission from SOC (35 vs. 22 $MtCO_2$) compared with GTAP-BIO, but the difference was compensated by the smaller emissions from foregone sequestration and larger agricultural biomass carbon sequestration. The higher crop yield and smaller shares of crop switching in area supply in GLOBIOM are main reasons for the larger agricultural biomass carbon sequestration. The emissions from peatland oxidation change were very small in both models for the corn ATJ-SPK from isobutanol pathway since the market-mediated impacts on palm oil production in Malaysia and Indonesia were negligible. As a result, the total emissions from GTAP-BIO (58 $MtCO_2$) and GLOBIOM (56 $MtCO_2$) are not very different.

Overall, the drivers to the results difference between the two models may include the coproduct (DDGS) displacement, corn yield responses, and land category and associated emission factors. However, the impacts from these drivers on the total ILUC emissions for this pathway are likely small as these drivers may compensate each other as the current results imply. The two models are in relatively close agreement in estimating ILUC emissions for the USA corn ATJ-SPK from isobutanol pathway.

5.2.2 **USA CORN ATJ-SPK FROM ETHANOL**

The 25-year ILUC emission intensity for the USA corn ATJ-SPK from isobutanol pathway is 24.9 g CO_2e/MJ from GTAP-BIO and 25.3 g CO_2e/MJ from GLOBIOM. Figure 19 compares the global land use change decomposition and emission decomposition between the two models for the USA corn ATJ-SPK from ethanol pathway. These decomposition results followed the same pattern with the results from the USA corn ATJ-SPK from isobutanol pathway, since the only major difference between the two pathways was that the USA corn ATJ-SPK from ethanol pathway has lower technology conversion yield.

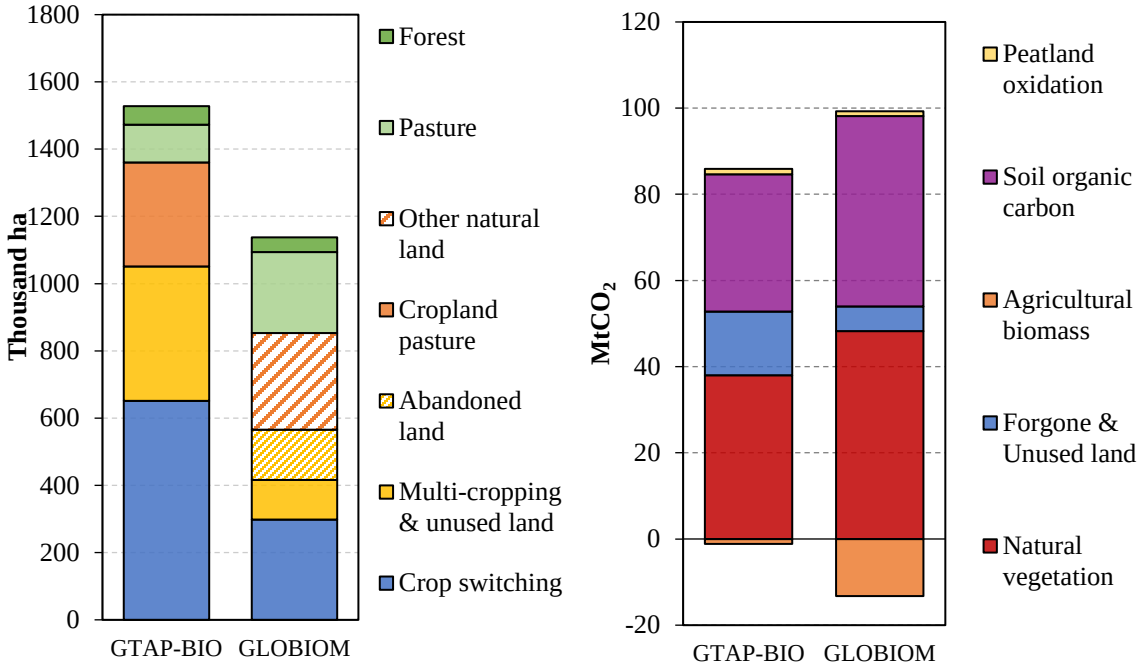

Figure 19: Land use change decomposition (left) and emission decomposition (right) for the USA corn alcohol (ethanol) to jet pathway

To produce 136 PJ ATJ-SPK from ethanol fuels, 20.9 million tons (Mt) of corn are directly needed, while 6.1 Mt DDGS would be coproduced for substituting corn or other feed crops in livestock sectors. GTAP-BIO projected the global corn production would increase by 13.8 Mt, and 91% of the increase would be grown in the USA. GLOBIOM estimated 11.6 Mt global corn increase with 96% of which being produced in the USA.

In GTAP-BIO, the shock of the USA corn ATJ led to a 1.53 Mha increase in the global coarse grains harvested area (1.38 Mha in the USA). The decomposition indicates that there is strong decrease in other crop areas or crop switching (0.65 Mha). Cropland pasture accounts for 0.31 Mha and multi-cropping and unused cropland provides 0.4 Mha with the rest provided by forest and pasture. In GLOBIOM, the global corn harvested area increased by 1.14 Mha due to the ATJ-SPK from ethanol shock, of which 0.30 Mha was from crop switching, 0.12 Mha was from multi-cropping, 0.44 Mha was from other natural land or abandoned land, and 0.29 Mha was from pasture (0.24 Mha) and forest.

GLOBIOM results showed larger emission from both natural vegetation (48 vs. 38 $MtCO_2$) and SOC (44 vs. 32 $MtCO_2$) compared with GTAP-BIO. The difference was compensated for by the smaller emissions from foregone sequestration and larger agricultural biomass carbon sequestration. The total emissions from GTAP-BIO (85 $MtCO_2$) and GLOBIOM (86 $MtCO_2$) are not very different.

5.2.3 BRAZIL SUGARCANE AND MOLASSES ATJ-SPK FROM ISOBUTANOL

The 25-year ILUC emission intensity for the Brazil sugarcane ATJ-SPK from isobutanol pathway is 7.4 g CO_2e/MJ from GTAP-BIO and 7.2 g CO_2e/MJ from GLOBIOM. Figure 20 compares the global land use change decomposition and emission decomposition between the two models for the Brazil sugarcane ATJ-SPK from isobutanol pathway. The (net) total bar level in the land use change decomposition indicates the feedstock cultivated area increase, which is a reflection of crop yield, technology conversion yield, and other market-mediated responses.

To produce 118 PJ ATJ-SPK from isobutanol fuels, 67.4 Mt of sugarcane are directly needed. GTAP-BIO projected the global sugarcane production would increase by 66.2 Mt, and almost all of the new sugarcane would be grown in Brazil. GLOBIOM estimated 66.9 Mt global sugarcane increase with over 98% of which is produced in Brazil.

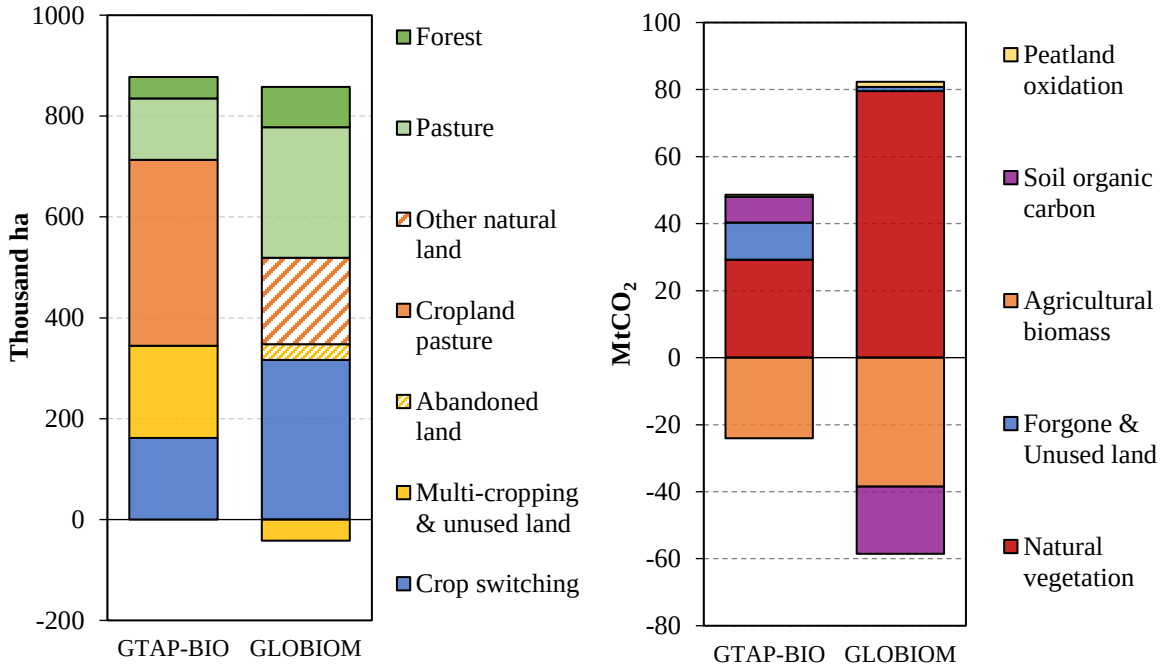

Figure 20: Land use change decomposition (left) and emission decomposition (right) for the Brazil sugarcane alcohol (isobutanol) to jet pathway

In GTAP-BIO, the shock of the Brazil sugarcane ATJ-SPK from isobutanol led to 0.88 Mha increase in the global sugarcane harvested area. The decomposition indicates that the major land source for sugarcane expansion is cropland pasture (0.37 Mha). Crop switching provides 0.16 Mha, and multi-cropping & unused cropland provides 0.18 Mha. There would also be 0.16 Mha decrease in global forest and pasture. In GLOBIOM, the global sugarcane harvested area increased by 0.82 Mha due to the ATJ-SPK from isobutanol shock, of which 0.32 Mha was from crop switching, 0.20 Mha was from other natural land and abandoned land, and 0.34 Mha was from pasture and forest. The sugarcane yield responses and the demand responses are comparable between the two models so that the total feedstock production and area increases are close. However, as indicated, the land transformation pattern is very different between the two models for the pathway.

Both GTAP-BIO and GLOBIOM estimated little land conversion from forest and pasture outside Brazil since more new sugarcane would be produced in Brazil and the international trade would not be significantly affected. GLOBIOM estimated much higher deforestation than GTAP-BIO (0.08 vs. 0.04 Mha).

GLOBIOM recently incorporated multi-cropping responses at crop level, but not for sugarcane since it is a perennial crop. Since sugarcane may expand on cropland that was able to apply multi-cropping practices in Brazil, the total harvested area supplied by multi-cropping decreased. Multi-cropping responses are modelled differently in GTAP-BIO. Cropland intensification responses through multi-cropping and unused land can become stronger as long as land rental prices become higher, which explains that these responses still played important role in supplying harvested area in this pathway.

For both models, the natural vegetation carbon change (29 $MtCO_2$ in AEZ-EF and 80 $MtCO_2$ in GLOBIOM) dominates the total emissions change, mainly because of the cropland expansion into natural land). In both AEZ-EF and GLOBIOM, sugarcane in Brazil was treated specially with higher soil organic carbon (SOC) since it is a perennial crop. However, results imply a net SOC sequestration effect in GLOBIOM (-20 $MtCO_2$) whereas it results in a net emissions in AEZ-EF (8 $MtCO_2$). Both AEZ-EF and GLOBIOM indicated strong carbon sequestration in agricultural biomass (-24 and -38 $MtCO_2$), mainly due to the high sugarcane crop yield. There was little foregone sequestration in GLOBIOM results, mainly because there was no abandoned land available in Brazil. The emissions from peatland oxidation change were very small in both models for the Brazil sugarcane ATJ-SPK from isobutanol pathway since the market-mediated impacts on palm oil production in Malaysia and Indonesia were negligible. As a result, the total emissions from GTAP-BIO (25 $MtCO_2$) and GLOBIOM (24 $MtCO_2$) are not very different.

Overall, even though the two models estimated comparable total sugarcane production and cultivated area changes, the land use change pattern was very different, mainly because of the difference in land category and land transformation related parameters. Nevertheless, the total ILUC emissions for the pathways from the two models converged when calculating emissions with their emission accounting models.

Molasses is being accounted as a co-product, as described in Section 1.4.7 of this Supporting Document, even though the feedstock is not the largest part of sugarcane product output. In line with the core-LCA protocol, the feedstock requirement for molasses ATJ-SPK from isobutanol was assumed the same as for sugar cane ATJ-SPK from isobutanol; therefore, the same ILUC values for sugar cane ATJ-SPK from isobutanol are used for this pathway.

5.2.4 **BRAZIL SUGARCANE ATJ-SPK FROM ETHANOL**

The 25-year ILUC emission intensity for the Brazil sugarcane ATJ-SPK from ethanol pathway is 9.0 g CO_2e/MJ from GTAP-BIO and 8.3 g CO_2e/MJ from GLOBIOM. Figure 21 compares the global land use change decomposition and emission decomposition between the two models for the Brazil sugarcane ATJ-SPK from ethanol pathway. The (net) total bar level in the land use change decomposition indicates the feedstock cultivated area increase. These decomposition results followed the same pattern with the results from the Brazil sugarcane ATJ-SPK from isobutanol pathway since the only major difference between the two pathways was that the Brazil sugarcane ATJ-SPK from ethanol pathway has a lower technology conversion yield.

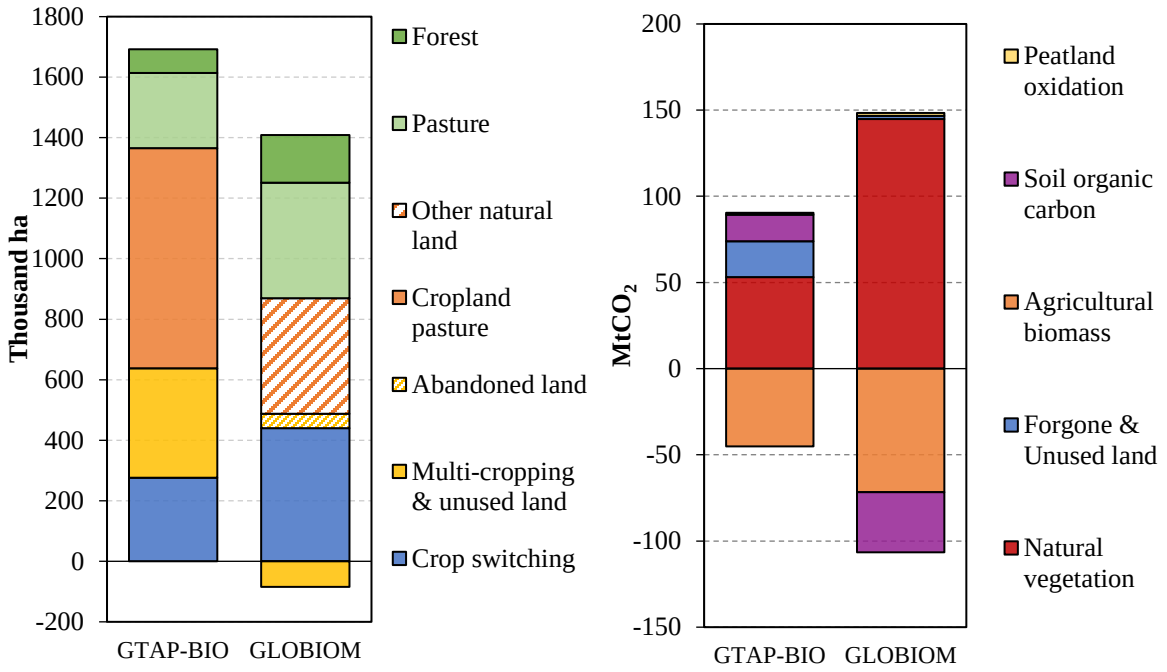

Figure 21: Land use change decomposition (left) and emission decomposition (right) for the Brazil sugarcane alcohol (ethanol) to jet pathway

For producing 168 PJ ATJ-SPK from ethanol fuels, 128.3 Mt of sugarcane are directly needed. GTAP-BIO projected the global sugarcane production would increase by 125.4 Mt, almost all of which would be grown in Brazil. GLOBIOM estimated 126.6 Mt global sugarcane increase with 99% of which being produced in Brazil.

In GTAP-BIO, the shock of the Brazil sugarcane ATJ-SPK from ethanol led to 1.69 Mha increase in the global sugarcane harvested area. The decomposition indicates that the major land source for sugarcane expansion is cropland pasture (0.73 Mha). Crop switching provides 0.28 Mha, and multi-cropping & unused cropland provides 0.36 Mha. There would also be 0.33 Mha decrease in global forest and pasture. In GLOBIOM, the global sugarcane harvested area increased by 1.32 Mha due to the ATJ-SPK from ethanol shock, of which 0.44 Mha was from crop switching, 0.43 Mha was from other natural land and abandoned land, and 0.54 Mha was from pasture and forest. Thus, the GLOBIOM forest and pasture share was considerably higher.

GLOBIOM results showed larger emission from natural vegetation (145 vs. 53 $MtCO_2$) and higher agricultural biomass sequestration (-72 vs. -45 $MtCO_2$) compared with GTAP-BIO. The total emissions from GTAP-BIO (45 $MtCO_2$) and GLOBIOM (42 $MtCO_2$) are not very different.

5.2.5 **BRAZIL SUGARCANE SYNTHESIZED ISO-PARAFFINS (SIP)**

The 25-year ILUC emission intensity for the Brazil sugarcane synthesized iso-paraffins (SIP) pathway is 14.2 g CO_2e/MJ from GTAP-BIO and 8.4 g CO_2e/MJ from GLOBIOM. Figure 22 compares the global land use change decomposition and emission decomposition between the two models for the Brazil sugarcane SIP pathway. The (net) total bar level in the land use change decomposition indicates the feedstock cultivated area increase. These decomposition results followed the similar pattern as the results from the Brazil sugarcane ATJ-SPK from isobutanol or ATJ-SPK from ethanol pathway.

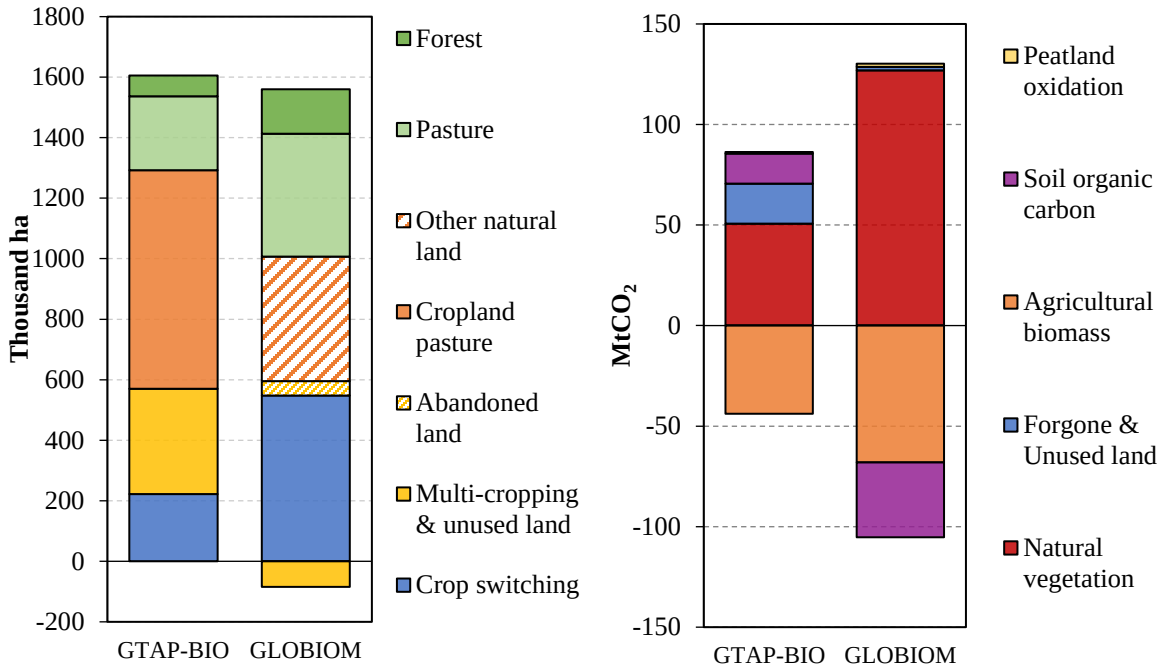

Figure 22: Land use change decomposition (left) and emission decomposition (right) for the Brazil sugarcane synthesized iso-paraffins (SIP) pathway

To produce 104 PJ SIP fuels along with 23 PJ biogas, 121.7 Mt of sugarcane are directly needed. GTAP-BIO projected the global sugarcane production would increase by 119.1 Mt, almost all of which would be grown in Brazil. GLOBIOM estimated 120.0 Mt global sugarcane increase with 99% being produced in Brazil.

In GTAP-BIO, the shock of the Brazil sugarcane SIP led to a 1.61 Mha increase in the global sugarcane harvested area. The decomposition indicates that the major land source for sugarcane expansion is cropland pasture (0.72 Mha). Crop switching provides 0.22 Mha, and multi-cropping & unused cropland provide 0.35 Mha. There would also be 0.31 Mha decrease in global forest and pasture. In GLOBIOM, the global sugarcane harvested area increased by 1.48 Mha due to the SIP shock, of which 0.55 Mha was from crop switching, 0.46 Mha was from other natural land and abandoned land, and 0.55 Mha was from pasture and forest.

GLOBIOM results showed larger emissions from natural vegetation (127 vs. 51 $MtCO_2$) and higher agricultural biomass sequestration (-68 vs. -44 $MtCO_2$) compared with GTAP-BIO. The total emissions are 45 $MtCO_2$ from GTAP-BIO and 25 $MtCO_2$ from GLOBIOM.

5.2.6 EU SUGAR BEET SYNTHESIZED ISO-PARAFFINS (SIP)

The 25-year ILUC emission intensity for the EU sugar beet synthesized iso-paraffins (SIP) pathway is 20.3 g CO_2e/MJ from GTAP-BIO and 20.0 g CO_2e/MJ from GLOBIOM. Figure 23 compares the global land use change decomposition and emission decomposition between the two models for the EU sugar beet SIP pathway. The (net) total bar level in the land use change decomposition indicates the sugar beet harvested area increase.

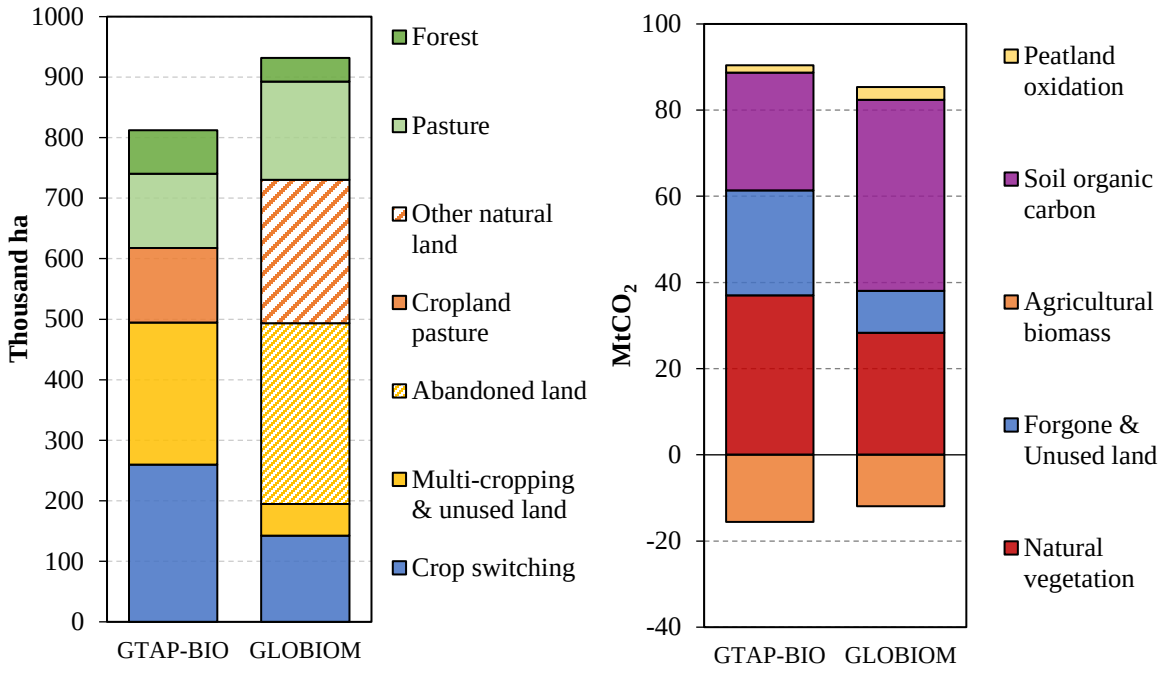

Figure 23: Land use change decomposition (left) and emission decomposition (right) for the EU sugar beet synthesized iso-paraffins (SIP) pathway

To produce 78 PJ SIP fuels along with 69 PJ biogas, 63.5 Mt of sugar beet are directly needed. GTAP-BIO estimated the global sugar beet production would increase by 63.0 Mt, all of which would be produced in EU. GLOBIOM estimated 67.3 Mt global sugar beet increase, and all of the new sugar beet would be cultivated in EU.

In GTAP-BIO, the shock of the EU sugar beet SIP led to 0.81 Mha increase in sugar beet harvested area. Globally, there would be 0.20 Mha decrease in forest and pasture. Crop switching (0.26 Mha) and multi-cropping & unused cropland (0.24 Mha) were major sources of area supply. Cropland pasture would also provide 0.12 Mha. In GLOBIOM, the sugar beet harvested area increased by 0.93 Mha due to the SIP shock, which can be decomposed into 0.14 Mha from crop switching, 0.54 Mha from other natural land and abandoned land, and 0.20 Mha was from pasture and forest. GTAP-BIO has higher crop yield responses for EU sugar beet compared with GLOBIOM so that less harvest area expansion was seen while the total production expansions were the same between the two models.

GLOBIOM results showed larger emission from SOC (44 vs. 27 $MtCO_2$) while GTAP-BIO had higher emissions from natural vegetation and converting unused land. The crop biomass carbon sequestrations were similar (-16 vs. -12 $MtCO_2$). The total emissions from GTAP-BIO (75 $MtCO_2$) and GLOBIOM (73 $MtCO_2$) are not very different.

5.2.7 USA SOY OIL HYDROPROCESSED ESTERS AND FATTY ACIDS (HEFA)

The 25-year ILUC emission intensity for the USA soy oil hydroprocessed esters and fatty acids (HEFA) pathway is 20.0 g CO_2e/MJ from GTAP-BIO and 50.4 g CO_2e/MJ from GLOBIOM. Figure 24 compares the global land use change decomposition and emission decomposition between the two models for the USA soy oil HEFA pathway. The (net) total bar level in the land use change decomposition indicates the feedstock harvested area increase.

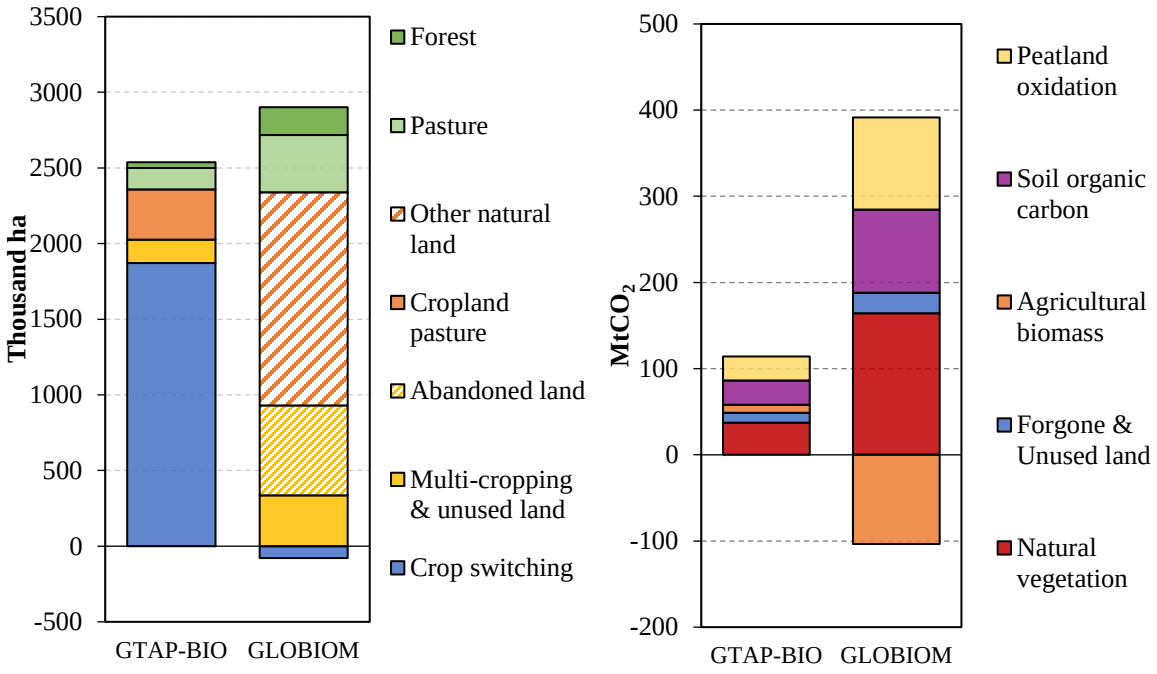

Figure 24: Land use change decomposition (left) and emission decomposition (right) for the USA soy oil hydroprocessed esters and fatty acids (HEFA) pathway

To produce 228 PJ HEFA fuels, 6.3 Mt of soy oil are directly needed. Driven by the increased soy oil demand, GTAP-BIO projected the global soybean production would increase by 9.1 Mt, and 93% of the increase would be produced in the USA. GLOBIOM estimated a 11.1 Mt global soybean increase, all of which would be produced in the USA. For crushing soybeans, the crushing rate is about 19 % (by weight) for soy oil and 80% for soy meal. The coproduced soymeal enters livestock sectors as feedstuff to provide protein. In both models, in addition to the newly crushed soy oil, substitutions among vegetable oils and a decrease in vegetable oil consumption played important roles in supplying the soy oil feedstock.

In GTAP-BIO, the shock of the USA soy HEFA led to a 2.54 Mha increase in global soybean harvested area. The decomposition indicates that crop switching (1.87 Mha) played the most important role in supplying soybeans. Cropland pasture accounts for 0.33 Mha and multi-cropping and unused cropland provides 0.15 Mha with the rest provided by forest and pasture. In GLOBIOM, the global soybeans harvested area increased by 2.82 Mha due to the HEFA shock, of which 2.00 Mha was from other natural land or abandoned land, 0.34 Mha was from multi-cropping, and 0.56 Mha was from pasture and forest. Note that, unlike GTAP-BIO, GLOBIOM projected an area expansion for other crops (0.08 Mha), so that crop switching played a negative role globally in supplying soybean area. This difference was driven by the significantly stronger livestock rebound effect that exists in GLOBIOM. When shocking a pathway generating feedstuff (protein) coproduct, the coproduced protein feedstuff enters livestock industries at a lower price, which benefits livestock sectors. Due to the feed ration requirements, cereal grains (energy feedstuff) are demanded to complement the excessive proteins to supply livestock sectors. In other words, the dispersion of the protein feedstuff leads to (1) growth in livestock production and (2) expansion in cereal grains area and production to meet feed ration requirement. This is called the livestock rebound effect.

The two models are in disagreement on the extent of the livestock rebound effect response. In the case of the US, GTAP-BIO and GLOBIOM both find similar magnitude of rebound effect in the US (0.23% for dairy, 0.13% for ruminant and 0.33% for non-ruminant for GTAP-BIO, versus 0.21%, 0.53% and 0.11% for GLOBIOM, respectively). But results differ for the rest of the world. Overall, at global level, GTAP-BIO results led to little net livestock rebound effect globally (0.012% for dairy, 0.003% for ruminant, and -0.004% for non-ruminant). The produced soy meal would substitute more largely existing feed crops,

which would provide land for soybean expansion. It explains the high crop switching in area decomposition in GTAP-BIO. Compared with GTAP-BIO, GLOBIOM livestock rebound effect remains high globally (0.17% for dairy, 0.09% for ruminant, and 0.037% for non-ruminant) which led to area expansions in other crops and higher natural land conversion. Differences can be explained by the location of the meal consumption in response to the shock. In GTAP-BIO, production of additional meal in the US creates an advantage for the domestic livestock industry in the global market and helps the US to export more livestock products to other regions. That causes reduction in livestock output in other regions. In GLOBIOM, two thirds of newly produced soybean meals are exported outside of the US and the comparative advantage effect is not playing a strong role.

Significant discussions took place on the question of the livestock rebound effect in models and the model specifications influencing it. The difference in the extent of livestock rebound effect between GLOBIOM and GTAP-BIO can be explained by: (1) GTAP-BIO and GLOBIOM have different feed representations. GTAP-BIO includes all animal feed crops and represents forage crops as part of cropland, whereas GLOBIOM complements its 18 crops used for feed with grass produced on grassland, which leads to less crop switching and more pasture response. (2) the two models assume different levels of flexibility in the feed mix for the livestock sector. GTAP-BIO uses nested functions allowing for different degree of substitutions among different categories of crops, whereas GLOBIOM includes substitution of predefined fixed feed bundles based on protein and energy requirement with some maximum incorporation constraints. Technologies in GTAP-BIO are modelled at the economic-wide level, which permits more flexible substitution. (3) GTAP-BIO includes more sector coverage so that there could be protein meal substitution from non-livestock sectors (e.g., processed food), and it includes all the oil crops and animal fats. (4) the two models represent differently livestock systems intensification. In GTAP-BIO, livestock intensification mainly operates through substitution of protein meal with other meals and grains, and through transition from ruminant meat production, less demanding in protein meal, to non-ruminant meat production (Taheripour et al., 2013). In GLOBIOM, the intensification primarily stimulates the development of intensive cattle systems and industrial scale monogastric production, in replacement of extensive cattle and smallholder livestock systems. This generates an increase in grain consumption from the market in addition to protein meals, to balance the ration in nutrient (energy and protein). Further research needs were identified to disentangle the dynamics above and improve the model specifications on this effect.

GTAP-BIO projected higher vegetable oil demand responses so that there was stronger consumption reduction due to the HEFA shock compared with GLOBIOM. GTAP-BIO projects 40% of the total soy oil biofuel feedstock demand for producing HEFA SAF in the US was newly produced or substituted by a new production of other vegetable oils from a global perspective. This means 60% of the vegetable oil refined for fuel is coming from displacement of other products than vegetable oil or from decrease in consumption. In contrast, production of new vegetable oil in GLOBIOM represents 59% of the fuel demand for the US soy oil HEFA pathway. A stronger reduction in demand would lead to less new production of vegetable oil and oilseeds, and thus smaller land use change and emissions.

The livestock rebound effect and the soy oil demand responses both drive important differences between the two models for this pathway. GLOBIOM estimated significantly higher land conversion of natural land or abandoned land compared with GTAP-BIO (AEZ-EF). This leads to considerably higher GLOBIOM emissions from natural vegetation (146 vs. 37 $MtCO_2$), SOC (97 vs. 28 $MtCO_2$), and foregone sequestration (24 vs. 12 $MtCO_2$). GLOBIOM finds higher agricultural biomass carbon sequestration (-103 vs. 9 $MtCO_2$). Furthermore, GLOBIOM estimated higher palm fruit production (6.4 Mt vs. 1.8 Mt) and palm cultivated area (0.43 vs. 0.09 Mha) expansion in Malaysia and Indonesia compared with GTAP-BIO. It explains the significantly higher peat oxidation from GLOBIOM (107 vs. 28 $MtCO_2$). However, a part of the peatland emissions is offset by the sequestration in the palm plantation biomass.

5.2.8 USA CARINATA OIL HYDROPROCESSED ESTERS AND FATTY ACIDS (HEFA)

The 25-year ILUC emission intensity for the USA carinata oil hydroprocessed esters and fatty acids (HEFA) pathway is -12.9 g CO_2e/MJ from GTAP-BIO and -25.9 g CO_2e/MJ from GLOBIOM. Figure 25 compares the global land use change decomposition and emission decomposition between the two models for the USA carinata oil HEFA pathway. The bar in the land use change decomposition indicates land use changes induced by expansion in carinata oil HEFA in the USA.

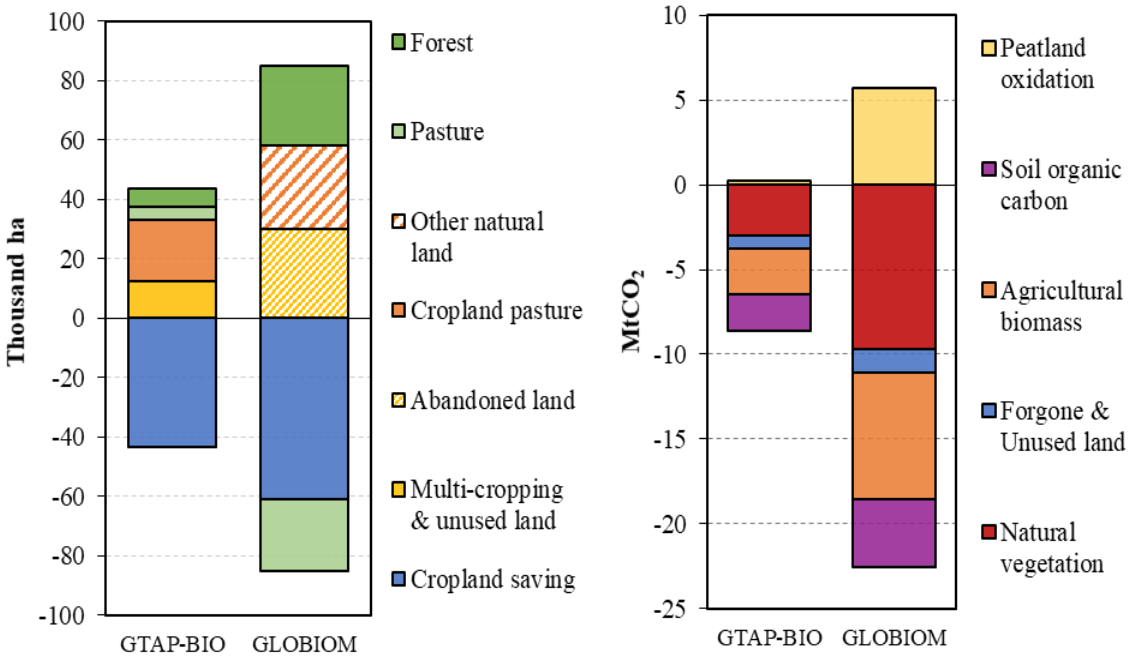

Figure 25: Land use change decomposition (left) and emission decomposition (right) for the USA carinata oil hydroprocessed esters and fatty acids (HEFA) pathway

To produce 26 PJ HEFA fuels from carinata oil, 0.69 Mt of carinata oil are directly needed. This needs an expansion in production of carinata by 1.7 Mt of carinata seed which requires an expansion in the area of carinata by 0.72 Mha in the USA. Since carinata is considered as a secondary crop produced in a double cropping system, it will be produced on the exiting active cropland with no expansion in cropland. However, conversion of produced carinata to HEFA fuels generates about 1.02 Mt of carinata meal. Carinata meal is having very similar content in protein as soybean meal. Therefore the expansion in carinata oil HEFA provides extra meals highly substitutable with soybean meal in the USA. The substitution between carinata meal and soybeans, indirectly affects production of soybeans and other crops used in animal feed rations. The indirect changes in crop production induced by the substitution in animal feed items generate some savings in cropland which eventually leads to changes in other land covers.

The GTAP-BIO model projects a saving in cropland at the global scale by .043 Mha due to the increase in carinata oil HEFA. That leads to relatively small expansions in cropland pasture, area of forest, and pasture land as shown in the left panel of Figure 25 on the GTAP-BIO bar. The saving in cropland, leads to an expansion in unused cropland or the need for multiple cropping. According to the GTAP-BIO results, these changes jointly drop the land use emissions by 8.4 $MtCO_2$, distributed mainly between natural vegetation, agricultural biomass and soil organic carbon, as shown the right panel of Figure 25 on the GTAP-BIO bar.

The GLOBIOM model projects a saving in cropland at the global scale by .061 Mha due to the increase in carinata oil HEFA. In addition, it projects a reduction in pasture area by 0.024 Mha as well. These reductions lead to small increases in other natural lands, abandoned land, and forest areas, as shown in the left panel of Figure 25 on the GLOBIOM bar. According to the GLOBIOM results, these changes jointly drop the land use emissions by 16.8 $MtCO_2$ distributed mainly between natural vegetation, agricultural biomass and soil organic carbon. For the case of GLOBIOM, all emission components are negative except for the peatland oxidation which shows an increase by 5.7 $MtCO_2$.

5.2.9 **BRAZIL SOY OIL HYDROPROCESSED ESTERS AND FATTY ACIDS (HEFA)**

The 25-year ILUC emission intensity for the Brazil soy oil hydroprocessed esters and fatty acids (HEFA) pathway is 22.5 g CO_2e/MJ from GTAP-BIO and 117.9 g CO_2e/MJ from GLOBIOM. Figure 26 compares the global land use change decomposition and emission decomposition between the two models for the Brazil soy oil HEFA pathway. Similar to the USA soy oil HEFA, the livestock rebound effect and the vegetable oil demand responses are the two major drivers of the difference in ILUC emissions for this pathway.

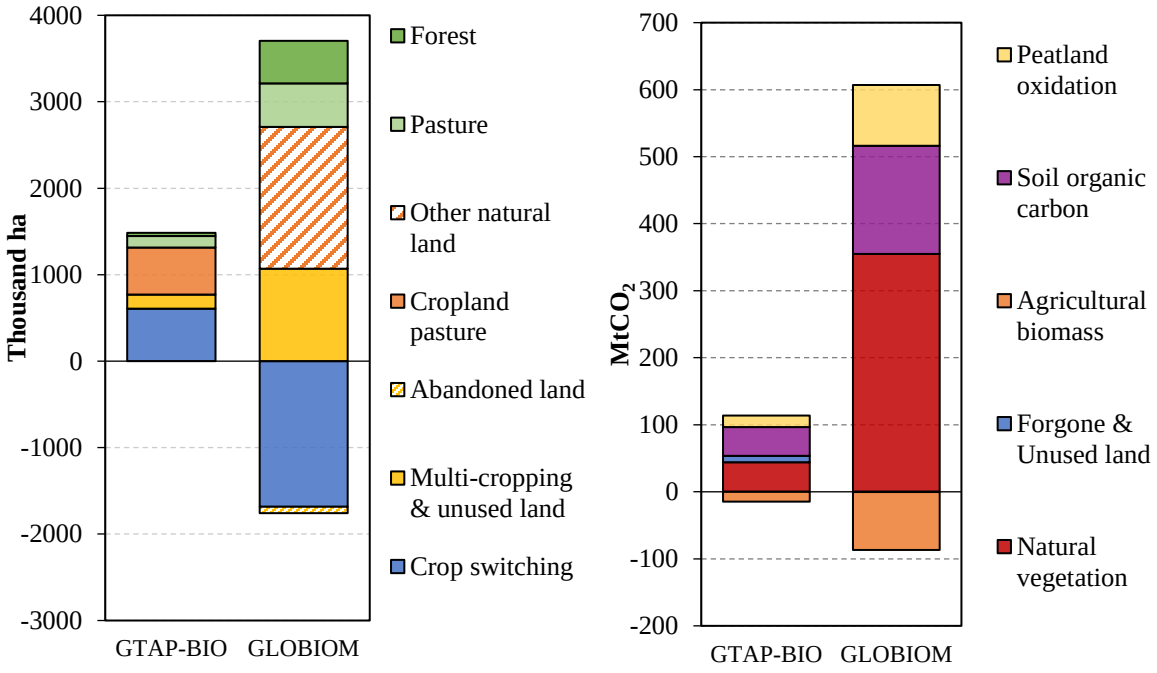

Figure 26: Land use change decomposition (left) and emission decomposition (right) for the Brazil soy oil hydroprocessed esters and fatty acids (HEFA) pathway

To produce 177 PJ HEFA fuels, 4.7 Mt of soy oil are directly needed. Driven by the increased soy oil demand, GTAP-BIO projected the global soybeans production would increase by 5.9 Mt. GLOBIOM estimated 6.2 Mt global soybeans increase. In GTAP-BIO, the HEFA shock led to 1.48 Mha increase in the global soybeans harvested area. The decomposition indicates that crop switching contributes 0.61 Mha. Cropland pasture accounts for 0.54 Mha and multi-cropping, and unused cropland provides 0.16 Mha with the rest provided by forest (0.04 Mha) and pasture (0.13 Mha). In GLOBIOM, the global soybeans harvested area increased by 1.95 Mha due to the HEFA shock, of which 1.64 Mha was from other natural land, 1.07 Mha was from multi-cropping, 0.51 Mha was from pasture, and 0.49 Mha was from forest. GLOBIOM

projected 1.67 Mha area expansion for other crops, mainly for producing energy feed crops as a response of the strong livestock rebound effect. No abandoned land is used in Brazil for expansion.

GLOBIOM estimated significantly higher conversion of natural land compared with GTAP-BIO (AEZ-EF), which explains the considerably higher GLOBIOM emissions from natural vegetation (355 vs. 44 $MtCO_2$) and SOC (161 vs. 43 $MtCO_2$). GLOBIOM also estimated higher agricultural biomass carbon sequestration (-86 vs. -15 $MtCO_2$), because of the stronger cropland expansion. Furthermore, GLOBIOM estimated higher palm fruit production (5.5 Mt vs. 1.1 Mt) and palm cultivated area (0.37 vs. 0.06 Mha) expansion in Malaysia and Indonesia compared with GTAP-BIO. This also explains the significantly higher peat oxidation from GLOBIOM (91 vs. 17 $MtCO_2$).

5.2.10 BRAZIL CARINATA OIL HYDROPROCESSED ESTERS AND FATTY ACIDS (HEFA)

The 25-year ILUC emission intensity for the Brazil carinata oil hydroprocessed esters and fatty acids (HEFA) pathway is -15.0 g CO_2e/MJ from GTAP-BIO and -24.9 g CO_2e/MJ from GLOBIOM. Figure 27 compares the global land use change decomposition and emission decomposition between the two models for the Brazil carinata oil HEFA pathway. The bar in the land use change decomposition indicates land use changes induced by expansion in carinata oil HEFA in Brazil.

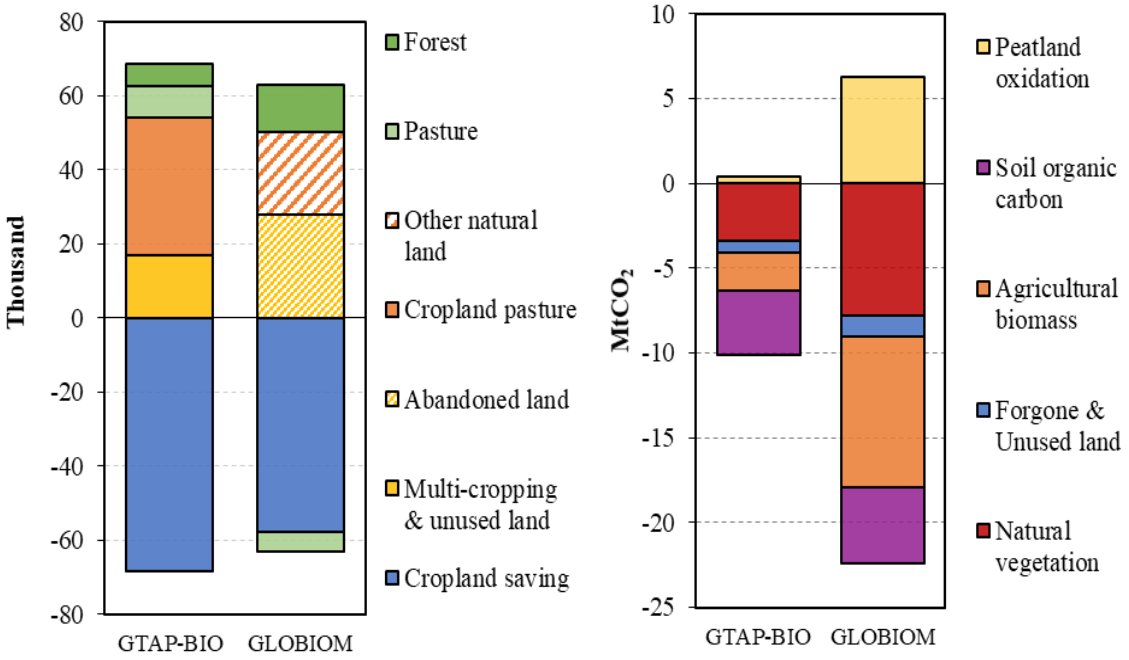

Figure 27: Land use change decomposition (left) and emission decomposition (right) for the Brazil carinata oil hydroprocessed esters and fatty acids (HEFA) pathway

To produce 26 PJ HEFA fuels from carinata oil, 0.69 Mt of carinata oil are directly needed. This needs an expansion in production of carinata by 1.7 Mt of carinata seed which requires an expansion in the area of carinata by 0.72 Mha in Brazil. Since carinata is considered as a secondary crop produced in a double cropping system, it will be produced on the exiting active cropland with no expansion in cropland. However, conversion of produced carinata to HEFA fuels generates about 1.02 Mt of carinata meal. Carinata meal is having very similar content in protein as soybean meal. Therefore the expansion in carinata oil HEFA provides extra meals highly substitutable with soybean meal in Brazil. The substitution between carinata meal and soybeans, indirectly affects production of soybeans and other crops used in animal feed rations.

The indirect changes in crop production induced by the substitution in animal feed items generate some savings in cropland which eventually leads to changes in land cover items.

The GTAP-BIO model projects a saving in cropland at the global scale by .069 Mha due to the increase in carinata oil HEFA. That leads to relatively small expansions in cropland pasture, area of forest, and pasture land as shown in the left panel of Figure 27 on the GTAP-BIO bar. The saving in cropland, leads to an expansion in unused cropland or the need for multiple cropping. According to the GTAP-BIO results these changes jointly drop the land use emissions by 9.7 $MtCO_2$ distributed mainly between natural vegetation, agricultural biomass and soil organic carbon, as shown the right panel of Figure 27 on the GTAP-BIO bar.

The GLOBIOM model projects a saving in cropland at the global scale by .058 Mha due to the increase in carinata oil HEFA. In addition, it projects a small reduction in pasture area by 0.005 Mha as well. These reductions lead to small increases in other natural lands, abandoned land, and forest areas, as shown in the left panel of Figure 27 on the GLOBIOM bar. According to the GLOBIOM results these changes jointly drop the land use emissions by 16.1 $MtCO_2$ distributed mainly between natural vegetation, agricultural biomass and soil organic carbon. For the case of GLOBIOM, all emission components are negative except for the peatland oxidation which shows an increase by 6.3 $MtCO_2$.

5.2.11 EU RAPESEED OIL HYDROPROCESSED ESTERS AND FATTY ACIDS (HEFA)

The 25-year ILUC emission intensity for the EU rapeseed oil hydroprocessed esters and fatty acids (HEFA) pathway is 20.7 g CO_2e/MJ from GTAP-BIO and 27.5 g CO_2e/MJ from GLOBIOM. Figure 28 compares the global land use change decomposition and emission decomposition between the two models for the EU rapeseed oil HEFA pathway.

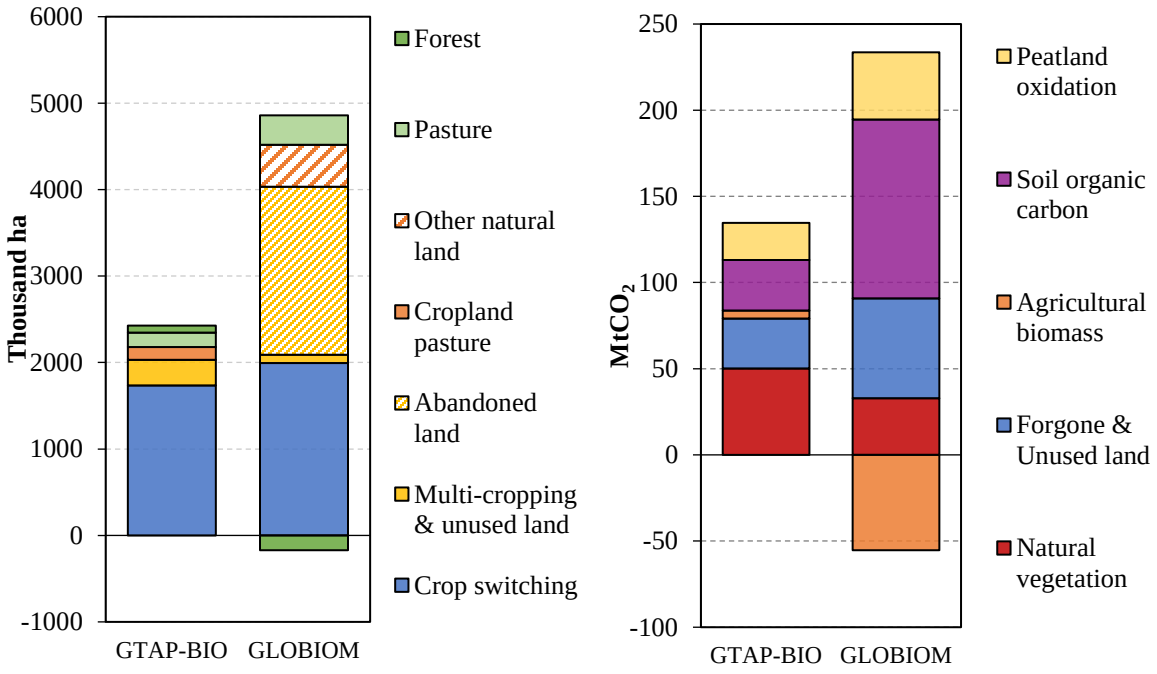

Figure 28: Land use change decomposition (left) and emission decomposition (right) for the EU rapeseed oil hydroprocessed esters and fatty acids (HEFA) pathway

To produce 260 PJ HEFA fuels, 7.1 Mt of rapeseed oil are directly needed. Driven by the increased rapeseed oil demand, GTAP-BIO projected the global rapeseed production would increase by 6.5 Mt, and 83% of

the increase would be produced in EU. GLOBIOM estimated a 14.6 Mt global rapeseed increase, only 31% of which would be produced in EU (5.9 Mt in Canada). The vegetable oil demand response is a major driver for the difference in rapeseed oil expansion. In GTAP-BIO, the HEFA shock led to 2.43 Mha increase in the global rapeseed harvested area. The decomposition indicates that crop switching contributes 1.74 Mha. Cropland pasture accounts for 0.15 Mha and multi-cropping, and unused cropland provides 0.29 Mha with the rest provided by forest (0.08 Mha) and pasture (0.16 Mha). In GLOBIOM, the global rapeseed harvested area increased by 4.69 Mha due to the HEFA shock, of which 2.43 Mha was from other natural land and abandoned land, 0.09 Mha was from multi-cropping, 0.34 Mha was from pasture, and 0.49 Mha was from forest. GLOBIOM projected 0.17 Mha of afforestation.

GTAP-BIO estimated lower emissions from foregone sequestration & unused land (29 vs. 58 $MtCO_2$) and SOC (29 vs. 104 $MtCO_2$) compared with GLOBIOM, corresponding to the higher land conversion from natural land and abandoned land. GLOBIOM had lower emissions from natural vegetation (33 vs. 50 $MtCO_2$), mainly because of the afforestation projected for the EU shock. Furthermore, GLOBIOM estimated higher palm fruit production (2.2 Mt vs. 1.4 Mt) and palm cultivated area (0.15 vs. 0.07 Mha) expansion in Malaysia and Indonesia compared with GTAP-BIO. This also explains the significantly higher peat oxidation from GLOBIOM (39 vs. 21 $MtCO_2$). However, this also leads in GLOBIOM to higher agricultural biomass carbon sequestration (-55 vs. 5 $MtCO_2$), because of sequestration in palm plantations.

5.2.12 MALAYSIA & INDONESIA PALM OIL HYDROPROCESSED ESTERS AND FATTY ACIDS (HEFA)

The 25-year ILUC emission intensity for the Malaysia & Indonesia palm oil hydroprocessed esters and fatty acids (HEFA) pathway is 34.6 g CO_2e/MJ from GTAP-BIO and 60.2 g CO_2e/MJ from GLOBIOM. Figure 29 compares the global land use change decomposition and emission decomposition between the two models for the Malaysia & Indonesia palm oil HEFA pathway. The (net) total bar level in the land use change decomposition indicates oil palm cultivated area increase.

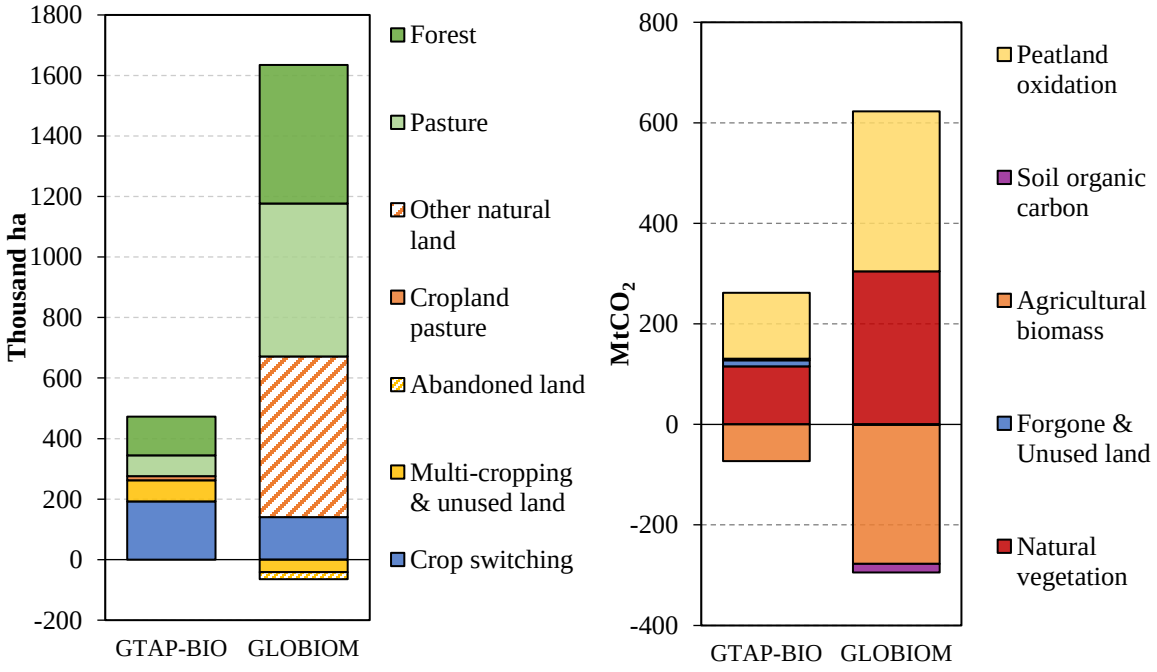

Figure 29: Land use change decomposition (left) and emission decomposition (right) for the Malaysia & Indonesia palm oil hydroprocessed esters and fatty acids (HEFA) pathway

To produce 208 PJ HEFA fuels, 5.7 Mt of palm oil are directly needed. Driven by the increased palm oil demand, GTAP-BIO projected the global palm fruit production would increase by 9.1 Mt, and 89% of the increase would be produced in Malaysia and Indonesia. GLOBIOM estimated 21.2 Mt global palm fruit increase, 95% which would be produced in the Malaysia and Indonesia. For crushing palm fruit, the crushing rate is about 24 % (by weight) for palm oil and palm kernel oil together. The vegetable oil demand and substitution responses are major drivers of the difference in palm oil expansion. GTAP-BIO showed a higher reduction in palm oil consumption and stronger substitutions with other materials. In GTAP-BIO, the HEFA shock led to 0.47 Mha increase in the global oil palm cultivated area, of which forest and pasture contributed 0.20 Mha, and crop switching accounted for 0.19 Mha. In GLOBIOM, the global oil palm cultivated area increased by 1.57 Mha, of which 0.96 Mha was from forest (0.46 Mha) and pasture, 0.53 was from other natural land and abandoned land.

Driven by the lower oil palm expansion and tropical deforestation, GTAP-BIO estimated lower emissions from natural vegetation (115 vs. 304 $MtCO_2$) and peat oxidation (131 vs. 318 $MtCO_2$) compared with GLOBIOM. Both models estimated agricultural biomass carbon sequestration (-73 vs. -276 $MtCO_2$), although GLOBIOM had higher sequestration due to the higher new palm plantation expansion.

5.2.13 USA MISCANTHUS FISCHER-TROPSCH JET FUEL (FT)

The 25-year ILUC emission intensity for the USA miscanthus Fischer-Tropsch jet fuel (FT) pathway is -37.3 g CO_2e/MJ from GTAP-BIO and -10.6 g CO_2e/MJ from GLOBIOM. Figure 30 compares the global land use change decomposition and emission decomposition between the two models for the USA miscanthus FT pathway. The (net) total bar level in the land use change decomposition indicates feedstock harvested area increase.

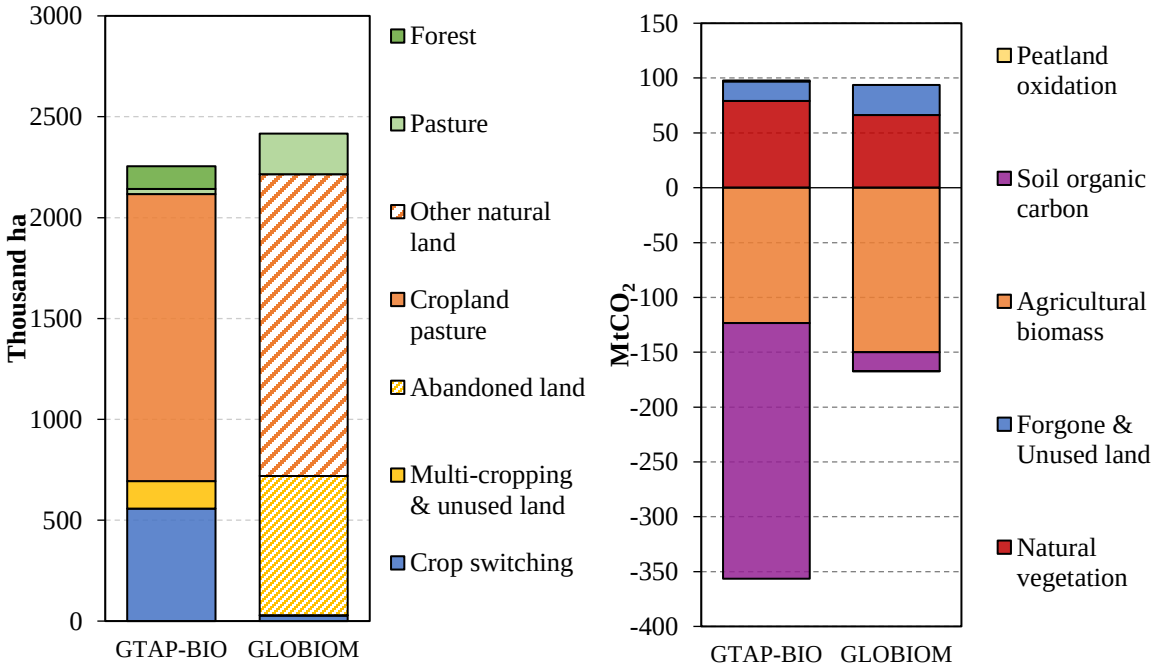

Figure 30: Land use change decomposition (left) and emission decomposition (right) for the USA miscanthus Fischer-Tropsch jet fuel (FT) pathway

To produce 277 PJ FT fuels, 34.1 Mt of miscanthus are directly needed. Since cellulosic crops are modelled as dedicated energy crop supplying only biofuels production in both GTAP-BIO and GLOBIOM and the technical conversion yields were reconciled, miscanthus production in both models would meet the direct requirement. There was a small difference in crop yield so that GTAP-BIO (2.25 Mha) used less land than GLOBIOM (2.42 Mha) for miscanthus production. Cropland pasture (1.42 Mha) is the major land source for miscanthus in GTAP-BIO, and crop switching also contributed 0.56 Mha. In GLOBIOM, other natural land (1.50 Mha) and abandoned land (0.69 Mha) are the major miscanthus land sources. The land sources for producing miscanthus and the associated emission factors are the drivers to the results difference between the two models, because the SOC impact of perennials differ depending on the type of land where plantations are grown.

Emission changes from natural vegetation (79 vs. 66 $MtCO_2$) and agricultural biomass carbon sequestration (-123 vs. -150 $MtCO_2$) are comparable for the USA miscanthus FT pathway. GTAP-BIO had higher SOC sequestration (-233 vs. -17 $MtCO_2$) in particular because of different emission factors and because the crop is assumed to expand into land types with soil poorer in SOC content. Driven by the high carbon sequestration in soil and crop, both models estimated negative ILUC emissions (-258 $MtCO_2$ for GTAP-BIO and -74 $MtCO_2$ from GLOBIOM).

5.2.14 USA MISCANTHUS ATJ-SPK FROM ISOBUTANOL

The 25-year ILUC emission intensity for the USA miscanthus ATJ-SPK from isobutanol pathway is -58.5 g CO_2e/MJ from GTAP-BIO and -8.7 g CO_2e/MJ from GLOBIOM. Figure 31 compares the global land use change decomposition and emission decomposition between the two models for the USA miscanthus ATJ-SPK from isobutanol pathway. The (net) total bar level in the land use change decomposition indicates feedstock harvested area increase. The land use change and emissions decomposition from this pathway have similar patterns to the USA miscanthus FT pathway.

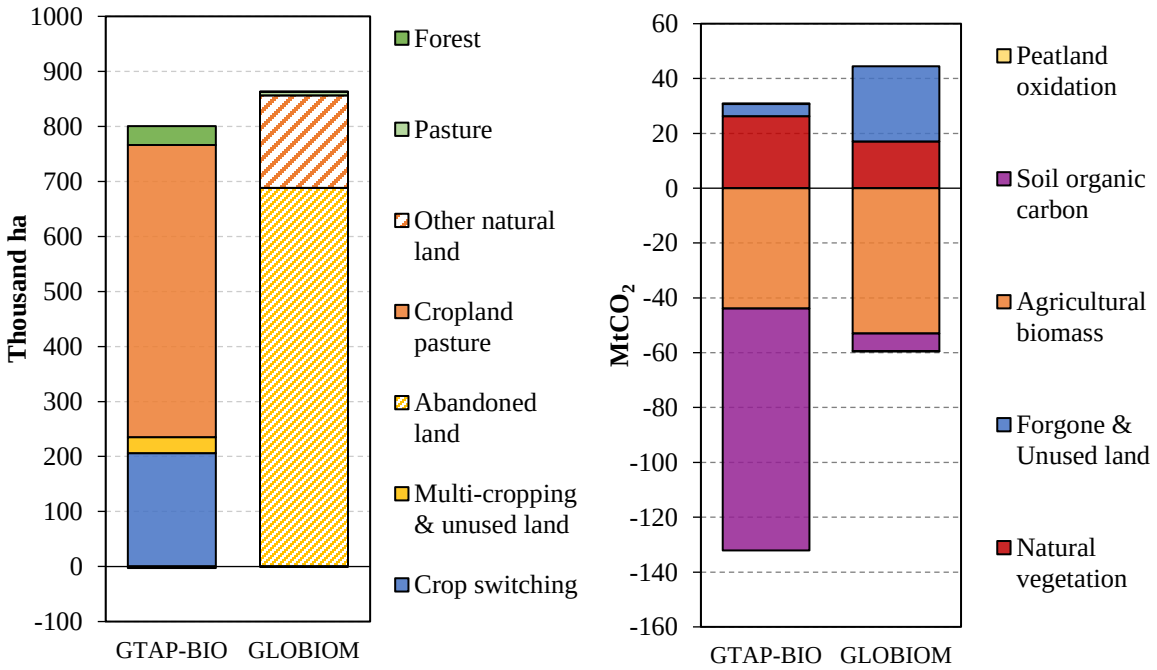

Figure 31: Land use change decomposition (left) and emission decomposition (right) for the USA miscanthus ATJ-SPK from isobutanol pathway

To produce 69 PJ ATJ-SPK from isobutanol fuels, 12.0 Mt of miscanthus are directly needed. The miscanthus production in both models would meet the direct requirement since cellulosic crops are modelled as a dedicated energy crop.

There was a small difference in crop yield so that GTAP-BIO (0.80 Mha) used less land than GLOBIOM (0.86 Mha) for miscanthus production. Cropland pasture (0.53 Mha) is the major land source for miscanthus in GTAP-BIO, and crop switching also contributed 0.21 Mha. In GLOBIOM, other natural land (0.17 Mha) and abandoned land (0.69 Mha) are the major miscanthus land sources. The land sources for producing miscanthus and the associated emission factors are the drivers of the different results from the two models.

GTAP-BIO had higher SOC sequestration (-88 vs. -7 $MtCO_2$) since it used generally higher emission (sequestration) factors for the USA miscanthus SOC compared with GLOBIOM, and expands into land types with soil poorer in SOC content. Emission changes from natural vegetation (26 vs. 17 $MtCO_2$), and agricultural biomass carbon sequestration (-44 vs. -53 $MtCO_2$) are not very different. GLOBIOM estimated 27 $MtCO_2$ foregone sequestration due to the use of abandoned land. Driven by the high carbon sequestration in soil and crop, both models estimated negative ILUC emissions (-101 $MtCO_2$ for GTAP-BIO and -15 $MtCO_2$ from GLOBIOM).

5.2.15 USA MISCANTHUS ATJ-SPK FROM ETHANOL

The 25-year ILUC emission intensity for the USA miscanthus ATJ-SPK from ethanol pathway is -47.1 gCO_2e/MJ from GTAP-BIO and -8.2 gCO_2e/MJ from GLOBIOM. Figure 32 compares the global land use change decomposition and emission decomposition between the two models for the USA miscanthus ATJ-SPK from ethanol pathway. The (net) total bar level in the land use change decomposition indicates feedstock harvested area increase. The land use change and emissions decomposition from this pathway are in line with the USA miscanthus ATJ-SPK from isobutanol and FTJ pathways.

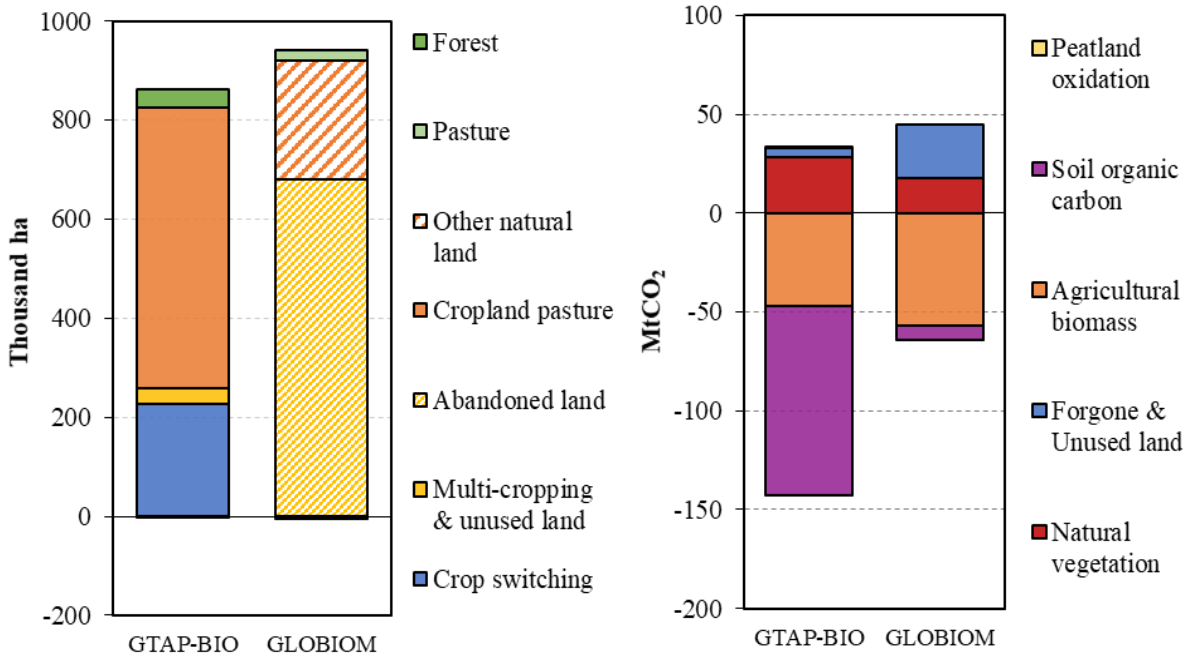

Figure 32: Land use change decomposition (left) and emission decomposition (right) for the USA miscanthus ATJ-SPK from ethanol pathway

For producing 93 PJ fuels from the ATJ-SPK from ethanol pathway, 13.0 Mt of miscanthus are directly needed. The miscanthus production in both models would meet the direct requirement since cellulosic crops are modelled as a dedicated energy crop.

Cropland pasture (0.57 Mha) is the major land source for miscanthus in GTAP-BIO, and crop switching also contributed 0.23 Mha. In GLOBIOM, other natural land (0.24 Mha) and abandoned land (0.68 Mha) are the major miscanthus land sources. The land sources for producing miscanthus and the associated emission factors are the drivers to the results difference between the two models.

GTAP-BIO had higher SOC sequestration (-40.9 vs. -3 gCO_2e/MJ) since its USA miscanthus expands into land cover types with higher emission (sequestration) factors for SOC compared with GLOBIOM. Emission changes from natural vegetation (12.1 vs. 7.6 gCO_2e/MJ), and agricultural biomass carbon sequestration (-20.3 vs. -24.6 gCO_2e/MJ) indicate similar patterns. GLOBIOM estimated 11.7 gCO_2e/MJ foregone sequestration due to the use of abandoned land where some biomass would otherwise regrow. Driven by the high carbon sequestration in soil and crop, both models estimated negative ILUC emissions (-47.1 gCO_2e/MJ for GTAP-BIO and -8.2 gCO_2e/MJ from GLOBIOM).

5.2.16 USA SWITCHGRASS FISCHER-TROPSCH JET FUEL (FT)

The 25-year ILUC emission intensity for the USA switchgrass Fischer-Tropsch jet fuel (FT) pathway is -8.2 g CO_2e/MJ from GTAP-BIO and 2.5 g CO_2e/MJ from GLOBIOM. Figure 33 compares the global land use change decomposition and emission decomposition between the two models for the USA switchgrass FT pathway. The land use change and emissions decomposition from this pathway are similar to the USA miscanthus FT pathway.

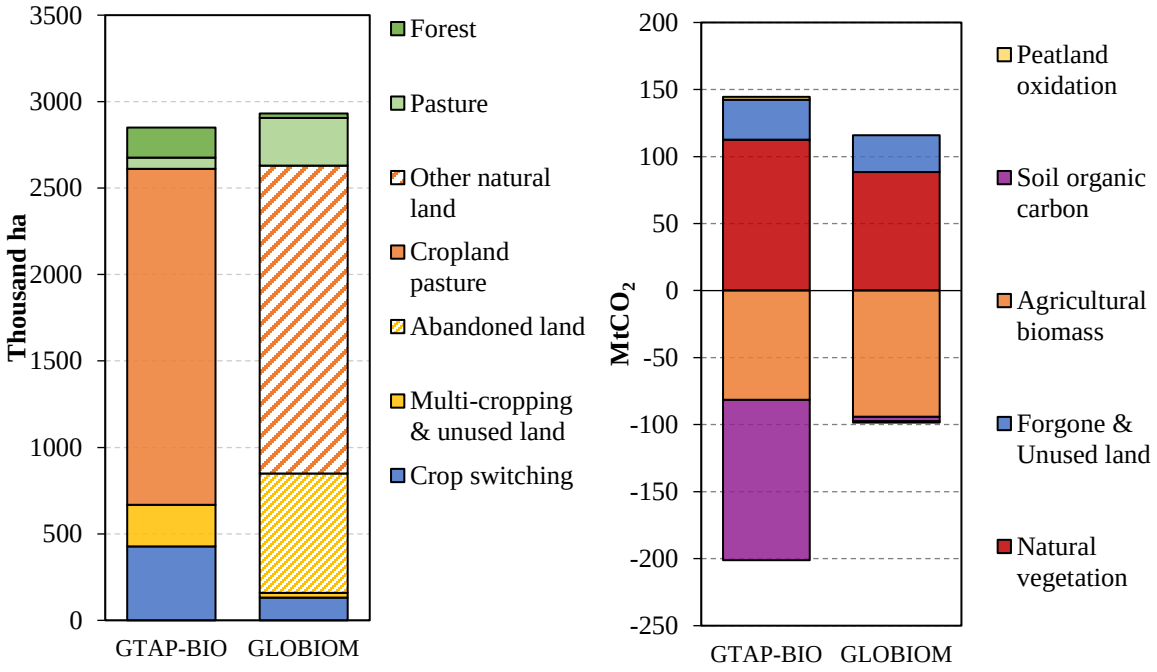

Figure 33: Land use change decomposition (left) and emission decomposition (right) for the USA switchgrass Fischer-Tropsch jet fuel (FT) pathway

To produce 277 PJ FT fuels, 33.0 Mt of switchgrass are directly needed. The switchgrass production in both models would meet the direct requirement since cellulosic crops are modelled as a dedicated energy crop.

In GTAP-BIO, the total miscanthus harvested area increased by 2.85 Mha. Cropland pasture (1.94 Mha) is the major land source for switchgrass in GTAP-BIO, and crop switching also contributed 0.43 Mha. In GLOBIOM, the total miscanthus harvested area increased by 2.93 Mha. Other natural land (1.78 Mha) and abandoned land (0.69 Mha) are the major switchgrass land sources. The land sources for producing switchgrass and the associated emission factors are the drivers of the different results from the two models.

GTAP-BIO had higher SOC sequestration (-119 vs. -3 $MtCO_2$) since it used generally higher emission (sequestration) factors for the USA switchgrass SOC compared with GLOBIOM, and expands into land types with soil poorer in SOC content. Emission changes from natural vegetation (112 vs. 89 $MtCO_2$), and agricultural biomass carbon sequestration (-82 vs. -94 $MtCO_2$) are not very different. GLOBIOM estimated 27 $MtCO_2$ foregone sequestration due to the use of abandoned land, while GTAP-BIO estimated 30 $MtCO_2$ from converting unused land. Driven by the high SOC sequestration, GTAP-BIO had significantly smaller total ILUC emissions (-57 $MtCO_2$ for GTAP-BIO and -17 $MtCO_2$ from GLOBIOM).

5.2.17 USA SWITCHGRASS ATJ-SPK FROM ISOBUTANOL

The 25-year ILUC emission intensity for the USA switchgrass ATJ-SPK from isobutanol pathway is -18.9 g CO_2e/MJ from GTAP-BIO and 10.2 g CO_2e/MJ from GLOBIOM. Figure 34 compares the global land use change decomposition and emission decomposition between the two models for the USA switchgrass ATJ-SPK from isobutanol pathway. The (net) total bar level in the land use change decomposition indicates feedstock harvested area increase. The land use change and emissions decomposition from this pathway have similar patterns to the USA switchgrass FT pathway.

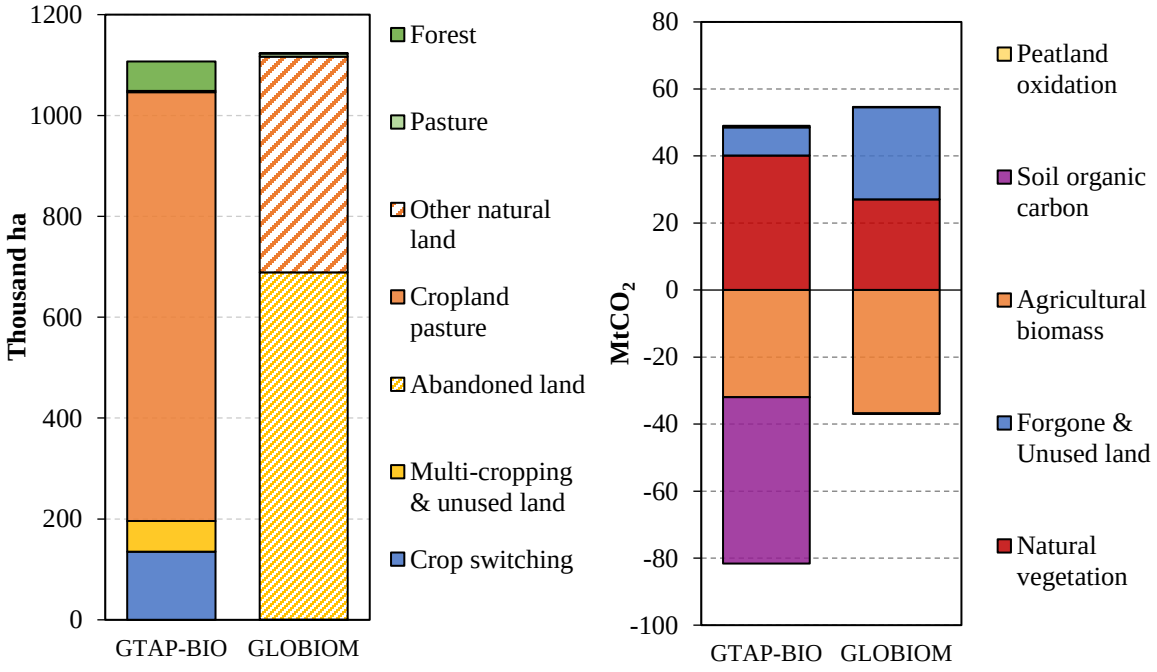

Figure 34: Land use change decomposition (left) and emission decomposition (right) for the USA switchgrass alcohol (isobutanol) to jet (ATJ) pathway

To produce 69 PJ ATJ-SPK from isobutanol fuels, 12.7 Mt of miscanthus are directly needed. Switchgrass production in both models would meet the direct requirement since cellulosic crops are modelled as a dedicated energy crop.

In GTAP-BIO, the total switchgrass harvested area increased by 1.11 Mha. Cropland pasture (0.85 Mha) is the major land source for switchgrass in GTAP-BIO, and crop switching also contributed 0.14 Mha. In GLOBIOM, the total switchgrass harvested area increased by 1.12 Mha. Other nature land (0.43 Mha) and abandoned land (0.69 Mha) are the major switchgrass land sources. The land sources for producing switchgrass and the associated emission factors are the drivers leading to different results from the two models.

GTAP-BIO had higher SOC sequestration (-20 vs. 0 $MtCO_2$) since it used generally higher emission (sequestration) factors for the USA switchgrass SOC compared with GLOBIOM, and expands into land types with soil poorer in SOC content. Emission changes from natural vegetation (40 vs. 27 $MtCO_2$), and agricultural biomass carbon sequestration (-32 vs. -37 $MtCO_2$) are not very different. GLOBIOM estimated 27 $MtCO_2$ foregone sequestration due to the use of abandoned land, while GTAP-BIO estimated 8 $MtCO_2$ from converting unused land. Driven by the high SOC sequestration, GTAP-BIO had smaller total ILUC emissions (-33 $MtCO_2$ for GTAP-BIO and 18 $MtCO_2$ from GLOBIOM).

5.2.18 **USA SWITCHGRASS ATJ-SPK FROM ETHANOL**

The 25-year ILUC emission intensity for the USA switchgrass ATJ-SPK from ethanol pathway is –15.2 gCO_2e/MJ from GTAP-BIO and 8.4 gCO_2e/MJ from GLOBIOM. Figure 35 compares the global land use change decomposition and emission decomposition between the two models for the USA Switchgrass ATJ-SPK from ethanol pathway. The (net) total bar level in the land use change decomposition indicates feedstock harvested area increase. The land use change and emissions decomposition from this pathway are in line with the US switchgrass ATJ and FTJ pathways.

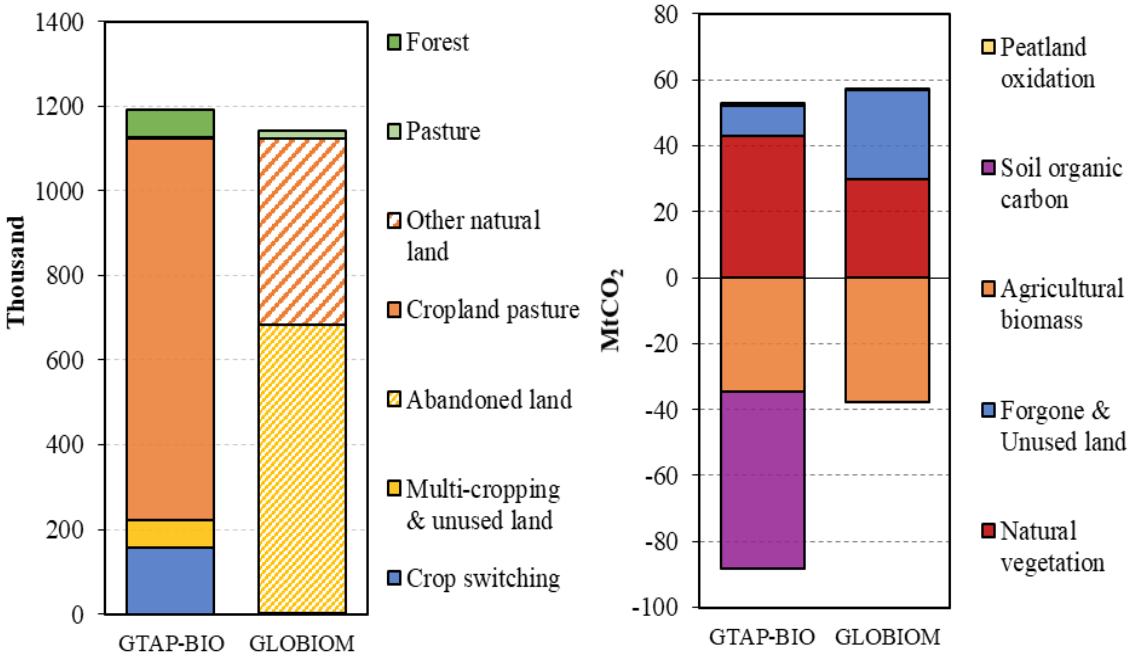

Figure 35: Land use change decomposition (left) and emission decomposition (right) for the USA switchgrass ATJ-SPK from ethanol pathway

For producing 93 PJ fuels from the ATJ-SPK from ethanol pathway, 13.0 Mt of switchgrass are directly needed. The switchgrass production in both models would meet the direct requirement since cellulosic crops are modelled as a dedicated energy crop.

Cropland pasture (0.90 Mha) is the major land source for switchgrass in GTAP-BIO, and crop switching also contributed 0.16 Mha. In GLOBIOM, other natural land (0.44 Mha) and abandoned land (0.68 Mha) are the major switchgrass land sources. The land sources for producing switchgrass and the associated emission factors are the drivers to the results difference between the two models.

GTAP-BIO had higher SOC sequestration (-23.1 vs. 0.1 gCO_2e/MJ) since a larger area of US switchgrass expands into land type with higher emission (sequestration) factors for SOC compared with GLOBIOM. Agricultural biomass carbon are relatively close (-14.8 vs. -16.2 gCO_2e/MJ), hence the total sequestration amount is larger in case of GTAP-BIO. GTAP-BIO emission changes from natural vegetation (18.5 vs. 12.8 gCO_2e/MJ), and foregone sequestration due to the use of abandoned land (3.9 vs. 11.7 gCO_2e/MJ) sum up to relatively close totals, which overall lead to more negative total emissions in GTAP-BIO results due to the larger sequestration effect in soil and crops. As a result, the GTAP-BIO model estimated net negative ILUC emissions (-15.2 gCO_2e/MJ) and GLOBIOM reports positive net emissions (8.4 gCO_2e/MJ) for the US switchgrass pathway.

5.2.19 USA POPLAR FISCHER-TROPSCH JET FUEL (FT)

The 25-year ILUC emission intensity for the USA poplar Fischer-Tropsch jet fuel (FT) pathway is -9.6 g CO_2e/MJ from GTAP-BIO and -0.6 g CO_2e/MJ from GLOBIOM. Figure 36 compares the global land use change decomposition and emission decomposition between the two models for the USA poplar FT pathway. The (net) total bar level in the land use change decomposition indicates feedstock harvested area increase. The land use change and emissions decomposition from this pathway have similar patterns to the USA miscanthus FT pathway.

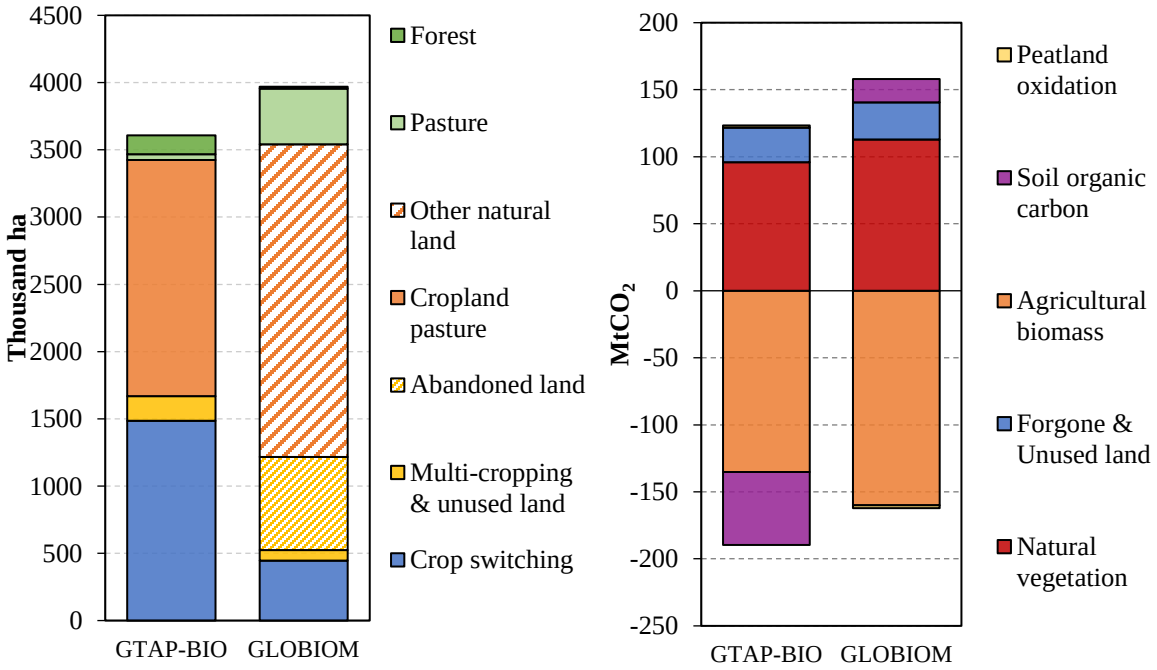

Figure 36: Land use change decomposition (left) and emission decomposition (right) for the USA poplar Fischer-Tropsch jet fuel (FT) pathway

To produce 277 PJ FT fuels, 30.8 Mt of poplar are directly needed. Poplar production in both models would meet the direct requirement since cellulosic crops are modelled as a dedicated energy crop.

In GTAP-BIO, the total poplar harvested area increased by 3.61 Mha. Cropland pasture (1.76 Mha) is the major land source for poplar in GTAP-BIO, and crop switching also contributed 1.49 Mha. In GLOBIOM, the total poplar harvested area increased by 3.97 Mha. Other natural land (2.33 Mha) and abandoned land (0.69 Mha) are the major poplar land sources. The land sources for producing poplar and the associated emission factors are the drivers of the different results from the two models.

GTAP-BIO had higher SOC sequestration (-54 vs. 17 $MtCO_2$) since it used generally higher emission (sequestration) factors for the USA poplar SOC compared with GLOBIOM, and expands into land types with soil poorer in SOC content. Emission changes from natural vegetation (96 vs. 113 $MtCO_2$) and agricultural biomass carbon sequestration (-135 vs. -160 $MtCO_2$) are not very different. GLOBIOM estimated 28 $MtCO_2$ foregone sequestration due to the use of abandoned land, while GTAP-BIO estimated 26 $MtCO_2$ from converting unused land. Driven by the high SOC sequestration, GTAP-BIO had smaller total ILUC emissions (-66 $MtCO_2$ for GTAP-BIO and -4 $MtCO_2$ from GLOBIOM).

5.2.20 EU MISCANTHUS FISCHER-TROPSCH JET FUEL (FT)

The 25-year ILUC emission intensity for the EU miscanthus Fischer-Tropsch jet fuel (FT) pathway is -9.3 g CO_2e/MJ from GTAP-BIO and -26.5 g CO_2e/MJ from GLOBIOM. Figure 37 compares the global land use change decomposition and emission decomposition between the two models for the EU miscanthus FT pathway. The (net) total bar level in the land use change decomposition indicates feedstock harvested area increase.

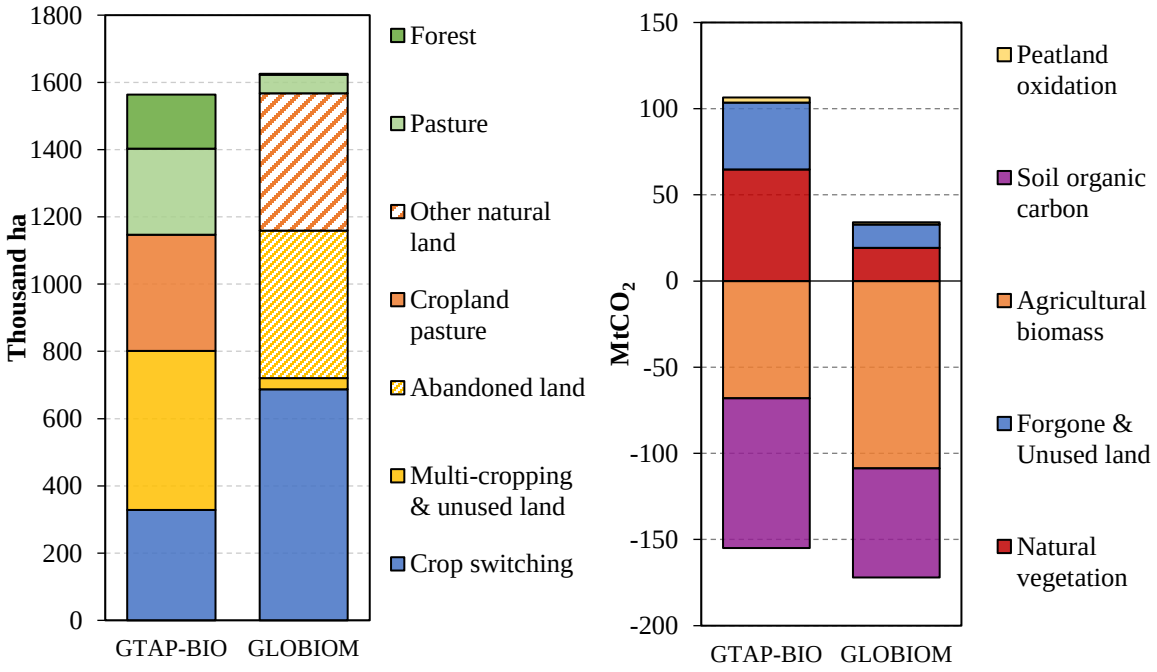

Figure 37: Land use change decomposition (left) and emission decomposition (right) for the EU miscanthus Fischer-Tropsch jet fuel (FT) pathway

To produce 208 PJ FT fuels, 25.6 Mt of miscanthus are directly needed. Miscanthus production in both models would meet the direct requirement since cellulosic crops are modelled as a dedicated energy crop.

In GTAP-BIO, the total miscanthus harvested area increased by 1.56 Mha. Multi-cropping & unused land (0.47 Mha) and cropland pasture (0.35 Mha) are the major land sources for miscanthus in GTAP-BIO, and crop switching also contributed 0.33 Mha. In GLOBIOM, the total miscanthus harvested area increased by 1.63 Mha. Crop switching (0.69 Mha), other natural land (0.41 Mha), and abandoned land (0.44 Mha) are the major miscanthus land sources. The land sources for producing miscanthus and the associated emission factors are the drivers of the different results from the two models.

GTAP-BIO had higher SOC sequestration (-87 vs. -63 $MtCO_2$) but lower crop biomass sequestration (-68 vs. -109 $MtCO_2$) compared with GLOBIOM. The emissions from natural vegetation (65 vs. 19 $MtCO_2$) are larger in GTAP-BIO mainly due to the larger deforestation projected. GLOBIOM estimated 14 $MtCO_2$ foregone sequestration due to the use of abandoned land, while GTAP-BIO estimated 39 $MtCO_2$ from converting unused land. Driven by the high SOC and crop biomass sequestration, both models had negative ILUC emissions (-49 $MtCO_2$ for GTAP-BIO and -138 $MtCO_2$ from GLOBIOM).

5.2.21 EU MISCANTHUS ATJ-SPK FROM ISOBUTANOL

The 25-year ILUC emission intensity for the EU miscanthus ATJ-SPK from isobutanol pathway is -16.6 g CO_2e/MJ from GTAP-BIO and -35.5 g CO_2e/MJ from GLOBIOM. Figure 38 compares the global land use change decomposition and emission decomposition between the two models for the EU miscanthus ATJ-SPK from isobutanol pathway. The (net) total bar level in the land use change decomposition indicates feedstock harvested area increase. The land use change and emissions decomposition from this pathway have similar patterns to the EU miscanthus FT pathway.

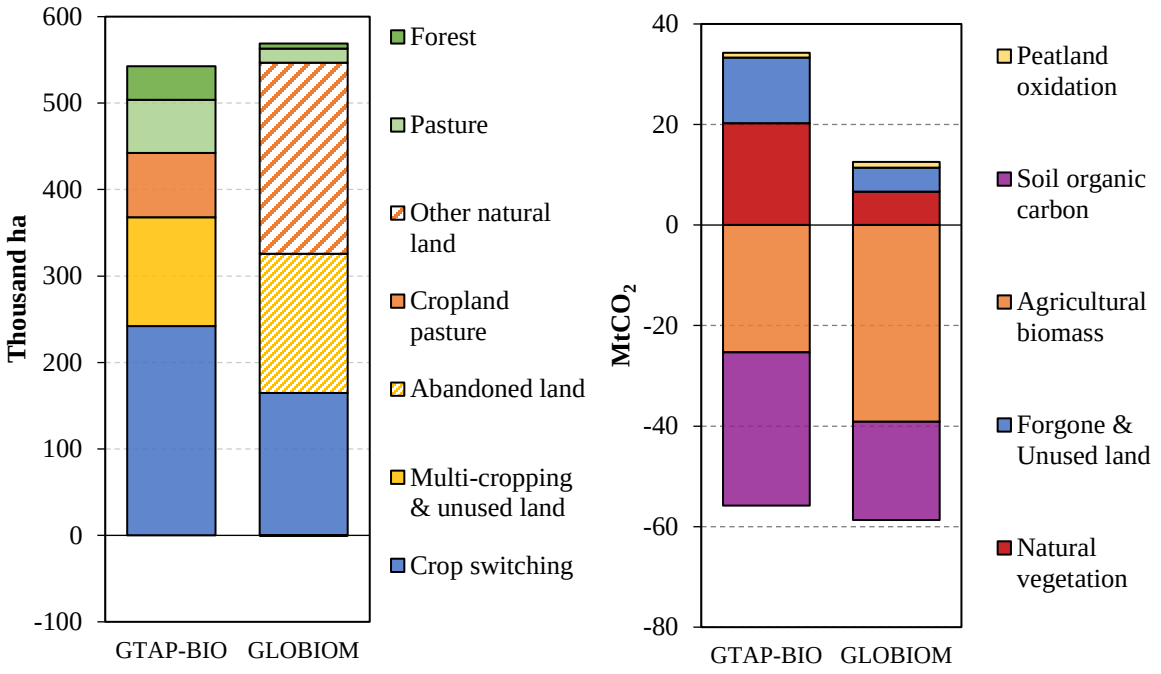

Figure 38: Land use change decomposition (left) and emission decomposition (right) for the EU miscanthus Fischer-Tropsch jet fuel (FT) pathway

To produce 52 PJ ATJ-SPK from isobutanol fuels, 34.1 Mt of miscanthus are directly needed. Miscanthus production in both models would meet the direct requirement since cellulosic crops are modelled as a dedicated energy crop.

In GTAP-BIO, the total miscanthus harvested area increased by 0.54 Mha. Crop switching (0.24 Mha), multi-cropping & unused land (0.13 Mha) and Cropland pasture (0.07 Mha) are the major land sources for miscanthus in GTAP-BIO. Forest and pasture together also contributed 0.1 Mha. In GLOBIOM, the total miscanthus harvested area increased by 0.57 Mha. Other natural land (0.22 Mha), Crop switching (0.17 Mha), and abandoned land (0.16 Mha) are the major miscanthus land sources. The land sources for producing miscanthus and the associated emission factors are the drivers of the different results from the two models.

GTAP-BIO had higher SOC sequestration (-30 vs. -20 $MtCO_2$) but lower crop biomass sequestration (-25 vs. -39 $MtCO_2$) compared with GLOBIOM. The emissions from natural vegetation (20 vs. 7 $MtCO_2$) are larger in GTAP-BIO mainly due to the higher deforestation projected. GLOBIOM estimated 5 $MtCO_2$ foregone sequestration due to the use of abandoned land, while GTAP-BIO estimated 13 $MtCO_2$ from converting unused land. Driven by the high SOC and crop biomass sequestration, both models had negative ILUC emissions (-22 $MtCO_2$ for GTAP-BIO and -46 $MtCO_2$ from GLOBIOM).

5.2.22 EU MISCANTHUS ATJ-SPK FROM ETHANOL

The 25-year ILUC emission intensity for the EU miscanthus ATJ-SPK from ethanol pathway is -12.7 gCO_2e/MJ from GTAP-BIO and -27.8 gCO_2e/MJ from GLOBIOM. Figure 39 compares the global land use change decomposition and emission decomposition between the two models for the EU miscanthus ATJ-SPK from ethanol pathway. The (net) total bar level in the land use change decomposition indicates feedstock harvested area increase. The land use change and emissions decomposition from this pathway are in line with the EU miscanthus ATJ-SPK from isobutanol and FTJ pathways.

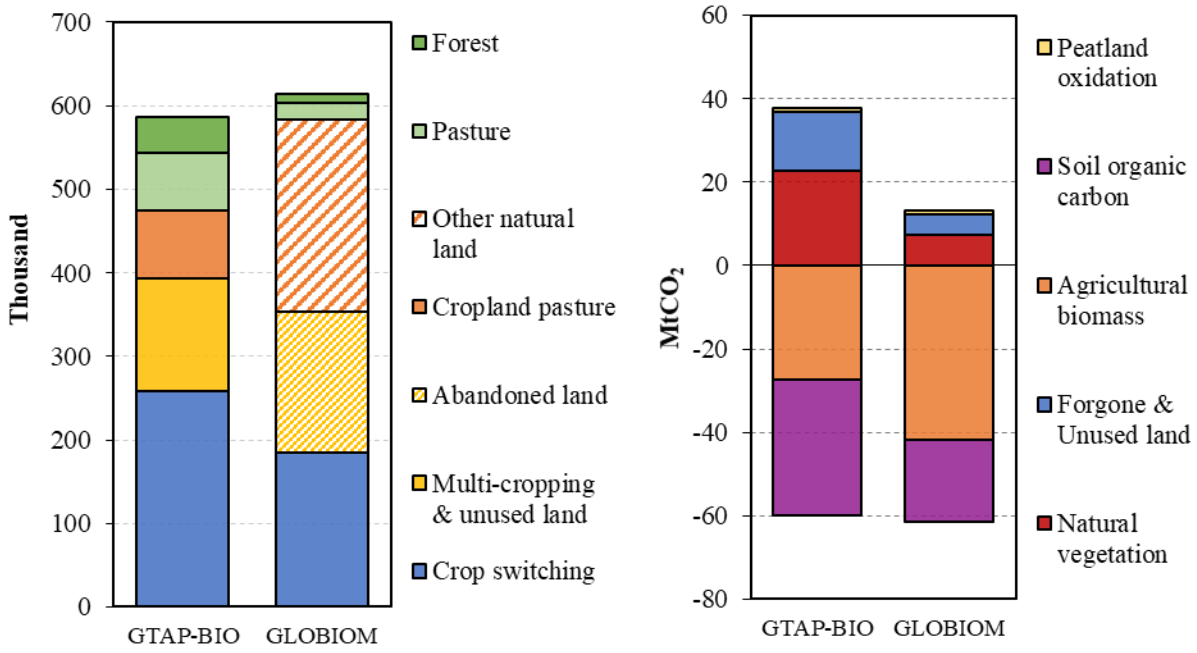

Figure 39: Land use change decomposition (left) and emission decomposition (right) for the EU miscanthus ATJ-SPK from ethanol pathway

For producing 70 PJ fuels from the ATJ-SPK from ethanol pathway, 9.8 Mt of miscanthus are directly needed. The miscanthus production in both models would meet the direct requirement since cellulosic crops are modelled as a dedicated energy crop.

Crop switching (0.26) and Changes in Multiple cropping & unused land (0.14 Mha) are the major land sources for miscanthus in GTAP-BIO. In GLOBIOM, other natural land (0.23 Mha) and abandoned land (0.17 Mha) are the major miscanthus land sources. The land sources for producing miscanthus and the associated emission factors are the drivers to the results difference between the two models.

GTAP-BIO had higher SOC sequestration (-18.6 vs. -11.3 gCO_2e/MJ) since a large area of the EU miscanthus expands in land with higher sequestration factors for SOC compared with GLOBIOM. Agricultural biomass carbon sequestration is different and GTAP has lower sequestration in this category (-15.7 vs. -24.0 gCO_2e/MJ) so the total sequestration amount is not very different between two models. GTAP emission changes from natural vegetation (12.9 vs. 4.2 gCO_2e/MJ), and foregone sequestration due to the use of abandoned land (8.14 vs. 2.9 gCO_2e/MJ) are both higher in case of GTAP-BIO. Driven by the high carbon sequestration in soil and crop, both models estimated negative ILUC emissions (-12.7 gCO_2e/MJ for GTAP-BIO and -27.8 gCO_2e/MJ from GLOBIOM).

5.2.23 INDIA JATROPHA HYDROPROCESSED ESTERS AND FATTY ACIDS (HEFA)

To model production of Jatropha oil HEFA in the ILUC models, input data were obtained from the existing literature. In particular, the map of jatropha suitability area and yields was obtained from the IIASA FAO GAEZ database.[20] According to this map, the average seed yield of irrigated Jatropha, with high input management, is about 3.24 metric tons per hectare in India after maturity. As a perennial crop, jatropha is

[20] https://gaez-data-portal-hqfao.hub.arcgis.com/

usually cultivated over 20 years life-cycle plantation cycles, but the crop has very low yield in the first two years of its plantation period. Hence, to obtain an average yield over the full plantation cycle, the Jatropha yield data were scaled down by a factor of 0.9.

As jatropha is a perennial crop with a 20-year lifespan, it sequesters some carbon in its biomass. Achten et al. (2013) was used to determine the above ground biomass collected by this plant over 20 years of its lifespan. Three cases of low, medium, and high biomass collection rates were considered. When adding below ground biomass (with a root-shoot ration of 0.386), these correspond to three average levels of 12.0, 17.8, and 21.4 tonnes carbon per hectare.

In order to choose between the three sequestration levels, additional information was mobilized from the literature on the relation between the carbon stock in the plantation and the seed yield, suggesting that the yield considered for the jatropha ILUC modelling would be located between the low and medium case scenario. Globally, the yield information used from GAEZ, with 2.5 t seed per ha, is closer to the low sequestration scenario. Fertilizer application assumptions from the core LCA group were also confronted with the yield observed in the literature. The application rates are also better aligned with a low yield case assumption. Furthermore, no irrigation is assumed for the core-LCA value; therefore, the low sequestration case was taken as the main assumption.

Results

The estimated ILUC values obtained from the GTAP-BIO and GLOBIOM models are presented in Table 105 for the 3 scenarios on the use of meals, assuming low sequestration rate in the plantation (see Appendix E - core LCA section for rationale on the scenario definitions). All ILUC values are negative due to the effect of carbon storage in the tree biomass of the plantations, and the soil organic carbon sequestration when plantations expand into cropland previously under annual crops. The results are relatively close across models for Scenario 1 and Scenario 3, under the three carbon stocks assumptions, with a difference less than 8.9 gCO_2/MJ. For scenario 2, the difference is a bit larger (10.7 gCO_2/MJ) with GLOBIOM showing more negative results due to larger savings associated to the meal coproduct effect on the feed market.

Table 105:. Estimated ILUC values for Jatropha oil HEFA produced in India (gCO_2e/MJ)

Scenario	GTAP-BIO	GLOBIOM	Reconciled
Scenario 1 - Fertilizer	-24.7	-20.0	**-22.4**
Scenario 2 - Feed meal	-41.9	-52.6	**-48.1**
Scenario 3 - Electricity	-29.8	-24.4	**-27.1**

For the core-LCA group, the three scenario value differences were lower than 8.9 gCO2/MJ. Adding the values of core-LCA and ILUC still maintain a difference lower than 8.9 gCO2/MJ for scenario 1 and 3. Therefore, scenarios 1 and 3 were merged, and two cases were considered for the final LCA analysis:

- Jatropha oil HEFA – meal used as fertilizer or electricity input [Scenario 1 and 3]
- Jatropha oil HEFA – meal used as animal feed after detoxification[Scenario 2]

For the core-LCA group, the three scenario value differences were lower than 8.9 gCO2/MJ. Adding the values of core-LCA and ILUC still maintain.

Detailed results on land use changes and their corresponding emissions for these scenarios are provided in sections below:

India jatropha oil hydroprocessed esters and fatty acids (HEFA) - Meal used as fertilizer or electricity input

The 25-year ILUC emission intensity for the India jatropha oil hydroprocessed esters and fatty acids (HEFA) pathway is -27.3 g CO_2e/MJ from GTAP-BIO and -22.2 g CO_2e/MJ from GLOBIOM, if meal coproducts are used as fertilizer. The ILUC value of each model represents an average value of the following two independent simulations: 1) non-fuel co-products are used as fertilizer and 2) non-fuel co-products used as feedstock for electricity production. This approach applies to other results for this pathway as well. Figure 40 compares the global land use change decomposition and emission decomposition between the two models for the India jatropha oil HEFA pathway. The (net) total bar level in the land use change decomposition indicates the feedstock harvested area increase.

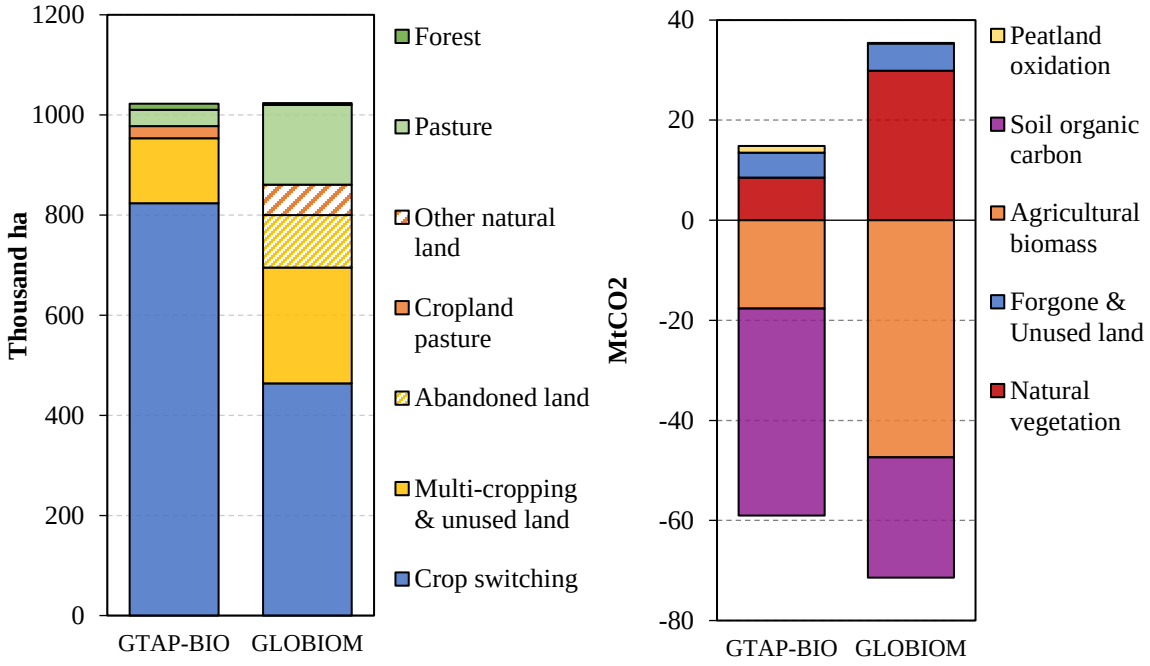

Figure 40. Land use change decomposition (left) and emission decomposition (right) for the India jatropha oil hydroprocessed esters and fatty acids (HEFA) pathway - Meal used as fertilizer or electricity input

For producing 45 PJ HEFA fuels, 1.15 Mt of jatropha oil are directly needed. This needs an increase in production of jatropha seed by 3.28 Mt, which requires an expansion in land under jatropha cultivation by 1.02 Mha in India. However, conversion of jatropha seeds to HEFA fuels generates about 0.91 Mt of jatropha meal, which will be used as fertilizer or for electricity generation.

In GTAP-BIO, the shock of the jatropha oil HEFA produced in India led to an expansion in harvested area of jatropha in this country of 1.02 Mha, as mentioned above. The decomposition of land area changes indicates that crop switching (0.82 Mha) played the most important role in supplying Jatropha. Cropland pasture accounts for 0.02 Mha and multi-cropping and unused cropland provides 0.13 Mha with the rest provided by small changes in forest and pasture. According to the GTAP-BIO results, these changes jointly lead to a land use emissions decrease by 44.2 $MtCO_2$, distributed mainly between agricultural biomass and soil organic carbon, as shown the right panel of Figure 40 on the GTAP-BIO bar. In GLOBIOM, the India jatropha harvested area increased by 1.02 Mha due to the Jatropha HEFA shock, of which 0.46 Mha was

from crop switching, 0.23 Mha from multi-cropping, 0.16 Mha was from grassland, 0.10 Mha was from abandoned land, and 0.07 Mha was from forest and other natural land.

India jatropha oil hydroprocessed esters and fatty acids (HEFA) - Meal used as animal feed after detoxification

The 25-year ILUC emission intensity for the India jatropha oil hydroprocessed esters and fatty acids (HEFA) pathway is -41.9 g CO_2e/MJ from GTAP-BIO and -52.6 g CO_2e/MJ from GLOBIOM, if meal coproducts are used as animal feed after detoxification. Figure 41 compares the global land use change decomposition and emission decomposition between the two models for the India jatropha oil HEFA pathway. The (net) total bar level in the land use change decomposition indicates the feedstock harvested area increase.

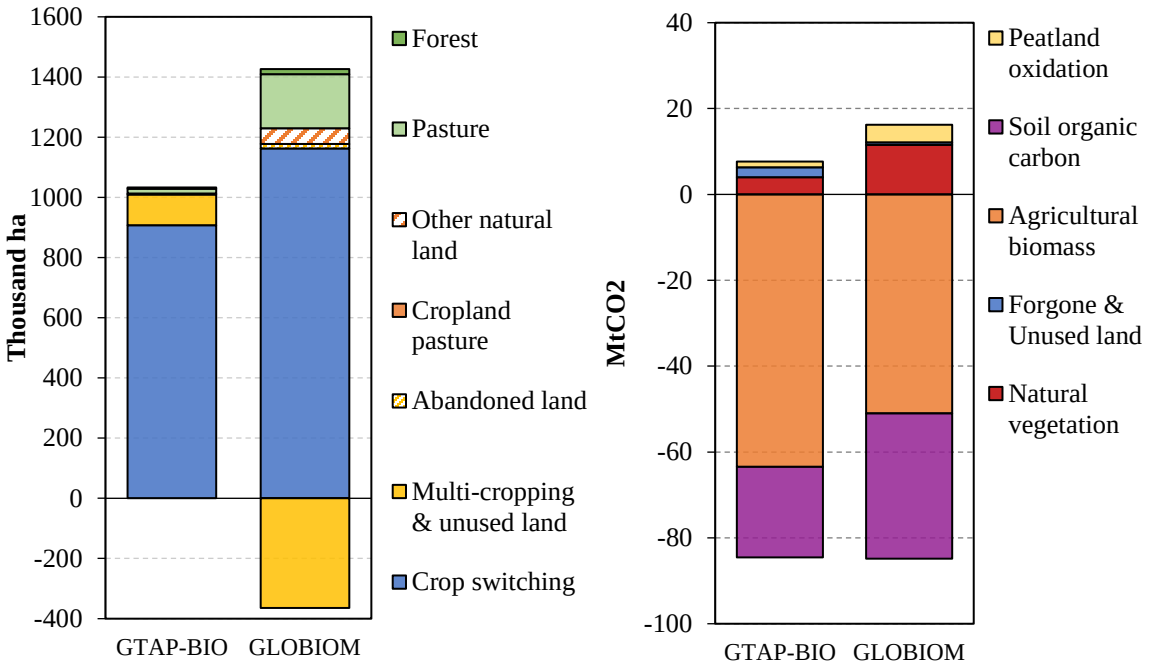

Figure 41. Land use change decomposition (left) and emission decomposition (right) for the India jatropha oil hydroprocessed esters and fatty acids (HEFA) pathway, if meal used as animal feed after detoxification

For producing 45 PJ HEFA fuels, 1.15 Mt of jatropha oil are directly needed. This needs an expansion in production of jatropha by 3.28 Mt of jatropha seed which requires an expansion in land under jatropha cultivation by 1.03 Mha in India. However, conversion of produced jatropha to HEFA fuels generates about 0.72 Mt of detoxicated jatropha meal, which will be used in animal feed rations. The substitution of jatropha meal, indirectly affects production of other crops used in animal feed rations. The indirect changes in crop production induced by the substitution in animal feed items generate some savings in cropland, which eventually leads to changes in other land covers. In GTAP-BIO, the decomposition of land area changes indicates that there is a reduction in other crop areas or crop switching (0.91 Mha). Multi-cropping and unused cropland provide 0.10 Mha with the rest provided by small changes in forest and pasture. According to the GTAP-BIO results, these changes jointly generate some land use emissions savings by 76.9 $MtCO_2$, distributed mainly between soil agricultural biomass and soil organic carbon as shown the right panel of Figure 41 on the GTAP-BIO bar. In GLOBIOM, the India jatropha harvested area increased by 1.06 Mha due to the Jatropha HEFA shock, of which 1.16 Mha was from crop switching, -0.36 Mha from a reduction in multi-cropping due to soybean production systems contraction, 0.18 Mha was from grassland, 0.05 Mha was from other natural land, and 0.03 Mha was from forest or abandoned land.

5.3 **GLOBAL ILUC VALUES**

Global default values have been developed to complement regional ILUC, such that potential SAF eligibility could be examined in all world regions. These global default ILUC values are based on simulations from GTAP-BIO and GLOBIOM, where equal shock sizes are applied across regions, independently from their share in the global production of each feedstock. For this method, the selection of the regions to be shocked was determined based on feedstock availability and the presence of biofuel policies. The shock applied to the selected regions was 0.25 Billion Gallon Gasoline Equivalent (BGGE) (30.2 PJ) of SAF demand. Table 106 and Table 107 display the regions selected for the global ILUC value simulation of each pathway and their corresponding shock sizes.

Table 106: Region selection for each feedstock for global default ILUC values

Region	Corn	Rapeseed	Soybean	Palm oil*	Sugarcane	Sugar beet	Carinata	Camelina	Miscanthus	Switchgrass	Poplar
USA	•		•			•	•	•	•	•	•
CAN		•					•	•			
BRA	•		•		•		•	•	•	•	•
CAC					•						
RSAM	•		•		•		•	•			
EU27	•	•				•	•	•	•	•	•
EECI	•	•				•					
MENA						•					
SSA					•						
IND					•						
RSA					•						
CHN					•	•					
IDMY											
JPN											
RAS					•						
OCE		•									

USA = United States of America, CAN = Canada, BRA = Brazil, CAC = Central America and Caribbean, RSAM = Rest of South America, EU27 = European Union, EECI = Rest of Europe and Commonwealth of Independent States, MENA = Middle East and North Africa, SSA = Sub-Saharan Africa, IND = India, RSA = Rest of South Asia, CHN = China, IDMY = Indonesia and Malaysia, JPN = Japan, RAS = Rest of Asia, OCE = Oceania.

* Palm oil HEFA is not modelled with a global default ILUC value.

Table 107: Shocks size used for modelling of global ILUC values

Pathways and targeted regions		Jet	Road	Total	Jet	Road	Total
Biojet pathways	Regions targeted in the global shock	PJ	PJ	PJ	BGGE	BGGE	BGGE
Corn ATJ-SPK from isobutanol	USA, BRA, RSAM, EU27, EECI	151	0	151	1.25	0.00	1.25

Corn ATJ-SPK from ethanol	USA, BRA, RSAM, EU27, EECI	151	47	198	1.25	0.39	1.64
Rapeseed HEFA	CAN, EU27, EECI, OCE	121	363	484	1.00	3.00	4.00
Soybean HEFA	USA, BRA, RSAM	91	272	363	0.75	2.25	3.00
Sugarcane ATJ-SPK from isobutanol	BRA, CAN, RSAM, SSA, IND, RSA, CHN, RAS	242	33	275	2.00	0.27	2.27
Sugarcane ATJ-SPK from ethanol	BRA, CAN, RSAM, SSA, IND, RSA, CHN, RAS	242	151	393	2.00	1.25	3.25
Sugarcane SIP	BRA, CAN, RSAM, SSA, IND, RSA, CHN, RAS	242	0	242	2.00	0.00	2.00
Sugar beet SIP	USA, EU27, EECI, MENA, CHN	151	0	151	1.25	0.00	1.25
Carinata HEFA	USA, CAN, BRA, RSAM, EU27	151	454	605	1.25	3.75	5.00
Camelina HEFA	USA, CAN, BRA, RSAM, EU27	151	454	605	1.25	3.75	5.00
Miscanthus FTJ	USA, BRA, EU27	91	272	363	0.75	2.25	3.00
Miscanthus ATJ-SPK from isobutanol	USA, BRA, EU27	91	0	91	0.75	0.00	0.75
Miscanthus ATJ-SPK from ethanol	USA, BRA, EU27	91	31	122	0.75	0.26	1.01
Switchgrass FT	USA, BRA, EU27	91	272	363	0.75	2.25	3.00
Switchgrass ATJ-SPK from isobutanol	USA, BRA, EU27	91	0	91	0.75	0.00	0.75
Switchgrass ATJ-SPK from ethanol	USA, BRA, EU27	91	31	122	0.75	0.26	1.01
Poplar FT	USA, BRA, EU27	91	272	363	0.75	2.25	3.00

*USA = United States of America, CAN = Canada, BRA = Brazil, CAC = Central America and Caribbean, RSAM = Rest of South America, EU27 = European Union, EECI = Rest of Europe and Commonwealth of Independent States, MENA = Middle East and North Africa, SSA = Sub-Saharan Africa, IND = India, RSA = Rest of South Asia, CHN = China, IDMY = Indonesia and Malaysia, JPN = Japan, RAS = Rest of Asia, OCE = Oceania.

The global default and regional ILUC estimates are available in Table 108. For 12 pathways out of 19, the difference in model results is lower than 8.9 gCO_2/MJ and the reconciled value is computed as a simple average. For the seven remaining pathways, the difference between the two models is larger than 8.9 gCO_2/MJ and the reconciled values is based on the lowest value of the two models' results plus 4.45 gCO_2/MJ. It is noteworthy however that the largest ILUC value modelled remains within the 8.9 gCO_2/MJ margin around the reconciled value for most pathways. Only three escape that rule: soybean oil HEFA (62.3 gCO_2/MJ higher for GLOBIOM), sugar cane SIP (15.7 gCO_2/MJ higher for GTAP-BIO) and miscanthus ATJ-SPK from isobutanol (9.7 gCO_2/MJ higher for GLOBIOM). The large difference between the two models for soybean oil HEFA was already noted in the regional ILUC values and extensively discussed by CAEP. The other deviations are lower and do not question feedstock eligibility, therefore they appear less critical.

Table 108: Default regional ILUC values and global ILUC values (gCO_2e/MJ)

Pathway	Regional ILUC values				Global default ILUC values		
	USA	EU	Brazil	IDN MYS	GTAP-BIO	GLOBIOM	Reconciled
Soy oil HEFA	24.5		27.0		21.3	88.1	25.8
Corn ATJ-SPK from isobutanol	22.1				37.7	25.2	29.7
Corn ATJ-SPK from ethanol	25.1				40.7	30.4	34.9
Rapeseed oil HEFA		24.1			24.1	27.8	26.0
Palm oil HEFA				39.1	-	-	-
Sugarcane ATJ-SPK from isobutanol			7.3		11.4	6.8	9.1
Sugarcane ATJ-SPK from ethanol			8.7		16.8	4.0	8.5
Sugarcane SIP			11.3		26.8	6.6	11.1
Molasses ATJ-SPK from isobutanol			7.3		11.4	6.8	9.1
Sugar beet SIP		20.2			13.0	9.5	11.2
Carinata HEFA	-21.4		-20.4		-9.8	-15.5	-12.7
Camelina HEFA					-11.4	-15.4	-13.4
Miscanthus FTJ	-32.9	-22.0			-16.7	-8.5	-12.6
Miscanthus ATJ-SPK from isobutanol	-54.1	-31.0			-28.0	-13.8	-23.6
Miscanthus ATJ-SPK from ethanol	-42.6	-23.3			-23.4	-11.0	-19.0
Switchgrass FTJ	-3.8				5.3	5.2	5.3
Switchgrass ATJ-SPK from isobutanol	-14.5				3.1	7.7	5.4
Switchgrass ATJ-SPK from ethanol	-10.7				3.7	5.9	4.8
Poplar FTJ	-5.2				11.4	5.8	8.6

Comparing global default and regional default ILUC values, one can see that most global default values are conservative, in the sense that they are higher than the regional ILUC values. Only three pathways are in a different configuration: sugarcane ATJ-SPK from ethanol, sugarcane SIP and sugar beet SIP. For these two sugarcane pathways, the difference between default ILUC value is however minor, with the regional value for Brazil being only 0.2 gCO_2/MJ larger than the global value. For sugar beet SIP, the difference is larger, with the regional value for the EU being 9 gCO_2/MJ larger than the global value.

Not all pathways are suited for receiving a global default value. Specifically, in the case of palm oil HEFA, the specificity of palm plantations and the impact of their expansion on ecosystems needed additional scrutiny on a region-by-region basis. This pathway is the only one without a global ILUC value.

Table 109 provides the ILUC results expressed in units normalized by the quantity of feedstock produced. These data complement usual ILUC values expressed in gCO_2/MJ as provided in Table 108. This metric provides more additional information that could aid in the evaluation of new SAF pathways and/or other energy uses.

Table 109: ILUC values for reconciled model results per unit of feedstock

Pathway	Feedstock unit of reference	Final energy content of feedstock [MJ/t]	Share of liquid fuel [%]	Regional ILUC values (CAEP 11) [kg CO_2e/t feedstock]				Global ILUC values (CAEP 12) [kg CO_2e/t feedstock]
				USA	EU	Brazil	IDN-MYS	
Soy oil HEFA	veg. oil	37,778	100	925.6		1,020.0		974.7
Corn ATJ-SPK from isobutanol	corn*	7,233	100	159.8				214.8
Corn ATJ-SPK from ethanol	corn*	6,511	100	163.4				227.2
Rapeseed oil HEFA	veg. oil	38,087	100		917.9			990.3
Palm oil HEFA	veg. oil	37,778	100				1,477.1	
Sugarcane ATJ-SPK from isobutanol	sugarcane	2,062	84.9			15.1		18.8
Sugarcane ATJ-SPK from ethanol	sugarcane	1,708	76.9			14.9		14.5
Sugarcane SIP	sugarcane	1,041	82.0			11.8		11.6
Sugar beet SIP	sugar beet	2,319	52.9		46.8			26.1
Molasses ATJ-SPK from isobutanol	sugarcane	2,062	84.9			15.1		18.8
Carinata HEFA	veg. oil	37,888	100	-810.8		-772.9		-481.2
Camelina HEFA	veg. oil	37,888	100					-507.7
Miscanthus FTJ	dry crop	8,117	100	-267.1	-178.6			-102.3
Miscanthus ATJ-SPK from isobutanol	dry crop	5,752	100	-311.2	-178.3			-135.7
Miscanthus ATJ-SPK from ethanol[#]	dry crop	7,154	100	-304.8	-166.7			-135.9
Switchgrass FTJ	dry crop	8,400	100	-31.9				44.5
Switchgrass ATJ-SPK from isobutanol	dry crop	5,441	100	-78.9				29.4
Switchgrass ATJ-SPK from ethanol	dry crop	7,154	100	-76.5				34.3
Poplar FTJ	dry crop	8,982	100	-46.7				77.2

* The ILUC value of corn includes here the feedback of coproducts.

Detailed results on land use changes and their corresponding emissions are provided in the sections hereafter for the global values.

5.3.1 GLOBAL SOY OIL HYDROPROCESSED ESTERS AND FATTY ACIDS (HEFA)

The 25-year ILUC emission intensity for the global soy oil hydroprocessed esters and fatty acids (HEFA) pathway is 21.3 g CO_2e/MJ from GTAP-BIO and 88.1 g CO_2e/MJ from GLOBIOM. Figure 42 compares the global land use change decomposition and emission decomposition between the two models for the global soy oil HEFA pathway. The (net) total bar level in the land use change decomposition indicates the feedstock harvested area increase.

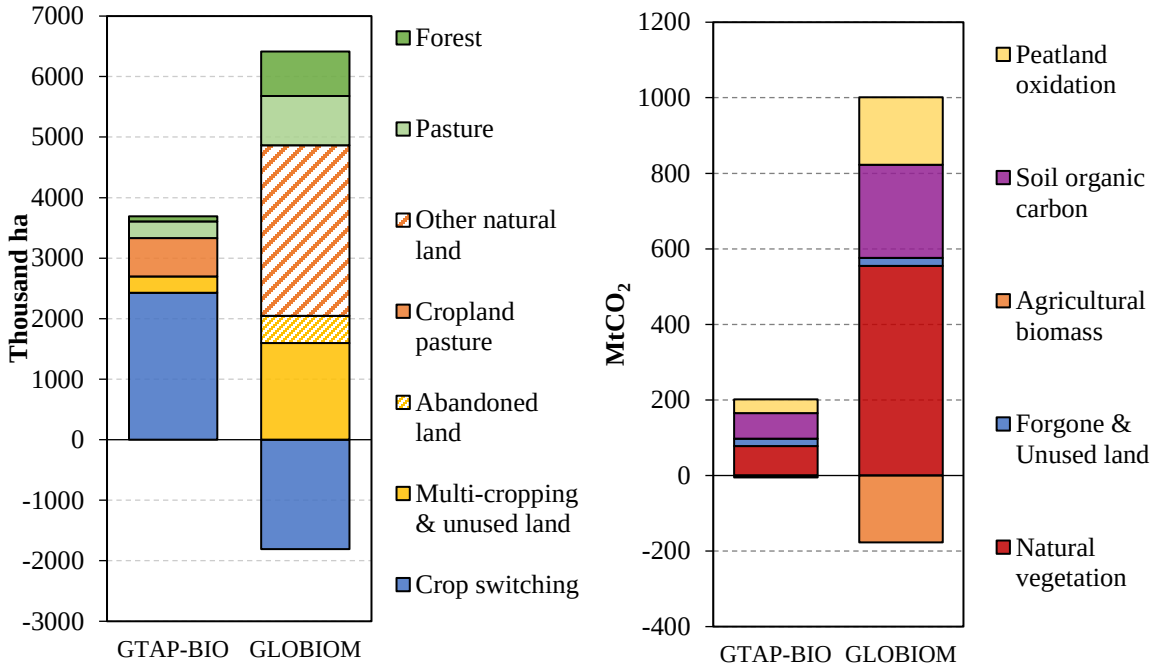

Figure 42. Land use change decomposition (left) and emission decomposition (right) for the global soy oil hydroprocessed esters and fatty acids (HEFA) pathway

For producing 363 PJ HEFA fuels, 9.6 Mt of soy oil are directly needed. Driven by the increased soy oil demand, GTAP-BIO projected the global soybeans production would increase by 14.0 Mt, and the increase would be mainly produced in the shocked regions. GLOBIOM estimated 15.1 Mt global soybeans increase, all produced in the shocked regions. For crushing soybeans, the crushing rate is about 19 % (by weight) for soy oil and 80% for soy meal. The coproduced soymeal enters livestock sectors as feedstuff to provide protein source. In both models, in addition to the newly crushed soy oil, substitutions among vegetable oils and a decrease in vegetable oil consumption played important roles in supplying the soy oil feedstock.

In GTAP-BIO, the shock of the soy HEFA led to 3.69 Mha increase in global soybean harvested area. The decomposition indicates that crop switching (2.43 Mha) played the most important role in supplying soybeans. Cropland pasture accounts for 0.64 Mha and multi-cropping and unused cropland provides 0.27 Mha with the rest provided by forest and pasture. In GLOBIOM, the global soybeans harvested area increased by 4.61 Mha due to the HEFA shock, of which 2.82 Mha was from other natural land or abandoned land, 1.60 Mha was from multi-cropping, and 1.55 Mha was from pasture and forest. Note that, unlike GTAP-BIO, GLOBIOM projected area expansion for other crops (1.81 Mha), so that crop switching played a negative role globally in supplying soybean area. This difference was driven by the significantly stronger livestock rebound effect in GLOBIOM. Those factors that explains the difference between the results of GTAP-BIO and GLOBIOM for soy oil HEFA applies to the corresponding global values as well (see section 5.8 for detail).

5.3.2 GLOBAL CORN ATJ-SPK FROM ISOBUTANOL

The 25-year ILUC emission intensity for the global corn ATJ-SPK from isobutanol pathway is 37.7 g CO_2e/MJ from GTAP-BIO and 25.2 g CO_2e/MJ from GLOBIOM. The two models also represent relatively different land use changes due various factors. Figure 43 compares the global land use change decomposition and emission decomposition between the two models for the global corn ATJ pathway. The (net) total bar level in the land use change decomposition indicates the feedstock harvested area increase, which is a reflection of crop yield, technology conversion yield, meal coproduct substitution, and other market-mediated responses.

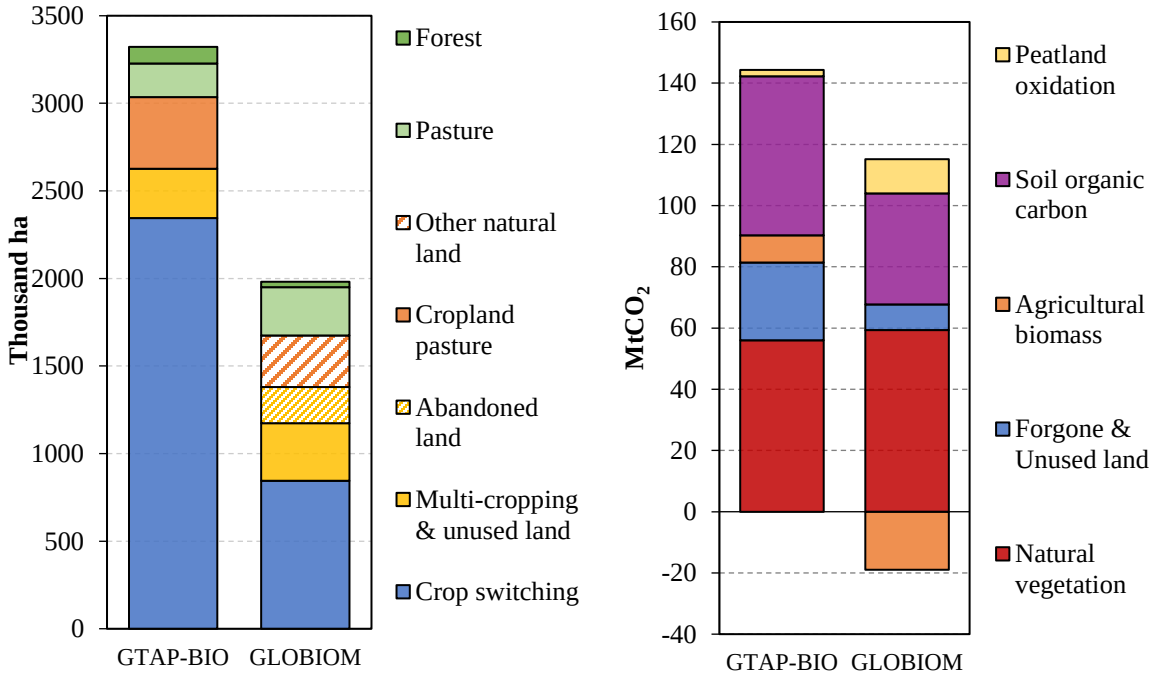

Figure 43. Land use change decomposition (left) and emission decomposition (right) for the global corn alcohol (isobutanol) to jet pathway

For producing 151 PJ ATJ-SPK from isobutanol fuels, 20.9 million tons (Mt) of corn are directly needed, while 6.4 Mt DDGS would be coproduced for substituting corn or other feed crops in livestock sectors. GTAP-BIO projected the global corn production would increase by 16.8 Mt, and most of the increase would be grown in the shocked regions. GLOBIOM estimated 13.0 Mt of global corn increase, mostly from the shocked regions. The corn demand responses and the DDGS displacement pattern are the two drivers to the difference in the total corn production.

In GTAP-BIO, the shock of the global corn ATJ-SPK from isobutanol led to 3.32 Mha increase in the global coarse grains harvested area. The decomposition indicates that there is strong decrease in other crop areas or crop switching (2.34 Mha). Cropland pasture accounts for 0.41 Mha and multi-cropping and unused cropland provides 0.28 Mha with the rest provided by forest and pasture. In GLOBIOM, the global corn harvested area increased by 1.98 Mha due to the global ATJ-SPK from isobutanol shock, of which 0.84 Mha was from crop switching, 0.33 Mha was from multi-cropping, 0.29 Mha was from other natural land or abandoned land, and 0.31 Mha was from pasture (0.28 Mha) and forest. GLOBIOM has stronger yield response for corn compared with GTAP-BIO, which partly explains the much smaller corn area increase in GLOBIOM.

Crop switching plays the most important role in supplying corn area in GTAP-BIO. This was because the coproduced DDGS also displaced other feed crops so that land originally growing those crops were

converted to growing corn. In GLOBIOM, DDGS displaced relatively less other feed crops but more corn, which explains the smaller crop switching and smaller total crop production increase. Both GTAP-BIO and GLOBIOM estimated little land conversion from forest and pasture due to global shock for this pathway.

The total emissions from natural vegetation are comparable between the two models (59-56 $MtCO_2$). GLOBIOM results showed smaller emission from SOC (36 vs. 52 $MtCO_2$) compared with GTAP-BIO, similarly smaller emissions from foregone sequestration and larger agricultural biomass carbon sequestration. The higher crop yield and smaller shares of crop switching in area supply in GLOBIOM are main reasons for the larger agricultural biomass carbon sequestration. As a result, the total emissions from GTAP-BIO (144 $MtCO_2$) is larger than the total emissions from GLOBIOM (96 $MtCO_2$). Overall, the drivers to the results difference between the two models may include the coproduct (DDGS) displacement, corn yield responses, and land category and associated emission factors.

5.3.3 GLOBAL CORN ATJ-SPK FROM ETHANOL

The 25-year ILUC emission intensity for the global corn ATJ-SPK from isobutanol (isobutanol) pathway is 40.7 g CO_2e/MJ from GTAP-BIO and 30.4 g CO_2e/MJ from GLOBIOM. Figure 44 compares the global land use change decomposition and emission decomposition between the two models for the global corn ATJ-SPK from ethanol pathway. These decomposition results followed the same pattern with the results from the global corn ATJ-SPK from isobutanol pathway, since the only major difference between the two pathways was that the global corn ATJ-SPK from ethanol pathway has lower technology conversion yield.

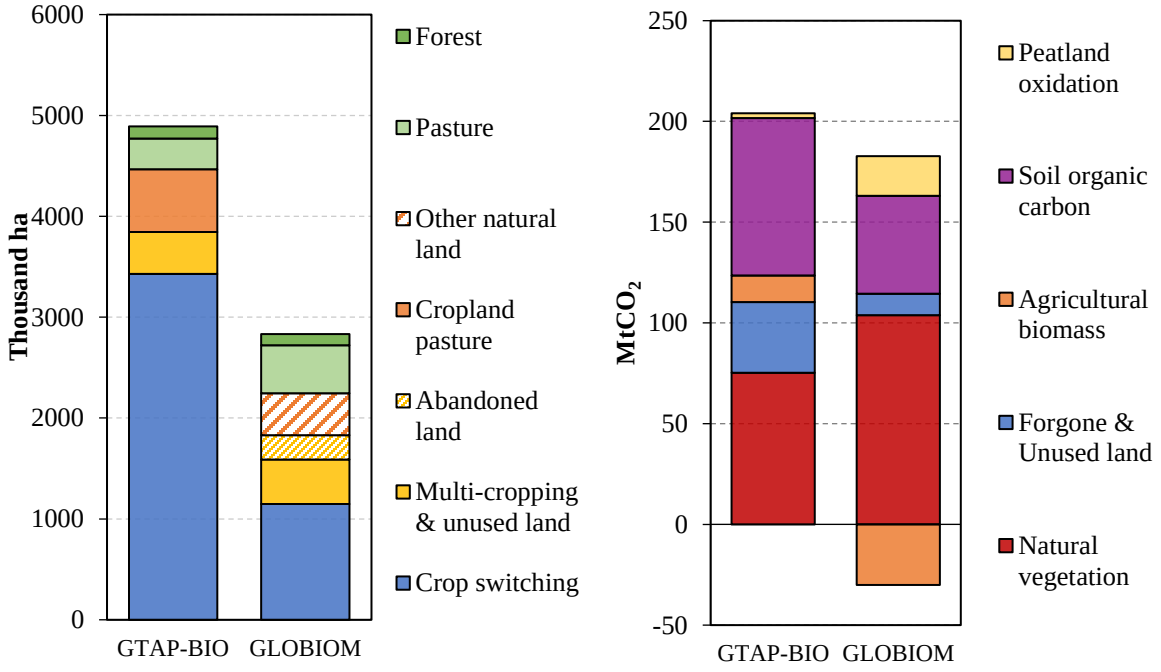

Figure 44. Land use change decomposition (left) and emission decomposition (right) for the global corn alcohol (ethanol) to jet pathway

For producing 198 PJ ATJ-SPK from ethanol fuels, 30.4 million tons (Mt) of corn are directly needed, while 8.9 Mt DDGS would be coproduced for substituting corn or other feed crops in livestock sectors. GTAP-BIO projected the global corn production would increase by 24.7 Mt, and 97% of the increase would be grown in the shocked regions. GLOBIOM estimated 19.0 Mt of global corn increase, mostly from the shocked regions.

In GTAP-BIO, the shock of the global corn ATJ-SPK from isobutanol led to 4.89 Mha increase in the global coarse grains harvested area. The decomposition indicates that there is strong decrease in other crop areas or crop switching (3.43 Mha). Cropland pasture accounts for 0.62 Mha and multi-cropping and unused cropland provides 0.41 Mha with the rest provided by forest and pasture. In GLOBIOM, the global corn harvested area increased by 2.83 Mha due to the global ATJ-SPK from isobutanol shock, of which 1.15 Mha was from crop switching, 0.44 Mha was from multi-cropping, 0.41 Mha was from other natural land or abandoned land, and 0.59 Mha was from pasture (0.47 Mha) and forest.

GLOBIOM results showed larger emission from natural vegetation (104 vs. 75 $MtCO_2$) and peatland oxidation (20 vs. 2 $MtCO_2$). But the difference was compensated by lower emissions from SOC (49 vs. 78 $MtCO_2$) and foregone sequestration (11 vs. 35 $MtCO_2$) and GLOBIOM's larger agricultural biomass carbon sequestration. Overall, the total emissions from GTAP-BIO (204 $MtCO_2$) is larger than GLOBIOM (153 $MtCO_2$).

5.3.4 GLOBAL RAPESEED OIL HYDROPROCESSED ESTERS AND FATTY ACIDS (HEFA)

The 25-year ILUC emission intensity for the global rapeseed oil hydroprocessed esters and fatty acids (HEFA) pathway is 24.1 g CO_2e/MJ from GTAP-BIO and 27.8 g CO_2e/MJ from GLOBIOM. Figure 45 compares the global land use change decomposition and emission decomposition between the two models for the global rapeseed oil HEFA pathway.

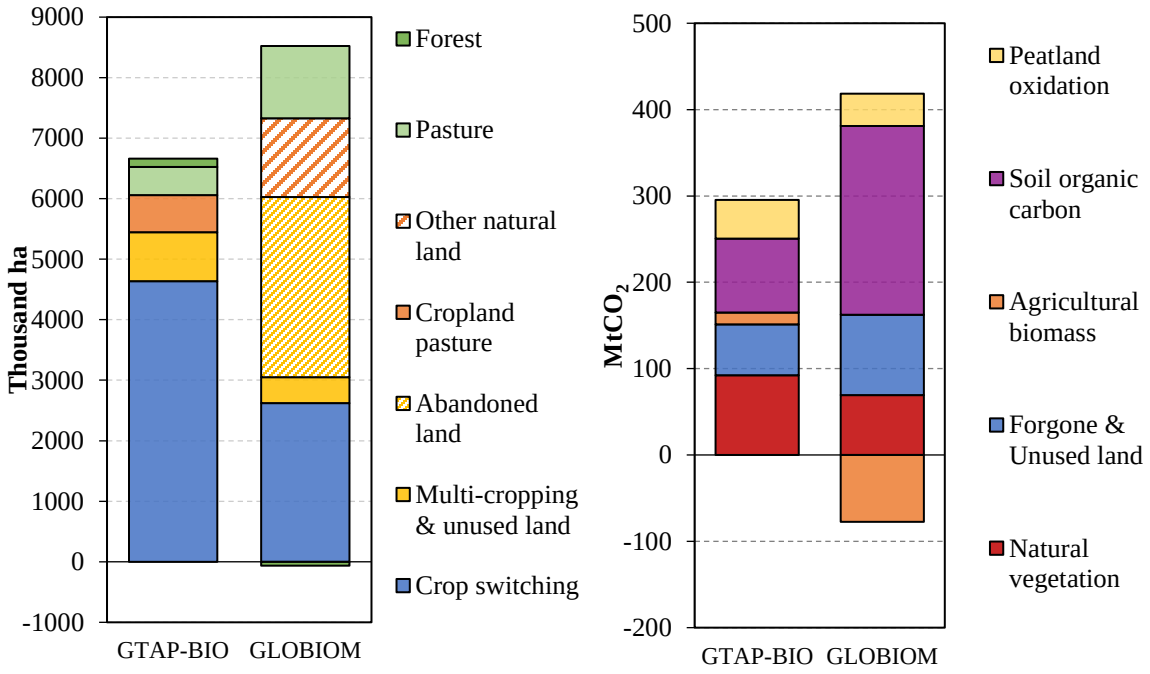

Figure 45. Land use change decomposition (left) and emission decomposition (right) for the global rapeseed oil hydroprocessed esters and fatty acids (HEFA) pathway

For producing 484 PJ HEFA fuels, 12.7 Mt of rapeseed oil are directly needed. Driven by the increased rapeseed oil demand, GTAP-BIO projected the global rapeseed production would increase by 12.3 Mt, and 94% of the increase would be produced in the shocked regions. GLOBIOM estimated 22.0 Mt of global rapeseed increase. The vegetable oil demand response is a major driver to the difference in rapeseed oil expansion. In GTAP-BIO, the HEFA global shock led to 6.66 Mha increase in the global rapeseed harvested area. The decomposition indicates that crop switching contributes 4.64 Mha. Cropland pasture accounts for 0.62 Mha and multi-cropping, and unused cropland provides 0.81 Mha with the rest provided by forest

(0.14 Mha) and pasture (0.46 Mha). In GLOBIOM, the global rapeseed harvested area increased by 8.46 Mha due to the global HEFA shock, of which 4.28 Mha was from other natural land and abandoned land, 0.43 Mha was from multi-cropping, and 1.19 Mha was from pasture. GLOBIOM projected 0.06 Mha area afforestation.

GTAP-BIO estimated lower emissions from foregone sequestration & unused land (59 vs. 93 $MtCO_2$) and SOC (86 vs. 219 $MtCO_2$) compared with GLOBIOM, corresponding to the higher land conversion from natural land and abandoned land. GLOBIOM had lower emissions from natural vegetation (69 vs. 92 $MtCO_2$), mainly because the afforestation projected for this shock. GLOBIOM estimated higher agricultural biomass carbon sequestration (-77 vs. 14 $MtCO_2$), because of the higher cropland expansion.

5.3.5 GLOBAL SUGARCANE AND MOLASSES ATJ-SPK FROM ISOBUTANOL

The 25-year ILUC emission intensity for the global sugarcane ATJ-SPK from isobutanol pathway is 11.4 g CO_2e/MJ from GTAP-BIO and 6.8 g CO_2e/MJ from GLOBIOM. Figure 46 compares the global land use change decomposition and emission decomposition between the two models for the global sugarcane ATJ-SPK from isobutanol pathway. The (net) total bar level in the land use change decomposition indicates the feedstock cultivated area increase, which is a reflection of crop yield, technology conversion yield, meal coproduct substitution, and other market-mediated responses.

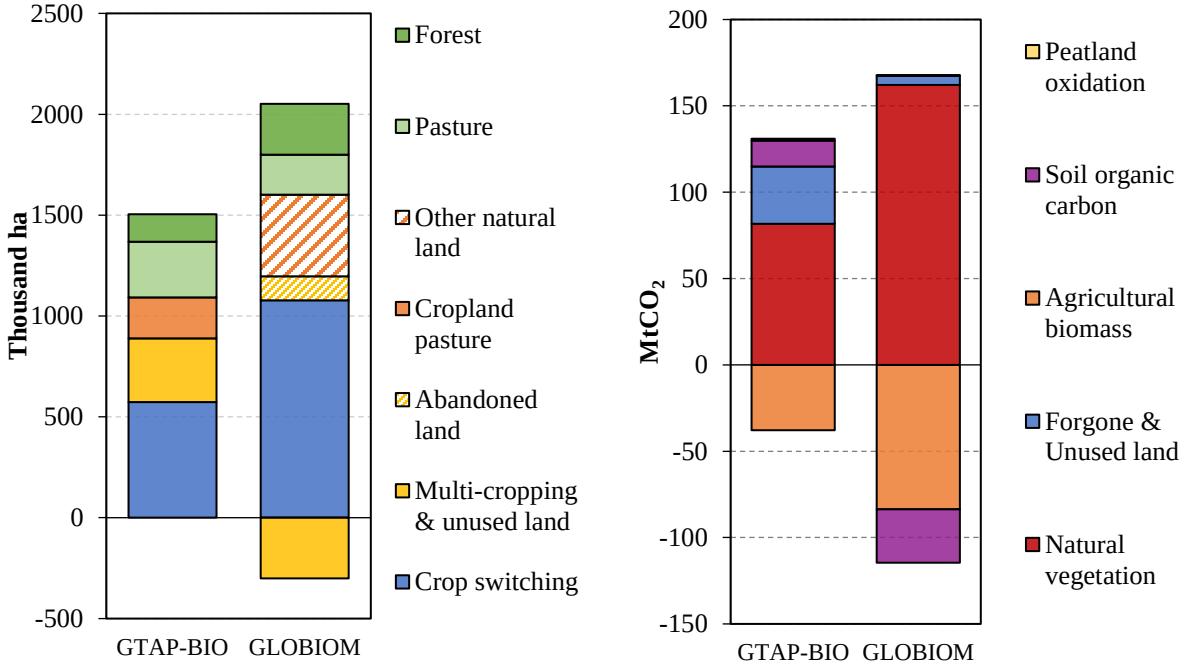

Figure 46. Land use change decomposition (left) and emission decomposition (right) for the global sugarcane alcohol (isobutanol) to jet pathway

For producing 275 PJ ATJ-SPK from isobutanol fuels, 157 Mt of sugarcane are directly needed. GTAP-BIO projected the global sugarcane production would increase by 119.3 Mt, and almost all of the new sugarcane would be grown in the shocked regions. GLOBIOM estimated 147.6 Mt of global sugarcane increase, from the same regions.

In GTAP-BIO, the shock of the global sugarcane ATJ-SPK from isobutanol led to 1.5 Mha increase in the global sugarcane harvested area. The decomposition indicates that the major land source for sugarcane expansion is cropland switching (0.57 Mha). Cropland pasture contributes by 0.2 Mha, and multi-cropping & unused cropland provides 0.32 Mha. There would also be 0.28 Mha decrease in global pasture area and

0.14 Mha deforestation. In GLOBIOM, the global sugarcane harvested area increased by 1.75 Mha due to the global ATJ-SPK from isobutanol shock, of which 1.08 Mha was from crop switching, 0.53 Mha was from other natural land and abandoned land, and 0.2 Mha was from pasture and 0.25 Mha from deforestation. The sugarcane yield responses and the demand responses are comparable between the two models so that the total feedstock production and area increases are close. However, as indicated, the land transformation pattern is slightly different between the two models for the pathway. Hence, both models estimated some land conversion from forest and pasture at the global scale for this global pathway.

For both models, the natural vegetation carbon change (81.6 $MtCO_2$ in GTAP-BIO and 162.1 $MtCO_2$ in GLOBIOM) dominates the total emissions change, mainly because of the cropland expansion into natural land). In both GTAP-BIO or GLOBIOM, sugarcane at the global scale was treated specially with higher soil organic carbon (SOC) since it is a perennial crop. However, the results imply higher total SOC sequestration in GLOBIOM (-30.6 $MtCO_2$) than in GTAP-BIO (14.9 $MtCO_2$). Both GTAP-BIO and GLOBIOM indicated strong carbon sequestration in agricultural biomass (-37.8 and -83.9 $MtCO_2$), mainly due to the high sugarcane biomass yield. There was little foregone sequestration in GLOBIOM results (5.2 $MtCO_2$) versus a more significant forgone sequestration projected form GTAP-BIO (33.3 $MtCO_2$). The emissions from peatland oxidation change were very small in both models for this global shock since the market-mediated impacts on palm oil production in Malaysia and Indonesia were negligible. As a result, the total emissions from GTAP-BIO (93.1 $MtCO_2$) and GLOBIOM (53.4 $MtCO_2$) were different.

Molasses is being accounted as a co-product, as described in Section 1.4.7 of this Supporting Document, even though the feedstock is not the largest part of sugarcane product output. In line with the core-LCA protocol, the feedstock requirement for molasses ATJ-SPK from isobutanol was assumed the same as for sugar cane ATJ-SPK from isobutanol; therefore, the same ILUC values for sugar cane ATJ-SPK from isobutanol are used for this pathway.

5.3.6 **GLOBAL SUGARCANE ATJ-SPK FROM ETHANOL**

The 25-year ILUC emission intensity for the global sugarcane ATJ-SPK from ethanol pathway is 16.8 g CO_2e/MJ from GTAP-BIO and 4.0 g CO_2e/MJ from GLOBIOM. Figure 47 compares the global land use change decomposition and emission decomposition between the two models for the global sugarcane ATJ-SPK from ethanol pathway. The (net) total bar level in the land use change decomposition indicates the feedstock cultivated area increase. These decomposition results followed the same pattern with the results from the global sugarcane ATJ-SPK from isobutanol pathway since the only major difference between the two pathways was that the global sugarcane ATJ-SPK from ethanol pathway has a lower technology conversion yield.

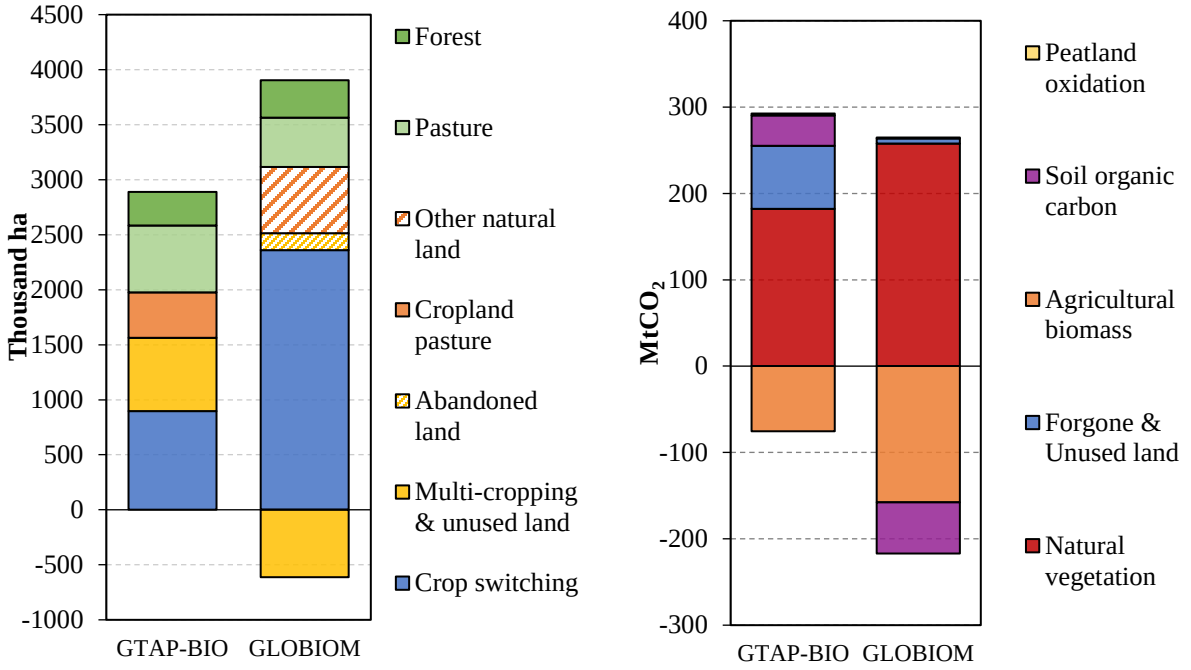

Figure 47. Land use change decomposition (left) and emission decomposition (right) for the global sugarcane alcohol (ethanol) to jet pathway

For producing 393 PJ ATJ-SPK from ethanol fuels, 298.9 Mt of sugarcane are directly needed. GTAP-BIO projected the global sugarcane production would increase by 227.6 Mt, almost all of which would be grown in the shocked regions. GLOBIOM estimated 279.4 Mt of global sugarcane increase from the same regions.

In GTAP-BIO, the shock of the global sugarcane ATJ-SPK from ethanol led to 2.89 Mha increase in the global sugarcane harvested area. The decomposition indicates that the major land source for sugarcane expansion is crop switching (0.9 Mha). Cropland pasture provides 0.41 Mha, and multi-cropping & unused cropland provides 0.67 Mha. There would also be 0.61 Mha decrease in global pasture and 0.31 Mha deforestation. In GLOBIOM, the global sugarcane harvested area increased by 3.29 Mha due to the global ATJ-SPK from ethanol shock, of which 2.36 Mha was from crop switching, 0.76 Mha was from other natural land and abandoned land, 0.45 Mha was from pasture, and 0.34 Mha from deforestation.

GLOBIOM results showed larger emission from natural vegetation (257.6 vs. 182.1 $MtCO_2$) and higher agricultural biomass sequestration (-157.9 vs. -75.6 $MtCO_2$) compared with GTAP-BIO. The total emissions from GTAP-BIO (217 $MtCO_2$) and GLOBIOM (47.9 $MtCO_2$) are very different.

5.3.7 GLOBAL SUGARCANE SYNTHESIZED ISO-PARAFFINS (SIP)

The 25-year ILUC emission intensity for the global sugarcane synthesized iso-paraffins (SIP) pathway is 26.8 g CO_2e/MJ from GTAP-BIO and 6.6 g CO_2e/MJ from GLOBIOM. Figure 48 compares the global land use change decomposition and emission decomposition between the two models for the global sugarcane SIP pathway. The (net) total bar level in the land use change decomposition indicates the feedstock cultivated area increase. These decomposition results followed the similar pattern with the results from the global sugarcane ATJ-SPK from isobutanol or ATJ-SPK from ethanol pathway.

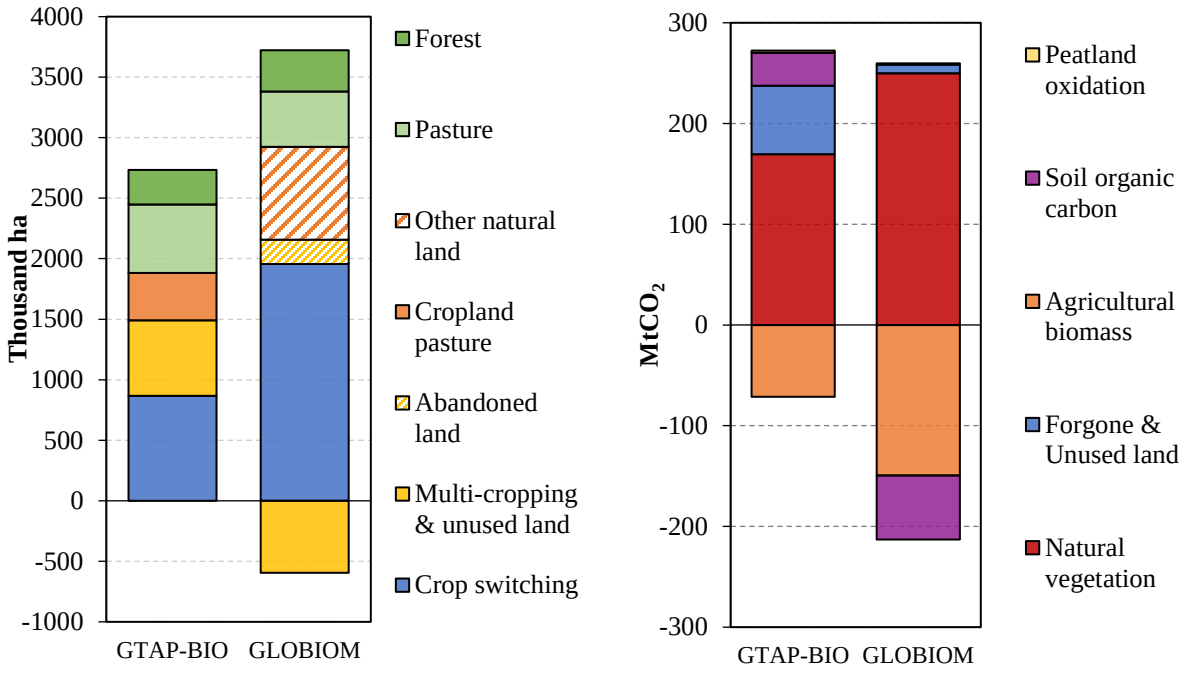

Figure 48. Land use change decomposition (left) and emission decomposition (right) for the global sugarcane synthesized iso-paraffins (SIP) pathway

For producing 242 PJ SIP fuels along with 53 PJ electricity, 283.5 Mt of sugarcane are directly needed. GTAP-BIO projected the global sugarcane production would increase by 215.6 Mt, almost all of which would be grown in the shocked regions. GLOBIOM estimated 264.9 Mt of global sugarcane increase from the same regions.

In GTAP-BIO, the global shock of sugarcane SIP led to 2.73 Mha increase in the global sugarcane harvested area. The decomposition indicates that the major land source for sugarcane expansion is crop switching (0.87 Mha). Cropland pasture provides 0.39 Mha, and multi-cropping & unused cropland provides 0.62 Mha. There would also be 0.57 Mha decrease in global pasture and 0.28 Mha deforestation. In GLOBIOM, the global sugarcane harvested area increased by 3.13 Mha due to the global SIP shock, of which 1.96 Mha was from crop switching, 0.97 Mha was from other natural land and abandoned land, and 0.458 Mha was from pasture and 0.34 Mha deforestation.

GLOBIOM results showed larger emission from natural vegetation (250 vs. 196.4 $MtCO_2$) and higher agricultural biomass sequestration (-149.6 vs. -71.3 $MtCO_2$) compared with GTAP-BIO. The total emissions are 201 $MtCO_2$ from GTAP-BIO and 46.8 $MtCO_2$ from GLOBIOM.

5.3.8 GLOBAL SUGAR BEET SYNTHESIZED ISO-PARAFFINS (SIP)

The 25-year ILUC emission intensity for the global sugar beet synthesized iso-paraffins (SIP) pathway is 13.0 g CO_2e/MJ from GTAP-BIO and 9.5 g CO_2e/MJ from GLOBIOM. Figure 49 compares the global land use change decomposition and emission decomposition between the two models for the global sugar beet SIP pathway. The (net) total bar level in the land use change decomposition indicates the sugar beet harvested area increase.

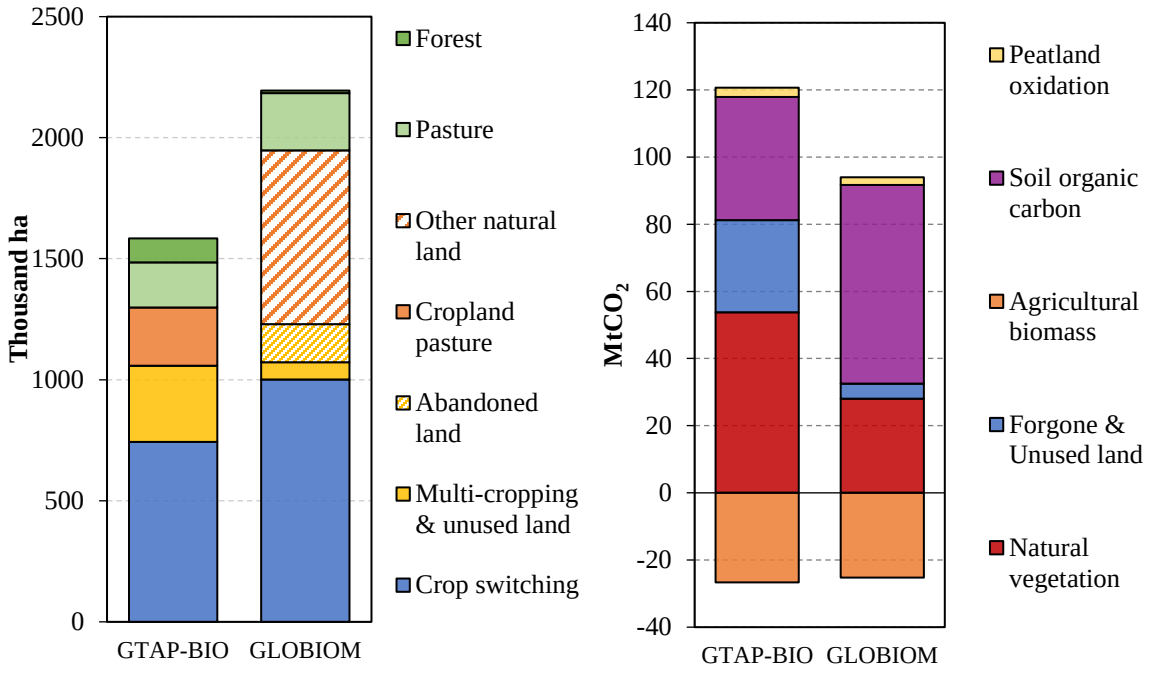

Figure 49. Land use change decomposition (left) and emission decomposition (right) for the global sugar beet synthesized iso-paraffins (SIP) pathway

For producing 151 PJ SIP fuels along with 134.5 PJ biogas, 123.2 Mt of sugar beet at 18% sugar content according to the corresponding core LCA assumption are directly needed. GTAP-BIO estimated the global sugar beet production would increase by 99.4 Mt, all of which would be produced in the shocked regions. GLOBIOM estimated 123.3 Mt global sugar beet increase, all of it cultivated in the targeted regions.

In GTAP-BIO, the global shock of sugar beet SIP led to 0.1.15 Mha increase in sugar beet harvested area. Globally, there would be 0.15 Mha decrease in forest and pasture. Crop switching (0.76 Mha) and multi-cropping & unused cropland (0.16 Mha) were major sources of area supply. Cropland pasture would also provide 0.09 Mha. In GLOBIOM, the global sugar beet harvested area increased by 2.2 Mha due to the SIP shock, which can be decomposed into 1.0 Mha from crop switching, 0.9 Mha from other natural land and abandoned land, and 0.2 Mha was from pasture and forest.

GLOBIOM results showed larger emission from SOC (59.2 vs. 36.7 $MtCO_2$) while GTAP-BIO had higher emissions from natural vegetation and converting unused land. The crop biomass carbon sequestrations were similar (-25.2 vs. -26.7 $MtCO_2$). The total emissions from GTAP-BIO (94 $MtCO_2$) and GLOBIOM (68.8 $MtCO_2$) are not very different.

5.3.9 GLOBAL MISCANTHUS FISCHER-TROPSCH JET FUEL (FTJ)

The 25-year ILUC emission intensity for the global miscanthus Fischer-Tropsch jet fuel (FTJ) pathway is -16.7 g CO_2e/MJ from GTAP-BIO and -8.5 g CO_2e/MJ from GLOBIOM. Figure 50 compares the global land use change decomposition and emission decomposition between the two models for the global miscanthus FTJ pathway. The (net) total bar level in the land use change decomposition indicates feedstock harvested area increase.

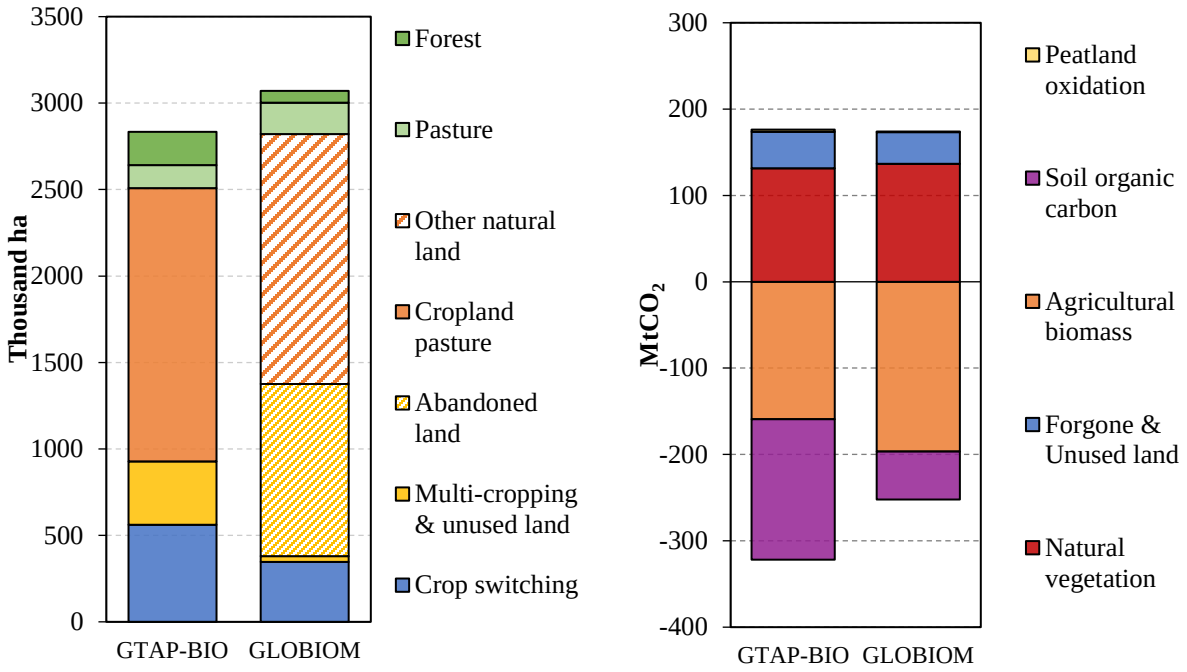

Figure 50. Land use change decomposition (left) and emission decomposition (right) for the global miscanthus Fischer-Tropsch jet fuel (FTJ) pathway

For producing 363 PJ FTJ fuels, 44.7Mt of miscanthus are directly needed. Since cellulosic crops are modelled as dedicated energy crop supplying only biofuels production in both GTAP-BIO and GLOBIOM and the technical conversion yields were reconciled, miscanthus production in both models would meet the direct requirement. There was a small difference in crop yield so that GTAP-BIO (2.83 Mha) used less land than GLOBIOM (3.07 Mha) for miscanthus production. Cropland pasture (1.58 Mha) is the major land source for miscanthus in GTAP-BIO, and crop switching also contributed 0.56 Mha. In GLOBIOM, other nature land (1.45 Mha) and abandoned land (1.0 Mha) are the major miscanthus land sources. The land sources for producing miscanthus and the associated emission factors are the drivers to the results difference between the two models.

Emission changes from natural vegetation (136.6 $MtCO_2$ of GLOBIOM vs. 131 $MtCO_2$ of GTAP-BIO) and agricultural biomass carbon sequestration (-196.5 $MtCO_2$ of GLOBIOM vs. -150 $MtCO_2$ of GTAP-BIO) are comparable for the global miscanthus FTJ pathway. GTAP-BIO had higher SOC sequestration (-162.7 vs. -55.8 $MtCO_2$) since it used generally higher emission (sequestration) factors for the miscanthus SOC compared with GLOBIOM. Driven by the high carbon sequestration in soil and crop, both models estimated negative ILUC emissions (-146.5 $MtCO_2$ for GTAP-BIO and -78.2 $MtCO_2$ from GLOBIOM).

5.3.10 GLOBAL MISCANTHUS ATJ-SPK FROM ISOBUTANOL

The 25-year ILUC emission intensity for the global miscanthus alcohol (isobutanol) to jet pathway is -28.0 g CO_2e/MJ from GTAP-BIO and -13.8 g CO_2e/MJ from GLOBIOM. Figure 51 compares the global land use change decomposition and emission decomposition between the two models for the global miscanthus ATJ-SPK from isobutanol pathway. The (net) total bar level in the land use change decomposition indicates feedstock harvested area increase. The land use change and emissions decomposition from this pathway have similar patterns to the global miscanthus FTJ pathway.

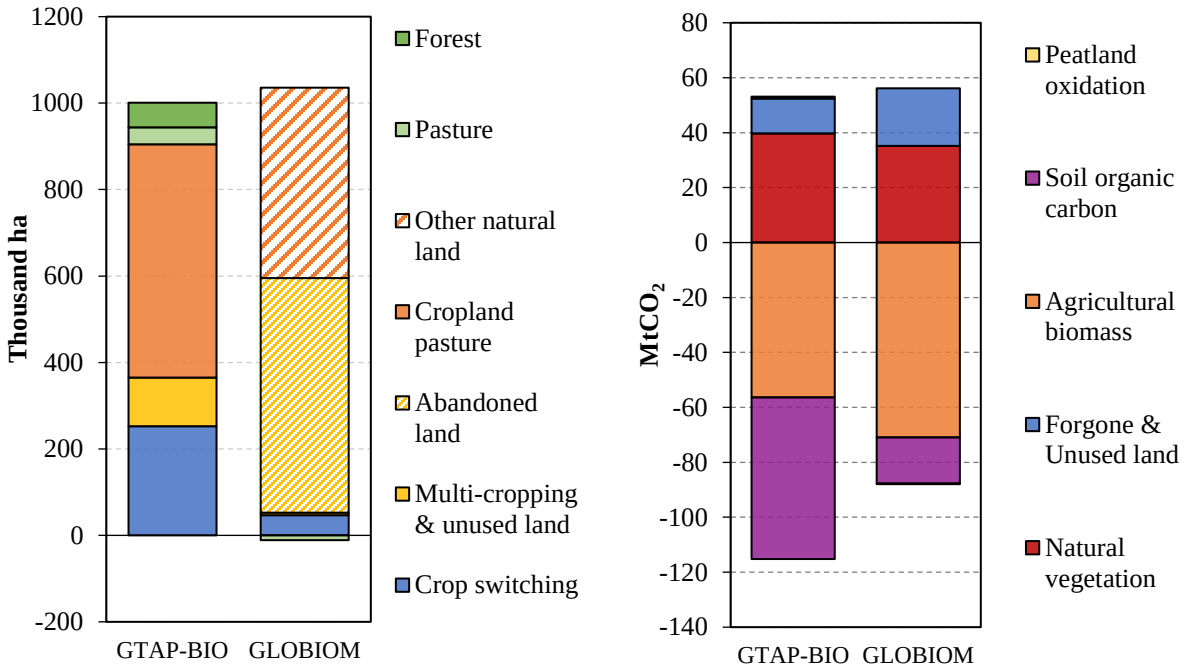

Figure 51. Land use change decomposition (left) and emission decomposition (right) for the global miscanthus ATJ-SPK from isobutanol pathway

For producing 91 PJ ATJ-SPK from isobutanol fuels, 15.80 Mt of miscanthus are directly needed. The miscanthus production in both models would meet the direct requirement since cellulosic crops are modelled as a dedicated energy crop. Cropland pasture (0.54 Mha) is the major land source for miscanthus in GTAP-BIO, and crop switching also contributed 0.25 Mha. In GLOBIOM, other nature land (0.44 Mha) and abandoned land (0.54 Mha) are the major miscanthus land sources. The land sources for producing miscanthus and the associated emission factors are the drivers to the results difference between the two models.

GTAP-BIO had higher SOC sequestration (-58.8 vs. -16.8 $MtCO_2$) since it used generally higher emission (sequestration) factors for the miscanthus SOC compared with GLOBIOM. Emission changes from natural vegetation (39.8 $MtCO_2$ of GTAP-BIO vs. 35.5 $MtCO_2$ of GLOBIOM), and agricultural biomass carbon sequestration (-56.4 $MtCO_2$ of GTAP-BIO vs. -70.9 $MtCO_2$ of GLOBIOM) are not very different. GTAP-BIO and GLOBIOM estimated 12.6 and 20.9 $MtCO_2$ foregone sequestration due to the use of abandoned land, respectively. Driven by the high carbon sequestration in soil and crop, both models estimated negative ILUC emissions (-62.0 $MtCO_2$ for GTAP-BIO and -31.8 $MtCO_2$ from GLOBIOM).

5.3.11 GLOBAL MISCANTHUS ATJ-SPK FROM ETHANOL

The 25-year ILUC emission intensity for the global miscanthus ATJ-SPK from ethanol pathway is -23.4 g CO_2e/MJ from GTAP-BIO and -11.0 g CO_2e/MJ from GLOBIOM. Figure 52 compares the global land use change decomposition and emission decomposition between the two models for the global miscanthus ATJ-SPK from ethanol pathway. The (net) total bar level in the land use change decomposition indicates feedstock harvested area increase. The land use change and emissions decomposition from this pathway have similar patterns to the global miscanthus FTJ or ATJ-SPK from isobutanol pathway.

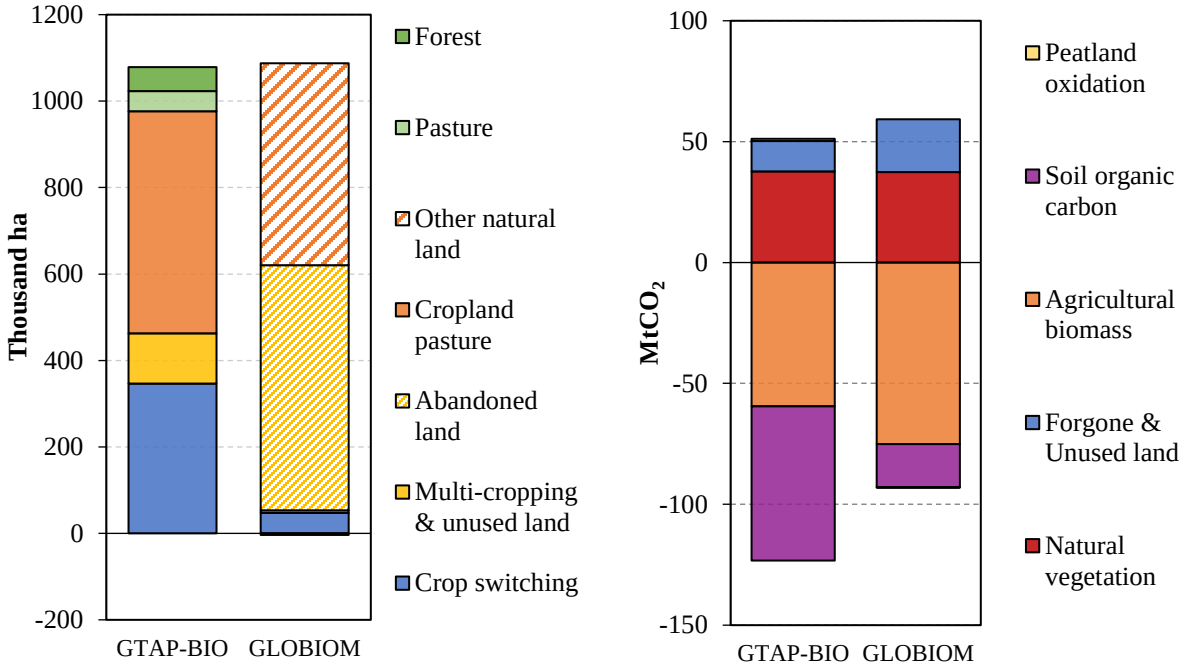

Figure 52. Land use change decomposition (left) and emission decomposition (right) for the global miscanthus ATJ-SPK from ethanol pathway

For producing 122 PJ ATJ-SPK from ethanol fuels, 17 Mt of miscanthus are directly needed. The miscanthus production in both models would meet the direct requirement since cellulosic crops are modelled as a dedicated energy crop.

Cropland pasture (0.51 Mha) is the major land source for miscanthus in GTAP-BIO, and crop switching also contributed 0.35 Mha. In GLOBIOM, other nature land (0.47 Mha) and abandoned land (0.57 Mha) are the major miscanthus land sources. The land sources for producing miscanthus and the associated emission factors are the drivers to the results difference between the two models.

GTAP-BIO had higher SOC sequestration (-162.7 vs. -55.8 $MtCO_2$) since it used generally higher emission (sequestration) factors for the miscanthus SOC compared with GLOBIOM. Emission changes from natural vegetation (131.6 $MtCO_2$ of GTAP-BIO vs. 136.6 $MtCO_2$ of GLOBIOM), and agricultural biomass carbon sequestration (-159 $MtCO_2$ of GTAP-BIO vs. 196.5 $MtCO_2$ of GLOBIOM) are not very different. GTAP-BIO and GLOBIOM estimated 41.9 $MtCO_2$ and 36.7 foregone sequestration. Driven by the high carbon sequestration in soil and crop, both models estimated negative ILUC emissions (-145.6 $MtCO_2$ for GTAP-BIO and -78.2 $MtCO_2$ from GLOBIOM).

5.3.12 GLOBAL SWITCHGRASS FISCHER-TROPSCH JET FUEL (FTJ)

The 25-year ILUC emission intensity for the global switchgrass Fischer-Tropsch jet fuel (FTJ) pathway is 5.3 g CO_2e/MJ from GTAP-BIO and 5.2 g CO_2e/MJ from GLOBIOM. Figure 53 compares the global land use change decomposition and emission decomposition between the two models for the global switchgrass FTJ pathway. The (net) total bar level in the land use change decomposition indicates feedstock harvested area increase. The land use change and emissions decomposition from this pathway have similar patterns to the global miscanthus FTJ pathway.

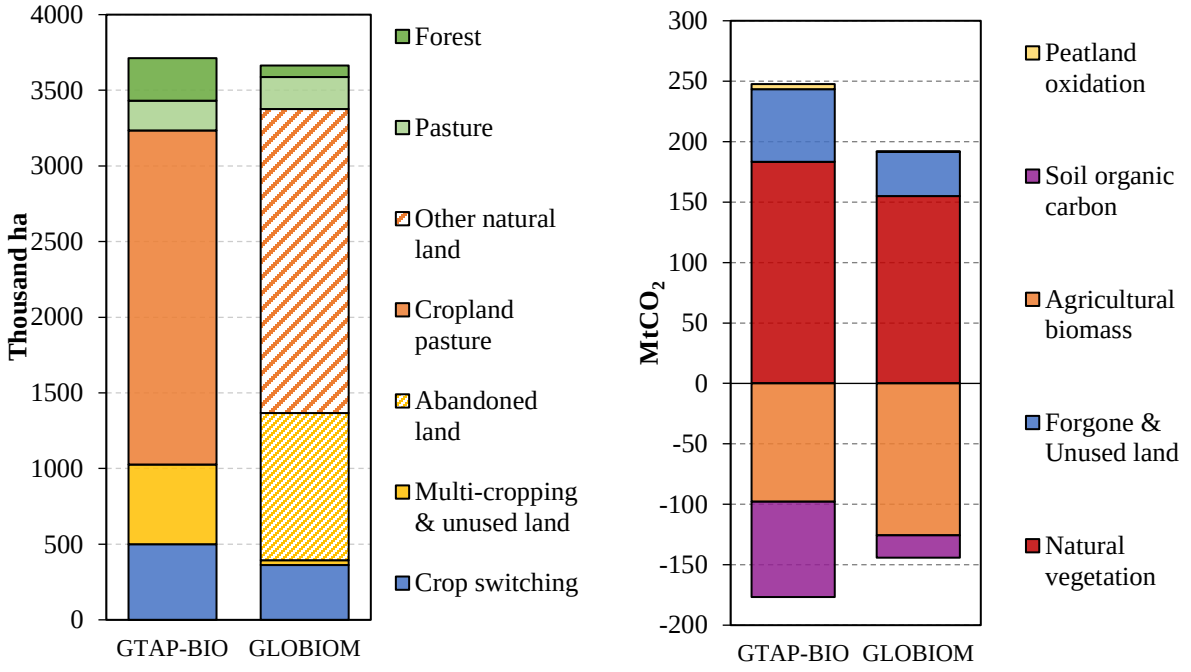

Figure 53. Land use change decomposition (left) and emission decomposition (right) for the global switchgrass Fischer-Tropsch jet fuel (FTJ) pathway

For producing 363 PJ FTJ fuels, 43.2 Mt of switchgrass are directly needed. The switchgrass production in both models would meet the direct requirement since cellulosic crops are modelled as a dedicated energy crop.

In GTAP-BIO, the total miscanthus harvested area increased by 3.71 Mha. Cropland pasture (2.21 Mha) is the major land source for switchgrass in GTAP-BIO, and crop switching also contributed 0.5 Mha. In GLOBIOM, the total miscanthus harvested area increased by 3.66 Mha. Other nature land (2.01 Mha) and abandoned land (0.97 Mha) are the major switchgrass land sources. The land sources for producing switchgrass and the associated emission factors are the drivers to the results difference between the two models.

GTAP-BIO had higher SOC sequestration (-78.9 vs. -18.6 $MtCO_2$) since it used generally higher emission (sequestration) factors for the switchgrass SOC compared with GLOBIOM. Emission changes from natural vegetation (188.3 $MtCO_2$ for GTAP-BIO and 155.1 $MtCO_2$ from GLOBIOM), and agricultural biomass carbon sequestration (-97.9 $MtCO_2$ for GTAP-BIO and -125.7 $MtCO_2$ from GLOBIOM) are not very different. GTAP-BIO and GLOBIOM estimated 60.2 $MtCO_2$ and 36.5 $MtCO_2$ foregone sequestration. Driven by the higher emissions due to natural vegetation, GTAP-BIO had significantly larger total ILUC emissions (70.9 $MtCO_2$ for GTAP-BIO and 46.6 $MtCO_2$ from GLOBIOM).

5.3.13 GLOBAL SWITCHGRASS ATJ-SPK FROM ISOBUTANOL

The 25-year ILUC emission intensity for the global switchgrass ATJ-SPK from isobutanol pathway is 3.1 g CO_2e/MJ from GTAP-BIO and 7.7 g CO_2e/MJ from GLOBIOM. Figure 54 compares the global land use change decomposition and emission decomposition between the two models for the global switchgrass ATJ-SPK from isobutanol pathway. The (net) total bar level in the land use change decomposition indicates feedstock harvested area increase. The land use change and emissions decomposition from this pathway have similar patterns to the global switchgrass FTJ pathway.

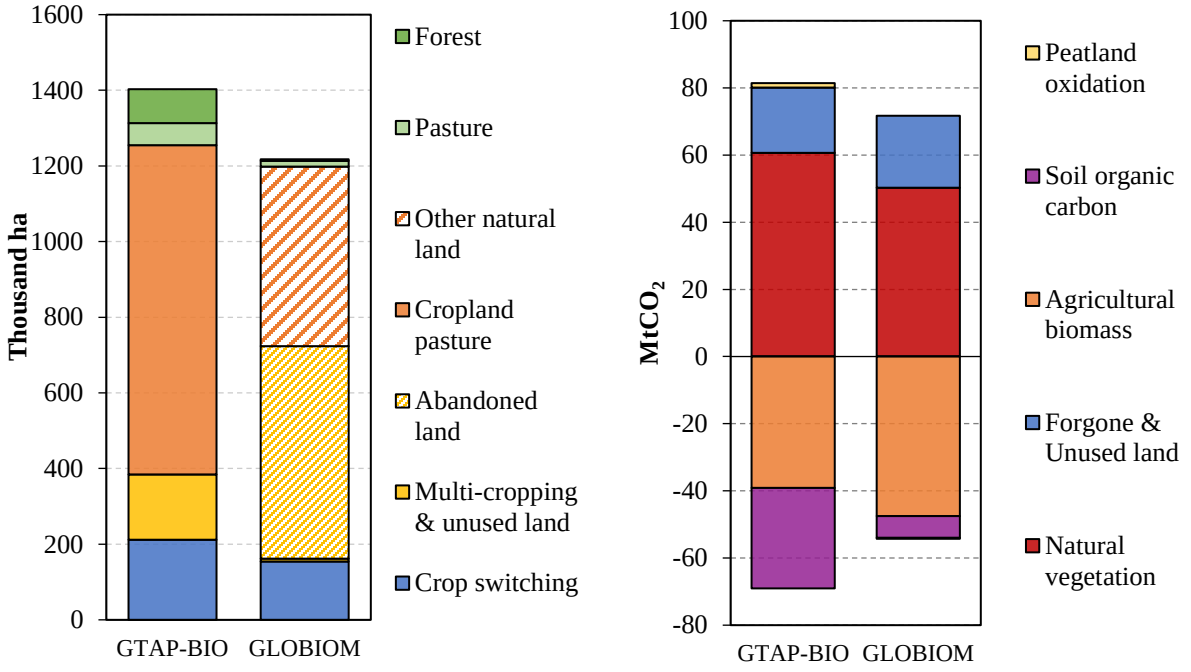

Figure 54. Land use change decomposition (left) and emission decomposition (right) for the global switchgrass ATJ-SPK from isobutanol pathway

For producing 91 PJ ATJ-SPK from isobutanol fuels, 16.7 Mt of miscanthus are directly needed. Switchgrass production in both models would meet the direct requirement since cellulosic crops are modelled as a dedicated energy crop.

In GTAP-BIO, the total switchgrass harvested area increased by 1.4 Mha. Cropland pasture (0.87 Mha) is the major land source for switchgrass in GTAP-BIO, and crop switching also contributed 0.21 Mha. In GLOBIOM, the total switchgrass harvested area increased by 1.22 Mha. Other nature land (0.48 Mha) and abandoned land (0.56 Mha) are the major switchgrass land sources. The land sources for producing switchgrass and the associated emission factors are the drivers to the results difference between the two models.

GTAP-BIO had higher SOC sequestration (-29.6 vs. -6.9 $MtCO_2$) since it used generally higher emission (sequestration) factors for the switchgrass SOC compared with GLOBIOM. Emission changes from natural vegetation (60.7 $MtCO_2$ for GTAP-BIO and 50.3 $MtCO_2$ from GLOBIOM), and agricultural biomass carbon sequestration ((-39.2 $MtCO_2$ for GTAP-BIO and -47.5 $MtCO_2$ from GLOBIOM) are not very different. GTAP-BIO and GLOBIOM estimated 19.4 $MtCO_2$ and 21.5 $MtCO_2$ foregone sequestration, respectively. GTAP-BIO had smaller total ILUC emissions (12.4 $MtCO_2$ for GTAP-BIO and 17.8 $MtCO_2$ from GLOBIOM).

5.3.14 GLOBAL SWITCHGRASS ATJ-SPK FROM ETHANOL

The 25-year ILUC emission intensity for the global switchgrass ATJ-SPK from ethanol pathway is 3.7 g CO_2e/MJ from GTAP-BIO and 5.9 g CO_2e/MJ from GLOBIOM. Figure 55 compares the global land use change decomposition and emission decomposition between the two models for the global switchgrass ATJ-SPK from ethanol pathway. The (net) total bar level in the land use change decomposition indicates feedstock harvested area increase. The land use change and emissions decomposition from this pathway have similar patterns to the global switchgrass FTJ or ATJ-SPK from isobutanol pathway.

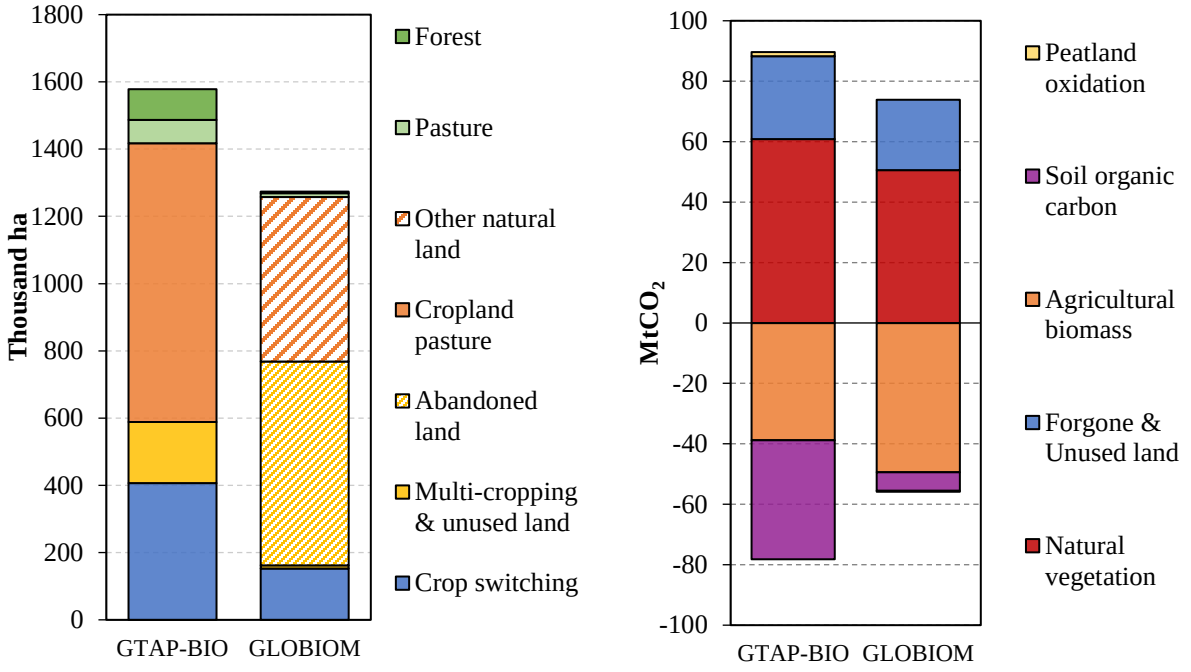

Figure 55. Land use change decomposition (left) and emission decomposition (right) for the global switchgrass ATJ-SPK from ethanol pathway

For producing 122 PJ ATJ-SPK from ethanol fuels, 17 Mt of miscanthus are directly needed. Switchgrass production in both models would meet the direct requirement since cellulosic crops are modelled as a dedicated energy crop.

In GTAP-BIO, the total switchgrass harvested area increased by 1.58 Mha. Cropland pasture (0.83 Mha) is the major land source for switchgrass in GTAP-BIO, and crop switching also contributed 0.41 Mha. In GLOBIOM, the total switchgrass harvested area increased by 1.27 Mha. Other nature land (0.49 Mha) and abandoned land (0.61 Mha) are the major switchgrass land sources. The land sources for producing switchgrass and the associated emission factors are the drivers to the results difference between the two models.

GTAP-BIO had higher SOC sequestration (- 29.9 vs. -6.5 $MtCO_2$) since it used generally higher emission (sequestration) factors for the switchgrass SOC compared with GLOBIOM. Emission changes from natural vegetation (60.7$MtCO_2$ for GTAP-BIO and 50.3 $MtCO_2$ from GLOBIOM), and agricultural biomass carbon sequestration (-39.2 $MtCO_2$ for GTAP-BIO and -47.5 $MtCO_2$ from GLOBIOM) are not very different. GTAP-BIO and GLOBIOM estimated 19.4 $MtCO_2$ and 21.5 $MtCO_2$ foregone sequestration, respectively. GTAP-BIO estimated smaller total ILUC emissions of 12.4 $MtCO_2$ compared with GLOBIOM of 17.5 $MtCO_2$.

5.3.15 GLOBAL POPLAR FISCHER-TROPSCH JET FUEL (FTJ)

The 25-year ILUC emission intensity for the global poplar Fischer-Tropsch jet fuel (FTJ) pathway is 11.4 g CO_2e/MJ from GTAP-BIO and 5.8 g CO_2e/MJ from GLOBIOM. Figure 56 compares the global land use change decomposition and emission decomposition between the two models for the global poplar FTJ pathway. The (net) total bar level in the land use change decomposition indicates feedstock harvested area increase. The land use change and emissions decomposition from this pathway have similar patterns to the global miscanthus FTJ pathway.

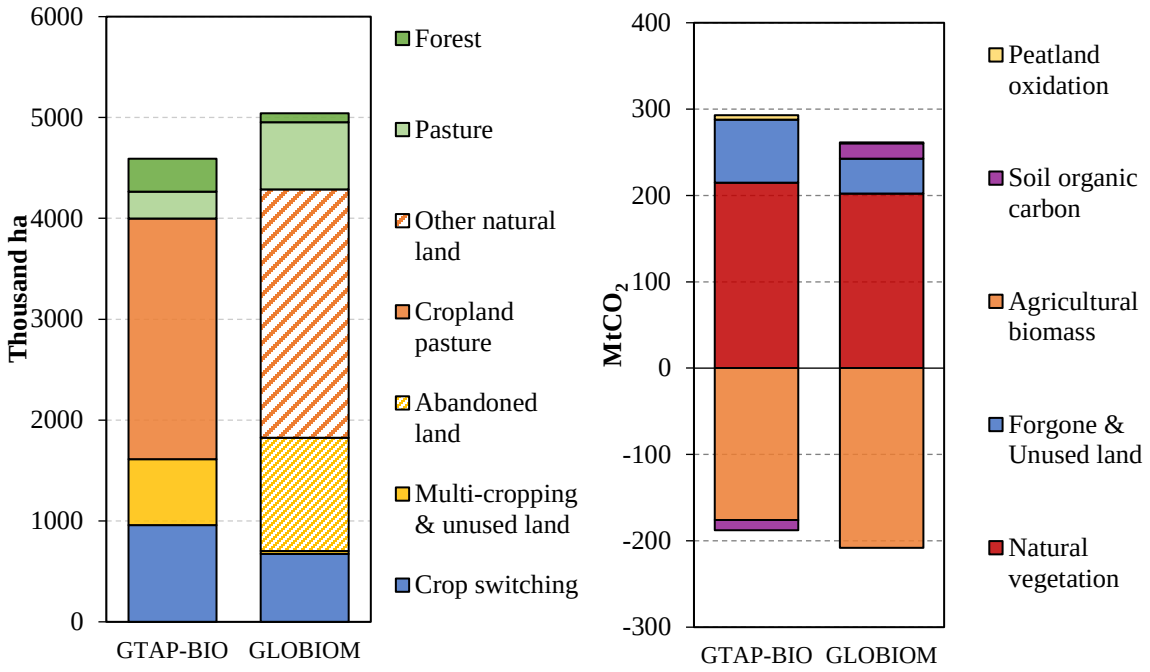

Figure 56. Land use change decomposition (left) and emission decomposition (right) for the global poplar Fischer-Tropsch jet fuel (FTJ) pathway

For producing 363 PJ FTJ fuels, 40 Mt of poplar are directly needed. Poplar production in both models would meet the direct requirement since cellulosic crops are modelled as a dedicated energy crop.

In GTAP-BIO, the total poplar harvested area increased by 4.59 Mha. Cropland pasture (2.38 Mha) is the major land source for poplar in GTAP-BIO, and crop switching also contributed 0.96 Mha. In GLOBIOM, the total poplar harvested area increased by 5.04 Mha. Other nature land (2.46 Mha) and abandoned land (1.12 Mha) are the major poplar land sources. The land sources for producing poplar and the associated emission factors are the drivers to the results difference between the two models.

GTAP-BIO had higher SOC sequestration (-12 vs. 18.1 $MtCO_2$) since it used generally higher emission (sequestration) factors for the global poplar SOC compared with GLOBIOM. Emission changes from natural vegetation (214.7 $MtCO_2$ for GTAP-BIO and 202.3 $MtCO_2$ from GLOBIOM) and agricultural biomass carbon sequestration -175.9 $MtCO_2$ for GTAP-BIO and -208.2 $MtCO_2$ from GLOBIOM) are not very different. GTAP-BIO and GLOBIOM estimated 73.1 $MtCO_2$ and 40.2 $MtCO_2$ foregone sequestration. GTAP-BIO estimated larger total ILUC emissions of 105 $MtCO_2$ compared with GLOBIOM of 53.3 $MtCO_2$.

5.3.16 GLOBAL CARINATA OIL HYDROPROCESSED ESTERS AND FATTY ACIDS (HEFA)

The 25-year ILUC emission intensity for the global carinata oil hydroprocessed esters and fatty acids (HEFA) pathway is -9.8 g CO_2e/MJ from GTAP-BIO and –15.5 g CO_2e/MJ from GLOBIOM. Figure 57 compares the global land use change decomposition and emission decomposition between the two models for the global carinata oil HEFA pathway. The bar in the land use change decomposition indicates land use changes induced by expansion in carinata oil HEFA.

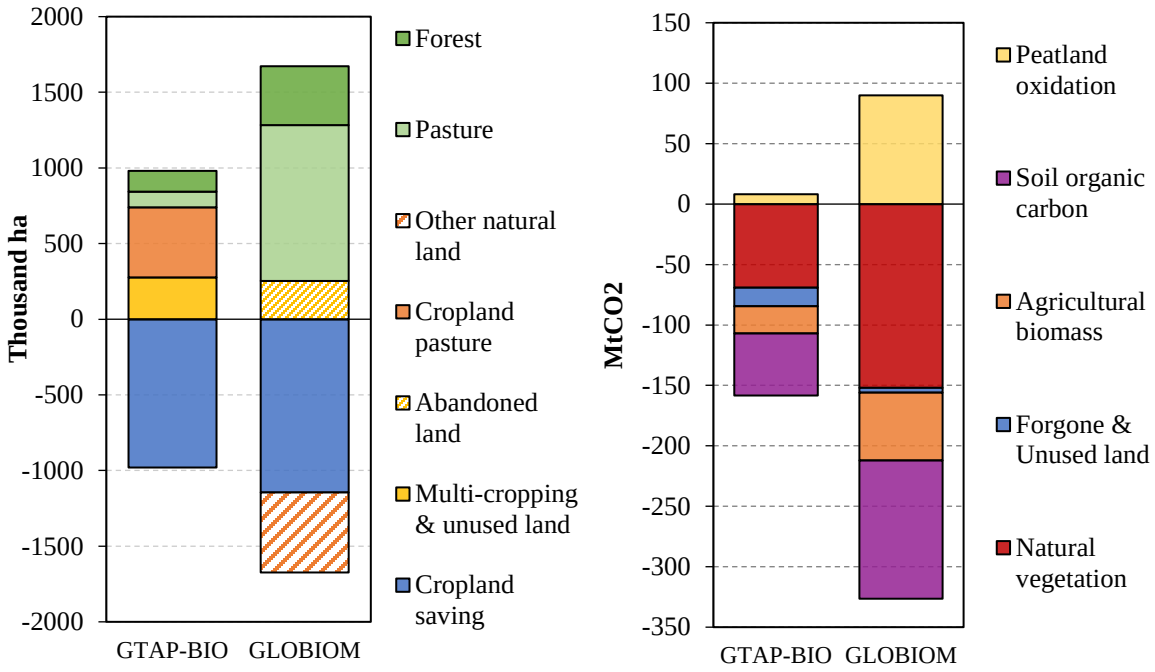

Figure 57. Land use change decomposition (left) and emission decomposition (right) for the global carinata oil hydroprocessed esters and fatty acids (HEFA) pathway

To produce 605 PJ HEFA fuels from carinata oil, 16.0 Mt of carinata oil are directly needed to be produced as secondary oil cover crop. This needs an expansion in production of carinata by 38.1 Mt of carinata seed which requires an expansion in the harvested area of carinata (in rotation with other crops) by 15.9 Mha in the shocked regions. Since carinata is considered as a secondary crop produced in a double cropping system, it will be produced on the exiting active cropland with no expansion in cropland. However, conversion of produced carinata to HEFA fuels generates about 22.1 Mt of carinata meal. Carinata meal is having very similar content in protein as soybean meal. Therefore, the expansion in carinata oil HEFA provides extra meals highly substitutable with soybean meal. The substitution between carinata meal and soybeans, indirectly affects production of soybeans and other crops used in animal feed rations. The indirect changes in crop production induced by the substitution in animal feed items generate some savings in cropland which eventually leads to changes in other land covers.

The GTAP-BIO model projects a saving in cropland at the global scale by 0.98 Mha due to the increase in carinata oil HEFA. That leads to relatively small expansions in cropland pasture, area of forest, and pasture land as shown in the left panel of Figure 57 on the GTAP-BIO bar. The saving in cropland, leads to an expansion in unused cropland or the need for multiple cropping. According to the GTAP-BIO results, these changes jointly drop the land use emissions by 150.2 $MtCO_2$, distributed mainly between natural vegetation, and soil organic carbon and agricultural biomass as shown the right panel of Figure 57 on the GTAP-BIO bar. A portion of this emissions savings is due to changes in forgone sequestration and agriculture biomass as well.

The GLOBIOM model projects a saving in cropland at the global scale by 1.15 Mha due to the increase in carinata oil HEFA. In addition, it projects a reduction in other natural land area by 0.53 Mha as well. These reductions lead to small increases in pasture, abandoned land, and forest areas, as shown in the left panel of Figure 57 on the GLOBIOM bar. According to the GLOBIOM results, these changes jointly drop the land use emissions by 236.7 $MtCO_2$ distributed mainly between natural vegetation, agricultural biomass

and soil organic carbon. For the case of GLOBIOM, all emission components are negative except for the peatland oxidation which shows an increase by 89.9 $MtCO_2$. A portion of this emissions savings is due to changes in forgone sequestration and agriculture biomass as well.

5.3.17 GLOBAL CAMELINA OIL HYDROPROCESSED ESTERS AND FATTY ACIDS (HEFA)

The 25-year ILUC emission intensity for the global camelina oil hydroprocessed esters and fatty acids (HEFA) pathway is -11.4 g CO_2e/MJ from GTAP-BIO and –15.4 g CO_2e/MJ from GLOBIOM. Figure 58 compares the global land use change decomposition and emission decomposition between the two models for the global camelina oil HEFA pathway. The bar in the land use change decomposition indicates land use changes induced by expansion in camelina oil HEFA.

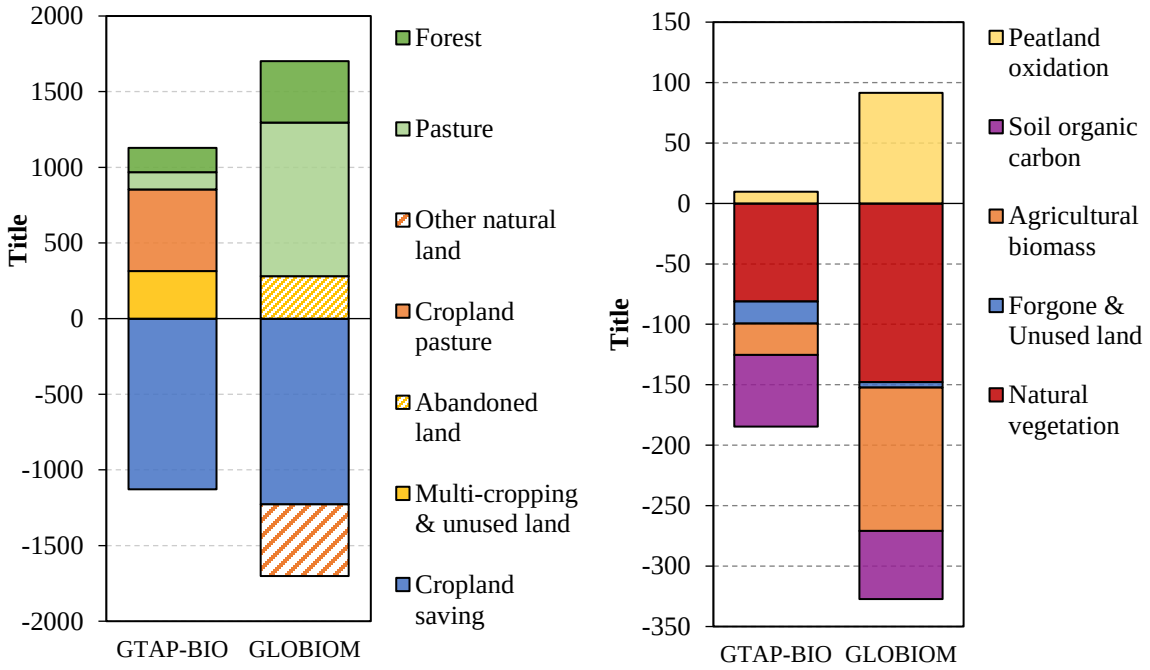

Figure 58. Land use change decomposition (left) and emission decomposition (right) for the global camelina oil hydroprocessed esters and fatty acids (HEFA) pathway

To produce 605 PJ HEFA fuels from camelina oil, 16.0 Mt of camelina oil are directly needed to be produced as second oil cover crop. This needs an expansion in production of camelina by 40.6 Mt of camelina seed which requires an expansion in the area of camelina (in rotation with other crops) by 18.2 Mha in the shocked regions. Since camelina is considered as a secondary crop produced in a double cropping system, it will be produced on the exiting active cropland with no expansion in cropland. However, conversion of produced camelina to HEFA fuels generates about 24.6 Mt of camelina meal. Camelina meal is having very similar content in protein as soybean meal. Therefore, the expansion in camelina oil HEFA provides extra meals highly substitutable with soybean meal. The substitution between camelina meal and soybeans, indirectly affects production of soybeans and other crops used in animal feed rations. The indirect changes in crop production induced by the substitution in animal feed items generate some savings in cropland which eventually leads to changes in other land covers.

The GTAP-BIO model projects a saving in cropland at the global scale by 1.13 Mha due to the increase in camelina oil HEFA. That leads to relatively small expansions in cropland pasture, area of forest, and pasture land as shown in the left panel of Figure 58 on the GTAP-BIO bar. The saving in cropland, leads to an expansion in unused cropland or the need for multiple cropping. According to the GTAP-BIO results, these changes jointly drop the land use emissions by 175.0 $MtCO_2$, distributed mainly between natural vegetation, and soil organic carbon and agricultural biomass as shown the right panel of Figure 58 on the GTAP-BIO bar. A portion of this emissions savings is due to changes in forgone sequestration and agriculture biomass as well.

The GLOBIOM model projects a saving in cropland at the global scale by 1.23 Mha due to the increase in camelina oil HEFA. In addition, it projects a reduction in other natural land area by 0.47 Mha as well. These reductions lead to an increase in pasture, abandoned land, and forest areas, as shown in the left panel of Figure 58 on the GLOBIOM bar. According to the GLOBIOM results, these changes jointly drop the land use emissions by 235.6 $MtCO_2$ distributed mainly between natural vegetation, agricultural biomass and soil organic carbon. For the case of GLOBIOM, all emission components are negative except for the peatland oxidation which shows an increase by 91.6 $MtCO_2$.

CHAPTER 6. **UNCERTAINTY AND SENSITIVITY ANALYSIS**

In the section above, all the analyses were performed using single-point estimates derived from the two selected models. However, estimation of ILUC emissions is subject to substantial uncertainties that need to be kept in mind to put results in perspective. In general, these uncertainties can be classified in four main categories: (1) methodology, (2) model design, (3) data, and (4) parameters.

Methodological uncertainty designates the calculation method chosen to determine ILUC emission intensities. This relates to the way land use models are shocked (one energy product, all energy coproducts, all-coproducts) and to the choice of a fully consequential approach (all effects on emissions of other products predicted by the model) versus an attributional framework (emissions are allocated across fuel and, if relevant, feed coproducts). But it also depends on the coverage of sectors and GHG emissions chosen (fertilizers, livestock emissions etc. to be included or not). Last, the reference period for LUC emission amortization plays a different role in the accounting. The baseline choice, as well as the time horizon considered can have important also implications for the level of emission intensities (Lemoine et al., 2010; O'Hare et al., 2009; Kloverpris and Muller, 2013). Any of the assumptions above are in principle independent of the model specifications but can play an important role in the results.

Model design uncertainty corresponds to the assumptions behind the land use model structure, the way they represent land use sectors, their linkages and their interactions. All models being simplification of reality, their results are always subject to some inherent limitations and uncertainties. Some model will focus on details of the sectoral representation, others the extent of sectoral coverage, and all models will assume different (mathematical) functional forms to represent producer, consumer or trade behaviors. Because no model can pretend completeness of the representation, the comparison of different model results can help address model design uncertainty (Plevin et al., 2010; Broch et al., 2013), as diversity of assumptions is generally expected following different interpretation of observations in economics as a social science.

Data uncertainty relates to the input to the model and current state of knowledge of the system analysed. In the case of land use, there are still many unresolved questions that are key to the analysis of land use change impacts and lead to some significant uncertainties in the model inputs, and therefore outputs. Exact extent of abandoned and unused land, current farmer practices in developing countries, proximate drivers of deforestation are still subject to significant uncertainty in spite of improving data collection, and limit the robustness of the modelling estimate on land use change (Fritz et al., 2013a,b; Erb et al., 2017). These data uncertainties are unfortunately difficult to overcome, although they should slowly decrease as more data are collected.

Parametric uncertainty relates to the parameter choices that determines the model behaviours. This corresponds to the choice of demand and trade elasticities, production and conversion costs on the supply side, and various non-linear cost components associated to the different function forms. CAEP also account in this category emission factors (EFs) of the different carbon pools because they are usually embedded in the models beside the economic parameters and also strongly influence the results on land use change emissions. Sensitivity analysis makes it possible to explore the parametric uncertainty and has been widely performed for earlier studies of biofuel land use change impacts (Golub et al., 2012; Laborde and Valin, 2012; Rajagopal and Plevin, 2013; Plevin et al., 2015, Valin et al. 2015).

Thanks to a clear protocol defined within CAEP, a number of sources of uncertainties related to the methodology have been treated explicitly, and choices were made for assumptions to be used in the analysis. The CAEP steering group agreed on a single amortization time of 25 years. While attributional analysis is used for core LCA, the consequential approach is used for induced land use change. However, the two models operate differently over time, with GTAP-BIO being comparative static and analysing shock from a base year of 2011, whereas GLOBIOM relies on a projected baseline to 2020. GTAP-BIO and GLOBIOM have different modelling structures (e.g., difference in representing multi-cropping, coproduct substitution, crop yield responses, international trade, etc). Many of these have been discussed in past CAEP meetings

and are documented above. The analysis partly reflects model design uncertainties because the two models represent two very different approaches to economic modelling. Each model is grounded in its own set of input data. Different data sources for land cover and emission factors introduce more variability in ILUC emissions results.

Sensitivity analysis has been conducted for some key data and parameters in GTAP-BIO and AEZ-EF for estimating SAF ILUC emissions. In the case of GLOBIOM, a grouped sensitivity analysis has been performed on 12 selected parameters with a Monte-Carlo analysis. Note that the sensitivity analysis results from the two models are not comparable, since, in most cases, there is no inherent mapping between parameters used in the two models given the different theoretical backgrounds. Also, the sensitivity tests conducted in the two models have a different focus. The sensitivity tests in GTAP-BIO use mostly boundary analysis, in which different boundary scenarios are tested on a single parameter, to study how sensitive the ILUC emission value is with regard to a parameter. A Monte-Carlo simulation on a group of parameters is not conducted in GTAP-BIO because a good estimation of parameter distributions is not available, and the correlation among the parameters is unknown. The Monte-Carlo analysis tested in GLOBIOM relied on assumptions of parameter distributions and assumed that the parameter distributions would be independent.

6.1 **SMALL SHOCK SENSITIVITY**

A sensitivity analysis on shock size was conducted by testing a very small shock size instead of the full projected SAF supply. A shock of 50 million gasoline gallon equivalent (MGGE) or 6.1 PJ was used for 11 pathways. Figure 59 compares ILUC emission values from the small shock with those from originally developed shock, as tested with GTAP-BIO. These tests indicate that ILUC emissions are not very sensitive to the shock size for most of the pathways, even for a fairly large shock decrease. As shock size increased, both the total induced land use change emissions (numerator) and fuel production (denominator) increased, so emission values did not change much. For example, for the US corn ATJ-SPK from isobutanol pathway, when the shock size decreased by about 94% from 104 PJ to 6.1 PJ, the total ILUC emissions decreased by about 95% (from 2.33 mil. tons to 0.13 mil tons). Thus, the emission intensity for this pathway decreased from 22.4 to 21.2 g CO_2e MJ^{-1}. The small non-linearity regarding shock size is mainly due to an extensification response in which new cropland has a lower yield than existing cropland. The same tests were also conducted in GLOBIOM, and similar conclusions were drawn, while those results are not included here since important updates had been made after those tests.

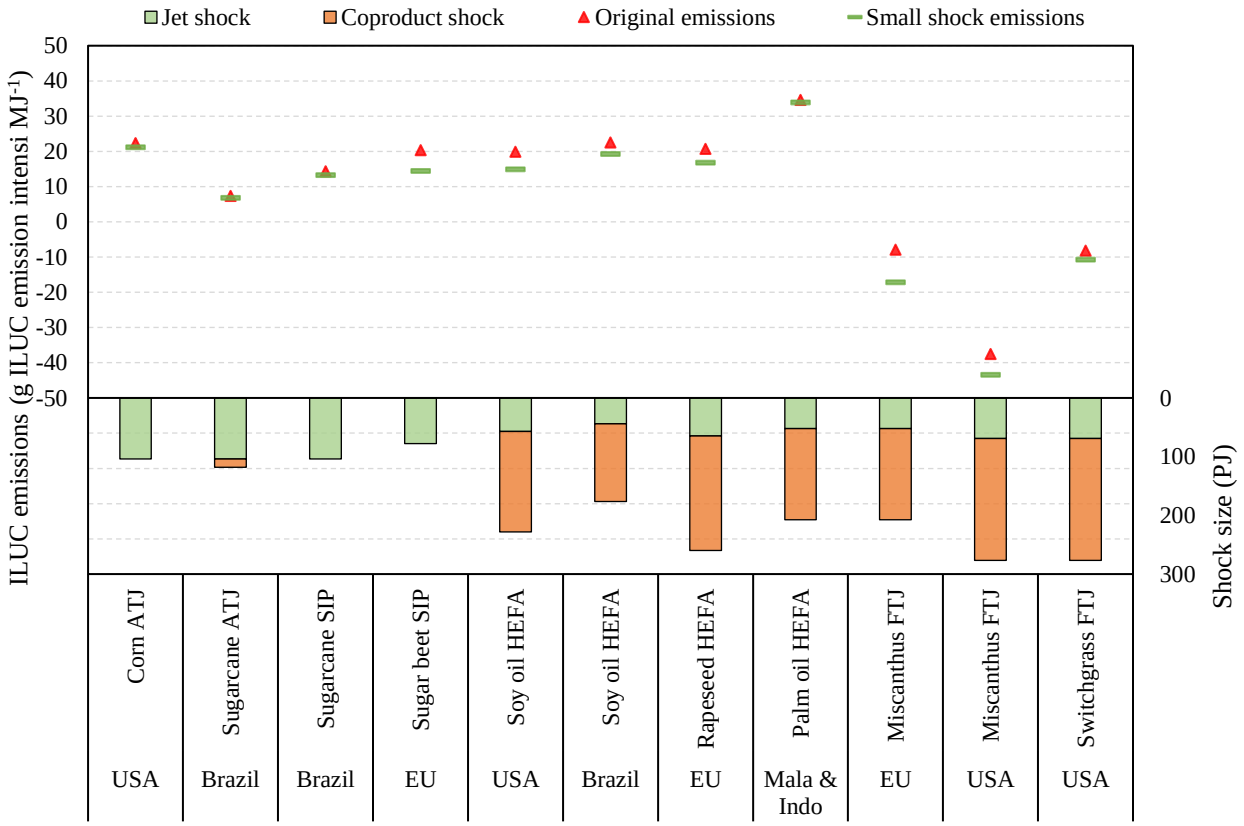

Figure 59: Comparison of ILUC emissions from small shock (50 MGGE or 6.1 PJ) and original shock, tested with GTAP-BIO

6.2 SENSITIVITY ANALYSIS CONDUCTED IN GTAP-BIO AND AEZ-EF

6.2.1 Peat oxidation and palm expansion on peatland

CAEP conducted sensitivity analysis to assess the impact of peat oxidation (PO) and palm expansion on peatland parameters on the ILUC emission intensity. The default PO emission factor in AEZ-EF was updated to 38.1 t CO_2/ha/year, which was calculated based on data provided in Miettinen et al. (2016) and Miettinen et al. (2017). Note that the IPCC PO parameters were mostly used in Miettinen et al. (2017) while the average of emission factors for acacia (20 t C/ha/year) and oil palm (11 t C/ha/year), 15 t C/ha/year was used for converting PSF to oil palm (IPCC, 2014). The weighted average PO emission factor would be around 24 t CO_2/ha/year if simply applying the IPCC emission factors for oil palm. However, the IPCC factor is representative of palm plantation cultivated on land for a long time, and it is possible that emission factors may be underestimating the peatland emissions of the first years after plantation establishment (Miettinen et al., 2017). Given the high uncertainty associated with peat oxidation, CAEP tested three scenarios for the peat oxidation factor: (1) a lower PO factor (30.8 t CO_2/ha/year), which was calculated based on a recent study from Austin et al. (2017), (2) the PO factor previously used by CAEP (60.8 t CO_2/ha/year), which was the mean value of nine literature studies reviewed in GLOBIOM documentation, and (3) another PO factor previously used by CAEP (95 t CO_2/ha/year) from Page et al. (2011), which was originally used by AEZ-EF.

Furthermore, AEZ-EF assumes an upper bound of 33% palm expansion in Malaysia and Indonesia (Mala & Indo) would be on peatland based on assumptions made in Edwards et al. (2010). This assumption has been used until now. However, GLOBIOM lowered the palm expansion on peatland to 20% from 32% in Indonesia but kept 34% for Malaysia. CAEP has not changed the default parameter since Malaysia and Indonesia are aggregated in GTAP-BIO, but tested a scenario of assuming 20% palm expansion on peatland.

The sensitivity test results for the eleven pathways are presented in Figure 60. The tests showed a significant impact of the PO factor on ILUC emission intensities for HEFA pathways, but very small impacts on results from other pathways. By increasing the peat oxidation factor from 38.1 t CO_2/ha/year to 95 t CO_2/ha/year, the ILUC emission intensity would be doubled for the Malaysia & Indonesia palm oil HEFA pathway and increase by about 25% - 30% for the other vegetable oil HEFA pathways. Similar to PO factors, decreasing palm expansion on peatland would have very small impacts on non-HEFA pathways but decrease ILUC emission intensity for HEFA pathways significantly. Given the increasing government and international attention to the deforestation and peat oxidation, both the peat oxidation factor and the share of palm expansion on peatland may decrease in future, which would reduce ILUC emissions for the HEFA pathways. However, it is uncertain to what extent policy changes will be enforced.

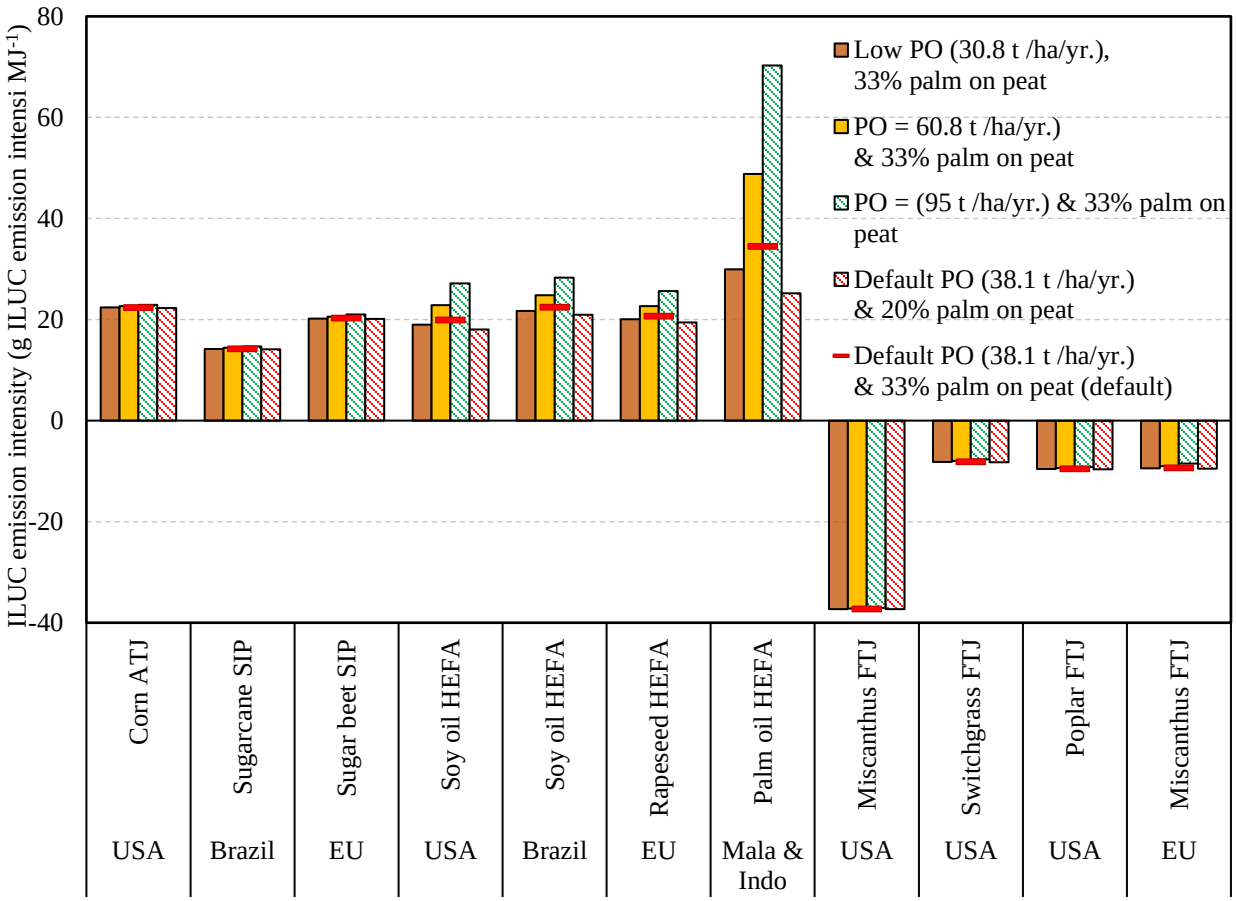

Figure 60: Sensitivity of ILUC emission intensity relative to the peat oxidation and palm expansion on peatland parameters

6.2.2 Emissions from converting unused land

CAEP did a sensitivity analysis on the impact of the unused land emission factor on the ILUC emission intensity for the eleven pathways. The default assumption used was that the emission factors for converting unused cropland are the same as those for converting cropland pasture (CP). Figure 61 shows the results

for scenarios assuming two lower emissions factors for unused land: 50% of cropland pasture emission factor and no unused land emissions. Including emissions from converting unused cropland (the default scenario) moderately increased the ILUC emission intensity for all pathways compared to the sensitivity cases with lower emissions factors. Results from the Brazil and EU pathways tend to be more sensitive to the unused land emission factor mainly due to the high cropland intensification responses and relatively high shares assigned to the use of unused land in these regions.

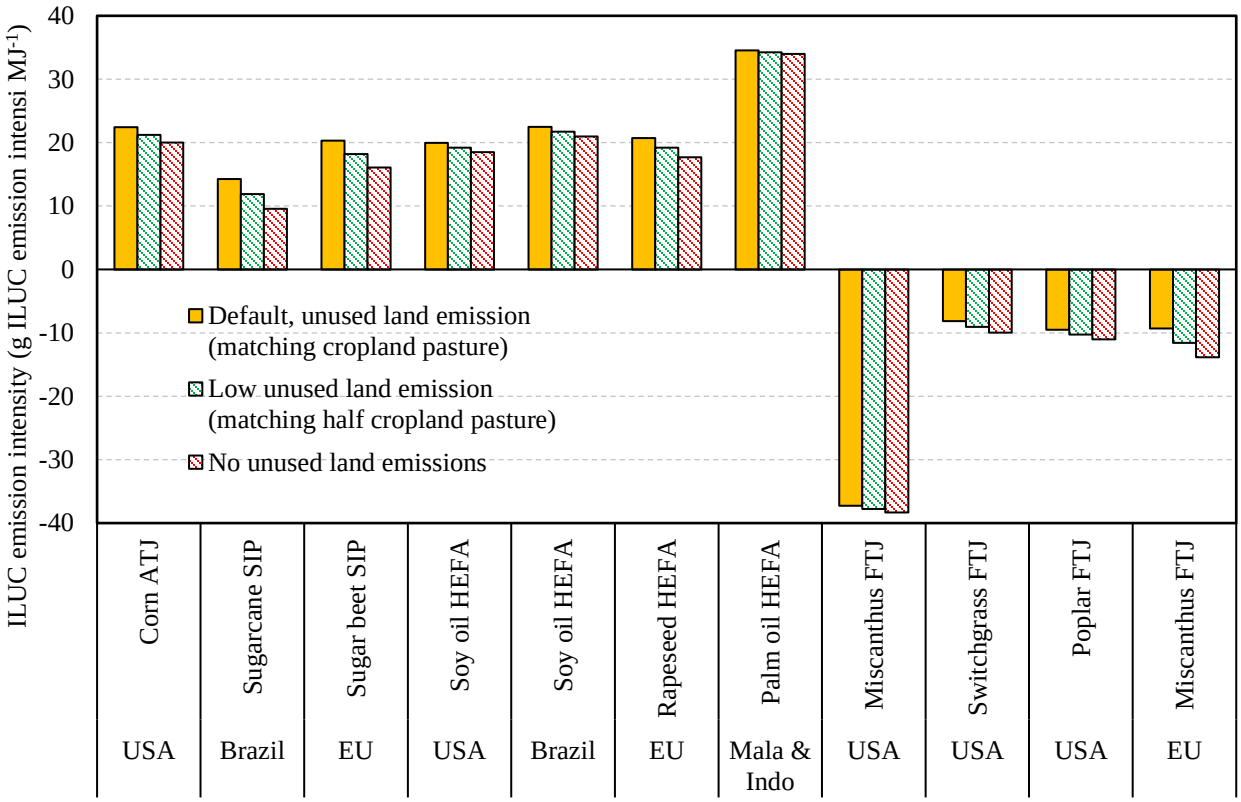

Figure 61: Sensitivity of ILUC emission intensity relative to the unused land emission factor

6.2.3 Yield price elasticity (YDEL)

YDEL is a parameter in GTAP-BIO governing crop yield response to crop prices (Keeney and Hertel, 2009). For example, if YDEL is 0.25 in a region, it implies a 1% increase in crop prices would lead to a 0.25% increase in crop yield. In a recent study from Taheripour et al. (2017a), the YDEL parameter was differentiated by region using real observations on productivity improvement across the world based on the FAO data. (e.g., 0.3 for the USA, 0.325 for Brazil, 0.25 for EU, 0.175 for East Asia and Oceania, and 0.3 for Malaysia & Indonesia). CAEP used these revised values in the current sensitivity analysis. The only exception is that CAEP decreased the YDEL for palm production in Malaysia & Indonesia to 0.05 to reflect the recent trend of palm yield growth. Prior to Taheripour et al. (2017a), 0.25 had been used uniformly across regions due to the lack of information (Keeney and Hertel, 2009). YDEL is an important parameter to allow crop producers to substitute land with other inputs as responses to relative price changes so the crop yield would increase through the intensification. CARB[21] tested a range of 0.05 to 0.35 for YDEL (Tyner et al., 2016). To be consistent with the CARB test, CAEP tested three scenarios for YDEL besides

[21] Note that the version of GTAP-BIO used for CARB was not updated with the new YDEL parameters suggested by Taheripour et al. (2017).

the default scenario: (1) 0.05 uniformly for the USA, Brazil, EU and Malaysia & Indonesia, (2) 0.15 uniformly for the USA, Brazil, EU and Malaysia & Indonesia, and (3) 0.35 uniformly for the USA, Brazil, EU and Malaysia & Indonesia. The YDEL parameters for other regions remain at the default values for all scenarios. CAEP will develop sensitivity tests with regional tuned YDEL values in the future. Note that for the default scenario of cellulosic FT pathways, CAEP fixed the cellulosic crop yield to be consistent with the Core LCA data and to help the reconciliation between GTAP-BIO and GLOBIOM for these pathways. However, YDEL may still play an important role for these pathways since it involves price-induced yield changes for all crops.

The results of the sensitivity test are presented in Figure 62. As expected, a higher YDEL value would result in relatively higher crop yields and, thus, lower ILUC emissions. Since the default YDEL values are mostly close to 0.35 (except palm in Mala & Indo), ILUC emissions did not decrease significantly when changing YDEL to 0.35 for the four regions. Conversely, ILUC emission values would increase considerably when decreasing YDEL to 0.05 for all pathways except palm HEFA in Mala & Indo. Similar to all other pathways, the ILUC emissions increase for cellulosic pathways with smaller price yield responses (lower YDEL). However, ILUC emissions would remain mostly negative (except for US switchgrass FT when YDEL is 0.05) for cellulosic pathways across these scenarios.

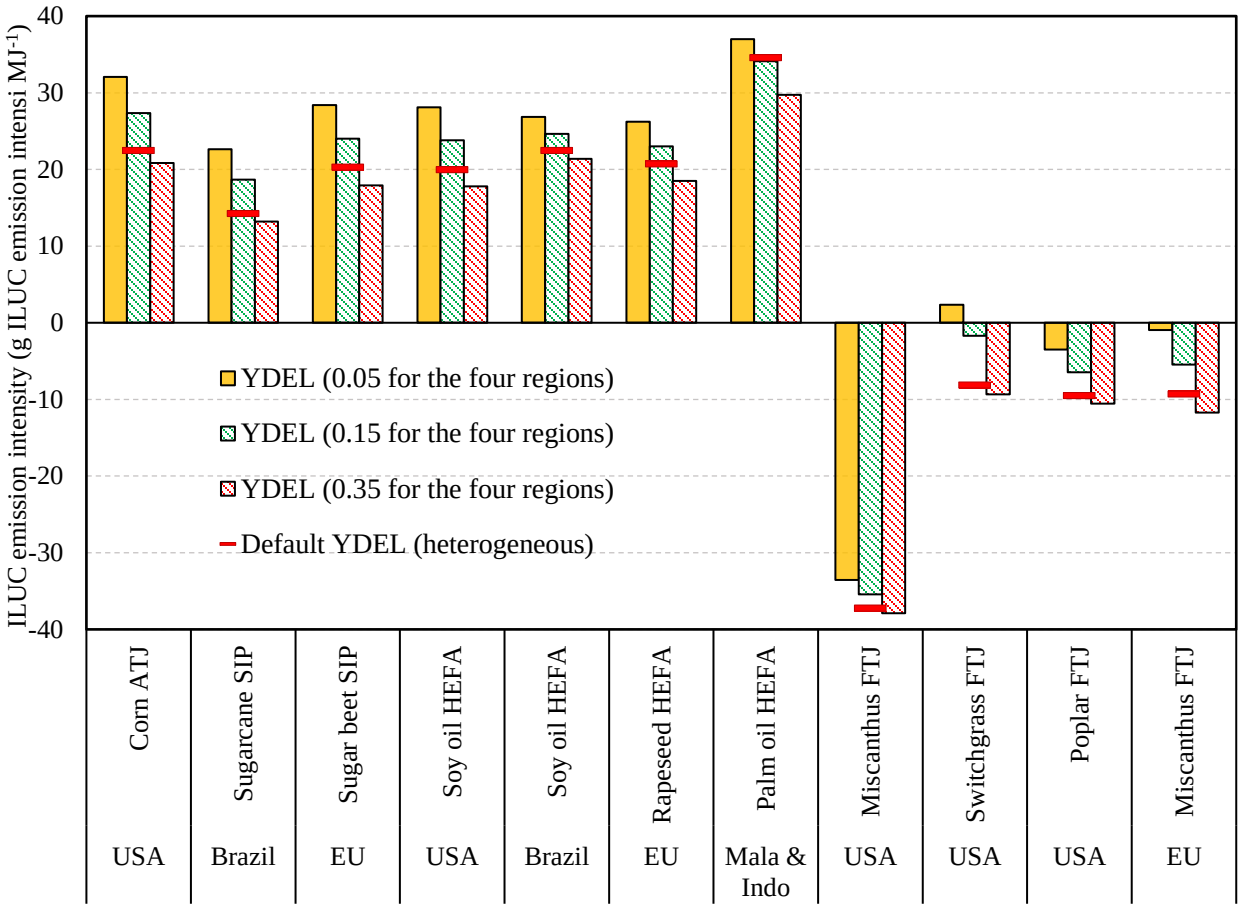

Figure 62: Sensitivity of ILUC emission intensity relative to the yield price elasticity (YDEL)

6.2.4 Armington elasticities

GTAP models employ the Armington structure, the workhorse for bilateral trade modelling, with parameters estimated for this structure. Armington elasticity is a measure of the degree of substitution between home and imported goods and also differentiation by exporting country. There are two Armington elasticities for each commodity: (1) ESUBD represents the ease of substitution between domestic and imported goods; and (2) ESUBM, represents the degree of substitution among different countries of origin for imports. In GTAP, ESUBM is set to twice ESUBD as a rule. The Armington elasticities vary by commodity. In general, larger Armington elasticities imply that products produced from different origins are more homogeneous to the importer, and the model would be closer to a homogeneous goods model (Heckscher-Ohlin). A homogeneous goods approach leads to stronger trade changes in response to price changes. The trade literature generally finds that an Armington structure better represents the reality in international trade compared with a world integrated market representation with perfectly substitutable homogeneous goods. However, Armington elasticities are still subject to uncertainty. Two scenarios were used for sensitivity testing: (1) using 150% of the default ESUBD and ESUBM parameters for agricultural, livestock, and forestry sectors, and (2) using 50% of the default ESUBD and ESUBM parameters for agricultural, livestock, and forestry sectors.

The sensitivity of ILUC emission intensity relative to Armington elasticities is presented in Figure 63. Cellulosic crop FT pathways are not included in the sensitivity tests here because cellulosic crops were assumed to be dedicated energy crops with no international trade. The results indicated heterogeneous impacts from Armington elasticities on ILUC emissions across pathways/regions. For the US and EU pathways, higher Armington values increase the accessibility to the international market so that relatively more feedstock would be produced internationally in regions with lower crop yield and higher deforestation rate. However, it was the opposite for the palm oil HEFA in Mala & Indo pathway, in which higher Armington elasticities permitted a reduction in palm oil exports and effectively increases the substitution from other vegetable oils. As a result, less palm oil would be produced, so that there would be less peat oxidation and tropical deforestation. The case for Brazil soy oil HEFA is similar to the Mala & Indo palm oil HEFA case given that Brazil has a relatively higher deforestation rate and associated emission factors compared with soy oil producing competitors (e.g., the USA). Furthermore, the impact of Armington elasticities on the sugarcane SIP pathway in Brazil is negligible mainly because sugar crops are hardly traded internationally, but sugar is.

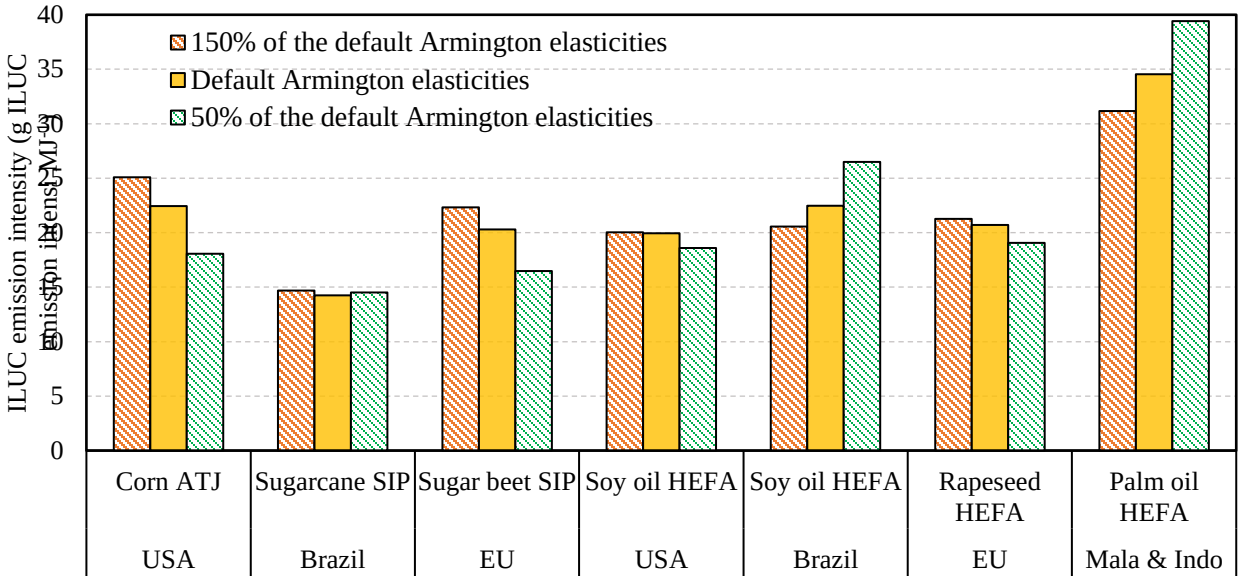

Figure 63: Sensitivity of ILUC emission intensity relative to Armington elasticities

6.2.5 Extensive margin parameter (ETA)

GTAP-BIO uses an extensive margin parameter, ETA, to govern the ratio of crop yields on converted land to the yield on existing cropland. The parameters are derived using the net primary productivity (NPP) information provided by the Terrestrial Ecosystems Model (TEM) at the AEZ and region level (Taheripour et al., 2012). The default values range from 0 to 1, where 0 indicates no productive land is available from a given AEZ in that region, and 1 suggests that converted land will be equally productive as existing cropland. Two scenarios were tested: using 120% of the default ETA and 80% of the default ETA, respectively. The results are presented in Figure 64. In general, a higher ETA value reduces land conversion and leads to lower ILUC emissions, and vice versa. The ILUC emission results are relatively more sensitive to Brazil and Mala & Indo pathways compared with the US and EU pathways, due to the higher emission factors for converting natural vegetation in Brazil and Mala & Indo.

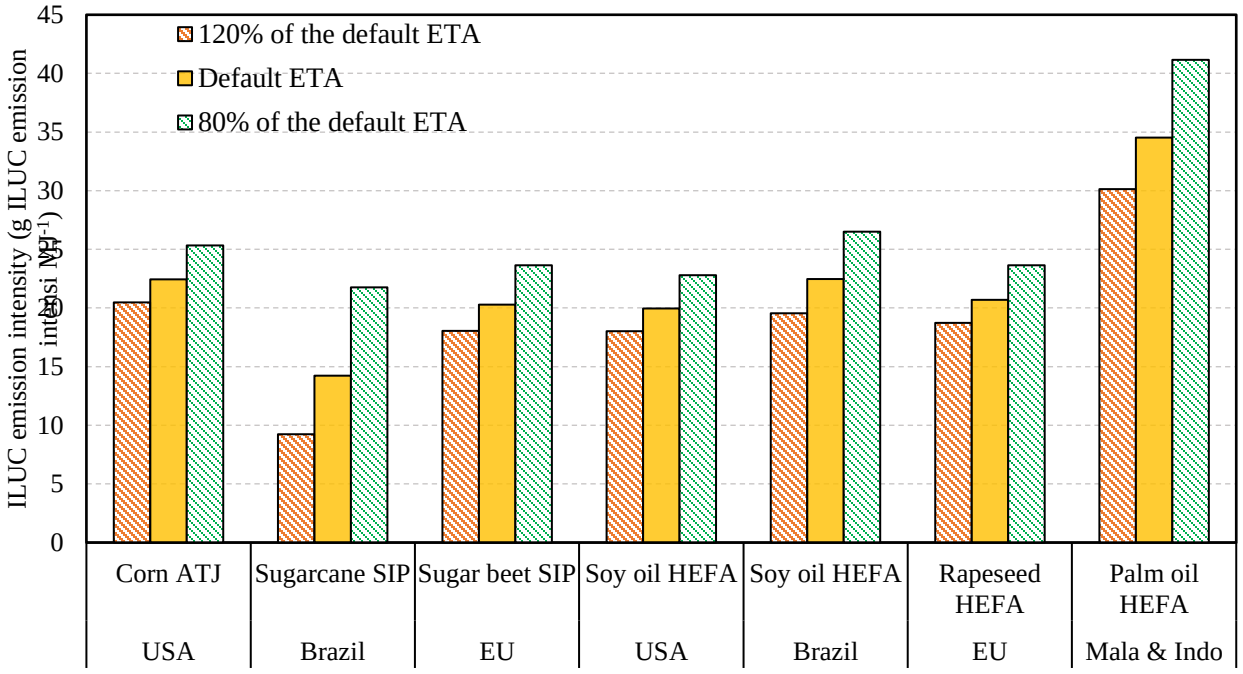

Figure 64: Sensitivity of ILUC emission intensity relative to extensive margin parameters (ETA)

6.2.6 Cellulosic crop yield, soil organic carbon, and agricultural biomass carbon

Cellulosic crops are modelled as dedicated energy crops for SAF production, and CAEP targeted crop yields used in the CLCA studies. As a result, the market-mediated responses are small for these pathways compared with pathways using regular crops. Cellulosic crop yield, soil organic carbon (SOC), and agricultural biomass carbon (ABC) are three important factors driving the ILUC emission results for cellulosic pathways. The after-loss dry crop yields from CLCA are 15.0 t/ha for US miscanthus, 11.4 t/ha for US switchgrass, 8.5 t/ha for US poplar, and 16.5 t/ha for EU miscanthus. SOC data from ANL were applied, and literature information has been used for calibrating the ABC calculation for cellulosic crops. The SOC data showed that there would be SOC sequestration in most of the land transition in any AEZ, while this is not the case for miscanthus and poplar. In the sensitivity tests, there are two scenarios for cellulosic crop yield (80% and 120% of the default CLCA cellulosic crop yield), two scenarios for SOC emission factors (increasing and decreasing by 30% relative to the default SOC emission factors), and two scenarios for ABC (increasing and decreasing by 30% relative to the default ABC emission factors).

The sensitivity results are shown in Figure 65. All the sensitivity tests are relative to the default scenario. For switchgrass and poplar pathways, just like other pathways using regular crops, an increase in crop yield would reduce land conversion from natural vegetation and related emissions. However, it is different for miscanthus since converting forest and pasture for miscanthus cultivation would increase SOC sequestration in most AEZs. Thus, a lower miscanthus crop yield entails relatively more land being converted for the crop and leads to higher total SOC sequestration. The ILUC emissions impacts from SOC and ABC are symmetric around the default value. Herbaceous crops based pathways were more sensitive to SOC relative to ABC, while the short rotation poplar pathway was more sensitive to ABC. In general, if conducting these sensitivity tests independently, the ILUC emission results for these pathways remain negative regardless of the sensitivity scenario.

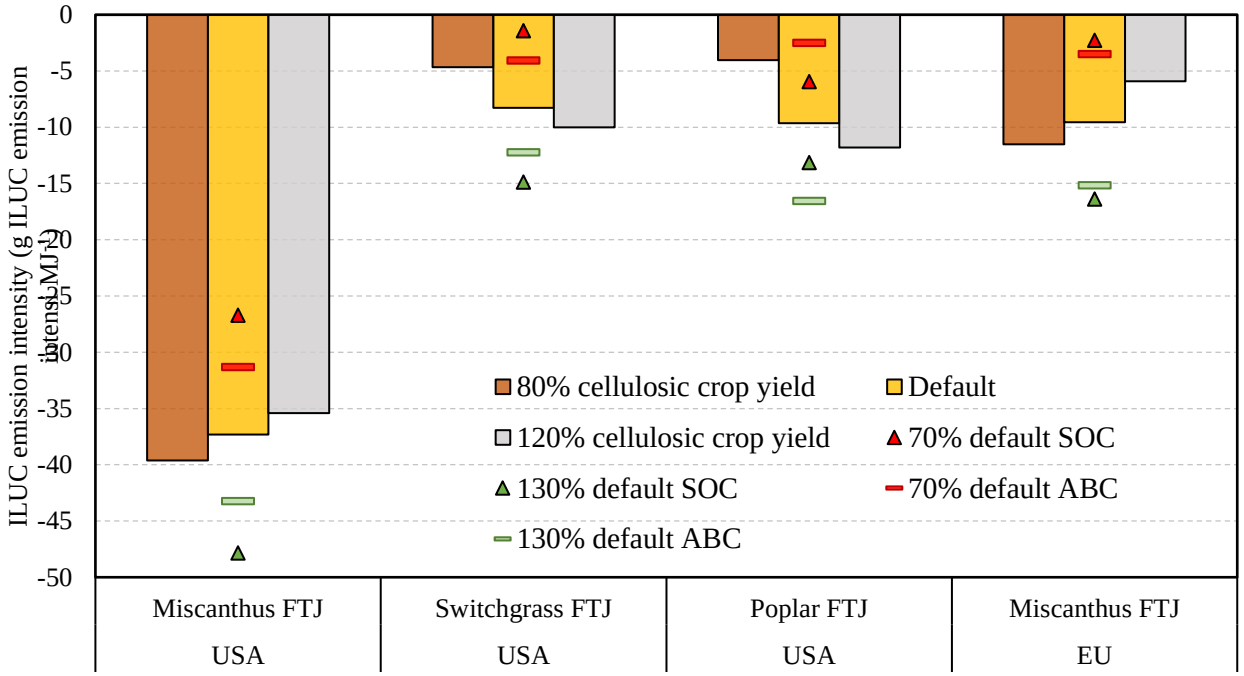

Figure 65: Sensitivity of ILUC emission intensity relative to cellulosic crop yield, SOC, and ABC

6.2.7 Demand response issues for HEFA pathways

Besides the livestock rebound effect, an important key driver of the different results between GTAP-BIO and GLOBIOM is the demand response. The previous comparison of the results indicated that GTAP-BIO had stronger demand responses, compared with GLOBIOM, in vegetable oil sectors so that there was greater reduction in consumption of vegetable oils due to the vegetable oil HEFA shocks. Generally, a stronger reduction in demand would lead to less production of new vegetable oil and oilseeds, and thus smaller land use change and emissions. In this section, GTAP-BIO was modified to weaken the demand responses in the vegetable oil sectors so that the consumption reduction would be closer to results from GLOBIOM. The tests would provide us with insights into the importance of this driver of the different results.

Table 110 provides a comparison between GTAP-BIO and GLOBIOM for the share of newly produced vegetable oil over vegetable oil feedstock demand in the world by the pathway. Results show that, for GTAP-BIO, 40% of the total soy oil biofuel feedstock demand for producing HEFA SAF in the US was newly produced or substituted by a new production of other vegetable oils from a global perspective. In contrast, 59% is the figure in GLOBIOM for the US soy oil HEFA pathway. The share was calculated as the sum of the product of newly produced oilseeds and the vegetable oil crushing rate at the world level. The 60% difference in GTAP-BIO corresponds to the change in consumption of vegetable oil, as also provided in Table 110. Compared to the initial level of global consumption, the 60% drop in consumption for the US soy HEFA shock corresponds to a global decrease in vegetable oil consumption of about 2.4%. While this comparison is somewhat simplistic, it does show an important model difference.

Table 110: Comparison of GTAP-BIO and GLOBIOM for share of calculated newly produced vegetable oil over feedstock demand in the world by pathway

Model	Share	US soy oil HEFA	Brazil soy oil HEFA	EU rape oil HEFA	Mala & Indo palm oil HEFA
GLOBIOM	New oil share over demand	59%	58%	81%	92%
GTAP	New oil share over demand	40%	30%	40%	55%
	Oil consumption decrease	2.4%	2.1%	2.7%	1.7%

However, demand response is an important issue, and sensitivity analysis were done in GTAP-BIO to force the GTAP-BIO results to become closer to GLOBIOM. Changes were made in the GTAP-BIO model and database to reduce the demand responses for vegetable oil in HEFA pathways in a direction towards GLOBIOM. CAEP noticed that there are differences between the value-based GTAP database and USDA statistics. For example, the GTAP database indicated oilseeds would have several uses including vegetable oil, food processing, feed, and households. The USDA data divides domestic consumption into only two categories: crushed and other uses. Usually, 92% goes to crush, and 8% goes to other uses. That is, the GTAP database represents uses of oilseeds in more activities. Furthermore, the GTAP database allows different prices across oilseed or vegetable oil domestic uses and exports as the database represents the real value flows in the base year. The heterogeneous prices across sectors also partly represent variation in quality of oilseeds. For these reasons, in general, GTAP may project a greater reduction in the consumption of vegetable oils. In addition, GTAP data base covers all type of oilseeds and fats, and hence it covers a broader consumption base, which allows greater substitution among various types of oils and fats. For the purpose of this test and to reduce the demand responses in GTAP-BIO, all of these issues were ignored, and adjustments were made to the value-based GTAP database to make it closer to the quantity-based USDA database with a uniform price. All the oilseed consumption in processed food and self-consumption categories were moved to the crushing sector.

A comparison between the original results and new results from using the adjusted database is presented in Table 111. The ILUC emissions would increase significantly due to the adjustment in the database, significantly decreasing the oilseed and vegetable oil consumption reduction for soy oil and rapeseed oil pathways, with a smaller reduction in the Mala & Indo palm oil HEFA pathway. With the adjusted database in GTAP-BIO, the share of new vegetable production over feedstock demand at the world level from the US soy oil HEFA pathways now is close to GLOBIOM, and ILUC emissions increased from 19.9 g CO_2e /MJ to 30.8 g CO_2e /MJ. However, for the other three pathways, GLOBIOM still has lower demand responses, particularly for Mala & Indo palm oil production. These tests indicate that the demand response is a key driver to the result differences between the two models, and the differences in the demand responses can be partly explained by the differences in the database and structure of the model. The sensitivity analysis also reveals important differences in the databases that help drive the differences in apparent demand response. The changes in the GTAP-BIO database that were made for this test illustrate a demand response closer to the demand response in GLOBIOM, as measured by the Table 110 calculation.

As shown in Table 112, even with the adjusted database in GTAP-BIO, the ILUC emissions from GLOBIOM are still larger for all these HEFA pathways. This points to other structural differences between the models that contribute to a difference in emissions.

Table 111: Results from GTAP-BIO with adjusted database

HEFA pathway	Original database			Adjusted database		
	New oil share over demand	Oil consumption decrease	ILUC emissions (g CO_2e /MJ)	New oil share over demand	Oil consumption decrease	ILUC emissions (g CO_2e /MJ)
US soy oil	40%	2.4%	19.9	60%	1.6%	30.8
Brazil soy oil	30%	2.1%	22.5	51%	1.6%	37.5
EU rape oil	40%	2.7%	20.7	61%	1.8%	26.6
Mala & Indo palm oil	55%	1.7%	34.5	59%	1.5%	36.5

Table 112: Comparison of ILUC emissions between GTAP-BIO and GLOBIOM for HEFA pathways (g CO2e /MJ)

HEFA pathway	GTAP-BIO		GLOBIOM
	Original database	Adjusted database	
US soy oil	19.9	30.8	50.4
Brazil soy oil	22.5	37.5	117.9
EU rape oil	20.7	26.6	27.5
Mala & Indo palm oil	34.5	36.5	60.2

6.3 SENSITIVITY ANALYSIS EXPLORATION WITH THE GLOBIOM MODEL

6.3.1 Monte-Carlo protocol for parametric uncertainty analysis.

To test sensitivity of the GLOBIOM results to different assumptions, the point-based estimates presented above were complemented with a full Monte-Carlo analysis targeting 10 different parameters in the model. Under a Monte-Carlo analysis, each parameter is assumed a probability distribution and a large number of simulations is performed, based on a number of randomized draws from the distribution of parameters. This method allows to test the overall sensitivity of the model results to parametric uncertainty, and if those are included in the analysis, to data uncertainty. However, this approach does not touch upon the design uncertainty of the models. Therefore, it does not tell what the overall probability of ILUC estimate would be, but what it would be under the current model structure. It should also be noted that for many parameters, the probability distribution is not very well known. This type of analysis is however extremely useful to inform on the overall degree of robustness of some particular estimates in the model. Although only GLOBIOM is here performing a Monte-Carlo analysis of its results, this type of analysis is relatively standard, although resource consuming. Similar analysis can be found in the literature for GTAP-BIO (Plevin et al. 2015) or MIRAGE-Biof CGE (Laborde and Valin, 2012) in the context of other biofuel policies.

Monte-Carlo analysis requires a large number of simulations to derive the results distribution (for the present analysis 300 runs per pathway). For this reason, CAEP performed the full analysis on 12 pathways out of the 22 (all HEFA except carinata, FT pathways, corn and sugar cane ATJ-SPK from isobutanol and corn ATJ-SPK from ethanol). Of the ten remaining pathways eight of them (sugar cane ATJ-SPK from ethanol and SIP, miscanthus and switchgrass ATJ-SPK from isobutanol and ATJ-SPK from ethanol) rely on the same feedstock-region combination as covered in the first 12, with only a different conversion efficiency assumed. No sensitivity is prepared for the carnina pathway of carinata. ILUC emission

intensities for these can therefore be computed ex-post based on the derived distribution from earlier runs by adjusting the energy efficiency of the pathway.

CAEP targeted 10 different key parameters, related to biophysical and economic behavior uncertainties. The selected parameters for the sensitivity analysis are listed in the Table 113 below. They comprise 6 parameters on economic responses and 4 on biophysical responses, all important for the ILUC estimation. These parameters are assumed distributed around the parameter used for estimation of the central value used for the single-point estimates. The distribution assumed can vary, depending on the nature of the uncertainty (experimental, conceptual), the presence of different underlying sources of uncertainty, and the overall level of knowledge of a variable. For instance, demand elasticities are more studied and therefore better known than supply elasticities, and their distribution will be assumed narrower. In general, as econometric parameters are less precisely known compared to biophysical ones, they are assumed here to follow a uniform distribution. Biophysical parameters, usually derived from direct measurement, are assumed to follow a normal distribution, which is the default probability distribution used in science around an observation. For some parameters however, log distribution is also considered (log-normal or log-uniform) when the effects to be measured do not correspond to single uncertain measurement but to a combination of uncertainties (e.g. peatland emissions, because different underlying uncertainties are multiplied on subsidence speed, bulk density, etc.). In the case of price elasticities, the log distribution reflects the logic that a response to a price change is assumed to be doubled (+100%) or halved (-50%), and the logarithmic scale is therefore used to vary the magnitude of the multiplicative effect. A discussion on probability distribution across scientific domains can be found in Limpert et al. (2001).

Table 113: List of parameters to be tested for Monte-Carlo simulations and range around the default parameter values

Parameter	Typical value range*		Distribution	Motivation for parameter selection and range
Behavioral parameters				
Demand elasticity	- 33%	+50%	Log-uniform	Degree of food consumption adjustment. Better documented parameter, reduced range compared to other elasticities.
Trade elasticity	-50%	+100%	Log-uniform	Trade response patterns.
Vegetable oil substitution elasticity	-50%	+100%	Log-uniform	Degree of substitution between different vegetable oils
Land expansion elasticity	-50%	+100%	Log-uniform	Distribution of expansion into the other land uses
Yield response on feedstock	Implicit elasticity – 0.05	Implicit elasticity + 0.1	Log-uniform	Degree of feedstock yield response to prices. Yield response in GLOBIOM is not defined through an explicit elasticity, therefore calculated differently.
Expansion response of palm into peat land	-50%	+50%	Normal	Degree of expansion of palm plantation into peatland in Indonesia and Malaysia
Biophysical/emission factors parameters				
Co-product protein content	-10%	+10%	Uniform	Degree of substitution of co-products
Peat land emissions factor on pristine forest	27 tCO_2 ha^{-1} yr^{-1}	113 tCO_2 ha^{-1} yr^{-1}	Lognormal	Level of peatland emissions in Indonesia and Malaysia
Emission factors of living biomass	Low bound IPCC range	High bound IPCC range	Normal	Determines emissions from the land use conversion category
Tillage impact	Low bound IPCC range	High bound IPCC range	Normal	Determines the SOC emission impact at the margin

* Typical value range corresponds to min/max for uniform distribution or to 95% probability range for normal or log normal distributions (approx. two standard deviations).

The sensitivity analysis presented here covers a number of interesting parameters influencing the results, however, some other key sources of impact on ILUC emission intensities are also deliberately excluded because these have been harmonized during the CAEP protocol. These however play a role in the final ILUC values obtained. Source of uncertainties not covered in the Monte-Carlo are in particular:

- amortization period for land use change emission
- feedstock yield
- pathway conversion efficiencies
- coproduct to fuel production ratio

In addition to these unconsidered factors, this document also discusses further below some other sources of uncertainty that have been identified as playing an important role in ILUC results but cannot be covered by the parametric sensitivity analysis as they relate to model methodology or design. These are in particular: i) the role of land cover converted by perennials crops ii) the role of the coproduct displacement and the livestock response iii) the dynamics of C accumulation on abandoned land. These are briefly discussed below.

6.3.2 Results from the Monte-Carlo analysis with GLOBIOM

Results of the various runs are illustrated in the Figure 66 below, which shows the distribution of the ILUC emission factors for each of the pathway tested. Boxes indicate the 50% central values in the distribution, whereas, whiskers indicate the span of the distribution for a 95% confidence interval and points are outliers. The sensitivity of the pathways to the tested assumption depends on the initial emission value, and the characteristics of land use change patterns associated to the results. Results with the lowest dispersion are the perennial crop pathways in the US, and sugar cane in Brazil for ATJ-SPK from isobutanol and ATJ-SPK from ethanol. For other pathways, larger variability can be observed, with the largest confidence intervals being observed for soybean in Brazil and palm oil in Southeast Asia. These two pathways are the only ones where the results go beyond 100 gCO_2e/MJ. In the case of palm oil, the results are also significantly skewed with a long tail for the high values due to peatland emissions.

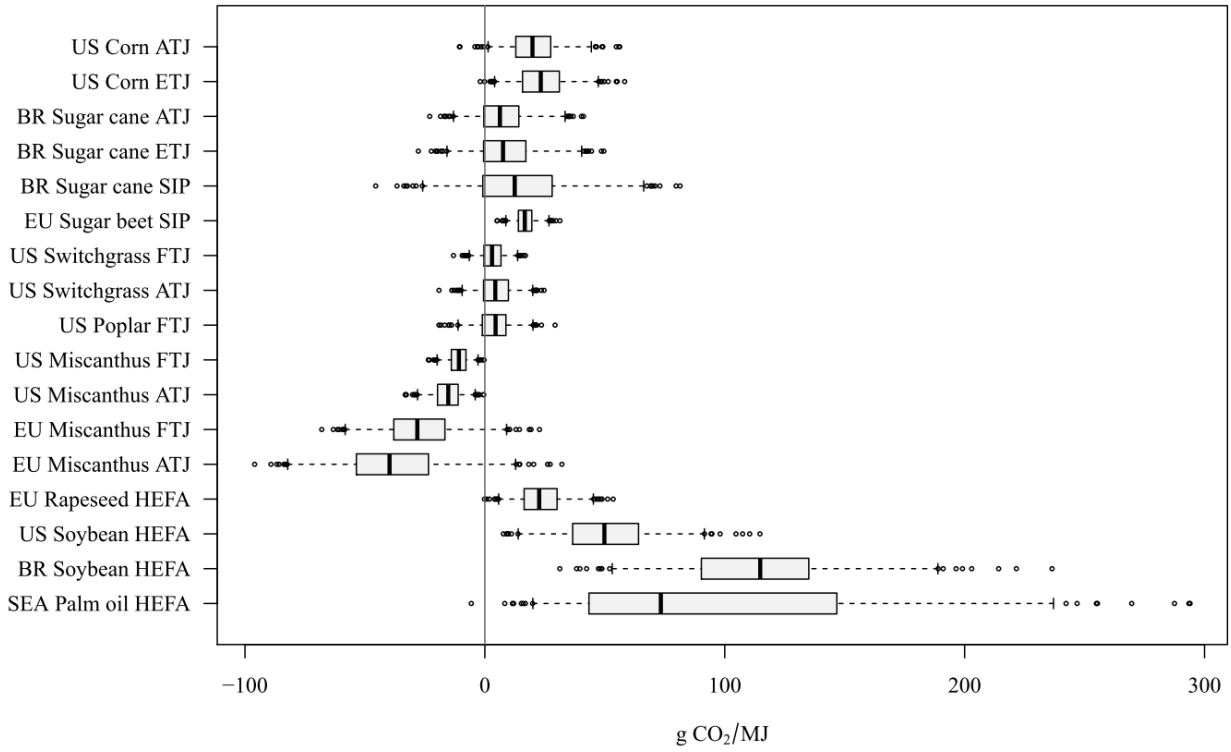

Figure 66: Results of Monte-Carlo analysis for the 17 aviation fuel pathways out of 22 examined pathways (300 runs per pathway), in gCO2e/MJ. Whiskers indicate the 95% interval of the results and the box indicates the 50% interval of the distribution. The horizontal bar in each box represents the median value of the distribution

The summary statistics of the sensitivity runs are indicated below in Table 114 and display the mean value of the distribution, the standard deviation, as well as the main quantiles for the 50% and 95% distribution confidence interval of the results distribution. The mean values are usually close to the single point estimate results presented earlier. They can however differ when the distribution of the results is skewed, which is the case notably with palm oil. Standard deviations also provide interesting information on the level of sensitivity around some estimates. For instance, in the case of sugar cane pathways, negative values are found possible, but also some notably positive ones, in particular in the case of sugar cane SIP, due to the lower yield, and this pathway ranks third in terms of standard deviation. Brazil soybean oil and Southeast palm oil HEFAs are the two pathways with both the largest mean and standard deviation values. The 95% confidence intervals on GLOBIOM parametric uncertainty are following a similar narrative as the standard deviation values. It is interesting to note that some pathways like EU miscanthus ATJ-SPK from isobutanol, due to the lower yield and uncertainty on the sequestration potential, can have significant spread in the values obtained (-82.2 to 12.8 g CO_2e/MJ). This range of value is much lower in the case of the US miscanthus due to the fact that US miscanthus is expanding in most scenarios outside of cropland for the US case (see discussion in next section). Median values are usually closer to single point estimates. In the case of palm however, the large number of carbon sources interacting (negative sequestration in palm trees and large positive emissions from peatland and land use conversion) prevents full convergence of the median value to the single point estimate. This uncertainty is also illustrated by the wide uncertainty range for the 50% central range of the distribution (44.9 to 148.7 gCO_2e/MJ).

Table 114: Summary statistics from sensitivity analysis on GLOBIOM results for 17 pathways out of 22 examined pathways (300 runs per scenario). Mean, standard deviation and quantiles

	Mean	SD	Quantiles				
			2.5%	25%	50%	75%	97.5%
US Corn ATJ-SPK from isobutanol	20.6	11.2	1.3	12.9	19.8	27.5	44.4
US Corn ATJ-SPK from ethanol	24.0	11.1	4.1	15.7	23.3	31.1	47.3
BR Sugar cane ATJ-SPK from isobutanol	7.1	11.7	-13.1	-0.4	6.3	14.2	33.4
BR Sugar cane ATJ-SPK from ethanol	8.6	14.1	-15.8	-0.5	7.6	17.1	40.4
BR Sugar cane SIP	14.1	23.2	-25.9	-0.9	12.4	28.1	66.2
EU Sugar beet SIP	16.9	4.4	8.8	14.0	16.7	19.6	26.9
US Switchgrass FT	3.2	5.2	-6.5	-0.4	3.0	6.7	13.7
US Switchgrass ATJ-SPK from isobutanol	4.6	7.6	-9.5	-0.6	4.3	9.8	20.0
US Poplar FT	4.0	7.9	-11.2	-1.1	4.5	8.8	20.1
US Miscanthus FT	-10.9	4.4	-19.9	-14.0	-10.8	-7.9	-2.9
US Miscanthus ATJ-SPK from isobutanol	-15.4	6.1	-28.1	-19.7	-15.3	-11.1	-4.0
EU Miscanthus FT	-27.1	16.3	-58.2	-38.0	-28.2	-16.7	9.1
EU Miscanthus ATJ-SPK from isobutanol	-38.2	22.9	-82.2	-53.6	-39.7	-23.5	12.8
US Soybean HEFA	50.8	20.1	13.9	36.6	49.8	64.1	91.5
BR Soybean HEFA	116.1	34.7	53.1	90.2	114.8	135.1	188.9
EU Rape oil HEFA	23.0	10.0	5.7	16.4	22.6	30.1	45.2
SE Asia Palm oil HEFA	98.6	65.1	15.9	44.9	76.8	148.7	240.9

6.4 **OTHER SOURCES OF UNCERTAINTY STUDIED IN GLOBIOM**

6.4.1 Land cover type converted by perennial crop expansion

The sensitivity analysis above reveals that, in spite of varying some of the model parameters, the range of results for miscanthus in the US and in the EU are not overlapping much, with US feedstock ILUC values being slightly negative and EU feedstocks being much more negative. Interestingly, this difference is also observed in the results of GTAP-BIO, although the patterns are reversed, with US miscanthus strongly negative and EU miscanthus much less. These differences are observed mainly by the type of land cover where the expansion of perennial plantations is taking place in the model. Even with sensitivity analysis on the conversion parameters, US miscanthus mostly expand in GLOBIOM in the "other natural land" land cover, which is already rich in soil organic carbon. Therefore, miscanthus do not sequester much more carbon in the soil. In the EU, a larger fraction of miscanthus expands in our results in cropland, which lead

to a much larger carbon sequestration. These results are therefore mainly driven by direct land use change associated to these pathways. The fact that the type of land cover into which the perennial plantation expands is not distinguished here is an important source of uncertainty, and this information would gain to be better discriminated to more precisely anticipate the sequestration potential of the crop. This source of uncertainty also very likely plays a role for the results of switchgrass and poplar pathways in the US, even if the EU counterpart were not tested here. The sequestration effect through SOC for these two feedstocks are however lower (Qin et al. 2016), therefore the difference between the two regions is expected to be lower.

6.4.2 Impact of the displacement effect

Some further experiments have also been conducted within GLOBIOM to assess the impact of keeping the displacement effect, by artificially freezing the final consumption of livestock product (consumers stop reacting to livestock product prices). The conclusion of the investigation was that the consumer response would play an important role, as cropland requirement would decrease by about 30% for soybean, and 15% for rapeseed in the case of complete absence of response. However, extending this absence of response to crops would increase ILUC, which shows that the effect can play a role in the two directions. Additionally, the representation of the feed substitution metric was found to play also an important role. In GLOBIOM, feed substitution patterns need to respect the matching of protein and energy requirement for each animal type. Switching from this nutrient balance substitution approach to an economic value-based substitution among feedstuff showed a large change in the model results, as protein meal (high economic value) are able to displace more cereals on value basis. Difference in land requirement in the Brazil soybean HEFA scenario was found to be 57% lower with a value-based displacement compared to nutrient balance substitution, and 48% less for the US soybean HEFA scenario. Due to the lower protein content, the difference is lower in the case of EU rapeseed (-13%). These results illustrate the crucial role of the substitution method choice for determining the impact of the soybean HEFA pathways.

6.4.3 Foregone sequestration accounting

Another important source of uncertainty is the carbon accumulation on marginal and abandoned land. Abandoned land is accounted for in the GLOBIOM framework when demand for agricultural products decreases (e.g. beef demand in the EU) or when agricultural yield improvement is faster than food demand change. Using abandoned land to grow bioenergy feedstock is part of the chain of impacts in the model when implementing a bioenergy demand shock. This implies a carbon sequestration opportunity cost if this land is being left without management for a long time in the counterfactual scenario (baseline). With an amortization period of 25 years for carbon stock change in the CAEP ILUC context, GLOBIOM is accounting for SOC regeneration and living biomass reversion on this land.

The carbon debt incurred from the use of abandoned land through living biomass C accumulation rate is the most sensitive to assumptions. GLOBIOM has been following different assumptions in the course of the CAEP work cycle, considering first a regrowth of vegetation to a mix of other natural vegetation and of natural forest reversion in the absence of land management, and more recently a more conservative approach where no forest would regrow on this land. The reason why this latter assumption was finally chosen was the concern that forest regrowth was not considered for some other land use types across the world, and feedstocks would be therefore treated differently depending on the region where they would be grown, due to different assessments of abandoned land in the future.

Assuming full forest regrowth over 25 years, or only natural vegetation regrowth, can lead to drastically different outcomes for the feedstocks. The choice was made for CAEP GLOBIOM simulations to only account for the reversion to other natural vegetation as part of the foregone sequestration to facilitate comparison of feedstock performance across regions. This means that the opportunity cost accounted for is at a rather low bound of possible estimates. Higher carbon sequestration rates leading to forest regrowth mix will be looked at as part of the sensitivity analysis of the results.

Figure 67 compares how the distribution of rapeseed would be shifted as an example, if carbon accumulation rate was considered higher than the default assumption in GLOBIOM in the case of the EU rapeseed HEFA pathway. As can be seen, changing the assumption of reversion from "other natural land" reversion to "mixed vegetation" reversion (other natural and forest regrowth) is increasing the ILUC emission intensity by 21 g CO_2e/MJ. Assuming natural vegetation regrowth into forest for 25 years would lead to an ILUC emission intensity of 39 gCO_2e/MJ higher. Factoring in this type of uncertainty in the distribution leads to the bar represented on the right of the figure ("Full range") which displays a much wider uncertainty range and a median value of 42 gCO_2e/MJ. The assumption on carbon accumulation on abandoned land for these scenarios leads after 25 years to 4tC/ha for "other natural land", i.e. only 0.2 tC/ha/year of carbon accumulation. In comparison, the previous forest-other natural vegetation mix regrowth corresponds to an average recovery of 22.1 tC/ha (0.9 tC/ha/yr), and 25-year forest regrowth is assumed an average carbon stock of 37 tC/ha (1.5 tC/ha/yr).

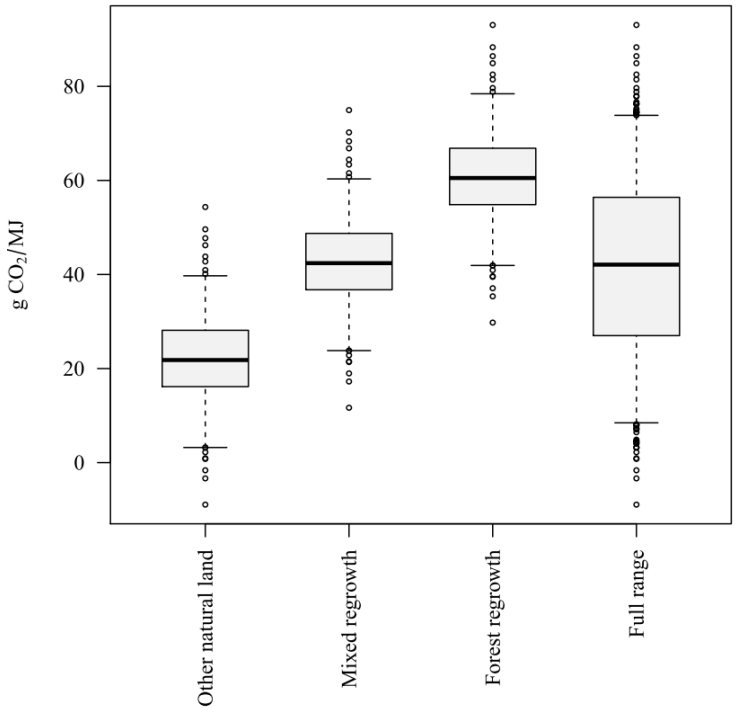

Figure 67: Role of foregone sequestration from natural vegetation regrowth under different assumptions for the EU rapeseed HEFA pathway

CHAPTER 7. **DEFAULT ILUC EMISSION INTENSITY FOR CORSIA**

The two models provide similar results for most of the sugar and starch pathways. Both models provide low or negative values for the cellulosic pathways, while the numerical values can be quite different. However, the biggest differences are in the oilseed values. GLOBIOM consistently provides higher ILUC values for oilseed pathways.

CAEP considered a number of options to determine an appropriate ILUC value in cases in which the estimates produced by the two models differ. The option set included using one model or the other, using the min, max, or average values and other possibilities. CAEP decided to use a similar approach to that used for the core LCA analysis that the mid-point can be used as default value when the estimates from the models are within 10 percent of the baseline fossil fuel value of 89 gCO_2e/MJ. That is, if the difference between the two model values for a particular region and pathway is 8.9 gCO_2e/MJ or less, then the proposed ILUC value is the average of the two model results. Following this approach, eight of the twenty two pathways use the average value, including six sugar or starch pathways, the EU rapeseed HEFA pathway, and the US corn ATJ-SPK from ethanol pathway (emissions for this pathway exceed the baseline value).

After a thorough debate of the pros and cons of the various options, CAEP decided to recommend the use, for the remaining sixteen pathways, of the lower of the two model values plus an adjustment factor of 4.45 gCO_2e/MJ. This adjustment factor represents half of the tolerance level of 8.9 gCO_2e/MJ discussed previously. It is therefore equal to the maximum difference between the lower model estimate and mid-point value for pathways where the difference between the two models is within the tolerance level of 8.9 gCO_2e/MJ. The calculated default ILUC values are provided in Table 115. The vast majority of CAEP experts thought this approach was a reasonable compromise. CAEP agreed that work to review the scientific evidence relating to ILUC should continue, and the ILUC values be subject to review as part of the regular CORSIA review process.

Table 115: Default ILUC emission values for SAF pathways, in g CO2e/MJ

Region	Feedstock	Conversion Process	Pathway Specifications	GTAP-BIO	GLOBIOM	Default ILUC Value
USA	Corn grain	ATJ-SPK from isobutanol		22.5	21.7	22.1
USA	Corn grain	Alcohol (ethanol) to jet (ATJ)		24.9	25.3	25.1
Brazil	Sugarcane and Molasses	ATJ-SPK from isobutanol		7.4	7.2	7.3
Brazil	Sugarcane	Alcohol (ethanol) to jet (ATJ)		9.0	8.3	8.7
Brazil	Sugarcane	Synthesized iso-paraffins (SIP)		14.2	8.4	11.3
EU	Sugar beet	Synthesized iso-paraffins (SIP)		20.3	20.0	20.2
USA	Soy oil	Hydroprocessed esters and fatty acids (HEFA)		20.0	50.4	24.5
USA	Carinata oil	Hydroprocessed esters and fatty acids (HEFA)	Feedstock is grown as a secondary crop that avoids other crops displacement	-12.9	-25.9	-21.4
Brazil	Soy oil	Hydroprocessed esters and fatty acids (HEFA)		22.5	117.9	27.0
Brazil	Carinata oil	Hydroprocessed esters and fatty acids (HEFA)	Feedstock is grown as a secondary crop that avoids other crops displacement	-15.0	-24.9	-20.4
EU	Rapeseed oil	Hydroprocessed esters and fatty acids (HEFA)		20.7	27.5	24.1
Malaysia & Indonesia	Palm oil	Hydroprocessed esters and fatty acids (HEFA)		34.6	60.2	39.1
USA	Miscanthus	Fischer-Tropsch (FT)		-37.3	-10.6	-32.9
USA	Miscanthus	ATJ-SPK from isobutanol		-58.5	-8.7	-54.1
USA	Miscanthus	ATJ-SPK from ethanol		-47.1	-8.2	-42.6
USA	Switchgrass	Fischer-Tropsch (FT)		-8.2	2.5	-3.8
USA	Switchgrass	ATJ-SPK from isobutanol		-18.9	10.2	-14.5
USA	Switchgrass	ATJ-SPK from ethanol		-15.2	8.4	-10.7
USA	Poplar	Fischer-Tropsch (FT)		-9.6	-0.6	-5.2
EU	Miscanthus	Fischer-Tropsch (FT)		-9.3	-26.5	-22.0
EU	Miscanthus	Alcohol (isobutanol) to jet (ATJ)		-16.6	-35.5	-31.0
EU	Miscanthus	ATJ-SPK from ethanol		-12.7	-27.8	-23.3
India	Jatropha	Hydroprocessed esters and fatty acids (HEFA)	Meal used as fertilizer or electricity input	-27.3	-22.2	-24.8
India	Jatropha	Hydroprocessed esters and fatty acids (HEFA)	Meal used as animal feed after detoxification	-41.9	-52.6	-1.3
Global	Soy oil	Hydroprocessed esters and fatty acids (HEFA)		21.3	88.1	25.8

Global	Corn grain	ATJ-SPK from isobutanol		37.7	25.2	29.7
Global	Corn grain	ATJ-SPK from ethanol		40.7	30.4	34.9
Global	Rapeseed oil	Hydroprocessed esters and fatty acids (HEFA)		24.1	27.8	26.0
Global	Sugarcane and Molasses	ATJ-SPK from isobutanol		11.4	6.8	9.1
Global	Sugarcane	ATJ-SPK from ethanol		16.8	4.0	8.5
Global	Sugarcane	Synthesized iso-paraffins (SIP)		26.8	6.6	11.1
Global	Sugar beet	Synthesized iso-paraffins (SIP)		13.0	9.5	11.2
Global	Miscanthus	Fischer-Tropsch (FT)		-16.7	-8.5	-12.6
Global	Miscanthus	ATJ-SPK from isobutanol		-28.0	-13.8	-23.6
Global	Miscanthus	ATJ-SPK from ethanol		-23.4	-11.0	-19.0
Global	Switchgrass	Fischer-Tropsch (FT)		5.3	5.2	5.3
Global	Switchgrass	ATJ-SPK from isobutanol		3.1	7.7	5.4
Global	Switchgrass	ATJ-SPK from ethanol		3.7	5.9	4.8
Global	Poplar	Fischer-Tropsch (FT)		11.4	5.8	8.6
Global	Carinata oil	Hydroprocessed esters and fatty acids (HEFA)	Feedstock is grown as a secondary crop that avoids other crops displacement	-9.8	-15.5	-12.7
Global	Camelina oil	Hydroprocessed esters and fatty acids (HEFA)	Feedstock is grown as a secondary crop that avoids other crops displacement	-11.4	-15.4	-13.4

CHAPTER 8. **REFERENCES**

Aguiar, A., Narayanan, B., McDougall, R., 2016. An overview of the GTAP 9 data base. Journal of Global Economic Analysis 1, 181-208.
Ahlgren, S., Di Lucia, L., 2014. Indirect land use changes of biofuel production–a review of modelling efforts and policy developments in the European Union. Biotechnology for biofuels 7, 35.
ASTM, 2018. Standard Specification for Aviation Turbine Fuel Containing Synthesized Hydrocarbons.
Austin, K.G., Mosnier, A., Pirker, J., McCallum, I., Fritz, S., Kasibhatla, P.S., 2017. Shifting patterns of oil palm driven deforestation in Indonesia and implications for zero-deforestation commitments. Land Use Policy 69, 41-48.
Broch, A., Hoekman, S.K., Unnasch, S., 2013. A review of variability in indirect land use change assessment and modeling in biofuel policy. Environmental Science & Policy 29, 147-157.
Buchspies, B., Kaltschmitt, M., 2016. Life cycle assessment of bioethanol from wheat and sugar beet discussing environmental impacts of multiple concepts of co-product processing in the context of the European Renewable Energy Directive. Biofuels 7, 141-153.
Câmara, G., Soterroni, A., Ramos, F., Carvalho, A., Andrade, P., Souza, R., Mosnier, A., Mant, R., Buurman, M., Pena, M., 2015. Modelling Land Use Change in Brazil: 2000–2050.
CEPCI, 2016. Economic indicators, Chemical Engineering.
Diederichs, G.W., Ali Mandegari, M., Farzad, S., Görgens, J.F., 2016. Techno-economic comparison of biojet fuel production from lignocellulose, vegetable oil and sugar cane juice. Bioresource Technology 216, 331-339.
Dohleman, F.G., Heaton, E.A., Arundale, R.A., Long, S.P., 2012. Seasonal dynamics of above- and below-ground biomass and nitrogen partitioning in Miscanthus × giganteus and Panicum virgatum across three growing seasons. GCB Bioenergy 4, 534-544.
Dunn, J.B., Mueller, S., Kwon, H.-y., Wang, M.Q., 2013. Land-use change and greenhouse gas emissions from corn and cellulosic ethanol. Biotechnology for Biofuels 6, 1-14.
Earles, J.M., Yeh, S., Skog, K.E., 2012. Timing of carbon emissions from global forest clearance. Nature Climate Change 2, 682.
Edwards, R., Mulligan, D., Marelli, L., 2010. Indirect land use change from increased biofuels demand. Comparison of models and results for marginal biofuels production from different feedstocks., EC Joint Research Centre, Ispra.
Edwards, R., O'Connell, A., Padella, M., Mulligan, D., Giuntoli, J., Agostini, A., Koeble, R., Moro, A., Marelli, L., 2016. Definition of input data to assess GHG default emissions from biofuels in EU legislation. JRC Science for Policy Report EUR 26853.
EEA, 2007. Estimating the Environmentally Compatible Bio-Energy Potential from Agriculture.
EEA, 2013. EU bioenergy potential from a resource-efficiency perspective. Publ. Office of the European Union.
EIA, 2015. International Energy Statistics.
EIA, 2016. Monthly Biodiesel Production Report.
Elgowainy, A., Han, J., Wang, M., Carter, N., Stratton, R., Hileman, J., Malwitz, A., Balasubramanian, S., 2012. Life-cycle analysis of alternative aviation fuels in GREET. Argonne National Laboratory (ANL).
EPA, 2010. Renewable Fuel Standard Program (RFS2) Regulatory Impact Analysis. Technical Report EPA-420-R-10-006. Assessment and Standards Division, Office of Transportation and Air Quality.
EPA, 2012. Federal Register, pp. 4300-4317.
FAO, 2010. Global forest resources assessment. Main report, FAO Forest paper 163.
FAOSTAT, 2017.
Garten, C.T., Smith, J.L., Tyler, D.D., Amonette, J.E., Bailey, V.L., Brice, D.J., Castro, H.F., Graham, R.L., Gunderson, C.A., Izaurralde, R.C., Jardine, P.M., Jastrow, J.D., Kerley, M.K., Matamala, R., Mayes, M.A., Metting, F.B., Miller, R.M., Moran, K.K., Post, W.M., Sands, R.D., Schadt, C.W., Phillips, J.R., Thomson, A.M., Vugteveen, T., West, T.O., Wullschleger, S.D., 2010. Intra-annual changes in biomass, carbon, and

nitrogen dynamics at 4-year old switchgrass field trials in west Tennessee, USA. Agriculture, Ecosystems & Environment 136, 177-184.
Garten, C.T., Wullschleger, S.D., Classen, A.T., 2011. Review and model-based analysis of factors influencing soil carbon sequestration under hybrid poplar. Biomass and Bioenergy 35, 214-226.
GFW, 2017. Oil palm concessions.
Gibbs, H., Yui, S., Plevin, R., 2014. New estimates of soil and biomass carbon stocks for global economic models. Center for Global Trade Analysis, Department of Agricultural Economics, Purdue University.
Harris, N., 2011. Revisions to land conversion emission factors since the RFS2 final rule. Winrock International report to EPA.
Havlík, P., Schneider, U.A., Schmid, E., Böttcher, H., Fritz, S., Skalský, R., Aoki, K., De Cara, S., Kindermann, G., Kraxner, F., 2011. Global land-use implications of first and second generation biofuel targets. Energy policy 39, 5690-5702.
Havlík, P., Valin, H., Herrero, M., Obersteiner, M., Schmid, E., Rufino, M.C., Mosnier, A., Thornton, P.K., Böttcher, H., Conant, R.T., 2014. Climate change mitigation through livestock system transitions. Proceedings of the National Academy of Sciences, 201308044.
Hertel, T.W., Golub, A.A., Jones, A.D., O'Hare, M., Plevin, R.J., Kammen, D.M., 2010. Effects of US maize ethanol on global land use and greenhouse gas emissions: estimating market-mediated responses. BioScience 60, 223-231.
Hugron, S., Bussières, J., Rochefort, L., 2013. Tree plantations within the context of ecological restoration of peatlands: practical guide. Peatland Ecology Research Group, Université Laval, Québec, Québec, Canada.
IEA, 2015a. Energy and Climate Change. International Energy Agency, www.iea.org, p. 200.
IEA, 2015b. Southeast Asia Energy Outlook 2015.
IPCC, 2006. 2006 IPCC guidelines for national greenhouse gas inventories.
IPCC, 2014. Climate change 2014: mitigation of climate change, in: Edenhofer, O., Pichs-Madruga, R., Sokona, Y. (Eds.).
Keeney, R., Hertel, T.W., 2009. The Indirect Land Use Impacts of United States Biofuel Policies: The Importance of Acreage, Yield, and Bilateral Trade Responses. American Journal of Agricultural Economics 91, 895-909.
Khanna, M., Crago, C.L., 2012. Measuring indirect land use change with biofuels: Implications for policy. Annu. Rev. Resour. Econ. 4, 161-184.
Khasanah, N.m., van Noordwijk, M., Ningsih, H., 2015. Aboveground carbon stocks in oil palm plantations and the threshold for carbon-neutral vegetation conversion on mineral soils. Cogent Environmental Science 1, 1119964.
Kicklighter, D.W., Gurgel, A.C., Melillo, J.M., Reilly, J.M., Paltsev, S., 2012. Potential direct and indirect effects of global cellulosic biofuel production on greenhouse gas fluxes from future land-use chage, MIT Joint Program on the Science and Policy of Global Change.
Klein-Marcuschamer, D., Turner, C., Allen, M., Gray, P., Dietzgen, R.G., Gresshoff, P.M., Hankamer, B., Heimann, K., Scott, P.T., Stephens, E., 2013. Technoeconomic analysis of renewable aviation fuel from microalgae, Pongamia pinnata, and sugarcane. Biofuels, Bioproducts and Biorefining 7, 416-428.
Laborde, D., Valin, H., 2012. Modeling land-use changes in a global CGE: assessing the EU biofuel mandates with the MIRAGE-BioF model. Climate Change Economics 3, 1250017.
Lewis, S.L., Lopez-Gonzalez, G., Sonké, B., Affum-Baffoe, K., Baker, T.R., Ojo, L.O., Phillips, O.L., Reitsma, J.M., White, L., Comiskey, J.A., 2009. Increasing carbon storage in intact African tropical forests. Nature 457, 1003.
Limpert, E., Stahel, W.A., Abbt, M., 2001. Log-normal Distributions across the Sciences: Keys and CluesOn the charms of statistics, and how mechanical models resembling gambling machines offer a link to a handy way to characterize log-normal distributions, which can provide deeper insight into variability and probability—normal or log-normal: That is the question. BioScience 51, 341-352.
Miettinen, J., Hooijer, A., Vernimmen, R., Liew, S.C., Page, S.E., 2017. From carbon sink to carbon source: extensive peat oxidation in insular Southeast Asia since 1990. Environmental Research Letters 12, 024014.

Miettinen, J., Shi, C., Liew, S.C., 2016. Land cover distribution in the peatlands of Peninsular Malaysia, Sumatra and Borneo in 2015 with changes since 1990. Global Ecology and Conservation 6, 67-78.
Mosnier, A., Havlík, P., Valin, H., Baker, J., Murray, B., Feng, S., Obersteiner, M., McCarl, B.A., Rose, S.K., Schneider, U.A., 2013. Alternative US biofuel mandates and global GHG emissions: The role of land use change, crop management and yield growth. Energy Policy 57, 602-614.
Myneni, R., Dong, J., Tucker, C., Kaufmann, R., Kauppi, P., Liski, J., Zhou, L., Alexeyev, V., Hughes, M., 2001. A large carbon sink in the woody biomass of Northern forests. Proceedings of the National Academy of Sciences 98, 14784-14789.
Page, S.E., Rieley, J.O., Banks, C.J., 2011. Global and regional importance of the tropical peatland carbon pool. Global Change Biology 17, 798-818.
Pearlson, M., Wollersheim, C., Hileman, J., 2013. A techno-economic review of hydroprocessed renewable esters and fatty acids for jet fuel production. Biofuels, Bioproducts and Biorefining 7, 89-96.
Peña-Lévano, L., Taheripour, F., Tyner, W., 2015. Development of the GTAP Land Use Data Base for 2011. GTAP Research Memorandum.
Perlack, R.D., Eaton, L.M., Turhollow Jr, A.F., Langholtz, M.H., Brandt, C.C., Downing, M.E., Graham, R.L., Wright, L.L., Kavkewitz, J.M., Shamey, A.M., 2011. US billion-ton update: biomass supply for a bioenergy and bioproducts industry.
Petter, R., Tyner, W.E., 2014. Technoeconomic and Policy Analysis for Corn Stover Biofuels. ISRN Economics 2014.
Plevin, R., 2017. AEZ-EF Cellulosic Model.
Plevin, R., Gibbs, H., Duffy, J., Yui, S., Yeh, S., 2014a. Agro-ecological Zone Emission Factor (AEZ-EF) Model (v47). Center for Global Trade Analysis, Department of Agricultural Economics, Purdue University.
Plevin, R., Gibbs, H., Duffy, J., Yui, S., Yeh, S., 2014b. Agro-ecological Zone Emission Factor (AEZ-EF) Model (v52). California Air Resources Board.
Plevin, R.J., Beckman, J., Golub, A.A., Witcover, J., O'Hare, M., 2015. Carbon Accounting and Economic Model Uncertainty of Emissions from Biofuels-Induced Land Use Change. Environmental Science & Technology 49, 2656-2665.
Radich, T., 2015. The Flight Paths for Biojet Fuel. U.S. Energy Information Administration.
Ray, D.K., Foley, J.A., 2013. Increasing global crop harvest frequency: recent trends and future directions. Environmental Research Letters 8, 044041.
Ruesch, A., Gibbs, H.K., 2008. New IPCC Tier-1 global biomass carbon map for the year 2000.
Saatchi, S.S., Harris, N.L., Brown, S., Lefsky, M., Mitchard, E.T., Salas, W., Zutta, B.R., Buermann, W., Lewis, S.L., Hagen, S., 2011. Benchmark map of forest carbon stocks in tropical regions across three continents. Proceedings of the National Academy of Sciences 108, 9899-9904.
Searchinger, T., Heimlich, R., Houghton, R.A., Dong, F., Elobeid, A., Fabiosa, J., Tokgoz, S., Hayes, D., Yu, T.-H., 2008. Use of U.S. Croplands for Biofuels Increases Greenhouse Gases Through Emissions from Land-Use Change. Science 319, 1238-1240.
Shean, M., 2012. Stagnating Palm Oil Yields Impede Growth. USA: United States Department of Agriculture.
Siebert, S., Portmann, F.T., Döll, P., 2010. Global patterns of cropland use intensity. Remote Sensing 2, 1625-1643.
Soterroni, A., Mosnier, A., Carvalho, A.X., Câmara, G., Obersteiner, M., Andrade, P.R., Souza, R.C., Brock, R., Pirker, J., Kraxner, F., 2018. Future environmental and agricultural impacts of Brazil's Forest Code. Environmental Research Letters.
Staples, M.D., Malina, R., Olcay, H., Pearlson, M.N., Hileman, J.I., Boies, A., Barrett, S.R.H., 2014. Lifecycle greenhouse gas footprint and minimum selling price of renewable diesel and jet fuel from fermentation and advanced fermentation production technologies. Energy Environ Sci 7.
Stratton, R.W., 2010. Life cycle assessment of greenhouse gas emissions and non-CO_2 combustion effects from alternative jet fuels. Massachusetts Institute of Technology.
Taheripour, F., Cui, H., Tyner, W.E., 2016. An Exploration of Agricultural Land Use Change at the Intensive and Extensive Margins: Implications for Biofuels Induced Land Use Change Modeling.

Taheripour, F., Cui, H., Tyner, W.E., 2017a. An Exploration of Agricultural Land Use Change at Intensive and Extensive Margins, Bioenergy and Land Use Change. John Wiley & Sons, Inc., pp. 19-37.
Taheripour, F., Hurt, C., Tyner, W.E., 2013. Livestock industry in transition: Economic, demographic, and biofuel drivers. Animal Frontiers 3, 38-46.
Taheripour, F., Tyner, W.E., 2013. Induced Land Use Emissions due to First and Second Generation Biofuels and Uncertainty in Land Use Emission Factors. Economics Research International 2013, 12.
Taheripour, F., Tyner, W.E., Wang, M.Q., 2011. Global land use changes due to the US cellulosic biofuel program simulated with the GTAP model. Purdue University, Department of Agricultural Economics: West Lafayette, IN, USA.
Taheripour, F., Tyner, W.E., Zhuang, Q., Lu, X., 2012. Biofuels, cropland expansion, and the extensive margin. Energy, Sustainability and Society 2, 1-11.
Taheripour, F., Zhao, X., Tyner, W.E., 2017b. The impact of considering land intensification and updated data on biofuels land use change and emissions estimates. Biotechnology for biofuels 10, 191.
Tyner, W.E., Taheripour, F., Hoekman, K., Broch , A., Liu, V., Lyons, J., 2016. Follow-on Study of Transportation Fuel Life Cycle Analysis: Review of Current CARB and EPA Estimates of Land use Change (LUC) Impacts. Sierra Research, Sacramento, CA, Coordinating Research Council (CRC).
Tyner, W.E., Taheripour, F., Zhuang, Q., Birur, D., Baldos, U., 2010. Land use changes and consequent CO2 emissions due to US corn ethanol production: A comprehensive analysis. Department of Agricultural Economics, Purdue University.
U.S. Bureau of Labor Statistics, 2018. Producer Price Index by Commodity for Chemicals and Allied Products: Industrial Chemicals.
USDA, 2016a. EU28 biofuels annual.
USDA, 2016b. EU28 sugar annual.
USDA, 2016c. Indonesia biofuels annual.
USDA, 2016d. Malaysia biofuels annual.
USDA, E., 2016e. Oil Crops Yearbook.
Valin, H., Havlik, P., Mosnier, A., Herrero, M., Schmid, E., Obersteiner, M., 2013. Agricultural productivity and greenhouse gas emissions: trade-offs or synergies between mitigation and food security? Environmental Research Letters 8, 035019.
Valin, H., Peters, D., Berg, M.v.d., Frank, S., Havlik, P., Forsell, N., Hamelinck, C., 2015. The land use change impact of biofuels consumed in the EU, European Commission.
Warner, E., Zhang, Y., Inman, D., Heath, G., 2014. Challenges in the estimation of greenhouse gas emissions from biofuel-induced global land-use change. Biofuels, Bioproducts and Biorefining 8, 114-125.
Wicke, B., Verweij, P., van Meijl, H., van Vuuren, D.P., Faaij, A.P., 2012. Indirect land use change: review of existing models and strategies for mitigation. Biofuels 3, 87-100.
Winans, K.S., Tardif, A.-S., Lteif, A.E., Whalen, J.K., 2015. Carbon sequestration potential and cost-benefit analysis of hybrid poplar, grain corn and hay cultivation in southern Quebec, Canada. Agroforestry Systems 89, 421-433.
Woodall, C., Heath, L., Smith, J., 2008. National inventories of down and dead woody material forest carbon stocks in the United States: challenges and opportunities. Forest Ecology and Management 256, 221-228.
You, L., Wood, S., 2006. An entropy approach to spatial disaggregation of agricultural production. Agricultural Systems 90, 329-347.
Zhuang, Q., Qin, Z., Chen, M., 2013. Biofuel, land and water: maize, switchgrass or Miscanthus ? Environmental Research Letters 8, 015020.

PART IV: LCA METHODOLOGIES FOR CORSIA LOWER CARBON AVIATION FUELS

The LCA methodology for CORSIA Lower Carbon Aviation Fuels is contained in Section 7 of the ICAO document “CORSIA Methodology For Calculating Actual Life Cycle Emissions Values”.

-END-